VNIVERSITAT DE VALÈNCIA

Facultat de Farmàcia

Departament de Medicina Preventiva i Salut Pública, Ciències de l'Alimentació, Toxicologia i Medicina Legal

Programa de Doctorat amb Menció cap a l'Excel·lència en Ciències de l'Alimentació

Efectos de las micotoxinas beauvericina y metabolitos de la zearalenona *in silico* e *in vitro* en células de neuroblastoma humano SH-SY5Y.

Tesi Doctoral

València, 2021

Presentada per:

Fojan Agahi

Dirigida per:

Dra. Ana Juan García

Dra. Cristina Juan García

Facultat de Farmàcia

La **Dra. Ana Juan García**, Professora Titular de l´àrea de Toxicologia, i la **Dra. Cristina Juan García**, Professora Titular de l´àrea de Nutrició i Bromatologia, de la Universitat de València,

CERTIFIQUEN QUE:

La Graduada en Nutrició Humana i Dietètica **Na. Fojan Agahi** ha realitzat baix la seua direcció el treball **"Efectos de las micotoxinas beauvericina y metabolitos de la zearalenona *in silico* e *in vitro* en células de neuroblastoma humano SH-SY5Y"**, i autoritzen la seua presentació per a optar al títol de Doctor per la Universitat de València.

I, perquè així conste, expedeixen i signen el present certificat.

Burjassot (València), Maig 2021.

Dra. Ana Juan García

Dra. Cristina Juan García

Aquest treball ha sigut plasmat en 5 articles, publicats o que es publicaran en les següents revistes:

1. *In silico* methods for metabolomic and toxicity prediction of zearalenone, α-zearalenone and β-zearalenone. Fojan Agahi, Cristina Juan, Guillermina Font and Ana Juan-García. 2020. Food and Chemical Toxicology 146, 111818. Impact factor: 4.679
2. Individual and combined effect of zearalenone derivates and beauvericin mycotoxins on SH-SY5Y Cells. Fojan Agahi, Guillermina Font, Cristina Juan and Ana Juan-García. 2020, Toxins, 12, 212. Impact factor: 3.531
3. Oxidative stress, glutathione, and gene expression key indicators in SH-SY5Y cells exposed to zearalenone metabolites and beauvericin. Fojan Agahi, Neda Álvarez-Ortega, Guillermina Font, Ana Juan-García and Cristina Juan. 2020. Toxicology Letters 334, 44–52. Impact factor: 3.569
4. Enzymatic defense system in neuroblastoma cells exposed to zearalenone's derivates and beauvericin. Fojan Agahi Ana Juan-García, Guillermina Font and Cristina Juan. 2021 Food and Chemical Toxicology. 152, 112227. Impact factor: 4.679
5. Neurotoxicity of zearalenone's metabolites and beauvericin mycotoxins via apoptosis and cell cycle disruption. Fojan Agahi, Cristina Juan, Guillermina Font and Ana Juan-García. 2021, Toxicology. 456, 152784. Impact factor: 4.099

Aquesta Tesi Doctoral Internacional s'engloba dins dels següents projectes:

1. Mitigación, biomarcadores, y toxicidad de micotoxinas legisladas y emergentes (**AGL2016-77610-R**).
2. Red Nacional sobre las micotoxinas y hongos micotoxigénicos y de sus procesos de descontaminación (**MICOFOOD**).
3. Biopreservación de pan de molde con suero de leche fermentado frente a micotoxinas y hongos toxigénicos. Seguridad de uso en presencia de carotenoides. (SAFEBIOBREAD) **PID2019-108070RB-I00ALI**
4. Evaluación de la toxicidad combinada de micotoxinas y metabolitos por métodos in vitro e in silico y su caracterización para el desarrollo de biomarcadores de exposición en humanos - Generalitat Valenciana **GV 2020/020**

Dra. Ana Juan García i Dra. Cristina Juan García en qualitat de Directores de l'estudiant Na. Fojan Agahi en els estudis de Doctorat en CIÈNCIES DE L'ALIMENTACIÓ, i en relació a la presentació de la Tesi doctoral com a compendi de publicacions

INFORMEN

Que les publicacions presentades per la doctoranda en la Tesi com a compendi de publicacions estan publicades, que els treball publicat en coautoria no han estat utilitzats en altra Tesi. i corresponen a la següent informació:

1) Autors / Autores: Fojan Agahi, Cristina Juan, Guillermina Font and Ana Juan-García.
Títol / Título: In silico methods for metabolomic and toxicity prediction of zearalenone, α-zearalenone and β-zearalenone.
Revista (vol. / nº / págs.): Food and Chemical Toxicology 146, 111818.
Any / Año: 2020 Factor d'impacte / Factor de impacto: 4.679
Classificació (ISI o SCOPUS) indicant quartil / Clasificación (ISI o SCOPUS) indicando cuartil: Q1 (ISI o / SCOPUS X)

2) Autors / Autores: Fojan Agahi, Guillermina Font, Cristina Juan and Ana Juan-García.
Títol / Título: Individual and combined effect of zearalenone derivates and beauvericin mycotoxins on SH-SY5Y Cells.
Revista (vol. / nº / págs.): Toxins, 12, 212.
Any / Año: 2020 Factor d'impacte / Factor de impacto: 3.531
Classificació (ISI o SCOPUS) indicant quartil / Clasificación (ISI o SCOPUS) indicando cuartil: Q1 (ISI o / SCOPUS X)

3) Autors / Autores: Fojan Agahi, Neda Álvarez-Ortega, Guillermina Font, Ana Juan-García and Cristina Juan.
Títol / Título: Oxidative stress, glutathione, and gene expression key indicators in SH-SY5Y cells exposed to zearalenone metabolites and beauvericin.
Revista (vol. / nº / págs.): Toxicology Letters 334, 44–52.
Any / Año: 2020 Factor d'impacte / Factor de impacto: 3.569
Classificació (ISI o SCOPUS) indicant quartil / Clasificación (ISI o SCOPUS) indicando cuartil: Q1 (ISI o / SCOPUS X)

4)Autors / Autores: Fojan Agahi, Cristina Juan, Guillermina Font y Ana Juan-García.

Títol / Título: Neurotoxicity of zearalenone's metabolites and beauvericin mycotoxins via apoptosis and cell cycle disruption.

Revista (vol. / nº / págs.): Toxicology *In press.*

Any / Año: 2021 Factor d'impacte / Factor de impacto: 4.099

Classificació (ISI o SCOPUS) indicant quartil / Clasificación (ISI o SCOPUS) indicando cuartil: Q1 (ISI o / SCOPUS X)

5)Autors / Autores: Fojan Agahi, Ana Juan-García, Guillermina Font y Cristina Juan.

Títol / Título: Study of enzymatic activity in human neuroblastoma cells SH-SY5Y exposed to zearalenone's derivates and beauvericin.

Revista (vol. / nº / págs.): Food and Chemical Toxicology *In press.*

Any / Año: 2021 Factor d'impacte / Factor de impacto: 4.679

Classificació (ISI o SCOPUS) indicant quartil / Clasificación (ISI o SCOPUS) indicando cuartil: Q1 (ISI o / SCOPUS X)

Burjassot, 3 de Maig de 2021

Directora: Dra. Ana Juan García

Directora: Dra. Cristina Juan García

Author rights

The below table explains the rights that authors have when they publish with Elsevier, for authors who choose to publish either open access or subscription. These apply to the corresponding author and all co-authors.

Author rights in Elsevier's proprietary journals	**Published open access**	**Published subscription**
Retain patent and trademark rights	√	√
Retain the rights to use their research data freely without any restriction	√	√
Receive proper attribution and credit for their published work	√	√
Re-use their own material in new works without permission or payment (with full acknowledgement of the original article): 1. Extend an article to book length 2. Include an article in a subsequent compilation of their own work 3. Re-use portions, excerpts, and their own figures or tables in other works.	√	√
Use and share their works for scholarly purposes (with full acknowledgement of the original article): 1. In their own classroom teaching. Electronic and physical distribution of copies is permitted 2. If an author is speaking at a conference, they can present the article and distribute copies to the attendees 3. Distribute the article, including by email, to their students and to research colleagues who they know for their personal use 4. Share and publicize the article via Share Links, which offers 50 days' free access for anyone, without signup or registration 5. Include in a thesis or dissertation (provided this is not published commercially) 6. Share copies of their article privately as part of an invitation-only work group on commercial sites with which the publisher has a hosting agreement	√	√

Author rights in Elsevier's proprietary journals	**Published open access**	**Published subscription**
Publicly share the preprint on any website or repository at any time.	√	√
Publicly share the accepted manuscript on non-commercial sites	√	√ using a CC BY-NC-ND license and usually only after an embargo period (see Sharing Policy for more information)
Publicly share the final published article	√ in line with the author's choice of end user license	×
Retain copyright	√	×

Índice

Lista de abreviaturas iii

Summary / Resumen viii

1. Introducción / Introduction 1

1.1. Micotoxinas 1

1.2. *Fusarium* micotoxinas 3

1.3. Zearalenona y sus metabolitos 4

1.3.1. Toxicidad *in vitro* de zearalenona y sus metabolitos 12

1.3.2. Inducción de estrés oxidativo de zearalenona y sus metabolitos 13

1.3.3. Interrupción del ciclo celular de la zearalenona y sus metabolitos 15

1.3.4. Actividad estrogénica de la zearalenona y sus metabolitos 16

1.4. Beauvericina 20

1.4.1. Efectos de toxicidad in vitro de beauvericina 22

1.4.2. Inducción de estrés oxidativo de beauvericina 24

1.4.3. Inducción del ciclo celular de beauvericina 25

1.5. Copresencia de micotoxinas 26

1.6. Estudio *in silico* de micotoxinas 28

1.7. Células de neuroblastoma humano 29

1.8. Producción de estrés oxidativo 32

1.9. Mecanismos de muerte celular y progresión del ciclo celular 37

1.10. Referencias 42

2. Objectivos / Objetives 65

3. Resultados / Results 67

3.1. Study 1: In silico methods for metabolomic and toxicity prediction of zearalenone, α-zearalenone and β-zearalenone 67

3.2. Study 2: Individual and combined effect of zearalenone derivates and beauvericin mycotoxins on SH-SY5Y cells 105

3.3. Study 3: Oxidative stress, glutathione, and gene expression key indicators in SH-SY5Y cells exposed to zearalenone metabolites and beauvericin 141

3.4. Study 4: Enzymatic defense system in neuroblastoma cells exposed to zearalenone's derivates and beauvericin 175

3.5. Study 5: Neurotoxicity of zearalenone's metabolites and beauvericin mycotoxins via apoptosis and cell cycle disruption 211

4. Discusión general / General discussion 243

4.1. *In silico* study for metabolomic and toxicity prediction of zearalenone, α-zearalenone and β-zearalenone 244

4.2. Cytotoxic effect of zearalenone's derivates and beauvericin mycotoxins on SH-SY5Y cells 248

4.2.1. Cytotoxicity effect of individual and combined mycotoxins 248

4.2.2. α-ZEL, β-ZEL, and BEA present in cell medium after treatment with binary and tertiary combination 250

4.3. Determination of oxidative stress production and enzymatic defense system in SH-SY5Y cells exposed to zearalenone metabolites and beauvericin 251

4.3.1. Intracellular ROS generation of individual and combined mycotoxins 252

4.3.2. Alteration of non-enzymatic defense system 252

4.3.3. Alteration of enzymatic defense system 253

4.4. Expression of apoptosis-related and estrogen receptors genes in SH-SY5Y cells exposed to zearalenone metabolites and beauvericin 256

4.5. Cell cycle disruption and cell death pathway analysis of zearalenone's metabolites and beauvericin 257

4.5.1. Cell cycle alteration in neuroblastoma cells exposed to zearalenone metabolites and beauvericin 257

4.5.2. Cell death pathway analysis in neuroblastoma cells exposed to zearalenone metabolites and beauvericin 260

4.6. References 261

5. Conclusiones / Conclusions 275

Annexo / Annex 281

Lista de abreviaturas

[3H]-NA	[3H]-noradrenalina
18S	Gen de referencia
A549	Células humanas de cáncer de pulmón
Acyl-coA	Colesterol aciltransferasa
Add	Aditivo
ADME	Absorción, Distribución, Metabolismo y Excreción
ADN/ DNA	ácido desoxirribonucleico/ Deoxyribonucleic acid
ANOVA	Análisis de la varianza
Ant	Antagonismo
BAX	Miembro de la familia genética *Bcl-2*
BBB	Barrera hematoencefálica/ Blood brain barrier
Bcl-2	B-cell lymphoma 2
BEA	Beauvericina
BEAS-2B	Células epiteliales bronquiales
Caco-2	Células de adenocarcinoma colorrectal humano
CASP3	Gen de caspasa 3
CAT	Catalasa/ Catalase
CCFAC	Comité del codex para aditivos y contaminantes alimentarios
CCRF-CEM	Células de leucemia humana
CdCl2	Cloruro de cadmio
CDK	Quinasa dependiente de ciclina
CDKI	Inhibidores de quinasa dependiente de ciclina
cDNA	ADN complementario /Complementary DNA
CDNB	1-chloro-2,4-dinitrobenzene
CE	Comisión Europea
CHO-K1	Células de ovario de hámster chino
IC/CI	Combination Index/Índice de combinación
CO_2	Dióxido de carbono
CYP450	Citocromo P450
DAPI	4',6-diamidina-2'- fenilandole dihidrocloruro
$DCFH_2$-DA	2',7'- diclorodihidrofluoresceína Diacetato
Dm	Dosis de efecto medio
DMEM/F-12	Dulbecco's Modified Eagle's Medium- F12
DMSO	Dimetil sulfóxido/Dimethyl sulfoxide
DON	Deoxinivalenol
EDTA	Ácido etilenodiaminetetraacetic
EFSA	Autoridad Europea de Seguridad Alimentaria/ European Food Safety Authorities

ELISA	Ensayo inmunosorbente vinculado a enzimas
ERs	Receptores de estrógeno
ERa	Receptor de estrógeno alfa
ERβ	Receptor de estrógeno beta
fa	Fracción afectada
FAO	Organización de la Agricultura y la Alimentación
FBS	Suero bovino fetal /Fetal bovine serum
FITC	Isotiacianato de fluoresceína /Fluorescein isothiocyanate
FSH	Hormona foliculoestimulante/ Follicle Stimulant Hormone
G0/G1	Segunda fase de ciclo celular
G2/M	Ultima fase de ciclo celular
GPER1	G receptor de estrógeno acoplado a proteínas
GPR30	Receptor de membrana de estrógeno no clásico 30
GPx	Glutatión peroxidasas/ Glutathione peroxidase
GR	Glutatión reductasa/ Glutathione reductase
GSH	Glutatión reducido/ Reduced glutathione
GSSG	Glutatión disulfuro/ Glutathione disulfide
GST	Glutatión-S-transferasa/ Glutathione S-transferase
H_2O_2	Peróxido de hidrógeno
HBA	Aceptadores de bonos de hidrógeno
HBD	Donantes de bonos de hidrógeno
HCG	Gonadotropina coriónica humana
HCT 116	Células de carcinoma de colon humano
HEK293	Células renales embrionarias humanas
Hek-293	Riñón embrionario humano 293 células
HepG2	Células de carcinoma de hígado humano
hESCs	Células madre embrionarias humanas
HIA	Absorción gastrointestinal humana
HL-60	Células de leucemia promielocítica humana
HMDB	Base de datos de Metabolome Humano
HMDB ID	Número de identificación de base de datos de metabolome humano
HSA	Agente único más alto
HSD	Hidroxisteroide deshidrogenasa
IARC	International Agency for Research in Cancer / Agencia Internacional de Investigación sobre el Cáncer
IBM SPSS	Soluciones estadísticas de productos y servicios
IC_{50}	Concentración inhibitoria cincuenta
IECs	Intestinal epithelial cells

JECFA	Comité Mixto de Expertos en Aditivos Alimentarios
KB-3-1	Células de carcinoma de cuello uterino humano
LC-ESI-qTOF-MS	Cromatografía líquida acoplada a espectrometría de masas/ Electrospray ionization-quadrupole time-of-flight mass spectrometry
LH	Hormona luteinizante
LOD	Límite de detección
LOQ	Límite de cuantificación
LPO	Peroxidación lipídica
MDA	Malondialdehído
MLTC-1	Células tumorales de Leydig de ratón
MnSOD	Superóxido de manganeso dismutasa
MR	Refracción molar
mRNA	ARN mensajero /Messenger RNA
MTT	3-(4,5-dimethylthiazol-2-yl)-2,5-diphenyltetrazolium bromide
MW	Peso molecular
n.a	No disponible /Not available
NADH	Dinucleótido de nicotinamida adenina
NADPH	Fosfato de dinucleótido de nicotinamida
NaN3	Azide de sodio
NEM	N-etillmaleimida
n-ROTB	Número de límites podridos
O_2	Oxigeno
$O_2^{\bullet-}$	Radical superóxido
OECD	Organización para la Cooperación y el Desarrollo Económicos
OMS	Organización Mundial de la Salud
OPT	O- fleloldehído
OTA	Ocratoxina A
Pa	Probabilidad de valores de activación
PASS	Predicción de espectros de actividad para sustancias
PBS	Solución salina de tampón de fosfato
PCa	Células de carcinoma de próstata
P-gp	P-glicoproteína
Pi	Probabilidad de valores de inactivación
PI	Yoduro de propidio
PS	Fosfatidilserina
RASFF	Sistema Europeo de Alertas Rápida para Alimentos y Piensos
RAW 264.7	Células de monocitos-macrófagos murinos

RE	Receptores de estrógenos
RNA	Ácido ribonucleico
RNAase	Ribonucleasa
RO5	Regla de cinco
ROS	Especies reactivas de oxígeno/ Reactive oxygen species
RT-PCR	Reacción en cadena de la polimerasa en tiempo real
SARS-COVID-19	Síndrome respiratorio agudo grave- enfermedad por coronavirus -2019
SD	Desviación estándar
SEM	Error estándar de la media
SH-SY5Y	Células de neuroblastoma humano/Human neuroblastoma cells
SIDA	Síndrome de inmunodeficiencia adquirida
SOD	Superóxido dismutasa/ Superoxide dismutase
STE	Sterigmatocystin
SubG0	Estado celular fuera del ciclo celular replicativo
Syn	Sinergismo
TPSA	Superficie polar topológica
Tris	tris(hidroximetil)aminometano
Triton-X 100	T-octilfenoxipolyethoxyethanol
U-937	Células de linfoma monocítico
UDPGT	Uridina difosfato glucuronil transferasas
UE	Unión Europea
ZAN	Zearalanona
ZEA	Zearalenona
α-ZAL	α-zearalanol
α-ZEL	α-zearalenol
β-NADPH	Fosfato de dinucleótido β-nicotinamida
β-ZAL	β-zearalanol
β-ZEL	β-zearalenol
ΔΔCT	Delta delta CT

RESUMEN

Las especies de hongos del género *Fusarium* sintetizan una amplia gama de micotoxinas muy variada química y estructuralmente. La zearalenona (ZEA) constituye uno de los grupos más grandes de micotoxinas producidas por *Fusarium*, que son los principales patógenos de los cereales. En esta Tesis Doctoral se ha realizado, en primer lugar, un estudio *in silico* del perfil metabolómico de la ZEA y sus derivados, α-zearalenol (α-ZEL) y β-zeralenol (β-ZEL), y de la predicción de sus efectos tóxicos. También se ha realizado un estudio de todos los productos de metabolización de las reacciones de fase I y II. En segundo lugar, debido a una característica común de las especies de *Fusarium* asociada a sintetizar ZEA, a la vez que ciertas micotoxinas emergentes como beauvericina (BEA), se ha realizado un estudio citotóxico *in vitro* de α-ZEL, β-ZEL y BEA en células SH-SY5Y sin diferenciar de neuroblastoma humano, se ha determinado el tipo de interacción (sinergismo, adición o antagonismo) de las combinaciones binarias y terciarias de estas micotoxinas y la recuperación de las micotoxina en el medio de cultivo celular con LC-qTOF-MS. En tercer lugar, y con el fin de evaluar cómo pueden actuar estas micotoxinas a nivel celular, se ha estudiado el estrés oxidativo mediante la evaluación de la generación de las especies reactivas de oxígeno y los sistemas de defensa intracelular de actividad antioxidante enzimática y no enzimática. Por último, se ha examinado la expresión de genes implicados en muerte celular por apoptosis (*CASP3, BAX* y *BCL2*) y receptores de estrógenos *(ERβ* and *GPER1)* por RT-PCR*;* y la progresión del ciclo celular y la vía de la muerte celular por citometría de flujo. Todos estos estudios se han realizado en las células

neuronales indiferenciadas de SH-SY5Y, un modelo biológico ampliamente utilizado para el estudio de la función neuronal.

Los resultados del estudio *in silico* demostraron que los productos del perfil metabolómico correspondían a O-glucuronidación, S-sulfatación e hidrólisis; además, los productos metabolitos tenían mejores propiedades para alcanzar la barrera hematoencefálica que las micotoxinas iniciales y el efecto de carcinogenecidad reveló ser el de mayor probabilidad.

Los resultados obtenidos *in vitro* demostraron que β-ZEL individualmente presentaba la mayor potencialidad citotóxica; mientras que el principal tipo de interacción detectado para todas las combinaciones de micotoxinas ensayadas fue sinergismo. La generación de especies reactivas de oxígeno se vio incrementada en combinaciones en las que participó α-ZEL. Además, el sistema de defensa enzimático y no enzimático se vio alterado para las dosis ensayadas, así como para diversas combinaciones. Los resultados obtenidos mediante la actividad de expresión génica revelaron que α-ZEL, β-ZEL y BEA pueden inducir la expresión de genes de apoptosis celular. Por último, en cuanto a la progresión del ciclo celular y la vía de la muerte celular se vio alterado en las células indiferenciadas SH-SY5Y como consecuencia de la exposición a las tres micotoxinas, α-ZEL, β-ZEL y BEA.

SUMMARY

Fusarium species synthesise a wide range of mycotoxins of diverse structure and chemistry. Zearalenone (ZEA) constitute one of the largest groups of mycotoxins produced by *Fusarium*, which are major pathogens of cereal plants. In this Doctoral Thesis, first it has been carried out an *in silico* study of the metabolomics profile of ZEA and its derivates, α-zearalenol (α-ZEL) and β-zeralenol (β-ZEL), and the prediction of their toxic effects. Metabolomic profile has been also defined and toxic effect evaluated for all metabolite products from Phase I and II reaction. Afterward, due to a common feature of *Fusarium* species as synthesising ZEA and its co-occurrence with certain emerging mycotoxins such as BEA, it has been performed an *in vitro* cytotoxic study of α-ZEL, β-ZEL and BEA to determine cell viability in human neuroblastoma SH-SY5Y cells, and additionally determined whether the interaction of binary and tertiary combinations of these mycotoxins is synergistic, additive, or antagonistic. Also, it has been investigated how these mycotoxins can act at the cellular level. Furthermore, it has been analysed the role of oxidative stress by evaluating reactive oxygen species generation and intracellular defence systems of enzymatic and non-enzymatic antioxidant activity. Also, it has been examined the expression of genes involved in cell apoptosis (*CASP3, BAX* y *BCL2*) and receptors of estrogens (*ERβ* and *GPER1)*; and ultimately, cell cycle progression and cell death pathway all on an undifferentiated SH-SY5Y neuronal cell line, which is widely used as a model of neuronal function.

Results of *in silico* study has been demonstrated that the metabolomics profile products were from O-glucuronidation, S-sulfation and hydrolysis, also metabolite products had better properties to reach blood brain barrier than initial

mycotoxins. Also, carcinogenicity reported the highest probability for zearalenone and its derivates to reach blood brain barrier.

Results obtained from in vitro study has been demonstrated that β-zearalenol alone presented the highest cytotoxicological potency; also, the main type of interaction detected between mycotoxins for all combinations assayed was synergism. The generation of reactive oxygen species has been increased in combinations where α-ZEL was involved. In addition, enzymatic and non-enzymatic defense system has been altered. Results obtained by gene expression activity has been revealed that α-ZEL, β-ZEL and BEA can induce the expression of cell apoptosis genes. Moreover, cell cycle progression and cell death pathway have been altered in SH-SY5Y cells as a consequence of being exposed to these three mycotoxins α-ZEL, β-ZEL y BEA.

RESUMEN

Las especies de hongos del género *Fusarium* sintetizan una amplia gama de micotoxinas muy variada química y estructuralmente. La zearalenona (ZEA) constituye uno de los grupos más grandes de micotoxinas producidas por *Fusarium*, que son los principales patógenos de los cereales. En esta Tesis Doctoral se ha realizado, en primer lugar, un estudio *in silico* del perfil metabolómico de la ZEA y sus derivados, α-zearalenol (α-ZEL) y β-zeralenol (β-ZEL), y de la predicción de sus efectos tóxicos. También se ha realizado un estudio de todos los productos de metabolización de las reacciones de fase I y II. En segundo lugar, debido a una característica común de las especies de *Fusarium* asociada a sintetizar ZEA, a la vez que ciertas micotoxinas emergentes como beauvericina (BEA), se ha realizado un estudio citotóxico *in vitro* de α-ZEL, β-ZEL y BEA en células SH-SY5Y sin diferenciar de neuroblastoma humano, se ha determinado el tipo de interacción (sinergismo, adición o antagonismo) de las combinaciones binarias y terciarias de estas micotoxinas y la recuperación de las micotoxina en el medio de cultivo celular con LC-qTOF-MS. En tercer lugar, y con el fin de evaluar cómo pueden actuar estas micotoxinas a nivel celular, se ha estudiado el estrés oxidativo mediante la evaluación de la generación de las especies reactivas de oxígeno y los sistemas de defensa intracelular de actividad antioxidante enzimática y no enzimática. Por último, se ha examinado la expresión de genes implicados en muerte celular por apoptosis (*CASP3, BAX* y *BCL2*) y receptores de estrógenos *(ERβ* and *GPER1)* por RT-PCR*;* y la progresión del ciclo celular y la vía de la muerte celular por citometría de flujo. Todos estos estudios se han realizado en las células

neuronales indiferenciadas de SH-SY5Y, un modelo biológico ampliamente utilizado para el estudio de la función neuronal.

Los resultados del estudio *in silico* demostraron que los productos del perfil metabolómico correspondían a O-glucuronidación, S-sulfatación e hidrólisis; además, los productos metabolitos tenían mejores propiedades para alcanzar la barrera hematoencefálica que las micotoxinas iniciales y el efecto de carcinogenecidad reveló ser el de mayor probabilidad.

Los resultados obtenidos *in vitro* demostraron que β-ZEL individualmente presentaba la mayor potencialidad citotóxica; mientras que el principal tipo de interacción detectado para todas las combinaciones de micotoxinas ensayadas fue sinergismo. La generación de especies reactivas de oxígeno se vio incrementada en combinaciones en las que participó α-ZEL. Además, el sistema de defensa enzimático y no enzimático se vio alterado para las dosis ensayadas, así como para diversas combinaciones. Los resultados obtenidos mediante la actividad de expresión génica revelaron que α-ZEL, β-ZEL y BEA pueden inducir la expresión de genes de apoptosis celular. Por último, en cuanto a la progresión del ciclo celular y la vía de la muerte celular se vio alterado en las células indiferenciadas SH-SY5Y como consecuencia de la exposición a las tres micotoxinas, α-ZEL, β-ZEL y BEA.

SUMMARY

Fusarium species synthesise a wide range of mycotoxins of diverse structure and chemistry. Zearalenone (ZEA) constitute one of the largest groups of mycotoxins produced by *Fusarium*, which are major pathogens of cereal plants. In this Doctoral Thesis, first it has been carried out an *in silico* study of the metabolomics profile of ZEA and its derivates, α-zearalenol (α-ZEL) and β-zeralenol (β-ZEL), and the prediction of their toxic effects. Metabolomic profile has been also defined and toxic effect evaluated for all metabolite products from Phase I and II reaction. Afterward, due to a common feature of *Fusarium* species as synthesising ZEA and its co-occurrence with certain emerging mycotoxins such as BEA, it has been performed an *in vitro* cytotoxic study of α-ZEL, β-ZEL and BEA to determine cell viability in human neuroblastoma SH-SY5Y cells, and additionally determined whether the interaction of binary and tertiary combinations of these mycotoxins is synergistic, additive, or antagonistic. Also, it has been investigated how these mycotoxins can act at the cellular level. Furthermore, it has been analysed the role of oxidative stress by evaluating reactive oxygen species generation and intracellular defence systems of enzymatic and non-enzymatic antioxidant activity. Also, it has been examined the expression of genes involved in cell apoptosis (*CASP3, BAX* y *BCL2*) and receptors of estrogens (*ERβ* and *GPER1)*; and ultimately, cell cycle progression and cell death pathway all on an undifferentiated SH-SY5Y neuronal cell line, which is widely used as a model of neuronal function.

Results of *in silico* study has been demonstrated that the metabolomics profile products were from O-glucuronidation, S-sulfation and hydrolysis, also metabolite products had better properties to reach blood brain barrier than initial

mycotoxins. Also, carcinogenicity reported the highest probability for zearalenone and its derivates to reach blood brain barrier.

Results obtained from in vitro study has been demonstrated that β-zearalenol alone presented the highest cytotoxicological potency; also, the main type of interaction detected between mycotoxins for all combinations assayed was synergism. The generation of reactive oxygen species has been increased in combinations where α-ZEL was involved. In addition, enzymatic and non-enzymatic defense system has been altered. Results obtained by gene expression activity has been revealed that α-ZEL, β-ZEL and BEA can induce the expression of cell apoptosis genes. Moreover, cell cycle progression and cell death pathway have been altered in SH-SY5Y cells as a consequence of being exposed to these three mycotoxins α-ZEL, β-ZEL y BEA.

1. INTRODUCCIÓN

2. INTRODUCCIÓN

1.1. Micotoxinas

Las micotoxinas son un grupo estructuralmente diverso de compuestos en su mayoría de bajo peso molecular, producidos por el metabolismo secundario de hongos y que pueden ser perjudiciales tras la ingesta, inhalación o contacto con la piel. Las enfermedades que causan, conocidas como micotoxicosis, no necesitan involucrar al hongo productor de toxinas. Por tanto, son peligros abióticos, pero de origen biótico. Debido a su complejidad estructural, las micotoxinas varían desde compuestos simples de cuatro carbonos, como la moniliformina, hasta sustancias complejas como Phomopsis y las micotoxinas tremorgénicas, que pueden provocar efectos adversos (carcinógenos, genotóxicos, hepatotóxicos, teratogénicos, estrogénicos, inmunosupresores, nefrotóxicos o neurotóxicos) en otros organismos, principalmente en seres humanos y/o animales, tras el consumo de alimentos/piensos contaminados. Las micotoxinas pueden aparecer en la cadena alimentaria debido a la infección fúngica de los cultivos, ya sea por ser consumidos directamente por el ser humano o utilizados como alimento para el ganado. Por la diversidad de su origen, difieren en su estructura, lo que lleva a marcadas diferencias en sus propiedades físico-químicas y biológicas. En consecuencia, sus efectos tóxicos varían mucho con el compuesto, pero también con la especie animal (Pieter y col., 1995).

El metabolismo de las micotoxinas ingeridas puede producir la acumulación de micotoxinas en diferentes órganos o tejidos y crear algunos efectos tóxicos con síntomas característicos observados en humanos y animales. El impacto de las micotoxinas en la salud depende de la cantidad de micotoxina

consumida, la toxicidad del compuesto, el peso corporal del individuo, la presencia de otras micotoxinas (efectos sinérgicos) y otros efectos dietéticos.

La Organización de las Naciones Unidas para la Agricultura y la Alimentación (FAO) estimó que aproximadamente el 25% de los cereales producidos en el mundo están contaminados por micotoxinas (JECFA, 2001). Si bien, se estima que este porcentaje ha aumentado. El trigo, el arroz y el maíz son los cereales más consumidos en todo el mundo; los últimos datos notificados por la FAO estimaron un consumo medio mundial anual de 66, 53.3 y 17.1 kg/per cápita de trigo, arroz y maíz, respectivamente. Además, la población española es uno de los mayores consumidores de trigo del mundo, con un consumo medio de 86.10 kg/per cápita (FAO, 2009). Otros alimentos, como nueces, especias, frutas y sus subproductos también pueden estar contaminados por estos metabolitos fúngicos. La producción de micotoxinas en cultivos agrícolas puede ocurrir en varios puntos de la cadena alimentaria: antes de la cosecha y durante la cosecha como en el proceso de secado y almacenamiento. Las malas prácticas agrícolas y de cosecha, el secado, la manipulación, el envasado, el almacenamiento y las condiciones de transporte inadecuados promueven el crecimiento de hongos, lo que aumenta el riesgo de producción de micotoxinas.

Los niveles de micotoxinas en los alimentos generalmente no producen un efecto adverso agudo en los consumidores, pero la exposición crónica puede representar un riesgo significativo para los consumidores que consumen estos productos con frecuencia; por ello, algunos países han adoptado regulaciones para limitar la exposición a micotoxinas. Su presencia no solo está relacionada con el efecto que puedan tener en la salud del consumidor, sino que también

puede tener un impacto en el comercio mundial. Según el informe anual Europeo del Sistema de Alerta Rápida para Alimentos y Piensos (RASFF) de 2019, las micotoxinas son el tipo de peligro y categoría de producto más registrados en productos alimenticios originarios de países no miembros. Además, se encuentran entre los principales peligros en las notificaciones de rechazo fronterizo en la Unión Europea (UE). En España, las micotoxinas son el segundo mayor peligro en alimentos, con 47 notificaciones anuales, y se encuentra entre los países con mayor número de notificaciones de la categoría de peligro de micotoxinas.

Los géneros fúngicos que principalmente producen micotoxinas son *Aspergillus, Penicillium, Alternaria, Fusarium* y *Claviceps*; mientras que los grupos de micotoxinas más relevantes que se encuentran en los alimentos son: las aflatoxinas, producidas por especies de Aspergillus; la ocratoxina A producida tanto por *Aspergillus* como por *Penicillium*; los tricotecenos (tipo A: toxina HT-2 y T-2, y tipo B: desoxinivalenol), zearalenona, fumonisinas B1 y B2, y las micotoxinas emergentes (fusaproliferina, moniliformina, beauvericina y enniatinas) producidas principalmente por especies de *Fusarium*; alcaloides del cornezuelo de centeno producidos por *Claviceps*; y altenuene, alternariol, alternariol metil éter, altertoxina y ácido tenuazónico producidos por especies de *Alternaria*.

1.2. Micotoxinas de *Fusarium*

Las micotoxinas de las especies de *Fusarium* se han asociado tradicionalmente con los cereales de zonas templadas, ya que estos hongos requieren temperaturas algo más bajas para el crecimiento y la producción de micotoxinas que las especies aflatoxigénicas de *Aspergillus*. Sin embargo, existen

numerosos estudios a escala mundial que indican la contaminación de los granos de cereales con varias micotoxinas de *Fusarium*. Las toxinas de *Fusarium*, como los tricotecenos y la zearalenona (ZEA), constituyen uno de los grupos más grandes, siendo los principales patógenos de las plantas de cereales en climas más moderados, causando tizón de la cabeza en el trigo y la cebada y pudrimiento de la mazorca en el maíz. Si bien estos contaminantes pueden ser de menor toxicidad que otras micotoxinas como las aflatoxinas, la ocratoxina A, etc., su presencia en productos alimenticios, consumidos muy ampliamente, implica que deben controlarse sus niveles de forma estricta tanto en alimentos como en piensos.

Las micotoxinas de *Fusarium* son de una diversidad estructural y química, y las más detectadas en los alimentos son las fumonisinas, tricotecenos, ZEA y entre las emergentes está la beauvericina (BEA), las enniatinas, la fusaproliferina y la moniliformin. Estas micotoxinas pueden encontrarse solas o simultáneamente con otras micotoxinas, una coexistencia habitual en los cereales, en particular las micotoxinas producidas por el mismo hongo. Hay que señalar que varias especies de *Fusarium* tienen la capacidad para sintetizar ZEA, por lo que puede detectarse junto a otras micotoxinas en un mismo alimento.

1.3. Zearalenona y sus metabolitos

ZEA (anteriormente conocida como toxina F-2) es una micotoxina estrogénica no esteroidal biosintetizada a través de la vía de los policétidos por una variedad de hongos *Fusarium*, incluyendo *F. Graminearum (Gibberella zeae), F. culmorum, F. cere-alis, F. equiseti, F. crookwellense* y *F. semitectum*, que son hongos comunes del suelo, en países templados y cálidos, y son contaminantes regulares de los cultivos de cereales en todo el mundo (Figura 1).

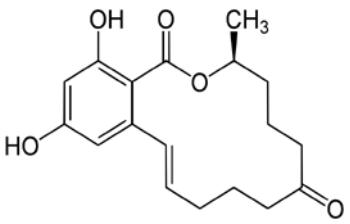

Figura 1. Estructura química de la zearalenona (ZEA)

ZEA es una micotoxina termoestable hasta 150°C y la degradación se ha observado solo a temperaturas más altas o en condiciones alcalinas. Es una lactona de ácido resorcíclico, químicamente descrita como lactona de ácido 6-[10-hidroxi-6-oxo-trans-1-undecenil] -B-resorcíclico. En los mamíferos, el grupo ceto en el carbono 8 se reduce a dos metabolitos esterioisoméricos de ZEA (isómeros α y β). Estos metabolitos de hongos productores de ZEA contaminan el maíz y también colonizan, en menor medida, cebada, avena, trigo, sorgo, mijo y arroz. Además, se ha detectado en productos de cereales como harina, malta, soja y cerveza. Los géneros de *Fusarium* infectan los cereales en el campo y la producción de toxinas tiene lugar principalmente antes de la cosecha, pero también puede ocurrir que se produzca después de la cosecha, si el cultivo no se manipula y seca adecuadamente (CCFAC, 2000). Aunque los cereales infectados con *Fusarium* que se encuentran en el campo pueden acumular ZEA antes de la cosecha, numerosos experimentos tienden a indicar que los altos niveles de ZEA que se registran, ocurren naturalmente en algunas muestras de alimentos para animales a base de maíz como resultado de un almacenamiento inadecuado en lugar de desarrollarse en el campo (Zinedine et al, 2007).

Por otro lado, la contaminación mundial de cereales y animales con micotoxinas de *Fusarium*, en particular ZEA, es muy elevada y la comercialización de estos productos puede contribuir a la dispersión mundial de esta micotoxina. Las concentraciones en alimentos y piensos varían en un amplio rango, dependiendo de las condiciones climáticas. Se ha detectado ZEA entre el 11-80% de las muestras de trigo y entre 7-68% de muestras de cebada para uso alimentario en el suroeste de Alemania en 1987 y 1989-93; con un contenido medio anual de 3-180 μg / kg en trigo (valor más alto, 8000 μg/kg) y 3-36 μg/kg en cebada (valor más alto, 310 μg/kg) (Müller et al., 1997a, b). En otro estudio, se analizó trigo para consumo humano de todas las regiones de Bulgaria (140 muestras) después de la cosecha de 1995, un año caracterizado por fuertes lluvias en primavera y verano y que influye en la presencia de hongos y producción de micotoxinas. La frecuencia de contaminación con ZEA en esas muestras fue del 69%, con una concentración promedio en muestras positivas de 17 μg/kg y un máximo de 120 μg/kg (Vrabcheva et al., 1996). También se detectó ZEA en el 30% de las 2271 muestras de maíz recolectadas en las provincias de Buenos Aires y Santa Fe de Argentina en 1983-94, a una concentración promedio de 165 μg / kg (variación anual, 46-300 μg/kg) y un máximo de 2000 μg/kg (Resnik et al., 1996). Se encontró ZEA en 40 de 201 muestras de granos, con concentraciones promedio de 24 μg/kg en trigo y 51 μg/kg en centeno en cultivos producidos alternativamente y 6 μg/kg en trigo y 4 μg/kg en centeno en muestras producidas convencionalmente. La concentración más alta de ZEA fue de 199 μg/kg, encontrada en el centeno cultivado alternativamente (Marx et al., 1995).

Las principales fuentes de ZEA son el trigo, el centeno y la avena en los países europeos, y el maíz, los productos de maíz y los productos de trigo en Canadá y Estados Unidos. Una incidencia que preocupa y que hace necesarios

controles rutinarios. El Reglamento (CE) no 1881/2006 de la Comisión, de 19 de diciembre de 2006, establece límites máximos para ZEA, en los cereales destinados al consumo humano directo, la harina de cereales, el salvado y el germen como producto final comercializados para el consumo humano directo, es de 75 µg / kg (Tabla 1). Además, las principales fuentes de ZEA son el trigo, el centeno y la avena en los países europeos, y el maíz, los productos de maíz y los productos de trigo en Canadá y Estados Unidos.

Tabla 1. Niveles máximos de contaminantes de micotoxinas de zearalenona en productos alimenticios (CE, No 1881/2006).

	Productos alimenticios	**Niveles máximos (µg/kg)**
1	Cereales sin transformar distintos del maíz	100
2	Maíz sin procesar	200
3	Cereales destinados al consumo humano directo, harina de cereales, salvado como producto final comercializado para consumo humano directo y germen, con excepción de los productos alimenticios enumerados en 4, 7 y 8	75
4	Maíz destinado al consumo humano directo, harina de maíz, harina de maíz, sémola de maíz, germen de maíz y aceite de maíz refinado	200
5	Pan (incluidos los pequeños productos de panadería), bollería, galletas, aperitivos de cereales y cereales para el desayuno, excepto los aperitivos de maíz y los cereales para el desayuno a base de maíz	50
6	Aperitivos de maíz y cereales para el desayuno a base de maíz	50
7	Alimentos elaborados a base de cereales (excluidos los alimentos elaborados a base de maíz) y alimentos infantiles para lactantes y niños pequeños	20
8	Alimentos elaborados a base de maíz para lactantes y niños pequeños	20

Según la Agencia Europea de Seguridad Alimentaria, EFSA en sus siglas en inglés (2011), entre los cereales para consumo humano, la frecuencia de aparición de ZEA en el maíz (33%) y el nivel de contenido medio (15 µg / kg)

son significativamente mayores. Esta tendencia se mantuvo en los productos de la molinería, aunque se determinaron niveles muy elevados en el salvado de trigo (33 µg/kg). Así, tanto la prevalencia como el nivel de ZEA en los productos de cereales para consumo humano analizados fue bajo excepto en los aceites vegetales (principalmente aceite de germen de maíz) con 86% de muestras positivas y un nivel medio de 72 µg/kg (Tabla 2).

Tabla 2. Zearalenona (µg/kg) en muestras de alimentos en la Unión Europea (EFSA, 2011).

Categoría de alimentos	*Nº* muestras	*Nº* muestras> LOD/LOQ	Media (µg/kg)	Mediana (µg/kg)	Máximo (µg/kg)
Granos para consumo humano	2190	372 (17%)	5.7	3,0	140
Productos de molienda de trigo	3088	432 (14%)	13	5,0	507
Productos de molienda de centeno	482	31 (6,4%)	4.1	3,0	50
Productos de molienda de maíz	838	369 (44%)	14	5,0	509
Pan y bollos	1247	94 (7,5%)	5.2	4.0	70
Pasta	330	13 (3,9%)	5.8	3,0	50
Cereales de desayuno	1377	120 (8,7%)	5.7	3,0	172
Productos de panadería fina	813	195 (24%)	7.7	5,0	98
Galletas	541	179 (33%)	9.0	5,0	98
Cerveza	35	2 (5,7%)	1.0	0,5	10
Maíz dulce	94	10 (11%)	4.8	4.0	50
Aceites vegetales	221	190 (86%)	72	49	823
Alimentos para bebés y niños pequeños	420	17 (4%)	7.0	6,7	20

[a]A las muestras <LOD se les dio el valor LOD. LOQ: 0.02 a 20 µg/kg

Se ha demostrado que la biotransformación de ZEA ocurre en hongos, plantas y mamíferos, e involucra tanto al macrociclo alifático como al anillo

aromático. Debido a la rápida biotransformación y excreción de ZEA en animales, la ingesta dietética a través de carne y productos derivados es, en principio, de poca importancia (Creppy, 2002). ZEA puede excretarse en la leche de las vacas lactantes tras la administración a dosis altas. Según Prelusky et al. (1990), las concentraciones máximas (6.1 μg/L ZEA, 4 μg/L α-zearalenol y 6.6 μg/L β-zearalenol) se encontraron en la leche de una vaca que recibió una dosis oral de 6000 mg ZEA (equivalente a 12 mg/kg de peso corporal), pero a dosis bajas, sin encontrarse ni ZEA ni sus metabolitos en la leche (<0.5 μg/L) de vacas lactantes alimentadas con 50 o 165 mg de ZEA (equivalente a 0.1 y 0.33 mg/kg de peso corporal) durante 21 días. Tampoco se ha detectado ZEA en huevos de producción comercial. Teniendo en cuenta los niveles medios de ZEA en los principales alimentos y su consumo, la ingesta diaria promedio de ZEA oscila en adultos de 0.8 a 29 ng/kg de peso corporal, mientras que los niños pequeños tienen las ingestas diarias media más altas, de 6 a 55 ng/kg de peso corporal/día (Minervini et al., 2005). Por lo tanto, se ha estimado que las ingestas dietéticas medias de ZEA en Canadá, Dinamarca y Noruega son 20 ng/kg pc/día, y en los EEUU son 30 ng/kg pc/día (Zinedine et al, 2007).

El Comité Mixto FAO/OMS establece una ingesta diaria máxima tolerable provisional (IDTMP) para ZEA de 0.5 μg/kg de peso corporal, basada en el NOEL de 40 μg/kg de pc/día obtenido en un estudio de 15 días en cerdos. El comité recomendó que la ingesta total de ZEA y sus metabolitos (incluido el α-zearalenol) no debería exceder este valor (CCFAC, 2000). Los niveles máximos tolerados de ZEA para el consumo humano se han establecido en 20 μg/kg en alimentos destinados a bebés y lactantes, 50 μg/kg en tortitas y cereales para el desayuno a base de maíz y 200 μg/kg en maíz sin procesar y ciertos productos de maíz (EFSA, 2011).

Los derivados de ZEA (α-zearalenol (α-ZEL), β-zearalenol (β-ZEL), α-zearalanol (α-ZAL), β-zearalanol (β-ZAL), zearalanona (ZAN)) se pueden detectar en mazorcas de maíz infectados con *Fusarium* en el campo (Bottalico et al., 1985) y en el cultivo de arroz (Richardson et al., 1985) (Figura 2). Además, se informa la presencia de α-ZEL y β-ZEL en subproductos de maíz, ensilaje de maíz y harina de soja a niveles bajos (Schollenberger et al. 2006). Se han identificado cuatro metabolitos fúngicos relacionados con ZEA en cultivos de *F. graminearum*, que son 13-formil-ZEA, 5,6-dehidro-ZEA y los dos estereoisómeros de 5-hidroxi-ZEA.

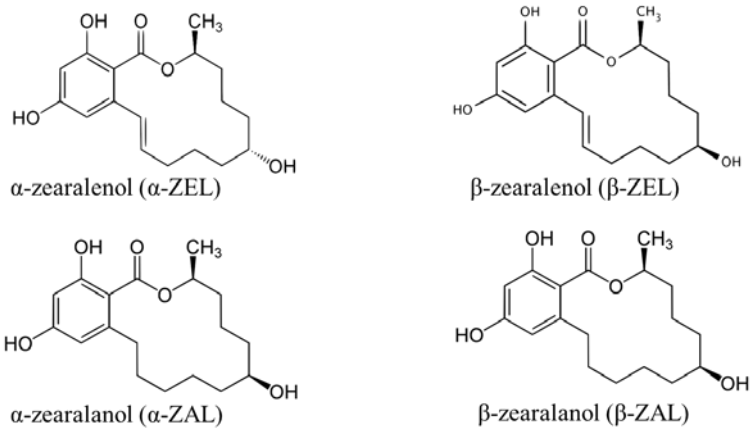

Figura 2. Estructura química de los derivados de la zearalenona

El metabolismo de ZEA se puede dividir en dos fases: metabolismo de fase I y metabolismo de fase II. Se ha sugerido que las 3α- y 3β-hidroxiesteroide deshidrogenasas (HSD) catalizan los metabolitos de fase I de ZEA en mamíferos, que eran los estereoisómeros de ZEL (α-ZEL y β-ZEL) y se ha demostrado que ocurren en el hígado de rumiantes (Mirocha et al., 1981), cerdos (James y Smith, 1982), pavos (Olsen et al., 1986) y gallinas (Dänicke et al., 2002),

eritrocitos de rata (Chang y Lin, 1984) y la mucosa intestinal de cerdos (Biehl et al., 1993). Son también capaces de convertir ZEA a α-ZAL y β-ZAL. De acuerdo con la fácil reducción del grupo 7-ceto, α- y β-ZEL se detectaron como metabolitos ZEA en la fracción de glucurónidos del plasma sanguíneo, orina o bilis de numerosas especies *in vivo*, incluidas ratas, cerdos, vacas, cabras y gallinas, (Dong et al., 2010; Zinedine et al., 2007).

Por otro lado, la conjugación de ZEA y sus metabolitos reductores α-ZEL y β-ZEL con ácido glucurónico catalizado por uridina difosfato glucuronil transferasas (UDPGT), representan la vía metabólica II, en animales domésticos y también en humanos (Biehl et al., 1993; Dänicke et al., 2005; Dong et al., 2010; Mirocha et al., 1981; Olsen et al., 1985; Zöllner et al., 2002). Los metabolitos glucurónidos son ZEA-glucurónido (ZEA-Glu), α-zearalenol-glucurónido (α-ZEL-Glu), β-zearalenol-glucurónido (β-ZEL-Glu), Zearalanona-glucurónido (ZAN-Glu),

De acuerdo con el estudio realizado por Ueno et al. (1983), α-ZEL fue el metabolito principal en hepatocitos cultivados de rata, ratón, cerdo, vaca y conejo a pH 4.5 con NADH o NADPH y a pH 7.4 con NADH, aunque a pH 7.4 con NADPH, β-ZEL fue el metabolito predominante. En cobayas, tanto α- como β-ZEL se produjeron en cantidades similares independientemente del pH y cofactor, mientras que en hámster β-ZEL fue el principal metabolito, lo que indica que hay dos tipos de ZEA reductasa que difieren en el pH óptimo. Además, se indica en otros estudios que ZEA se metaboliza a α-ZEL y β-ZEL por la mucosa intestinal de cerdas *in vitro* con predominio del isómero β-ZEL (Olsen et al., 1987). Malekinejad y col. (2006), mostró que los cerdos convierten ZEA predominantemente en α-ZEL, mientras que en los bovinos β-ZEL es el

metabolito hepático dominante. Aunque se encontraron diferencias significativas en el perfil metabólico de ZEA entre especies animales, se dispone de datos muy limitados para humanos.

Las concentraciones de ZEA, α-ZEL y β-ZEL en la orina de un voluntario masculino 6, 12 y 24 h después de una dosis oral única de 100 mg de ZEA fueron de 3.7 y 3 μg/ml y no se detectaron después de 6 h; 6.9, 6 y 2.7 μg/ml después de 12 h; y 2,7, 4 y 2 μg/ml después de 24 h (Mirocha et al., 1981). En rumiantes, ZEA y sus metabolitos se detectan en la bilis a tasas respectivas de 68% de β-ZEL, 24% de α-ZEL y 8% de ZEA (Danicke et al., 2002); también aumentaron en el hígado y la bilis a la dosis administrada (Döll et al., 2003). Sin embargo, ni ZEA ni sus metabolitos se detectan en músculos, riñones, hígado, vejiga, grasa dorsal de bovinos macho que ingieron 0.1 mg de ZEA/día/kg de alimento (Danicke et al., 2002).

1.3.1. Toxicidad *in vitro* de zearalenona y sus metabolitos

La toxicidad de ZEA y sus metabolitos es causada no solo por efectos estrogénicos, sino también por otros mecanismos como la citotoxicidad. Se ha evidenciado que el metabolito α-ZEL muestra una toxicidad mayor que β-ZEL, pero ambos son menos citotóxicos que ZEA (Abid-Essefi et al., 2004). Minervini et al. (2001, 2006) y Alm et al. (2002) que investigaron la maduración de ovocitos porcinos, equinos y bovinos *in vitro* por metabolitos ZEA obtuvieron resultados similares. En ambos estudios, α-ZEL demostró un efecto negativo sobre la progresión meiótica de los ovocitos, mientras que β-ZEL no mostró ningún efecto o mostró un efecto positivo débil solo a concentraciones altas. Por el contrario, Abid-Essefi et al., (2009) encontraron que β-ZEL era más citotóxico que α-ZEL, mientras que ambos eran menos citotóxicos que ZEA.

Además, en otro estudio de Benzoni et al., (2008) demostraron que tanto α-ZEL como β-ZEL reducen la viabilidad de los espermatozoides de una manera dependiente de la dosis y el tiempo, específicamente se encontró que β-ZEL era más citotóxico que α-ZEL, sin embargo, se encontró que la ZEA era la más citotóxica en comparación con sus dos derivados. Por otro lado, Wollenhaupt et al., (2004) detectaron un efecto antiproliferativo de la micotoxina β-ZEL en células endometriales porcinas; el resultado se reflejó en una reducción significativa de las células en la fase S, acompañada de una detención de las células en la fase G0/G1. Además, α-ZEL mostró un marcado efecto inhibidor sobre la proliferación celular, incluso a dosis muy bajas, esencialmente mediado por apoptosis en células Jurkat-T (Luongo et al., 2006). Además, ZEA, α-ZEL y β-ZEL también inducen citotoxicidad en líneas de células inmunes.

1.3.2. Inducción de estrés oxidativo de zearalenona y sus metabolitos

La citotoxicidad de ZEA y sus metabolitos puede producirse por varios mecanismos como el estrés oxidativo, la peroxidación lipídica y el daño del ADN en células *in vitro*. Se ha evidenciado que la ZEA puede inducir estrés oxidativo durante la formación de sus metabolitos al generar especies reactivas de oxígeno (ROS), lo que produce un daño en el ADN (Minervini y Dell'Aquila, 2008; So et al., 2014; Tatay et al., 2017b). Diversos autores han evidenciado que ZEA induce daño oxidativo y apoptosis e inhibe la síntesis de ADN y proteínas en células de hepatocito humano HepG2 (Ayed-Boussema et al., 2008; Hassen et al., 2007). Gazzah y col. (2010) y El Golli Bennour et al. (2009) también demostraron una mayor producción de ROS a través de modificaciones indirectas del estado oxidativo después de la exposición a ZEA en células HepG2 y Ayed-Boussema

et al. (2008) observaron un aumento en la producción de ROS dependiente del tiempo, así como, Venkataramana et al. (2014) en células de neuroblastoma humano (SH-SY5Y) expuestas a ZEA. En las células CHO-K1 se detectó inducción de ROS cuando las células se expusieron a ZEA (Ferrer et al., 2009). Efectos similares se observaron en células tumorales de Leydig de ratón (MLTC-1) y células epiteliales bronquiales (BEAS-2B) por Li et al., (2014) y So et al., (2014). Gao et al., (2013) expusieron células renales embrionarias humanas (HEK293) a ZEA y registraron un aumento en la producción de ROS; se observaron alteraciones lisosomales que resultan en daño mitocondrial como resultado de la exposición a ZEA. Abid-Essefi et al., (2004) ha demostrado que estos metabolitos son capaces de aumentar la peroxidación lipídica de manera dependiente de la concentración según se infiere por la cantidad de malondialdehído (MDA) generada, lo que indica un aumento de la producción de radicales libres, en células Vero tratadas con ZEA. Banjerdpongchai et al., (2010) también evidenciaron la capacidad de ZEA para generar ROS en células HL-60.

Son pocos los estudios publicados sobre los metabolitos de ZEA y los mecanismos implicados en la generación intracelular de ROS. Pero se ha observado que estas micotoxinas causan efectos citotóxicos y estrés oxidativo en varias líneas celulares como CHO-K1 (Tatay et al., 2014; Ferrer et al., 2009), células HepG2 (Tatay et al, 2017b), y en células de adenocarcinoma Caco-2 colorrectal (Abid-Essefi et al., 2009; Pfeiffer et al., 2011; Kouadio et al., 2005). Además, Lu et al. (2013) observaron un aumento de ROS en células de macrófagos RAW264.7, tratadas con α-ZEL y β-ZEL. Othmen et al. (2008) determinaron el efecto de α-ZEL y β-ZEL sobre el estrés oxidativo midiendo niveles de MDA en células Vero y encontraron que estas micotoxinas inducen

peroxidación lipídica (LPO) de una manera dependiente de la concentración en las células. Las micotoxinas reducen la viabilidad celular correlacionada con los aumentos de la generación de ROS y la formación de MDA de manera dependiente de la concentración y el tiempo. Ben Salem et al., (2016) demostraron que α-ZEL y β-ZEL aumentaron el nivel de superóxido de aniones mitocondriales en las células HEK293. Además, ZEA podría alterar la maquinaria antioxidante celular y afectar los niveles y actividades de las enzimas de detoxificación, incluidas glutatión reducido (GSH), superóxido dismutasa (SOD), MDA, glutatión peroxidasas (GPx) y catalasa (CAT) en diferentes tipos de células (Tatay et al., 2017b; Zheng et al., 2018b).

1.3.3. Interrupción del ciclo celular de la zearalenona y sus metabolitos

Varios estudios han sugerido que ZEA y sus derivados reducen el número de células al inducir la apoptosis celular, también se ha sugerido que la sobreproducción de ROS está involucrada en el proceso de detención del ciclo celular inducido por ZEA en la fase G2/M y también en apoptosis celular (Zheng et al., 2018b). Por lo tanto, el estrés oxidativo puede explicar por qué ZEA causa daño al ADN e induce la detención del ciclo celular en diferentes tipos de células. La exposición a ZEA y α-ZEL provocó un aumento simultáneo de las poblaciones sub-G0 y S + G2/M en células de granulosa cultivadas de ovarios equinos (Minervini et al., 2006). Además, se observó que ZEA redujo el número de células al retrasar la regeneración de las células de Leydig (Zhou et al., 2018). ZEA podría inducir apoptosis y necrosis en células de Sertoli de rata a través de las vías apoptóticas extrínsecas e intrínsecas (Xu et al., 2016). Después de la exposición a ZEA (30 y 50 μM) durante 12 h, se detectaron células

apoptóticas tempranas; mientras que después de la exposición a ZEA durante 24 h, se observaron principalmente células apoptóticas tardías (Chen et al., 2015a).

1.3.4. Actividad estrogénica de la zearalenona y sus metabolitos

Según la reunión de la OCDE (Organización para la Cooperación y el Desarrollo Económicos) sobre la Evaluación y Pruebas de Disruptores Endocrinos en abril de 2011, un posible disruptor endocrino es "una sustancia química que puede alterar el funcionamiento del sistema endocrino"; pero las consecuencias de los efectos adversos de esa alteración de la información en un organismo intacto son inciertas (OCDE, 2011).

Ciertos compuestos químicos pueden imitar o antagonizar la acción de los estrógenos naturales como el 17β-estradiol (E2). Estos compuestos tienen poca similitud estructural obvia con los estrógenos naturales, pero pueden unirse a los receptores de estrógenos (RE en castellano o ER de sus siglas en inglés), influir en la expresión de genes regulados por estrógenos, regular el crecimiento de células dependientes de estrógenos y producir respuestas fisiológicas de estrógenos *in vivo* (Darbre et al., 2002; EFSA, 2013). Dado que estas sustancias pueden interferir con el funcionamiento normal de los procesos endocrinos, pueden causar varios trastornos de salud relacionados con las hormonas en humanos y animales, incluida la pubertad temprana en las mujeres, la reducción del recuento de espermatozoides, la alteración de las funciones de los órganos reproductivos, la obesidad, comportamientos sexuales alterados y una mayor incidencia de algunos cánceres de mama, ovario, testículo y próstata (Bittner et al., 2014). Los tejidos que responden al estrógeno, como el útero, la glándula mamaria, los huesos, el hígado, el cerebro y otros, contienen dos tipos de *ER*,

ERa y *ERβ*, cuya expresión es específica de tejido; sin embargo, además de los efectos sobre los tejidos reproductivos, las células del sistema inmunológico también tienen RE; por ejemplo, *ERa* se expresa en células T, células NK y macrófagos, mientras que *ERβ* se expresa más prominentemente en células B y monocitos.

Se ha indicado que la actividad estrogénica de ZEA y sus metabolitos está mediada por su afinidad de unión a RE e imitando la actividad de los estrógenos naturales; siendo tan potentes como el cumestrol y la genisteína, dos fitoestrógenos que alteran el sistema endocrino. Sin embargo, a diferencia de los fitoestrógenos, que se unen preferentemente a *ERβ*, la afinidad de ZEA y sus metabolitos reductores por *ERβ* es aproximadamente igual a su afinidad por los receptores *ERa* (Le Guevel y Pakdel, 2001; Bang et al., 2004; Grassi et al., 2013; Xiao et al., 2013). Según Tashiro et al., (1980) la afinidad de unión relativa de ZEA y sus derivados al receptor citoplásmico uterino de rata fueron según el siguiente orden α-ZAL> α-ZEL> β-ZAL> ZEA> β-ZEL. Además, en otro estudio sobre células de cáncer de mama humano, las actividades estrogénicas se clasificaron como α-ZEL = α-ZAL> ZAN> ZEA = β-ZAL> β-ZEL (Parveen et al., 2009). Minervini et al., (2005) han indicado que ZEA y sus derivados mostraron propiedades estrogénicas similares, con la excepción de α-ZEL que indujo una actividad estrogénica más alta que ZEA y β-ZEL, el mismo resultado se observó años después en Tatay et al., (2017a). Los estereoisómeros de ZEL difieren considerablemente en su estrogenicidad, siendo α-ZEL aproximadamente 10 veces más potente que ZEA y β-ZEL 50 veces menos (Olsen y Kiessling, 1983). Las diferencias de especies en la unión del receptor también pueden contribuir a la alta sensibilidad en algunos animales como los cerdos: cuando se comparó la afinidad de unión relativa de α-ZEL a los RE de

cerdo, rata y pollo, el RE porcino mostró la mayor afinidad y el RE de pollo la menor (Fitzpatrick et al., 1989).

Varios estudios también han demostrado que ZEA no solo puede interrumpir la pubertad y el ciclo estral, sino que también podría afectar los eventos tempranos del embarazo, incluida la fertilidad, el desarrollo del embrión y la implantación del embrión (Zhao et al., 2014). También se ha demostrado que ZEA disminuye la fertilidad debido a trastornos del tracto reproductivo y desarrollo fetal anormal, reduce el tamaño y peso de las glándulas suprarrenales y pituitarias en animales y altera el ciclo de ovulación (Parveen et al., 2009; Cortinovis et al., 2013; EFSA, 2016). Además, también se indicó que la exposición a ZEA puede adelantar el momento de la pubertad humana. ZEA y sus metabolitos se han visto implicados en una serie de incidentes relacionados con la pubertad precoz entre las niñas de varios países (Mukherjee et al., 2014). Se sospecha que ZEA es un factor desencadenante del desarrollo de la pubertad precoz en niñas (Massart et al., 2008). ZEA también redujo el peso testicular, ovárico y uterino en ratas de 2 días (Kuiper-Goodmann et al., 1987), mientras que en ratones recién nacidos presentaron cornificación vaginal, celo persistente, fertilidad reducida, anovulación y disminución de la producción de hormonas gonadotrópicas por la hipófisis; además, en las hembras porcinas se observó una disminución de las camadas vivas y un aumento de la pseudo-preñez (Young y King, 1984). ZEA y α-ZEL también podrían inhibir la síntesis de la producción de andrógenos inducida por gonadotropina coriónica humana (HCG) en cultivos primarios de células de Leydig y líneas celulares de Leydig *in vitro* (Gao et al., 2018; Li et al., 2014). Además, muchos estudios han indicado que ZEA y sus derivados podrían perturbar la producción de estradiol (Belli et al., 2010; Wang et al., 2010); perturbar la producción de progesterona (Chen et al., 2015b;

Savard et al., 2016) y disminuir la síntesis y secreción de la hormona folículo estimulante (FSH) en cerdas a través del receptor acoplado a proteína G del receptor de membrana de estrógeno no clásico 30 (*GPR30*) *in vitro* (He et al., 2018).

La función principal de las células de la granulosa es producir esteroides sexuales. Durante la fase folicular del ciclo menstrual, la FSH estimula las células de la granulosa de la pituitaria anterior para convertir los andrógenos en estradiol vía aromatasa. Además, después de la ovulación, las células de la granulosa se convierten en células de luteína de la granulosa, que pueden producir progesterona (Garzo y Dorrington, 1984). Por tanto, la función y la viabilidad de las células de la granulosa son de vital importancia para la síntesis y secreción de los esteroides sexuales, incluidos el estradiol y la progesterona. Varios estudios han indicado que ZEA puede alterar la función, inhibir la viabilidad y causar la muerte celular en las células de la granulosa. Los estudios *in vitro* demostraron que ZEA podría alterar la función y la estabilidad genómica de las células de la granulosa porcina y disminuir la tasa de apoptosis (Zhang et al., 2017; Liu et al., 2018), también inducir apoptosis y necrosis en las mismas células a través de la vía de señalización mitocondrial dependiente de caspasa 3 y caspasa 9 (Zhu et al., 2012). Además, ZEA y sus metabolitos alteraron la proliferación celular, la producción de esteroides y la expresión génica en células de la granulosa de folículos pequeños bovinos *in vitro* (Pizzo et al., 2016), y también disminuyeron la síntesis y secreción de FSH y LH a través de receptores estrógenos no clásicos de membrana *GPR30* en glándulas pituitarias porcinas y bovinas (He et al., 2018a; Nakamura y Kadokawa, 2015).

1.4. Beauvericina

BEA es un hexadepsipéptido cíclico que consta de una secuencia alterna de tres grupos d-α-hidroxi-isovalerilo y tres N-metil-1-fenilalanilo (Figura 3). Originalmente se aisló de *Beauveria bassiana* y desde entonces se ha detectado en varias especies de hongos, incluido especies de *Fusarium*, que es parásito del maíz, el trigo, el arroz y otros productos básicos importantes.

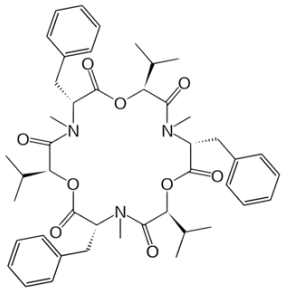

Figura 3. Estructura química de Beauvericina

Se ha detectado que BEA inhibe la contracción tónica provocada por un alto contenido en potasio (K^+) en cobayas *Taenia Coli*, y que también podría disminuir una alta fuerza contráctil inducida por K^+ en el íleo terminal y en los músculos papilares estimulados eléctricamente (Nakajyo y col., 1987; Lemmens-Gruber et al, 2000). El ion calcio (Ca^{2+}), el mensajero celular que media la función celular y los mecanismos fisiológicos, puede convertirse en una señal de muerte cuando se administra en un momento y lugar determinados y en determinadas circunstancias (Berridge et al, 2000; Hajnoczky et al, 2000). Por otro lado, se ha demostrado que la transferencia de Ca^{2+} desde el retículo endoplásmico a las mitocondrias es necesaria para el inicio de la apoptosis (Scorrano et al, 2003). Es interesante ya que BEA inhibió la corriente de Ca^{2+} en la línea celular neuronal NG 108-15 y permitió un flujo de cationes en las células

del canal, aumentando así el Ca^{2+} intracelular. En última instancia, puede activar varias vías biológicas que conducen a la muerte celular. Además, se demostró que reduce la retención de calcio en mitocondrias aisladas (Tonshin et al., 2010). Este efecto podría cooperar con la entrada de Ca^{2+} a través de la membrana plasmática para activar la apertura de los poros de transición de la permeabilidad mitocondrial y colapsar el potencial de la membrana mitocondrial. Por lo tanto, se ha descrito que la citotoxicidad de esta micotoxina para varias líneas celulares se basa en la inducción de apoptosis a través de la vía mitocondrial (Jow et al., 2004, Lin et al., 2005). Se evidenció que BEA causa apoptosis atribuida a la familia *Bcl-2*, citocromo C y caspasa 3; por otro lado, incrementos de calcio citoplasmático, aberraciones cromosómicas, fragmentación del ADN, alteraciones de micronúcleos y que es el inhibidor específico más potente de colesterol aciltransferasa (Acyl -coA) (Mallebrera et al., 2016). La incidencia de fragmentación nuclear y formación de cuerpos apoptóticos aumentó significativamente en las células CCRF-CEM tratadas con BEA, además, de un incremento en el citosol de actividad caspasa-3 de forma dosis dependiente (Jow et al., 2004).

También se ha propuesto que BEA tiene propiedades inhibidoras antibióticas, apoptóticas y de colesterol aciltransferasa y funciona como agente de control biológico activo sobre plagas de insectos que afectan a plantas de importancia agrícola (Hamill y col., 1969; Ojcius et al, 1991; Tomoda y col., 1992; Wagner y Lewis, 2000). Por tanto, puede acumularse en el medio ambiente y entrar en la cadena alimentaria.

Si bien varias micotoxinas de *Fusarium* aparecen en el reglamento (CE Nº 165/2010) y recomendaciones de la CE (Recomendación, 2006/583/CE), BEA

no está legislada ni incluida en el Reglamento de la Comisión (CE) Nº 1881/2006 que establece el máximo niveles de contaminantes específicos para la protección de la salud pública, sin embargo, los esfuerzos se centran en esta micotoxina, ya que en 2018 la EFSA publicó un Informe Científico relacionado con la toxicidad y genotoxicidad *in vivo* de BEA basado en el hecho de que no hay datos suficientes para establecer sus valores de referencia. No obstante, se han reportado altos niveles de contaminación, hasta 10-500 mg/kg, para la suma de BEA y enniatinas en trigo, cebada y maíz del sur, centro y norte de Europa (Uhlig et al., 2007, Jestoi, 2008). BEA también se ha encontrado como contaminante natural del maíz en Italia, Austria, Polonia, Sudáfrica y EE. UU. (Krska et al., 1996, Logrieco et al., 1993, Munkvold et al., 1998, Ritieni et al., 1997, Shephard et al., 1999); así como en 17 de 64 muestras totales (26.5%) de cereales crudos (trigo, maíz y cebada), con frecuencias de contaminación de 19, 28 y 50%, en maíz, trigo y cebada respectivamente de Marruecos, y en 21 de 64 muestras totales (32.8%) con frecuencias de contaminación de 42.8%, 21.4% y 50% en trigo, maíz y cebada respectivamente (Zinedine et al, 2011; Meca et al, 2010).

1.4.1. Efectos de toxicidad *in vitro* de Beauvericina

Varios estudios relacionados con BEA sugirieron que ejerce un efecto citotóxico sustancial en células de invertebrados y mamíferos. Indujo apoptosis en linfocitos de sangre periférica de pavo (Dombrink-Kurtzman, 2003), en la línea celular de carcinoma humano (Lin et al., 2005), linfocitos B humanos IARC/ LCL 171 (Logrieco et al., 1996), hematopoyéticos humanos, epiteliales y células fibroblastoides (Logrieco et al., 1997) y colangiocitos de roedores (Que et al., 1997). Fornelli et al, (2004) demostraron que la viabilidad tanto de las células U-937 como de las células HL-60 se vio afectada y disminuyó en los

cultivos expuestos a BEA. Para varias líneas celulares de cáncer humano, se ha descrito que la citotoxicidad de BEA se basa en la inducción de apoptosis a través de la vía mitocondrial. Además, se encontró que era citotóxico en las células de mastocitoma murino P815, células de linfoma Yac-1 y células de timoma EL-4 (Ojcius et al., 1991), las células RBL-1 de mastocitos de rata, el fibroblastoide de simio CV-1, las células IARC/BL 41 humanas (de linfoma de Burkitt), células HeLa (de carcinoma cervical), células HepG2 de hepatoma, carcinoma de colon humano HCT 116 (Macchia et al., 1995, Logrieco et al., 2002); y disminuir la viabilidad celular de una manera dependiente de la dosis y el tiempo, en células Caco-2 (Prosperini et al, 2013a).

En un estudio realizado por Juan-García et al., (2019) en células HepG2 expuestas a BEA individualmente y combinadas con ocratoxina A (OTA), se demostró una mayor citotoxicidad de BEA en la proliferación celular al interferir en ella, lo que sucedió de manera similar en las células PK15 por Klarić et al., (2010). Los datos obtenidos por Jow et al., (2004) revelaron que BEA induce la muerte celular en células de leucemia humana (CCRF-CEM) de una manera dosis y tiempo dependientes. Los mismos resultados obtenidos por Chen et al., (2006) donde BEA también indujo la muerte celular en células CCRF-CEM. Otros estudios también indicaron inhibición de la proliferación celular en varias líneas celulares: células CHO-K1, células Caco2, células Vero, células H4IIE, células HCT 116, células C6 y células Jurkat-T (Zouaoui et al, 2016; Ferrer et al. 2009; Ruiz et al., 2011a, Ruiz et al., 2011b, Watjen et al., 2014; Manyes et al., 2018). BEA también tiene efecto citotóxico en dos líneas celulares humanas de origen mieloide: las células de linfoma monocítico U-937 y las células de leucemia promielocítica HL-60 (Calò et al., 2004). Por otro lado, se han obtenido resultados negativos de BEA en el ensayo de mutagenicidad del Test de Ames,

en el que se encontró sólo un efecto moderadamente tóxico de BEA con el ensayo de bioluminiscencia bacteriana (Fotso y Smith, 2003).

1.4.2. Inducción de estrés oxidativo de Beauvericina

La citotoxicidad y el daño celular pueden producirse induciendo la producción de ROS y el daño de la actividad mitocondrial como consecuencia de la exposición a BEA, y ha sido evidenciado por varios estudios en diferentes líneas celulares. Por ejemplo, se ha evidenciado un aumento significativo en la producción de ROS (de 1.3 a 4.0 veces mayor que el control) después de la exposición a BEA en células Caco-2 (Prosperini et al., 2013a), también lo demostró Ferrer et al., (2009) que esta micotoxina podría dañar el metabolismo celular de las células CHO-K1 a través de la generación de ROS y la producción de MDA de manera dependiente de la concentración y del tiempo. En otro estudio sobre la misma línea celular, BEA también mostró un nivel elevado de producción de ROS (Mallebrera et al., 2015); evidenciando que la inducción de la LPO y el agotamiento del GSH están involucrados en los niveles de ROS, y su activación podría contribuir a la citotoxicidad de algunos compuestos. En un estudio realizado por Klarić et al, (2007), el nivel de GSH intracelular como marcador de la capacidad celular antioxidante, se redujo significativamente después de exponerse a la micotoxina BEA en células PK15, especulando que la acción ionofórica de BEA altera la estructura de la membrana lipídica y produce peróxido de hidrógeno, que a su vez disminuye la capacidad antioxidante celular. Prosperini et al., (2013a) también confirmaron que la generación de ROS juega un papel en los eventos moleculares por BEA que conducen al daño celular, particularmente por la inducción de agotamiento de LPO y GSH en células Caco-2. De manera similar, Juan-García et al., (2020) proporcionaron evidencia

de generación de LPO y ROS en células HepG2 expuestas a BEA individualmente y en combinación con OTA que se relacionaron con alteraciones detectadas para los niveles de glutatión reducido (GSH) y oxidado (GSSG). Paciolla et al., (2004) también observaron que BEA aumentaba los niveles de peróxido de hidrógeno y disminuia la actividad de la enzima depuradora de ROS, la catalasa (CAT) en protoplastos de tomate, lo que sugiere la participación del estrés oxidativo en el daño celular. Además, la exposición a BEA en las células CHO-K1 indujo un aumento significativo en los niveles de GSH, la actividad de GPx y glutatión-S-transferasa (GST) como sistema de defensa antioxidante (Mallebrera et al, 2014). Por el contrario, Dornetshuber et al. (2009b) no observaron ninguna producción de ROS en células de leucemia promielocítica humana (HL60) y células de carcinoma de cuello uterino humano (KB-3-1), y de manera similar sucedió en las células Jurkat-T que no se observó producción de ROS cuando se expusieron a BEA (Manyes et al., 2018).

1.4.3. Inducción del ciclo celular de Beauvericina

Generalmente, las micotoxinas que perturban la progresión del ciclo celular inician su actividad tóxica con efecto antiproliferativo, seguido de la acumulación de células en una o más fases del ciclo celular. Prosperini et al., (2013a) demostraron que las células Caco-2 tratadas con BEA reducían de forma significativa del porcentaje de células en la fase G0/G1 y producían detención en las fases G2/M y S. De manera similar, se obtuvieron los mismos resultados en células de monocitos-macrófagos murinos (RAW 264.7), cáncer de pulmón de células humanas (A549) y células Caco-2, para las enniatinas, unas micotoxinas estructuralmente relacionada con BEA (Dornetshuber et al., 2007; Gammelsrud et al., 2012; Prosperini et al., 2013b). También se demostró que

BEA inhibió la proliferación celular al detener las células CHO-K1 en la fase G0/G1 después de 24 h y un resultado opuesto después de 48 h y 72 h donde la detención celular sucedió a través de la fase G2/M e impidió la entrada de las células a la mitosis (Mallebrera et al, 2016). Aunque existen pocos estudios sobre el efecto de las micotoxinas combinadas en la alteración del ciclo celular, Juan-García et al., (2019) investigaron el efecto de la micotoxina BEA de forma individual y combinada con OTA en células HepG2. Los resultados de BEA mostraron una disminución significativa en todas las fases del ciclo celular, pero solo en la fase G0/G1 cuando se combinó con OTA. En otro estudio en células Jurkat-T, se observó la detención de S y la disminución en el porcentaje de células en la fase G2/M a las concentraciones más altas de BEA (Manyes et al., 2018).

1.5. Copresencia de micotoxinas

La coexistencia de micotoxinas en alimentos y piensos y su importante papel en la salud humana es un fenómeno bien conocido. Sin embargo, debido al gran número de micotoxinas y a la complejidad resultante de los diseños experimentales de estudios adecuados para la investigación de efectos combinatorios (por ejemplo, con respecto a las proporciones de compuestos, rangos de concentración, selección de criterios de valoración toxicológicos razonables, etc.), la evaluación de riesgos para la salud que tiene en cuenta dicha copresencia sigue siendo un desafío. Si bien, el estudio del impacto de las micotoxinas y sus combinaciones en piensos y productos alimenticios ha ganado atención en los últimos años, debido a la capacidad de la mayoría de *Fusarium* spp. para producir simultáneamente diferentes micotoxinas. Por ello, la EFSA ha publicado recientemente un borrador de documento de orientación donde se

describe una metodología de evaluación de riesgos armonizada para la exposición combinada a múltiples sustancias químicas en todas las áreas relevantes (EFSA, 2019). Hasta la fecha, la mayoría de los datos sobre los efectos combinatorios de las micotoxinas proceden de estudios *in vitro*, por lo que queda por ver si los resultados pueden confirmarse *in vivo*. Hay varias combinaciones de micotoxinas que ya se han probado *in vitro*. La mayoría de estos estudios investigaron principalmente los efectos citotóxicos en diferentes modelos celulares (Juan-García et al, 2016; Juan-García et al, 2015; Ruiz et al; 2011a; Zouaoui et al, 2016; Juan-García et al, 2019; Ferrer et al, 2009). Con base en estos estudios, parece que el impacto de la combinación de micotoxinas varía sustancialmente dependiendo de la proporción de compuestos aplicados, el rango de concentración y el modelo celular, que van desde efectos antagónicos a aditivos e incluso sinérgicos.

Un tema crítico, pero aún ignorado, en la evaluación del riesgo para la salud de las micotoxinas se refiere a los efectos combinados no solo de la micotoxina original y sus formas modificadas, sino también con otras sustancias presentes en los alimentos. Esto parece particularmente importante en el caso de ZEA y sus formas modificadas, ya que se estima que la exposición a ZEA y sus formas modificadas está cerca o incluso por encima del valor del grupo-TDI, al menos para algunos grupos de edad (EFSA 2011, 2014). Además, ZEA no solo coexiste con sus metabolitos, sino también con otras micotoxinas de *Fusarium* que no están reguladas por EFSA, como BEA (Ferrer et al, 2009).

Para los compuestos tóxicos se han desarrollado varios métodos matemáticos implementados en programas informáticos para evaluar el efecto de la combinación de compuestos y los efectos que contribuyen a la toxicología

computacional: Chou (2006) y Chou and Talalay (1984) mediante isobologramas, adición simple de efecto, análisis factorial de varianza mediante el uso de dos vías simples, ANOVA, criterio de independencia de Bliss, Ley de aditividad de Loewe, Modelo de agente único más alto (HSA) (no interacción de Gaddums), etc. (Kifer et al., 2020). Para la evaluación de mezclas de micotoxinas, el método de Choy y Talalay se ha utilizado ampliamente en la predicción de efectos potenciales (sinergismo, adición y antagonismo) (Juan-García et al, 2016, 2019a, 2019b; Agahi et al., 2020) incluso con fuertes diferencias en estructuras químicas, así como en la variedad de especies de hongos productores.

1.6. Estudio *in silico* de micotoxinas

Hoy en día, el desarrollo de programas informáticos y computacionales facilita la predicción de enfoques experimentales en toxicología que deben confirmarse con ensayos adicionales. Estos sistemas utilizan estructuras químicas, parámetros y descriptores que, en comparación con otros compuestos estudiados, pueden dar como resultado un conocimiento empírico de su efecto para prevenir la exposición o incluso para promover el desarrollo de terapias para evitar o disminuir los efectos tóxicos.

El escenario de investigación global para nuevas terapias y desarrollo de nuevos medicamentos para enfermedades comunes, o como está sucediendo hoy en día en la pandemia mundial SARS-COVID-19 por efectos secundarios en la salud, el uso de técnicas de detección virtual es una buena alternativa para ayudar en el descubrimiento de nuevas estrategias y sin utilizar o evitar los ensayos biológicos a largo plazo. Todas estas estrategias terminan explorando el perfil de efectos mediante la aplicación de programas informáticos. Uno de estos programas alternativos es PASS-on line (predicción de espectros de actividad

para sustancias), un enfoque *in silico* que revela las actividades biológicas de los compuestos, sus mecanismos de acción y los efectos secundarios relacionados (Lagunin et al., 2000). La versión PASS-on line predice más de 4000 tipos de actividad biológica, incluidos efectos farmacológicos, mecanismos de acción, efectos tóxicos y adversos, interacción con enzimas metabólicas y transportadores, influencia en la expresión génica, etc., como se describe en su página web (www.pharmaexpert.ru/passonline) (Lagunin et al., 2000). La predicción se basa en el análisis de relaciones estructura-actividad para más de 250.000 sustancias biológicamente activas, incluidos fármacos, candidatos a fármacos, conductores y compuestos tóxicos (Lagunin et al., 2000).

El soporte de los descubrimientos de nuevos compuestos y el conocimiento de su toxicidad viene dado por otros programas en línea que trabajan con diferentes parámetros, algunos de ellos son: SwissADME, MetaTox, GUSAR, ROSC-Pred, etc. Cada programa está enfocado en brindar diferentes predicciones; por ejemplo, mientras MetaTox predice los productos de metabolitos de Fase I y II que se pueden generar a partir de un compuesto (Rudik et al., 2017), SwissADME es un programa computacional que permite calcular descriptores fisicoquímicos, así como parámetros de ADME, propiedades farmacocinéticas, naturaleza farmacológica y compatibilidad con la química medicinal de una o varias moléculas pequeñas (Daina et al., 2017).

1.7. Células de neuroblastoma humano

Las pruebas toxicológicas y neurotoxicológicas se basan principalmente en modelos animales experimentales, pero se han desarrollado varios modelos de cultivo celular y tejidos para estudiar el mecanismo de neurotoxicidad. En general, las células de origen humano son alternativas atractivas a los modelos

animales de exploración de la toxicidad del ser humano. La línea celular de neuroblastoma humano SH-SY5Y, derivada de una biopsia de médula ósea humana, deriva de un ganglio simpático y se usa ampliamente como modelo de función neuronal, enfocándose en la neurotoxicidad, neuroprotección y patogénesis de la neurodegeneración. Además esta línea celular posee muchas características de las neuronas dopaminérgicas, es un modelo celular popular para la investigación de enfermedades neurodegenerativas. Dado que las células SH-SY5Y son de origen humano, expresan una serie de proteínas e isoformas de proteínas específicas para humanos que no estaran presentes de forma inherente en cultivos primarios de roedores. Por ejemplo, estas células expresan tirosina hidroxilasa y dopamina-beta-hidroxilasa, así como el transportador de dopamina, normalmente bloqueado en una etapa de diferenciación neuronal temprana (Oyarce et al, 1991). Las células SH-SY5Y indiferenciadas expresan captación de alta afinidad y liberación dependiente de Ca^{2+} evocada por despolarización de [3H]-noradrenalina ([3H]-NA). Estas células expresan proteínas que han sido implicadas en el acoplamiento y fusión de vesículas sinápticas durante la exocitosis (Goodall et al., 1997) lo que lleva a la suposición de que pueden realizar esta función en las SH-SY5Y. Además, se ha demostrado que estas células son un buen modelo celular en el estudio de diferentes micotoxinas (Kalagatur et al, 2021; Zingales et al, 2020; Venkataramana et al, 2014). También se ha evidenciado que las células SH-SY5Y indiferenciadas expresan RE, que funcionan como factores de transcripción activados por ligandos para regular la transcripción de genes (Grassi et al, 2013; Ding et al, 2019).

Las células de neuroblastoma pueden diferenciarse en células similares a las neuronas mediante la adición de compuestos específicos a los cultivos

celulares, mostrando fenotipos colinérgicos, adrenérgicos o dopaminérgicos. Las células SH-SY5Y indiferenciadas proliferan continuamente, expresan marcadores neuronales inmaduros y carecen de marcadores neuronales maduros; también se considera que recuerdan a las neuronas catecolaminérgicas inmaduras. Después de la estimulación con varios agentes, adquieren un fenotipo similar a una neurona más madura caracterizado por una forma fusiforme con procesos ramificados largos y un aumento de marcadores neuronales dopaminérgicos, lo que los convierte en una herramienta de investigación útil para dilucidar los mecanismos de toxicidad de varias drogas, incluidas las drogas de abuso que tienen efectos neurotóxicos, muchos de los cuales están mediados por el sistema dopaminérgico (Presgraves et al. 2004; Takeuchi et al. 2009). La diferenciación de las células SH-SY5Y induce una disminución en la tasa de proliferación a medida que las células se retiran del ciclo celular, y un aumento en la actividad de la enolasa específica de neuronas, una isoenzima que está presente en los tejidos neuronales y neuroendocrinos (Encinas et al, 2000). Además, la diferenciación sincroniza el ciclo celular, que puede fluctuar drásticamente en células SH-SY5Y indiferenciadas y otras líneas celulares de uso común, para producir una población de células neuronales homogénea. La diferenciación neuronal implica una serie de eventos específicos, incluida la formación y extensión de procesos neuríticos, aumento de la excitabilidad eléctrica de la membrana plasmática, formación de sinapsis funcionales positivas para sinaptofisina e inducción de enzimas, neurotransmisores y receptores de neurotransmisores específicos de neuronas. Por lo tanto, al determinar si se deben utilizar células indiferenciadas o diferenciadas para un experimento particular, se deben tener en cuenta todas estas propiedades.

Por otro lado, todos los organismos con un sistema nervioso central bien desarrollado tienen una barrera hematoencefálica (BBB) creada por las células endoteliales que forman las paredes de los capilares en el cerebro y la médula espinal de los seres humanos (Abbott et al., 2005). Se ha demostrado que la BBB funciona como una barrera protectora de las sustancias neurotóxicas que circulan en la sangre, que pueden ser metabolitos o proteínas endógenos, o xenobióticos ingeridos en la dieta o adquiridos del medio ambiente. Varios estudios han demostrado que las micotoxinas de *Fusarium* son capaces de atravesar la BBB y causar la muerte de las células neuronales (Krug et al., 2018; Taevernier et al., 2016; Behrens et al., 2015). Por ejemplo, BEA alcanza el BBB si pasa a la circulación sistémica y, por lo tanto, es capaz de ejercer efectos sobre el sistema nervioso central como se demostró en un estudio *in vitro* del transporte de BBB (con homogeneizados de cerebro de ratón) (Taevernier et al., 2016). Además, las micotoxinas de la misma familia (enniatin B y B_1) en un modelo de BBB porcino utilizando diferentes líneas celulares demostraron llegar al parénquima cerebral, destacando el efecto neurotóxico de estas micotoxinas (Krug et al., 2018). Sin embargo, existen muy pocos estudios y estos son limitados sobre los efectos de los derivados de ZEA y la BEA sobre la BBB, por lo que su estudio de forma individual y combinada son interesante llevarlos a cabo.

1.8. Producción de estrés oxidativo

Las células de mamíferos han desarrollado mecanismos de protección para minimizar los eventos nocivos que resultan de las sustancias químicas tóxicas y los productos oxidativos normales del metabolismo celular. El estrés oxidativo se caracteriza por una sobreproducción de especies reactivas de oxígeno (ROS)

y es una consecuencia del metabolismo aeróbico que, en células eucariotas, ocurre principalmente en las mitocondrias y puede conducir a daño mitocondrial de varias formas. La reducción de oxígeno en la cadena respiratoria implica la formación de intermediarios de oxígeno tóxicos. Aproximadamente el 2-5% del consumo de O_2 mitocondrial genera peróxido de hidrógeno (H_2O_2). El H_2O_2, si no se reduce, puede conducir a la formación del radical hidroxilo muy reactivo y provocar la formación de hidroperóxidos lipídicos que pueden dañar membranas, ácidos nucleicos, proteínas y alterar sus funciones.

En condiciones fisiológicas normales, del 1 al 5% del oxígeno se convierte en ROS, por lo que la mayoría de las estimaciones sugieren que la mayor parte de la producción de ROS intracelulares deriva de las mitocondrias. La producción de radicales superóxido mitocondriales tiene lugar principalmente en dos puntos discretos de la cadena de transporte de electrones, a saber, en el complejo I (nicotinamida adenina dinucleótido deshidrogenasa) y el complejo III (ubiquinona-citocromo C reductasa). En condiciones metabólicas normales, el complejo III es el sitio principal de producción de ROS. El daño del ADN y del ADN mitocondrial no reparado que conduce a una función defectuosa del complejo I y/o III puede resultar en una mayor reducción de electrones de O_2 para formar el ion superóxido. El aumento del flujo de superóxido resultante de este tipo de lesiones del ADN mitocondrial podría contribuir posteriormente al estrés oxidativo metabólico, la inestabilidad genómica, y lesión celular. El ADN mitocondrial representa un objetivo crítico para tal daño oxidativo. Una vez dañado, el ADN mitocondrial puede amplificar el estrés oxidativo al disminuir la expresión de proteínas críticas importantes para el transporte de electrones, lo que conduce a un círculo vicioso de ROS y desregulación de orgánulos que eventualmente desencadena en apoptosis. La exposición crónica a ROS puede

resultar en daño oxidativo a proteínas, lípidos y ácidos nucleicos mitocondriales y celulares, y la exposición aguda a ROS puede inactivar los centros de hierro-azufre (Fe-S) de los complejos de cadena de transporte de electrones I, II y III, y aconitasa del ciclo del ácido tricarboxílico, que provoca la interrupción de la producción de energía mitocondrial.

Las mitocondrias normalmente están protegidas del daño oxidativo por una red multicapa de sistemas antioxidantes mitocondriales, que está formada por antioxidantes enzimáticos y no enzimáticos. Los antioxidantes enzimáticos consisten en SOD, CAT, GPx y glutatión reductasa (GR) junto con una serie de antioxidantes de bajo peso molecular como el α-tocoferol y ubiquinol, con el agregado de los provenientes de la ingesta alimentaria como zeaxantina, luteína, polifenoles presentes en las bayas de goji y café entre otros (Montesano et al., 2020; Juan et al., 2020; Juan-García et al., 2019a). Estas moléculas son particularmente efectivas para eliminar radicales peroxilo de lípidos y prevenir las reacciones en cadena de radicales libres de peroxidación de lípidos. Sin embargo, estos sistemas antioxidantes no son perfectos.

La enzima de la matriz mitocondrial manganeso superóxido dismutasa (MnSOD o SOD2) o SOD de cobre / zinc (Cu / ZnSOD o SOD1) en el espacio intermembrana mitocondrial y el citosol convierte $O_2^{\bullet-}$ en peróxido de hidrógeno (H_2O_2) en la reacción $O_2^{\bullet-} + O_2^{\bullet-} + 2H^+ \rightarrow H_2O_2 + O_2$. El H_2O_2 es más estable que el $O_2^{\bullet-}$ y puede difundirse desde las mitocondrias hacia el citosol y el núcleo y, en consecuencia, iniciar cascadas de peroxidación de lípidos en las membranas. Además, los productos de la oxidación de azúcares, proteínas y lípidos pueden causar daños secundarios a las proteínas, que pueden perder la función catalítica y sufrir una degradación selectiva. Posteriormente, el H_2O_2 es

metabolizado por GPx en las mitocondrias y el citosol usando GSH como sustrato, y por CAT en peroxisomas, ambos convirtiéndolo en H_2O. Por otro lado, la enzima CAT también participa en catalizar la descomposición de H_2O_2 junto con GPx. Las enzimas CAT son abundantes en los peroxisomas de las células hepáticas, pero no tanto en las células neuronales, y GPx es abundante en las mitocondrias y el compartimento del citosol. Además, GST es una familia de enzimas que catalizan la conjugación de GSH con multitud de sustratos para desintoxicar los compuestos exógenos y endógenos. Estas enzimas intervienen en la desintoxicación de xenobióticos y en el mecanismo protector frente al daño celular, como el estrés oxidativo.

Además de los sistemas protectores enzimáticos, las células de mamíferos están equipadas con un sistema antioxidante endógeno protector formado por un antioxidante no enzimático llamado ciclo redox del glutatión, que consiste en GSH y GSSG mencionado anteriormente en la metabolización del peróxido de hidrógeno.

El GSH actúa como eliminador nucleofílico de numerosos compuestos y sus metabolitos, mediante mecanismos enzimáticos y químicos, convirtiendo los centros electrofílicos en enlaces tioéter, y como sustrato en la destrucción de hidroperóxidos mediada por peroxidasa de GSH. El agotamiento de GSH hasta aproximadamente el 20-30% de los niveles totales de glutatión puede afectar la defensa de la célula contra las acciones tóxicas de dichos compuestos y puede provocar lesiones celulares y la muerte. GSH se mantiene en una pareja redox con GSSG dentro de la célula y es regenerado por GSH reductasa, una enzima citosólica dependiente de NADPH. Además, el GSH mitocondrial puede ser importante en la regulación de la permeabilidad de la membrana interna al

mantener los tioles intramitocondriales en estado reducido. Debido a que las mitocondrias no tienen catalasa, dependen únicamente de la peroxidasa GSH para desintoxicar los hidroperóxidos. Un sistema redox de glutatión completo consta de GSH, GR, GPx y NADPH generados a partir de NADH por transhidrogenación. GPx utiliza los equivalentes reductores de GSH, el tiol no proteico celular más abundante, del cual entre un 10% y un 15% se encuentra en las mitocondrias. También fue propuesto en primer lugar por Meredith & Reed, (1982 y 1983), que el GSH mitocondrial tiene un papel protector de la citotoxicidad. Demostraron que el inicio de la lesión de cel1 en hepatocitos de rata aislados por ácido etacrínico se correlacionaba con el agotamiento del GSH mitocondrial, mientras que el grupo citosólico podría agotarse sin afectar la viabilidad celular. También fue propuesto en primer lugar por Meredith & Reed, (1982 y 1983), que el GSH mitocondrial tiene un papel protector de la citotoxicidad. Demostraron que el inicio de la lesión de cel1 en hepatocitos de rata aislados por ácido etacrínico se correlacionaba con el agotamiento del GSH mitocondrial, mientras que el grupo citosólico podría agotarse sin afectar la viabilidad celular. También fue propuesto en primer lugar por Meredith & Reed, (1982 y 1983), que el GSH mitocondrial tiene un papel protector de la citotoxicidad. Demostraron que el inicio de la lesión de cel1 en hepatocitos de rata aislados por ácido etacrínico se correlacionaba con el agotamiento del GSH mitocondrial, mientras que el grupo citosólico podría agotarse sin afectar la viabilidad celular.

Debido a que ningún sistema de defensa es completamente eficiente, la gama completa de enzimas antioxidantes endógenas disponibles no puede neutralizar completamente las ROS emitidas por las mitocondrias. Las lesiones oxidativas acumulativas de las mitocondrias, desencadenadas por procesos

metabólicos endógenos y/o influencias oxidativas exógenas, hacen que las mitocondrias se vuelvan cada vez menos eficientes. A medida que las mitocondrias pierden progresivamente su integridad funcional, proporciones cada vez mayores de moléculas de oxígeno que las alcanzan se convierten en ROS, que socavan el sistema de defensa mitocondrial. Además, se cree que la tasa de liberación de GSSG es proporcional a la actividad de la peroxidasa de GSH (Akerboom et al. 1980), y la proporción de par redox GSH/GSSG es un marcador importante de estrés oxidativo debido a su función antioxidante y alta concentraciones en las células.

1.9. Mecanismos de muerte celular y progresión del ciclo celular

La apoptosis ha sido reconocida y aceptada como un modo distintivo e importante de muerte celular "programada", que implica la eliminación determinada genéticamente de células. La apoptosis ocurre normalmente durante el desarrollo y el envejecimiento y como mecanismo homeostático para mantener las poblaciones de células en los tejidos. La apoptosis también ocurre como un mecanismo de defensa, como en las reacciones inmunes o cuando las células son dañadas por enfermedades o agentes nocivos. Aunque existe una amplia variedad de estímulos y condiciones, tanto fisiológicas como patológicas, que pueden desencadenar la apoptosis, no todas las células morirán necesariamente en respuesta al mismo estímulo. La irradiación o los fármacos utilizados para la quimioterapia contra el cáncer dañan el ADN de algunas células, lo que puede provocar la muerte por apoptosis a través de una vía dependiente de p53. Algunas hormonas, como los corticosteroides, puede conducir a la muerte apoptótica en algunas células (p. ej., timocitos) aunque otras células no se ven afectadas o incluso estimuladas. Otra cuestión relacionada es

la de distinguir la apoptosis de la necrosis, dos procesos que pueden ocurrir de forma independiente, secuencial y simultánea (Hirsch, 1997; Zeiss, 2003). En algunos casos, es el tipo de estímulo y/o el grado de estímulo lo que determina si las células mueren por apoptosis o necrosis. A dosis bajas, una variedad de estímulos perjudiciales como el calor, la radiación, la hipoxia y los fármacos citotóxicos contra el cáncer pueden inducir la apoptosis, pero estos mismos estímulos pueden provocar necrosis a dosis más altas. Finalmente, la apoptosis es un proceso coordinado y, a menudo, dependiente de la energía que implica la activación de un grupo de cisteína proteasas llamadas "caspasas" y una compleja cascada de eventos que vinculan los estímulos iniciadores con la desaparición final de la célula.

Durante el proceso temprano de apoptosis, las células parecen ser de tamaño más pequeño debido a la contracción celular y, en consecuencia, el citoplasma es denso y los orgánulos están más apretados. La alternativa es la muerte celular por necrosis, que se considera un proceso tóxico en el que la célula es una víctima pasiva y sigue un modo de muerte independiente de energía. Algunos de los principales cambios morfológicos que ocurren con la necrosis incluyen hinchazón celular; formación de vacuolas citoplasmáticas; retículo endoplásmico distendido; formación de ampollas citoplasmáticas; mitocondrias condensadas, hinchadas o rotas; desagregación y desprendimiento de ribosomas; membranas de orgánulos rotos; lisosomas hinchados y rotos; y eventualmente ruptura de la membrana celular. Aunque los mecanismos y morfologías de la apoptosis y la necrosis difieren, existe una superposición entre estos dos procesos. La evidencia científica indica que la necrosis y la apoptosis representan expresiones morfológicas de una red bioquímica compartida descrita como el "*apoptosis-necrosis continuum*" (Zeiss, 2003). La necrosis es un proceso pasivo e

incontrolado que generalmente afecta a grandes campos de células, mientras que la apoptosis es controlada y dependiente de la energía y puede afectar a individuos o grupos de células. La lesión de las células necróticas está mediada por dos mecanismos principales: la interferencia con el suministro de energía de la célula y el daño directo a las membranas celulares.

Hasta la fecha, las investigaciones indican que existen dos vías apoptóticas principales: la vía extrínseca o del receptor de muerte y la vía intrínseca o mitocondrial. Las células apoptóticas exhiben varias modificaciones bioquímicas tales como escisión de proteínas, entrecruzamiento de proteínas, ruptura del ADN y reconocimiento fagocítico que, en conjunto, dan como resultado la patología estructural distintiva descrita anteriormente (Hengartner, 2000). Las caspasas se expresan ampliamente en una forma de proenzima inactiva en la mayoría de las células y, una vez activadas, a menudo pueden activar otras procaspasas, lo que permite el inicio de una cascada de proteasas. Algunas procaspasas también pueden agregarse y autoactivarse. Esta cascada proteolítica, en la que una caspasa puede activar otras caspasas, amplifica la vía de señalización apoptótica y, por tanto, conduce a una muerte celular rápida. Una vez que las caspasas se activan inicialmente, parece haber un compromiso irreversible con la muerte celular. Hasta la fecha, se han identificado diez caspasas principales y se han categorizado ampliamente en iniciadores (caspasa-2, -8, -9, -10), efectores o verdugos (caspasa-3, -6, -7) y caspasas inflamatorias (caspasa-1, -4, -5). El control y la regulación de los eventos mitocondriales apoptóticos ocurre a través de miembros de la familia de proteínas *Bcl-2* que gobierna la permeabilidad de la membrana mitocondrial y puede ser proapoptótica o antiapoptótica. También se ha implicado a muchos de los miembros de la familia *Bcl-2* en la regulación de la muerte celular en el sistema

nervioso. Hasta la fecha, se han identificado un total de 25 genes en la familia *Bcl-2*. Algunas de las proteínas anti-apoptóticas incluyen *Bcl-2, Bcl-x, Bcl-XL, Bcl-XS, Bcl-w, BAG*, y algunas de las proteínas proapoptóticas incluyen *Bcl-10, Bax, Bak, Bid, Bad, Bim, Bik* y *Blk*.

Así como la apoptosis está controlada por una maquinaria altamente conservada, el ciclo celular es un mecanismo altamente conservado por el cual proliferan las células eucariotas. Las anomalías en la regulación de la muerte celular pueden ser un componente importante de enfermedades como el cáncer, el síndrome linfoproliferativo autoinmune, el SIDA, la isquemia y enfermedades neurodegenerativas como la enfermedad de Parkinson, la enfermedad de Alzheimer, la enfermedad de Huntington y la esclerosis lateral amiotrófica. Algunas afecciones presentan una apoptosis insuficiente, mientras que otras presentan una apoptosis excesiva.

Curiosamente, la apoptosis y el ciclo celular comparten algunos factores comunes, incluidos Rb, E2F y p53, y exhiben similitudes morfológicas de redondeo celular y condensación de cromatina (King y Cidlowski, 1995). Esto sugiere que ambos procesos podrían estar regulados hasta cierto punto por mecanismos moleculares similares. El ciclo celular se divide en cuatro fases: G1 (primer espacio), S (síntesis de ADN), G2 (segundo espacio) y M (mitosis). La progresión a través de estas fases está regulada por la expresión, activación e inhibición secuenciales de los complejos de quinasa dependiente de ciclina (CDK) y sus subunidades de activación, las ciclinas, así como por los inhibidores de quinasa dependiente de ciclina (CDKI). En la proliferación celular, el progreso del ciclo celular está estrictamente controlado a través de puntos de control (en las fases G0/G1 y G2/M) que funcionan como interruptores

moleculares que aseguran que los eventos críticos en una fase del ciclo celular se completen antes de que se pueda ingresar a la siguiente fase de crecimiento con proliferación celular, coordinando así la división y el crecimiento celular. Las células bloqueadas en cualquiera de los puntos de control volverán a G0 y se volverán a diferenciar (si se detienen en el punto de control G1), o bien, las células morirán por apoptosis (Liu y Greene, 2001a; Nagy, 2000).

Varios factores alteran el proceso por el cual una célula experimenta la división celular que es la progresión del ciclo celular. Los puntos de control del ciclo celular se activan mediante una cascada de señales y detienen temporalmente la progresión del ciclo celular. Para mantener la integridad genómica se activan las diferentes proteínas de los puntos de control induciendo la detención del ciclo celular para reparar el daño o si la lesión excede la capacidad reparadora de la célula para activar la muerte celular (Damia & Broggini, 2003). Generalmente, las micotoxinas que perturban la progresión del ciclo celular inician su actividad tóxica con efecto antiproliferativo, seguido de la acumulación de células en una o más fases del ciclo celular.

1.10. References

Abbott, N.J. 2005. Dynamics of CNS Barriers: Evolution, Differentiation, and Modulation. Cellular and Molecular Neurobiology. 25, 5–23.

Abid-Essefi S., Bouaziz C., El Golli-Bennour E., Ouanes Z., Bacha H., 2009. Comparative study of toxic effects of zearalenone and its two major metabolites α-zearalenol and β-zearalenol on cultured human Caco-2 cells. J. Biochem. Mol. Toxicol., 23, 233-243.

Abid-Essefi, S., Ouanes, Z., Hassen, W., Baudrimont, I., Creppy, E., Bacha, H., 2004. Cytotoxicity, inhibition of DNA and protein syntheses and oxidative damage in cultured cells exposed to zearalenone. Toxicol. In Vitro 18, 467–474.

Akerboom, T. P. M., Bilzer, M., Sies, H. 1980. The relationship of biliary glutathione disulfide efflux and intracellular glutathione disulfide content in perfused rat liver. 1. Bioi. Chem. 257:4248-52.

Alm, H., Greising, T., Brussow, K.P., Torner, H., Tiemann, U., 2002. The influence of the mycotoxins deoxynivalenol and zearalenol on in vitro maturation of pig oocytes and in vitro culture of pig zygotes. Toxicol. In Vitro 16 (6), 643–648.

Ayed-Boussema I., Bouaziz C., Rjiba K., Valenti K., Laporte F, Bacha H, Hassen W. 2008. The mycotoxin Zearalenone induces apoptosis in human hepatocytes (HepG2) via p53-dependent mitochondrial signaling pathway, Toxicology in Vitro, 22(7), 1671-1680.

Bang O.Y., Hong H.S., Kim D.H., Kim H., Boo J.H., Huh K., Mook-Jung I., 2004. Neuroprotective effect of genistein against beta amyloid-induced neurotoxicity Neurobiology of Disease, 16 (1), 21-28.

Behrens M., Hüwel S., Galla H.J., Humpf H.U. 2015. Blood-brain barrier effects of the Fusarium mycotoxins deoxynivalenol, 3 acetyldeoxynivalenol, and moniliformin and their transfer to the brain. PLoS One, 10 (11), 0143640.

Ben Salem, I., Boussabbeh, M., Prola, A., Guilbert A., Bacha H., Lemaire C., Abid-Essefi S., 2016. Crocin protects human embryonic kidney cells (HEK293) from α- and β-Zearalenol-induced ER stress and apoptosis. Environ Sci Pollut Res, 23, 15504–15514.

Benzoni, E., Minervini, F., Giannoccaro, A., Fornelli, F., Vigo, D., Visconti, A., 2008. Influence of in vitro exposure to mycotoxin zearalenone and its derivatives on swine sperm quality. Reprod. Toxicol. 25 (4), 461–467.

Berridge M.J., Lipp P., Bootman M.D., 2000. The versatility and universality of calcium signaling Nature Rev. Mol. Cell Biol., 1, 11-21.

Biehl, M.L., Prelusky, D.B., Koritz, G.D., Hartin, K.E., Buck, W.B. and Trenholm, H.L., 1993. Biliary excretion and enterohepatic cycling of zearalenone in immature pigs. Toxicology and Applied Pharmacology 121: 152-159.

Bittner GD, Denison MS, Yang CZ, Stoner MA, He G. 2014. Chemicals having estrogenic activity can be released from some bisphenol a-free, hard and clear, thermoplastic resins. Environ Health 13: 103.

Bottalico, A., Visconti, A., Logrieco, A., Solfrizzo, M., Mirocha, C.J., 1985. Occurrence of zearalenols (diastereomeric mixture) in corn stalk rot and their production by associated Fusarium species. Appl. Environ. Microbiol. 49, 547–551.

Calò L., Fornelli F., Ramires R., Nenna S., Tursi A., Caiaffa MF., Macchia L., 2004. Cytotoxic effects of the mycotoxin beauvericin to human cell lines of myeloid origin Pharmacol. Res., 49, 73-77.

Chang, W.-M. and Lin, J.-K., 1984. Transformation of zearalenone and zearalenol by rat erythrocytes. Food and Chemical Toxicology 22: 887-891.

Chen B.F., Tsai M.C., Jow G.M., 2006. Induction of calcium influx from extracellular fluid by beauvericin in human leukemia cells. Biochem. Biophys. Res. Commun., 34, (2006), pp. 134-139.

Cortinovis C, Pizzo F, Spicer LJ, Caloni F., 2013. Fusarium mycotoxins: Effects on reproductive function in domestic animalsdA review. Theriogenology 80: 557–564.

Creppy, E.E., 2002. Update of survey, regulation and toxic effects of mycotoxins in Europe. Toxicol. Lett. 127, 19–28.

Daina A., Michielin O., Zoete V., 2017. SwissADME: a free web tool to evaluate pharmacokinetics, drug-likeness and medicinal chemistry friendliness of small molecules. Sci. Rep., 7, 42717.

Damia G., Broggini M., 2003. Cell cycle checkpoint proteins and cellular response to treatment by anticancer agents. Cell Cycle, 3, 46-50.

Dänicke, S., Ueberschär, K.-H., Halle, I., Matthes, S., Valenta, H. and Flachowsky, G., 2002, Effect of addition of a detoxifying agent to laying hen diets containing uncontaminated or Fusarium toxin-contaminated maize on performance of hens and on carryover of zearalenone. Poultry Science 81: 1671-1680.

Darbre PD, Byford JR, Shaw LE, Horton RA, Pope GS, Sauer MJ., 2002. Oestrogenic activity of isobutylparaben in vitro and in vivo. J Appl Toxicol. 22: 219-226.

David M.O, Zychlinsky A., Zheng L.M, Young J.D.E., 1991. Ionophore-induced apoptosis: Role of DNA fragmentation and calcium fluxes, Experimental Cell Research, 197(1), 43-49.

Ding X.W., Gao T., Gao P., Meng Y.Q., Zheng Y., Dong L., Luo P., Zhang G.H., Shi X.Y., Rong W.F., 2019. Activation of the G protein-coupled estrogen receptor elicits store calcium release and phosphorylation of the Mu-opioid receptors in the human neuroblastoma SH-SY5Y cells. Frontiers in Neurosci., 13, 1351.

Döll, S., Danicke, S., Schnurrbusch, U., 2003. The effect of increasing concentrations of Fusarium toxins in the diets of piglets on histological parameters of uterus. Mycotox. Res. 19, 73–76.

Dombrink-Kurtzman M.A., 2003. Fumonisin and beauvericin induce apoptosis in turkey peripheral blood lymphocytes Mycopathologia, 156, 357-364.

Dong, M., He, X.J., Tulayakul, P., Li, J.-Y., Dong, K.-S., Manabe, N., Nakayama, H. and Kumagai, S., 2010. The toxic effects and fate of intravenously administered zearalenone in goats. Toxicon 55: 523-530.

Dornetshuber R., Heffeter P., Kamyar M.-R., Peterbauer T., Beregr W., Lemmens-Gruber R., 2007. Enniatin exerts p53-dependent cytostatic and p53-independent cytotoxic activities against human cancer cells. Chem. Res. Toxicol., 20, 465-473.

Dornetshuber R., Heffeter P., Lemmens-Gruber R., Elbling L., Marko D., Micksche M., Berger W., 2009. Oxidative stress and DNA interactions are not involved in enniatin- and beauvericin-mediated apoptosis induction. Mol. Nutr. Food Res., 53, 1112-1122.

EFSA Panel on Contaminants in the Food Chain (CONTAM). 2016. Appropriateness to set a group health-based guidance value for zearalenone and its modified forms. EFSA J. 14: 4425-4471. doi:10.2903/j.efsa.2016.4425.

EFSA Scientific Committee. 2013. Scientific Opinion on the hazard assessment of endocrine disruptors: scientific criteria for identification of endocrine disruptors and appropriateness of existing test methods for assessing effects mediated by these substances on human health and the environment. EFSA J. 11: 3132 (84 pp).

EFSA. Guidance on harmonised methodologies for human health, animal health and ecological risk assessment of combined exposure to multiple chemicals. EFSA J. 2019, 17, 5634.

Encinas M., Iglesias M., Liu Y., Wang H., Muhaisen A., Cena V., Gallego C., Comella J.X., 2000. Sequential treatment of SH-SY5Y cells with retinoic acid and brain-derived neurotrophic factor gives rise to fully differentiated, neurotrophic factor-dependent, human neuron-like cells. J Neurochem 75(3):991–1003.

European Food Safety Authority (EFSA) Scientific opinion on the risks for public health related to the presence of zearalenone in food. EFSA J., 9 (2011), p. 2197.

European Food Safety Authority, 2011. Scientific opinion on the risk for public health related to the presence of zearalenone in food. Eur. Food Saf. Auth. J.9, 1–124.

FAO, 2009. Food Balance Sheet. <http://faostat.fao.org/> (accessed 01.26.13).

Ferrer E., Juan-García A., Font G., Ruiz M.J., 2009. Reactive oxygen species induced by beauvericin, patulin and zearalenone in CHO-K1 cells. Toxicol. Vitro, 23, 1504-1509.

Fitzpatrick, D.W., Picken, C.A., Murphy, L.C. and Buhr, M.M., 1989. Measurement of the relative binding affinity of zearalenone, α-zearalenol and β-zearalenol for uterine and oviduct estrogen receptors in swine, rats and chickens: an indicator of estrogenic potencies. Comparative Biochemistry and Physiology 94C: 691-694.

Fink-Gremmels J., Malekinejad H., 2007. Clinical effects and biochemical mechanisms associated with exposure to the mycoestrogen zearalenone. Animal Feed Science and Technology, 137, 3–4, 326-341.

Forsell, J.H and Pestka, J.J., 1985. Relation of 8-ketotrichothecene and zearalenone analog structure to inhibition of mitogen-induced human lymphocyte blastogenesis. Appl. Environ. Microbiol. 50 (5), 1304–1307.

Fotso J., Smith J.S., 2003. Evaluation of beauvericin toxicity with the bacterial bioluminescence assay and the AMES mutagenicity bioassay. J. Food Sci., 68 (6), 1938-1941.

Gammelsrud A., Solhaug A., Dendelé B., Sanberg W.J., Ivanova L., Kochbach Bølling A., Lagadic-Gossmann D., Refsnes M., Becher R., Eriksen G., Holme J.A., 2012. Enniatin B-induced cell death and inflammatory responses in RAW 267.4 murine macrophages. Toxicol. Appl. Pharmacol., 261, 74-87.

Goodall A.R., Danks K., Walker J.H., Ball S.G., Vaughan P.F.T., 1997. Occurrence of two types of secretory vesicles in the human neuroblastoma SH-SY5Y. J. Neurochem., 68, 1542-1552.

Grassi D., Bellini M.J., Acaz-Fonseca E., Panzica G., Garcia-Segura L.M., 2013. Estradiol and testosterone regulate arginine-vasopressin expression in SH-SY5Y human female neuroblastoma cells through estrogen receptors-α and-β Endocrinology, 154, 2092-2100.

Hajnoczky G., Csordas G., Madesh M., Pcher P., 2000. Control of apoptosis by IP3 and ryanodine receptor driven calcium signals. Cell Calcium, 28, 349-363.

Hamill R.L., Higgens C.E., Boaz H.E., Gorman M., 1969. The structure op beauvericin, a new depsipeptide antibiotic toxic to artemia salina, Tetrahedron Letters, 10(49), 4255-4258.

Hassen, W., Ayed-Boussema, I., Azqueta Oscoz, A., De Cerain Lopez, A., Bacha, H., 2007. The role of oxidative stress in zearalenone-mediated toxicity in Hep G2 cells: oxidative DNA damage, gluthatione depletion and stress proteins induction. Toxicology 232, 294–302.

Hengartner MO., 2000. The biochemistry of apoptosis. Nature. 407:770–6.

James, L.J. and Smith, T.K., 1982. Effect of dietary alfalfa on zearalenone toxicity and metabolism in rats and swine. Journal of Animal Sciences 55: 110-118.

JECFA, 2001. Joint FAO/WHO Expert Committee on Food Additives (JECFA). Safety Evaluation of Certain Mycotoxins in Food. Food and Agriculture Organization, Rome, Italy, 281–320.

Jestoi M., 2008. Emerging Fusarium-mycotoxins fusaproliferin, beauvericin, enniatins, and moniliformin: a review Crit. Rev. Food Sci. Nutr., 48, 21-49.

Jow G.M., Chou C.J., Chen B.F., Tsai J.H., 2004. Beauvericin induces cytotoxic effects in human acute lymphoblastic leukemia cells through cytochrome c release, caspase 3 activation: the causative role of calcium, Cancer Letters, Volume 216(2), 165-173.

Juan-García A., Carbone S., Ben-Mahmoud M., Sagratini G., Mañes J., 2020. Beauvericin and ochratoxin A mycotoxins individually and combined in

HepG2 cells alter lipid peroxidation, levels of reactive oxygen species and glutathione. Food and Chemical Toxicology, 139, 111247.

Juan-García, A.; Juan, C.; König, S.; Ruiz, M.J. 2015. Cytotoxic effects and degradation products of three mycotoxins: Alternariol, 3-acetyl-deoxynivalenol and 15-acetyl-deoxynivalenol in liver hepatocelular carcinoma cells. Toxicol. Lett, 235, 8–16.

Juan-García, A.; Juan, C.; Manyes, L.; Ruiz, M.J. 2016. Binary and tertiary combination of alternariol, 3-acetyl-deoxynivalenol and 15-acetyl-deoxynivalenol on HepG2 cells: Toxic effects and evaluation of degradation products. Toxicol. In Vitro, 34, 264–273.

Juan-García, A.; Tolosa, J.; Juan, C.; Ruiz, M.J. 2019. Cytotoxicity, Genotoxicity and Disturbance of Cell Cycle in HepG2 Cells Exposed to OTA and BEA: Single and Combined Actions. Toxins, 11, 341.

Kalagatur N.K., Abd_Allah E.F., Poda A., Kadirvelu K., Hashem A., Mudili V., Siddaiah C., 2021. Quercetin mitigates the deoxynivalenol mycotoxin induced apoptosis in SH-SY5Y cells by modulating the oxidative stress mediators. Saudi Journal of Biological Sciences, 28(1), 465-477.

Kifer D., Jakši D., Klari M.S., 2020. Assessing the effect of mycotoxin combinations: which mathematical model is (the most) appropriate? Toxins, 12, 153.

King, K.L., Cidlowski, J.A., 1995. Cell cycle and apoptosis: common pathways to life and death. J. Cell Biochem. 58, 175–180.

Klarić M.S., Pepeljnjak S., Domijan A.M., Petrik J., 2007. Lipid Peroxidation and Glutathione Levels in Porcine Kidney PK15 Cells after Individual and Combined Treatment with Fumonisin B1, Beauvericin and Ochratoxin A. Basic & Clinical Pharmacology & Toxicology, 100, 157–164.

Klarić, M.Š., Daraboš, D., Rozgaj, R. Kašuba V., Pepeljnjak S., 2010. Beauvericin and ochratoxin A genotoxicity evaluated using the alkaline comet assay: single and combined genotoxic action. Arch Toxicol 84, 641–650.

Krska R., Schuhmacher R., Grasserbauer M., Scott P.M., 1996. Determination of the Fusarium mycotoxin beauvericin at μg/kg levels in corn by high-performance liquid chromatography with diode-array detection. Journal of Chromatography A, 746, 233-238.

Krug I., Behrens M., Esselen M., Humpf H.U., 2018. Transport of enniatin B and enniatin B1 across the blood-brain barrier and hints for neurotoxic effects in cerebral cells. PLOS ONE.

Kuiper-Goodman, T., Scott, P.M., Watanabe, H., 1987. Risk assessment of the mycotoxin zearalenone. Regul. Toxicol. Pharmacol. 7, 253–306.

Lagunin A., Stepanchikova A., Filimonov D., Poroikov V., 2000. PASS: prediction of activity spectra for biologically active substances. Bioinformatics, 16 (8), 747-748.

Lang, T.J. Estrogen as immunomodulator. Clin. Immunol. 2004, 113, 224–230.

Le Guevel, R., Pakdel, F., 2001. Assessment of oestrogenic potency of chemicals used as growth promoter by in-vitro methods. Human Reproduction. 16, 1030–1036.

Lemmens-Gruber, R., Rachoy, B., Steininger, E., Kouri, K., Saleh, P., Krska, R., Josephs, R., and Lemmens, M., 2000. The effect of the Fusarium metabolite beauvericin on electromechanical and physiological properties in isolated smooth and heart muscle preparations of guinea pigs. Mycopathologia 149, 5-12.

Lin H.I., Lee Y.J., Chen B.F., Tsai M.C., Lu J.L., Chou C.J., Jow G.M., 2005. Involvement of Bcl-2 family, cytochrome c and caspase 3 in induction of apoptosis by beauvericin in human non-small cell lung cancer cells Cancer Lett., 230, 248-259.

Liu, D.X., Greene, L.A., 2001b. Regulation of neuronal survival and death by E2F-dependent gene repression and derepression. Neuron 32, 425–438.

Logrieco A., Moretti A., Fornelli F., Fogliona V., Ritieni A., Caiaffa M.F., Randazzo G., Bottalico A., Macchia L., 1996. Fusaproliferin production by Fusarium subglutinans and its toxicity to Artemia salina, SF-9 insect cells, and IARC/LCL 171 human B lymphocytes Appl. Environ. Microbiol., 62, 3378-3384.

Logrieco A., Moretti A., Ritieni A., Caiaffa M.F., Macchia L., 2002. Beauvericin: chemistry biology and significance. R Upadhyay (Ed.), Advances in Microbial Toxin Research and its Biotechnological Exploitation, Kluwer Academic, New York, 23-30.

Logrieco A., Moretti A., Ritieni A., Chelkowski J., Altomare C., Bottalico A., Randazzo, G., 1993. Natural occurrence of beauvericin in preharvest Fusarium subglutinans infected corn ears in Poland. Journal of Agricultural and Food Chemistry, 41, 2149-2152.

Logrieco A., Ritieni A., Moretti A., Randazzo G., Bottalico A., 1997. Beauvericin and fusaproliferin: new emerging Fusarium toxins Cereal Res. Commun., 25, 407-413.

Luongo, D., Severino, L., Bergamo, P., De Luna, R., Lucisano, A., Rossi, M., 2006. Interactive effects of fumonisin B1 and alpha-zearalenol on proliferation and cytokine expression in Jurkat T cells. Toxicol. In Vitro 20 (8), 1403–1410.

Macchia, L., Di Paola, R., Fornelli, F., Nenna, S., Moretti, A., Napoletano, R., Logrieco, A., Caiaffa, M.F., Tursi, A. and Bottalico, A., 1995. Cytotoxicity of beauvericin to mammalian cells. In: Proceedings of the International Seminar on Fusarium Mycotoxin, Taxonomy and Pathogenicity, 1995 May 9–13; Martina Franca, Bari, Italy. Abstract book, pp. 72–73.

Malekinejad, H., Maas-Bakker, R., Fink-Gremmels, J., 2006. Species differences in the hepatic biotransformation of zearalenone. Vet. J. 172, 96–102.

Mallebrera B., Brandolini V., Font G., Ruiz M.J., 2015. Cytoprotective effect of resveratrol diastereomers in CHO-K1 cells exposed to beauvericin. Food Chem. Toxicol., 80, 319-327.

Mallebrera B., Font G., Ruiz M.J., 2014. Disturbance of antioxidant capacity produced by beauvericin in CHO-K1 cells, Toxicology Letters, 226(3), 337-342.

Mallebrera B., Juan-Garcia A., Font G., Ruiz M.J., 2016. Mechanisms of beauvericin toxicity and antioxidant cellular defense. Toxicol. Lett., 246, 28-34.

Manyes L., Escrivá L., Ruiz M.J., Juan-García A., 2018. Beauvericin and enniatin B effects on a human lymphoblastoid Jurkat T-cell model. Food Chem Toxicol, 115, 127-135.

Marx, H., Gedek, B. & Kollarczik, B., 1995. Comparative investigations of mycotoxological status of alternatively and conventionally grown crops. Z. Lebensm. Unters. Forsch., 201, 83-86.

Massart, F.; Meucci, V.; Saggese, G.; Soldani, G., 2008. High growth rate of girls with precocious puberty exposed to estrogenic mycotoxins. J. Pediatr. 152, 690–695.

Meca G., Zinedine A., Blesa J., Font G., Mañes J., 2010. Further data on the presence of Fusarium emerging mycotoxins enniatins, fusaproliferin and beauvericin in cereals available on the Spanish markets, Food and Chemical Toxicology, Volume 48(5), 1412-1416.

Meredith, M. J., Reed, D. J., 1982. Status of mitochondrial pool of glutathione in the isolated hepatocyte. J. Bioi. Chem. 257:3747-53

Meredith, M. J., Reed, D. J. 1 983. Depletion in vitro of mitochondrial glutathione in rat hepatocytes and enhancement of lipid peroxidation by Adriamycin and 1 ,3-bis(2-chlorocthyl)-I -nitrosourea (BCNU). Biochem. Pharmacal. 32: 1 383-88.

Minervini, F., Dell Aquila, M.E., Maritato, F., Minoia, P., Visconti, A., 2001. Toxic effects of the mycotoxin zearalenone and its derivatives on in vitro maturation of bovine oocytes and 17 Beta-estradiol levels in mural granulosa cell cultures. Toxicol. In Vitro 15, 489–495.

Minervini, F., Giannoccaro, A., Cavallini, A., Visconti, A., 2005. Investigations on cellular proliferation induced by zearalenone and its derivatives in relation to the estrogenic parameters. Toxicol. Lett. 159, 272–283.

Minervini, F., Giannoccaro, A., Fornelli, F., Dell'Aquila, M.E., Minoia, P., Visconti, A., 2006. Influence of mycotoxin zearalenone and its derivatives (alpha and beta zearalenol) on apoptosis and proliferation of cultured granulosa cells from equine ovaries. Reprod. Biol. Endocrinol. 4, 62.

Minervini, F.; Dell'Aquila, M.E., 2008. Zearalenone and Reproductive Function in Farm Animals. Int. J. Mol. Sci. 9, 2570-2584.

Mirocha, C.J., Pathre, S.V. and Robinson, T.S., 1981. Comparative metabolism of zearalenone and transmission into bovine milk. Food and Cosmetics Toxicology 19: 25-30.

Mukherjee D, Royce SG, Alexander JA, Buckley B, Isukapalli SS, Bandera E.V, Zarbl H, Georgopoulos P.G., 2014. Physiologically-Based Toxicokinetic Modeling of Zearalenone and Its Metabolites: Application to the Jersey Girl Study. PLOS ONE 9(12).

Müller, H.M., Reimann, J., Schumacher, U., Schwadorf, K., 1997a. Natural occurrence of Fusarium toxins in barley harvested during five years in an area of southwest Germany. Mycopathologia, 137, 185-192.

Müller, H.M., Reimann, J., Schumacher, U., Schwadorf, K., 1997b. Fusarium toxins in wheat harvested during six years in an area of southwest Germany. Nat. Toxins, 5, 24-30.

Munkvold G., Stahr H.M., Logrieco A., Moretti A., Ritieni A., 1998. Occurrence of fusaproliferin and beauvericin in Fusarium-contaminated livestock feed in Iowa Applied and Environmental Microbiology, 64, 3923-3926.

Murata, H., Sultana, P., Shimada, N., Yoshioka, M., 2003. Structure-activity relationships among Zearalenone and its derivatives based on bovine neutrophil chemiluminescence. Vet. Hum. Toxicol. 45, 18–20.

Nagy, Z., 2000. Cell cycle regulatory failure in neurones: causes and consequences. Neurobiol. Aging 21, 761–769.

Nakajyo, S., Matsuoka, K., Kitayama, T., Yamamura, Y., Shimizu, K., Kimura, M., and Urakawa, N., 1987. Inhibitory effect of beauvericin on a high K+-induced tonic contraction in guinea-pig taenia coli. Jpn. J. Pharmacol. 45, 317-325.

Ojcius D.M., Zychlinsky A., Zheng L.M., Young J.D., 1991. Ionophore induced apoptosis: role of DNA fragmentation and calcium fluxes. Exp. Cell. Res., 197, 43-49.

Olsen, M., Kiessling, K.H., 1983. Species differences in zearalenone-reducing activity in subcellular fractions of liver from female domestic animals. Acta Pharmacologica and Toxicologica (Copenhagen) 52: 287-291.

Olsen, M., Mirocha, C.J., Abbas, H.K., Johansson B., 1986. Metabolism of high concentrations of dietary zearalenone by young male turkey poults. Poultry Science 65: 1905-1910.

Olsen, M., Pettersson, H., Kiessling, K.H., 1981. Reduction of zearalenone to zearalenol in female rat liver by 3 alpha-hydroxysteroid dehydrogenase. Acta Pharmacol. Toxicol. (Copenh) 48, 157–161.

Olsen, M., Pettersson, H., Sandholm, K., Visconti, A., Kiessling, K.H., 1987. Metabolism of zearalenone by sow intestinal mucosa in vitro. Food Chem. Toxicol. 25, 681–683.

Organisation for Economic Co-operation and Development (OECD). 2011. In Environment, Health and Safety News: The OECD Environment, Health and Safety Programme: Achievements, no. 27 on December 2011, [online: http://www.oecd.org/env/chemicalsafetyandbiosafety/49171557.pdf]

Oyarce A.M., Patrick J., 1991. Fleming, Multiple forms of human dopamine β-hydroxylase in SH-SY5Y neuroblastoma cells, Archives of Biochemistry and Biophysics, 290(2), 503-510.

Paciolla C, Dipierro N, Mule G, Logrieco A, Dipierro S., 2004. The mycotoxins beauvericin and T-2 induce cell death and alteration to the ascorbate metabolism in tomato protoplasts. Physiol Mol Plant Pathol, 65:49–56.

Parveen M, Zhu Y, Kiyama R., 2009. Expression profiling of the genes responding to zearalenone and its analogues using estrogen-responsive genes. FEBS Lett. 583: 2377-2384.

Pieter S.S., 1995. Mycotoxins, general view, chemistry and structure. Toxicology Letters, 82–83, 843-851.

Prelusky, D.B., Scott, P.M., Trenholm, H., Lawrence, G.A., 1990. Minimal transmission of earalenone to milk of dairy cows. J. Environ. Sci. Health B 25, 87–103.

Presgraves S.P., Ahmed T., Borwege S., Joyce J.N., 2004. Terminally differentiated SH-SY5Y cells provide a model system for studying neuroprotective effects of dopamine agonists. Neurotox Res 5:579–598.

Prosperini A., Juan-García A., Font G., Ruiz M.J., 2013a. Beuvericin induced cytotoxicity via ROS production and mitochondrial damage in Caco-2 cells. Toxicol. Lett., 222, 204-211.

Prosperini A., Juan-García A., Font G., Ruiz M.J., 2013b. Reactive oxygen species involvement in apoptosis and mitochondrial damage in Caco-2 cells induced by enniatins A. A1, B and B1. Toxicol. Lett., 222, 36-44.

Que F.G., Gores G.J., Larusso N.F., 1997. Development and initial application of an in vitro model of apoptosis in rodent cholangiocytes. Am. J. Physiol., 35, 106-115.

RASFF — The Rapid Alert System for Food and Feed — Annual Report 2019: file:///C:/Users/fozhan/Downloads/EWAC20001ENN.en.pdf.

Resnik, S., Neira, S., Pacin, A., Martinez, E., Apro, N. & Latreite, S., 1996. A survey of the natural occurrence of aflatoxins and zearalenone in Argentine field maize: 1983-1994. Food Addit. Contam., 13, 115-120.

Richardson, K.E., Hagler, W.M., Mirtocha, C.J., 1985. Production of zearalenone α - and β -zearalenol and α- and β-zearalanol by Fusarium spp. in rice culture. J. Agric. Food Chem. 33, 862–866.

Ritieni A., Moretti A., Logrieco A., Bottalico A., Randazzo G., S.M. Monti, Ferracane, R., Fogliano, V., 1997. Occurrence of fusaproliferin, fumonisin B1 and beauvericin in maize from Italy Journal of Agricultural and Food Chemistry, 45, 4011-4016.

Rudik A.V., Bezhentsev V.M., Dmitriev A.V., Druzhilovskiy D.S., Lagunin A.A., Filimonov D.A., Poroikov V.V., 2017. MetaTox: web application for predicting structure and toxicity of xenobiotics' metabolites. J. Chem. Inf. Model., 57, 638-642.

Ruiz M.J., Franzova P., Juan-Garcia A., Font G., 2011a. Toxicological interactions between the mycotoxins beauvericin, deoxynivalenol and T-2 toxin in CHO-K1 cells in vitro. Toxicon, 58, 315-326.

Ruiz M.J., Macakova P., Juan-Garcia A., Font G., 2011b. Cytotoxic effects of mycotoxin combination in mammalian kidney cells. Food Chem. Toxicol., 49, 2718-2724.

Schollenberger, M., Müller, H.M., Rüfle, M., Suchy, S., Planck, S., Drochner, W., 2006. Natural occurrence of 16 fusarium toxins in grains and feedstuffs of plant origin from Germany. Mycopathologia 161, 43–52.

Scorrano L., Oskes S.A., Opferman J.T., Cheng E.H., Sorcinelli M.D., Pozzan T., Korsmeyer S.J., 2003. BAX and BAK regulation of endoplasmic reticulum Ca2+: a control point for apoptosis Science, 300, 135-139.

Shephard G.S., Sewram V., Nieuwoudt T.W., Marasas W.F.O., Ritieni A., 1999. Production of the mycotoxins fusaproliferin and beauvericin by South

African isolates in the Fusarium section Liseola Journal of Agricultural and Food Chemistry, 47, 5111-5115.

So M.Y, Tian Z, Phoon Y.S, Sha S, Antoniou M.N, Zhang J, Wu R.S.S., Tan-Un K.C., 2014. Gene Expression Profile and Toxic Effects in Human Bronchial Epithelial Cells Exposed to Zearalenone. PLoS ONE 9(5): e96404.

Szüts, P.; Mesterházy, Á.; Falkay, G.Y.; Bartók, T., 1997. Early thelarche symptoms in children and their relations to zearalenone contamination in foodstuffs. Cereal Res. Commun. 25, 429–441.

Taevernier L., Bracke N., Veryser L., Wynendaele E., Gevaert B., Peremans K., De Spiegeleer B., 2016. Blood-brain barrier transport kinetics of the cyclic depsipeptide mycotoxins beauvericin and enniatins. Toxicology Letters, 258, 175-184.

Takeuchi H., Yanagida T., Inden M., Takata K., Kitamura Y., Yamakawa K., Sawada H., Izumi Y., Yamamoto N., Kihara T., Uemura K., Inoue H., Taniguchi T., Akaike A., Takahashi R., Shimohama S., 2009. Nicotinic receptor stimulation protects nigral dopaminergic neurons in rotenone-induced Parkinson's disease models. J Neurosci Res 87:576–585.

Tashiro, F., Kawabata, Y., Naoi, M. & Ueno, Y., 1980. Zearalenone-estrogen receptor interaction and RNA synthesis in rat uterus. In: Preuser, H.J., ed., Medical Mycology, Stuttgart: Fischer, Suppl. 8, pp. 311-320.

Tatay, E; Espín, S; García-Fernández, A.J; Ruiz, M.J., 2017a. Estrogenic activity of zearalenone, α-zearalenol and β-zearalenol assessed using the E-Screen assay in MCF-7 cells. Toxicology Mechanisms and Methods, 1–15.

Tatay, E., Espin, S., Garcia-Fernandez, A.J., Ruiz, M.J., 2017b. Oxidative damage and disturbance of antioxidant capacity by zearalenone and its metabolites in human cells. Toxicology In Vitro, 45, 334-339.

Tatay, E., Meca, G., Font, G., Ruiz, M.J., 2014. Interactive effects of zearalenone and its metabolites on cytotoxicity and metabolization in ovarian CHO-K1 cells. Toxicology in Vitro. 28, 95-103.

Tomoda H., Huang X.H., Cao J., Nishida H., Nagao R., Okuda S., Tanaka H., Omura S., Arai H., Inoue J.K., 1992. Antibiot. (Tokyo), 45, 1626-1632.

Tonshin, A.A., Teplova, V.V., Andersson, M.A., Salkinoja-Salonen, M.S., 2010. The Fusarium mycotoxins enniatins and beauvericin cause mitochondrial dysfunction by affecting the mitochondrial volume regulation, oxidative phosphorylation and ion homeostasis. Toxicology, 276, 49-57.

Ueno, Y. and Tashiro, F., 1981. α-Zearalenol, a major hepatic metabolite in rats of zearalenone, an estrogenic mycotoxin of Fusarium species. Journal of Biochemistry 89: 563-571.

Ueno, Y., Ayaki, S., Sato, N. and Ito, T., 1977. Fate and mode of action of zearalenone. Annales de la Nutrition et de l'Alimentation 31: 935-948.

Ueno, Y., Tashiro, F., Kobayashi, T., 1983. Species differences in zearalenone-reductase activity. Food Chem. Toxicol. 21, 167–173.

Uhlig S., Jestoi M., Parikka P., 2007. Fusarium avenaceum—the North European situation Int. J. Food Microbiol., 119, 17-24.

Venkataramana, M.; Chandra Nayaka, S.; Anand, T.; Rajesh, R.; Aiyaz, M.; Divakara, S.T.; Murali, H.S.; Prakash, H.S.; Lakshmana Rao, P.V., 2014. Zearalenone induced toxicity in SHSY-5Y cells: The role of oxidative stress evidenced by N-acetyl cysteine. Food Chem. Toxicol. 65, 335–342.

Vrabcheva, T., Gessler, R., Usleber, E. & Märtlbauer, E., 1996. First survey on the natural occurrence of Fusarium mycotoxins in Bulgarian wheat. Mycopathologia, 136, 47-52.

Wagner B.L., Lewis L.C., 2000. Colonization of corn, Zea mays by the entomopathogenic fungus Beauveria bassiana Appl. Environ. Microbiol, 66, 3468-3473.

Watjen W., Debbab A., Hohlfeld A., Chovolou Y., Proksch P., 2014. The mycotoxin beauvericin induces apoptotic cell death in H4IIE hepatoma cells accompanied by an inhibition of NF-κB-activity and modulation of MAP-kinases. Toxicol. Lett., 231, 9-16.

Wollenhaupt, K., Jonas, L., Tiemann, U., Tomek, W., 2004. Influence of the mycotoxins alpha- and beta-zearalenol on regulators of cap-dependent translation control in pig endometrial cells. Reprod. Toxicol. 19 (2), 189–199.

Xiao Z., Huang C., Wu J., Sun L., Hao W., Leung L.K., Huang J.., 2013. The neuroprotective effects of ipriflavone against H_2O_2 and amyloid beta

induced toxicity in human neuroblastoma SH-SY5Y cells European journal of pharmacology, 721, 286-293.

Young, L.G. and King, G.J., 1984. Zearalenone and swine reproduction. Journal of the American Veterinary Medical Association 185: 334-335.

Zeiss CJ., 2003. The apoptosis-necrosis continuum: insights from genetically altered mice. Vet Pathol. 40:481–95.

Zheng, W., Wang, B., Si, M., Zou H., Song R., Gu J., Yuan Y., Liu X., Zhu G., Bai J., Bian J., Liu Z.P., 2018a. Zearalenone altered the cytoskeletal structure via ER stress- autophagy- oxidative stress pathway in mouse TM4 Sertoli cells. Sci Rep, 8, 3320.

Zheng, W.L.; Wang, B.J.; Wang, L.; Shan, Y.P.; Zou, H.; Song, R.L.; Wang, T.; Gu, J.H.; Yuan, Y.; Liu, X.Z.; Zhu, G.Q.; Bai, J.F.; Liu, Z.P.; Bian, J.C., 2018b. ROS-Mediated Cell Cycle Arrest and Apoptosis Induced by Zearalenone in Mouse Sertoli Cells via ER Stress and the ATP/AMPK Pathway. Toxins, 10, 24.

Zhou S., Wang Y., Ma L., Chen X., Lü Y., Ge F., Chen Y., Chen X., Lian Q., Jin X.D., Ge R.S., 2018. Zearalenone Delays Rat Leydig Cell Regeneration, Toxicological Sciences, Volume 164(1), 60–71.

Zinedine A., Meca G., Mañes J., Font G., 2011. Further data on the occurrence of Fusarium emerging mycotoxins enniatins (A, A1, B, B1), fusaproliferin and beauvericin in raw cereals commercialized in Morocco. Food Control, 22(1), 1-5.

Zinedine, A., Soriano, J.M., Moltó, J.C. and Mañes, J., 2007. Review on the toxicity, occurrence, metabolism, detoxification, regulations and intake of zearalenone: an oestrogenic mycotoxin. Food and Chemical Toxicology 45: 1-18.

Zingales V., Fernández-Franzón M., Ruiz M.J., 2020. Sterigmatocystin-induced cytotoxicity via oxidative stress induction in human neuroblastoma cells. Food and Chemical Toxicology., 136, 110956.

Zouaoui N., Mallebrera B., Berrada H., Abid-Essefi S., Bacha H., Ruiz M.J., 2016. Cytotoxic effects induced by patulin, sterigmatocystin and beauvericin on CHO–K1 cells. Food and Chemical Toxicology, 89, 92-103.

2. OBJETIVOS

3. OBJETIVOS

El objetivo principal de esta Tesis Doctoral fue el de estudiar los efectos de las micotoxinas alfa-zearalenol (α-ZEL), beta-zearalenol (β-ZEL) y beauvericina (BEA) *in silico* e *in vitro* en la línea celular de neuroblastoma humano, SH-SY5Y.

Para llevar a cabo este objetivo, las células SH-SY5Y estuvieron expuestas a tratamientos individuales y combinados de α-ZEL, β-ZEL y BEA para alcanzar los siguientes objetivos parciales:

1. Predecir el perfil metabolómico de zearalenona, α-ZEL y β-ZEL y sus efectos tóxicos mediante metodología *in silico*.
2. Determinar el tipo de interacción toxicológicos (sinergismo, adición o antagonismo) en las combinaciones binarias y terciarias de las micotoxinas estudiadas y determinar la micotoxina más involucrada en dicho efecto cuantificándolas por LC-qTOF-MS en el medio de cultivo celular.
3. Analizar el rol de estrés oxidativo mediante la evaluación de la generación de especies reactivas de oxígeno y la actividad de las enzimas implicadas en el sistema de defensa enzimático y no enzimático.
4. Examinar la expresión de genes implicados en el proceso de muerte celular por apoptosis (*CASP3*, *BAX y BCL2*) y de receptores de estrógenos (*ERβ* y *GPER1*) por RT-PCR.
5. Evaluar la progresión del ciclo celular y la activación de la ruta de muerte celular por citometría de flujo.

2. OBJECTIVES

The main objective of this Doctoral Thesis is the study of the effects of the mycotoxins alfa-zearalenol (α-ZEL), beta-zearalenol (β-ZEL) and beauvericin (BEA) *in silico* and *in vitro* on human neuroblastoma cells SH-SY5Y.

To carry out these objectives, SH-SY5Y cells were exposed to individual and combined treatments of α-ZEL, β-ZEL and BEA to achieve the following specific objectives:

1. Predict the metabolomics profile of zearalenone, α-ZEL and β-ZEL, and their toxic effects via an *in silico* study.
2. Determine the toxicological interactions (synergism, additive or antagonism) in binary and tertiary combinations of assayed mycotoxins and determine the most involved mycotoxin in mentioned effect, quantifying them with LC-qTOF-MS in cell culture medium.
3. Analyse the role of oxidative stress by evaluating the generation of reactive oxygen species and intracellular defense systems of enzymatic and non-enzymatic activity.
4. Examine the expression of genes involved in cell death process by apoptosis (*CASP3*, *BAX, BCL2*) and receptors of estrogens (*ERβ* and *GPER1*) by RT-PCR.
5. Evaluate the cell cycle progression and activation of cell death pathway by flow cytometry.

3. RESULTADOS

Study 1

In silico methods for metabolomic and toxicity prediction of zearalenone, α-zearalenone and β-zearalenone

Fojan Agahi, Cristina Juan*, Guillermina Font, Ana Juan-García

Laboratory of Toxicology and Food Chemistry, Faculty of Pharmacy, University of Valencia, Burjassot 46100, Valencia, Spain

Agahi et al., 2020a. Food and Chemical Toxicology 146, 111818

Abstract

Zearalenone (ZEA), α-zearalenol (α-ZEL) and β-zearalenol (β-ZEL) (ZEA's metabolites) are co/present in cereals, fruits or their products. All three with other compounds, constitute a cocktail-mixture that consumers (and also animals) are exposed and never entirely evaluated, nor in vitro nor in vivo. Effect of ZEA has been correlated to endocrine disruptor alterations as well as its metabolites (α-ZEL and β-ZEL); however, toxic effects associated to metabolites generated once ingested are unknown and difficult to study. The present study defines the metabolomics profile of all three mycotoxins (ZEA, α-ZEL and β-ZEL) and explores the prediction of their toxic effects proposing an *in silico* workflow by using three programs of predictions: MetaTox, SwissADME and PASS online. Metabolomic profile was also defined and toxic effect evaluated for all metabolite products from Phase I and II reaction (a total of 15 compounds). Results revealed that products describing metabolomics profile were: from O-glucuronidation (1z and 2z for ZEA and 1 ab, 2 ab and 3 ab for ZEA's metabolites), S-sulfation (3z and 4z for ZEA and 4 ab, 5 ab and 6 ab for ZEA's metabolites) and hydrolysis (5z and 7 ab for ZEA's metabolites, respectively). Lipinsky's rule-of-five was followed by all compounds except those coming from O-glucuronidation (HBA>10). Metabolite products had better properties to reach blood brain barrier than initial mycotoxins. According to Pa values (probability of activation) order of toxic effects studied was carcinogenicity > nephrotoxic > hepatotoxic > endocrine disruptor > mutagenic (AMES TEST) > genotoxic. Prediction of inhibition, induction and substrate function on different isoforms of Cytochrome P450 (CYP1A1, CYP1A2, CYP2C9 and CYP3A4) varied for each compounds analyzed; similarly, for activation of caspases 3 and 8. Relying to our findings, the metabolomics profile of ZEA, α-ZEL and β-ZEL analyzed by in silico programs predicts alteration of systems/pathways/mechanisms that ends up causing several toxic effects, giving an excellent sight and direct studies before starting *in vitro* or *in vivo* assays contributing to 3Rs principle; however, confirmation can be only demonstrated by performing those assays.

Keywords: Zearalenone; Metabolomics; Prediction; SwissADME; PASS online; MetaTox; In silico

1. Introduction

Mycotoxins are low-molecular-weight toxic compounds synthetized by different types of molds belonging mainly to the genera *Aspergillus*, *Penicillium*, *Fusarium* and *Alternaria* (Berthiller et al., 2013; Juan et al., 2020, Pascari et al., 2019). Effects associated are diverse according to the chemical structure which provides a great variety in ADME/T characteristics (absorption, distribution, metabolism, and excretion/toxicity) and still to elucidate for most of them.

Zearalenone (ZEA) is a *Fusarium* mycotoxin of primary concern. It is commonly found in cereals like barley, sorghum, oats, wheat, millet, and rice (Juan et al., 2017a, 2017b; Stanciu et al., 2017; Bakker et al., 2018; Oueslati et al., 2020). When ingested and metabolized, two major metabolites, α-zearalenol (α-ZEL) and β-zearalenol (β-ZEL), can be found in various tissues; nonetheless, their presence is starting to be commonly found in food and feed as natural contaminants (EFSA et al., 2011, 2017). Once ingested by the consumer, further metabolite products from all three mycotoxins (ZEA, α-ZEL and β-ZEL) can be generated by Phase I and II reactions, although their effect is unknown. Studies of these compounds contribute to metabolomics profile for following the compound transformation (metabolic changes) whose identification and quantification will help to elucidate the complete toxic effects. It can help to understand global metabolic disturbances.

Effects associated to ZEA, α-ZEL and β-ZEL have been studied in vitro and in vivo and estrogenic effect, oxidative stress, cytotoxicity, DNA damage, among others have been reported (Eze et al., 2019; Frizzell et al., 2011; Agahi et al., 2020; Juan-García et al., 2020). On the other hand, the entire implication of these compounds in producing toxic effects are unknown, same as with its metabolite products originated in Phase I and II reactions. So that, there are

many indirect or side effects associated yet not studied and their involvement in pathways, cascade or routes still need to be discovered. Nowadays, the development of computational and informatics programs facilitates to predict experimental approaches in toxicology which need to be confirmed with further assays. These systems use chemical structures, parameters and descriptors which by comparison with other studied compounds, can give as a result empirical knowledge of their effect to prevent against exposure or even to promote the development of therapeutics to avoid or decrease toxic effects, concerning drugs.

Combination of compounds is a routine practice in medicine for palliate diseases achieving successful results. Previous to this practice it is necessary to evaluate the potential effects that this might cause. For toxic compounds there have been developed several mathematical methods implemented in informatics programs for assessing the effect of compounds combination and effects contributing to computational toxicology: Chou and Talalay by using isobolograms, Simple Addition of Effect, Factorial Analysis of Variance by using simple 2-way ANOVA, Bliss Independence Criterion, Loewe's Additivity Law, Highest Single Agent (HSA) Model (Gaddums non-interaction), etc. (Kifer et al., 2020). For mycotoxins' mixture assessment, Choy and Talalay method has been widely used in predicting potential effects (synergism, addition and antagonism) (Juan-García et al, 2016, 2019a, 2019b; Agahi et al., 2020) even with strong differences in chemical structures as well as in the variety of fungi spp. producer.

The global research scenario for new therapies and development of new drugs for common diseases, or as it is happening nowadays in the global world pandemic SARS-COVID-19 for health side-effects, the use of virtual screening techniques for helping in the discovery of new strategies and without using or

avoiding long-term biological assays, is a good alternative. All these strategies end-up in exploring profile of effects by application of computer programs. One of this alternative programs is PASS online (Prediction of Activity Spectra for Substances) an in silico approach that reveals biological activities of compounds, their mechanisms of action and connected side-effects (Lagunin et al., 2000). The available PASS online version predicts over 4000 kinds of biological activity, including pharmacological effects, mechanisms of action, toxic and adverse effects, interaction with metabolic enzymes and transporters, influence on gene expression, etc. as described on its web page (www.pharmaexpert.ru/passonline) (Lagunin et al., 2000). Prediction is based on the analysis of structure activity-relationships for more than 250,000 biologically active substances including drugs, drug-candidates, leads and toxic compounds (Lagunin et al., 2000).

The support of new compounds discoveries and knowledge of its toxicity is given by other on-line programs which work with different parameters, some of them are: SwissADME, Meta-Tox, GUSAR, ROSC-Pred, etc. Each program is focused in providing different predictions, and for example while MetaTox predicts the Phase I and II metabolite products that can be generated from one compound (Rudik et al., 2017), SwissADME is a computational program that allows to compute physicochemical descriptors as well as ADME parameters, pharmacokinetic properties, drug-like nature and medicinal chemistry friendliness of one or multiple small molecules (Daina et al., 2017).

To escape long-term biological assays and implementing the computational programs for testing compounds and their predicted metabolites, here it is presented an in silico working procedure and the prediction of the entire potential effects of three mycotoxins (zearalenone (ZEA), α-zearalenol (α-ZEL) and β-zearalenol (β-ZEL)) and its Phase I and II metabolite products, by

using three in silico programs described for computational toxicology: MetaTox, SwissADME and PASS online; all available on-line.

2. Materials and methods

Mycotoxins herein studied for this predictive *in silico* study displayed endocrine disruptor effects associated and correspond to: zearalenone (ZEA) (MW: 318,37 g/mol), α-zearalenol (α-ZEL) and β-zearalenol (β-ZEL) (MW: 320,38 g/mol) (Figure 1).

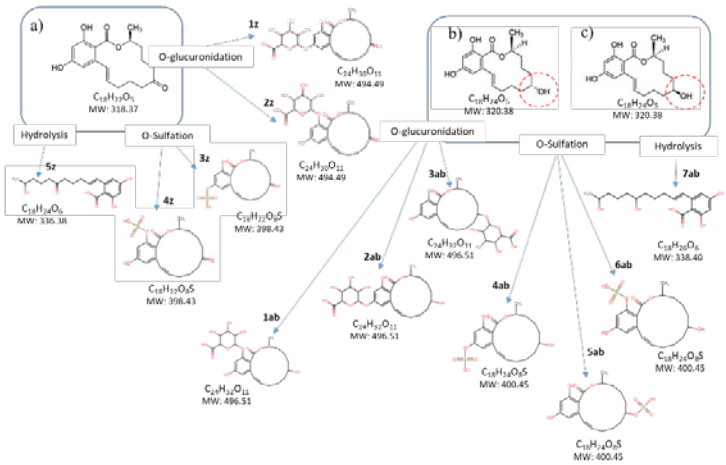

Figure 1. Metabolomic profile and chemical structures of mycotoxins predicted by MetaTox: ZEA (a), α-ZEL (b) and β-ZEL (c).

2.1. Procedure followed (workflow)

Firstly, prediction of Phase I and II metabolites products was obtained by MetaTox software (http://way2drug.com/mg2/) with a molecular sketcher based on Marvin JS chemical editor. This editor is used for input and visualization of molecular structure (in canonical SMILE) of each mycotoxin, obtaining a metabolomic profile. "No-limit" in metabolite likeness and "all"

reactions in predicting metabolites for drawn structure were selected (Rudik et al., 2017). Secondly, all compounds predicted from reactions and mycotoxins were evaluated through i)SwissADME by obtaining physicochemical descriptors (http://www.swissadme.ch/index.php) (Daina et al., 2017; Cheng et al., 2012; Yang et al., 2018) and following the Lipinski's rule of five (RO5) (see section 2.2. below) and ii)SwissSimilarity which provides an identification number HMDB (Human Metabolome Database version 4.0, https://hmdb.ca/) with a score associated (Zoete et al., 2016). Afterwards, all compounds were predicted as active compounds or inactive compounds according to probability of activation values (Pa) and probability of inactivation values (Pi), respectively; as well as their biological activities through PASS online software (http://www.pharmaexpert.ru/passonline/info.php) (Workflow 1). Lastly, potential toxic effects were predicted for Pa > Pi with PASS online software.

2.2. *In silico* software: MetaTox, SwissADME and PASS online

Three *in silico* softwares available online for studying prediction of toxicity and biological activities were used: MetaTox, SwissADME and PASS online.

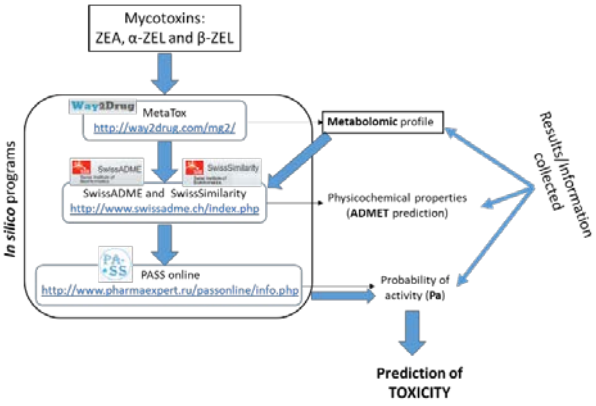

Workflow 1. Procedure followed to predict the toxic effect of mycotoxins and its metabolite products by using different *in silico* programs.

MetaTox is a software based in generating metabolites and calculating probability of their formation where metabolism pathway generation is integrated with the prediction of acute toxicity. Metabolomics' profile is predicted by the formation from nine classes of reactions (aliphatic and aromatic hydroxylation, N and O-glucuronidation, N-, S- and C-oxidation, and N- and O-dealkylation) that are catalyzed by five human isoforms of cytochromes P450s (1A2, 2C19, 2C9, 2D6, 3A4) and by human UDP glucuronosyltransferase without differentiation into isoforms. The calculation of probability for generated metabolites is based on analyses of "structure-biotransformation reactions" and "structure-modified atoms" relationships using a Bayesian approach (Rudik et al., 2017).

SwissADME is a web tool that enables to predict the computation of key physicochemical properties, pharmacokinetics, mycotoxin-likeness and medicinal chemistry friendliness (for one or multiple molecules), (Daina et al., 2017; Cheng et al., 2012; Yang et al., 2018). This predictive in silico model shows statistical significance, predictive power, intuitive interpretation, and straight forward translation to molecular design. This program uses Lipinski's rule-of-five (RO5) for the lead compounds. The compounds were then filtered through that rule (RO5) to predict their mycotoxins likeliness. Lipinski's descriptors evaluate the molecular properties for compound pharmacokinetics in the human body, especially for oral absorption. The rule states molecules to have: molecular weight (MW) ≤500, number of hydrogen bond donors (HBD) ≤5, number of hydrogen bond acceptors (HBA) ≤10, cLogP ≤5 and number of rotable bounds (n-ROTB) ≤10. Molar reactivity in the range of 40–130 and topological polar

surface area (TPSA) were also considered. Targets of p-glycoprotein (P-gp) efflux and isoforms of cytochrome P450 that metabolize the majority of toxic compounds (CYP3A4, CYP2C9, CYP2C19, CYP1A1 and CYP1A2) were investigated.

The biological prediction of activity spectra for mycotoxins and metabolite products were obtained by PASS online (available in www.pharmaexpert.ru/passonline) (Lagunin et al., 2000). This software was used to evaluate the general biological potential of all compounds and provided simultaneous prediction of several types of biological activity based on their chemical structure. It also estimated the predicted activity spectrum of mycotoxins as probable activity (Pa, probability to be active) and probable inactivity (Pi, probability to be inactive). Both probabilities, Pa and Pi values, vary from 0.000 to 1.000; nevertheless, values are expressed as percentage of probability (%).

Among all toxic effects for all three mycotoxins and products of Phase I and II reactions provided from PASS, prediction was evaluated for: carcinogenesis, endocrine disruption, nephrotoxicity, mutagenicity (with and without AMES test), genotoxicity and hepatotoxicity. Biological activities prediction inhibiting, inducing or as substrate was evaluated for different isoforms of Cytochrome P450 and caspases 3 and 8. All predictions of probabilities were expressed as percentage of probability (%).

3. Results

3.1. Meta-Tox for predicting metabolite products: describing the metabolomics profile.

Metabolite prediction included in MetaTox uses dictionaries of biotransformation based on preliminary prediction of possible classes of

biotransformation describing also the metabolomics profile of the compounds. Mycotoxins' canonical SMILE structure were used to predict metabolite products in MetaTox. Figure 1 collects chemical structure of mycotoxins and metabolite products predicted by MetaTox (five from ZEA (from 1z to 5z) and 7 for each ZEA's metabolite (from 1 ab to 7 ab)). Metabolite products predicted for ZEA were from: reaction of O-glucuronidation (metabolites 1z and 2z), reaction of S-sulfation (metabolites 3z and 4z) corresponding to Phase II products and one from reaction of hydrolysis (5z) corresponding to Phase I products. For α-ZEL and β-ZEL, products were equal for each one with a total of seven products for each isoform and corresponding to same reactions as ZEA: O-glucuronidation (metabolites: 1 ab, 2 ab and 3 ab), S-sulfation (metabolites: 4 ab, 5 ab and 6 ab) and hydrolysis (metabolite 7 ab) reactions. A total of 12 compounds were proposed as predicted metabolites products form Phase I and II reactions.

3.2. SwissADME for physicochemical descriptors of zearalenone, α-zearalenol, β-zearalenol and phase I and II metabolite products

Target of mycotoxins in organs and systems are wide and unknown for most of them; however, they are able to activate several routes or pathways. ZEA, α-ZEL and β-ZEL were analyzed through SwissADME online sever for molecular properties to validate them as potential inducers/activators of toxic mechanisms. All three mycotoxins were filtered through Lipinski's RO5 to predict their mycotoxin likeliness (Table 1). All three mycotoxins and metabolite products were studied and only metabolites coming from O-glucuronidation of ZEA (metabolites 1z and 2z) or α-ZEL and β-ZEL (metabolites 1 ab, 2 ab and 3 ab) violated Lipinski's rule because of HBA (hydrogen bond acceptor) (Table 1). It is also reported the human metabolome database identification number

(HMDB ID) and the score of similarity predicted provided from SwissSimilarity. All compounds had one or more HMDB ID with score >50% (Table 1). To notice that values were the same for metabolite products coming from the same metabolization reaction.

Table 1. Lipinski's molecular descriptors for ZEA, ZEA's metabolites (α-ZEL and β-ZEL) and its products of reaction (from O-glucuronidation, O sulfation and hydrolysis) from SwissADME and SwissSimilarity.

	HMDB ID	MW (≤500)	HBD (≤5)	HBA (≤10)	cLog P (<5)	MR (≤10)	n-ROTB (≤10)	TPSA
ZEA	31752 (99.6%)	318.37	2	5	3.58	88.40	0	83.83
O-Glucuronidation								
Metabolite 1z*	34753 (74.1%)	494.49	5	11*	1.14	121.13	3	180.05
Metabolite 2z*	60634 (84.3%)							
O-Sulfation								
Metabolite 3z	33623 (99.6%)	398.43	2	8	3.06	98.60	2	135.58
Metabolite 4z	31752 (87.6%)							
Hydrolysis								
Metabolite 5z	31752 (52.4%)	336.38	4	6	3.10	92.16	10	115.06
α-ZEL and β-ZEL	41838 (99.8%) 41824 (99.7%)	320.38	3	5	3.37	89.36	0	86.99
O-Glucuronidation								
Metabolite 1ab*	34753 (86.8%)							
Metabolite 2ab*	60634 (75.6%)	496.51	6	11*	0.94	122.09	3	183.21
Metabolite 3ab*	31752 (53.9%)							
O-Sulfation								
Metabolite 4ab	33623 (91.5%)							
Metabolite 5ab	31752 (90.4%)	400.45	3	8	2.85	99.56	2	138.74
Metabolite 6ab	41838 (91.1%)							
Hydrolysis								
Metabolite 7ab	41824 (50.6%)	338.40	5	6	2.89	93.12	10	118.22

HMDB ID = Human Metabolome Database Identification; MW = Molecular weight; g/mol (acceptable range: <500); HBD = Hydrogen bond donor (acceptable range: ≤5); HBA = Hydrogen bond acceptor (acceptable range: ≤10); cLogP = High lipophilicity (expressed as LogP, acceptable range: <5); MR = Molar refractivity (acceptable range: 40–130); n-ROTB: number of rotatable bounds; TPSA = Topological polar surface area; Å2. *Denotes violation of Lipinski's RO5.

Probability for ADMET and toxicity profile for all compounds was evaluated. Table 2 reports values for mycotoxins, while Table 3 for metabolite products of Phase I and II's reactions of all three mycotoxins. Results reveal that ZEA mycotoxin has very low prediction for BBB crossing (28.22%) and similar tendency was obtained for α-ZEL and β-ZEL (31.47%). However, high gastrointestinal absorption was reported for all three mycotoxins (HIA >97%, Caco-2 permeability >48% and P-glycoprotein substrate >84%) (Table 2). The results indicate moderate to high absorption by the gastrointestinal tract, but unlikely to penetrate into the brain on its current form unless metabolized (Table 3). Distribution (P-gp substrate) was favored with probability >84%. For metabolism prediction, several cytochrome P450 (CYP450) isoenzymes were evaluated showing similar pattern for all three mycotoxins. Probability of ZEA as substrate in CYP450 went from 55.40% (isoform 3A4) to 86.69% (isoform 2D6); while as inhibitor of CYP450 from 68.95% (isoform 1A2) to 91.60% (isoform 2D6). For α-ZEL and β-ZEL, as substrates of CYP450 probability went from 60.44% (isoform 2C9) to 83.54% (isoform 2D6); while as substrate from 72.46% (isoform 2C19) to 90.07% (isoform 2D6) (Table 2). For toxicity evaluation, ZEA reported higher values than α-ZEL and β-ZEL (Table 2).

For Phase I and II metabolite products of all three mycotoxins, ADMET probability values revealed that all 12 compounds (5 metabolite products from ZEA and 7 products from α-ZEL and β-ZEL) were able to pass the gastrointestinal tract (>70%), especially metabolite products originated in S-Sulfation and hydrolysis. Probability of BBB crossing was >95% for all same metabolites originated in same reaction mentioned above although quite low for O-glucuronidation metabolite products (<37%) (Table 3). Distribution (P-gp substrate) was favored for all compounds originated from all reactions (>73%).

It is noticed that as long as the Phase I and II reactions take place, metabolite products become more suitable to reach BBB compartment (Table 3).

Table 2. Probability of ADMET and toxicity profile for ZEA, α-ZEL and β-ZEL.

	ZEA	**α-ZEL and β-ZEL**
	Probability (%)	Probability (%)
Absorption & Distribution		
BBB	28.22	31.47
HIA	97.61	97.50
P-gp substrate	85.50	84.12
Caco-2 permeability	48.84	59.94
LogPapp (cm/s)	-5.67	-5.39
Metabolism		
CYP450 2C9 substrate	57.95	60.44
CYP450 2D6 substrate	86.69	83.54
CYP450 3A4 substrate	55.40	57.08
CYP450 1A2 inhibitor	68.95	76.60
CYP450 2C9 inhibitor	84.90	89.37
CYP450 2D6 inhibitor	91.60	90.07
CYP450 2C19 inhibitor	75.95	72.46
CYP450 3A4 inhibitor	79.60	76.82
Toxicity		
AMES toxicity	90.0	85.00
Carcinogens	90.0	66.04
Rat acute toxicity (LD_{50}, mol/Kg)	1.88	1.94

BBB: blood-brain barrier; HIA: human gastrointestinal absorption; P-gp: P-glycoprotein.

Table 3. Probability of ADMET and toxicity profile of products predicted by MetaTox from ZEA α-ZEL and β-ZEL.

	Metabolomic profile of ZEA					Metabolomic profile of α-ZEL and β-ZEL						
Reaction	**O-Glucuronidation**		**S-Sulfation**		**Hydrolysis**	**O-Glucuronidation**			**S-Sulfation**			**Hydrolysis**
Metabolites	**1z**	**2z**	**3z**	**4z**	**5z**	**1ab**	**2ab**	**3ab**	**4ab**	**5ab**	**6ab**	**7ab**
Probability (Prob)	Prob (%)	Prob (%)	Prob (%)	Prob (%)	Prob (%)	Prob (%)	Prob (%)	Prob (%)	Prob (%)	Prob (%)	Prob (%)	Prob (%)
Absorption & Distribution												
BBB	37.65	37.65	97.05	97.05	79.17	31.47	50.00	37.65	97.00	97.04	97.00	79.17
HIA	72.33	70.65	95.94	96.20	96.75	97.50	68.84	71.40	95.72	96.97	95.90	97.43
P-gp substrate	89.04	78.58	82.69	75.15	75.38	84.12	78.48	80.17	81.59	80.54	73.72	73.06
Caco-2 permeability	81.87	87.20	76.48	80.89	62.41	59.94	86.25	86.09	66.51	55.72	70.99	61.16
LogPapp (cm/s)	-7.85	-8.24	-6.58	-6.97	-6.51	-7.96	-7.57	-7.42	-6.29	-6.14	-6.69	-6.16
Metabolism												
CYP450 2C9 substrate	100	100	79.13	59.58	59.92	60.44	79.88	80.22	58.95	61.28	61.74	61.90
CYP450 2D6 substrate	87.97	88.12	86.54	86.41	86.75	83.54	87.85	87.74	85.62	86.69	85.35	86.83
CYP450 3A4 substrate	63.85	64.20	60.69	61.92	50.71	57.08	64.36	63.41	62.04	60.19	63.23	51.50
CYP450 1A2 inhibitor	57.71		74.19		73.02	76.60	53.79	57.71	69.70	72.83	69.70	64.06
CYP450 2C9 inhibitor	92.01		82.74		84.24	89.37	92.95	92.01	82.61	81.81	82.61	79.70
CYP450 2D6 inhibitor	92.29		87.55		90.45	90.07	91.41	92.29	87.62	86.89	87.62	90.48
CYP450 2C19 inhibitor	74.09		77.83		82.96	72.46	79.05	74.09	75.21	76.29	75.21	74.04
CYP450 3A4 inhibitor	73.18		84.7		64.02	76.82	73.89	73.18	75.62	78.53	75.62	61.88
Toxicity												
AMES toxicity	68.00	66.00	73.00	66.00	79.00	85.00	67.00	70.00	68.79	76.79	60.79	74.00
Carcinogens	65.75	65.74	88.57	88.57	77.10	66.04	61.54	65.74	62.12	64.01	62.12	75.52
Rat acute toxicity (LD50, mol/Kg)	2.65	2.22	2.50	2.03	2.36	1.94	2.36	2.45	2.77	2.37	2.3	2.27

BBB: blood-brain barrier; HIA: human gastrointestinal absorption; P-gp: P-glycoprotein.

In metabolism, all ZEA's predicted products were substrate of CYP450 with probability from 100% (metabolites 1z and 2z) to 59.58% (metabolite 4z); while for α-ZEL and β-ZEL metabolites predicted products, it ranged from 51.5% (metabolite 7 ab) to 87.85% (metabolite 2 ab) (Table 3). Compounds were predicted as inhibitor for CYP450 with probabilities from 57.71% to 92.29% (metabolites 1z and 2z) for ZEA's predicted products; while from 53.79% (metabolite 2 ab) to 92.29% (metabolite 3 ab) for α-ZEL and β-ZEL's predicted products (Table 3). To notice that as inhibitors of CYP450 (for all five isoenzymes), ZEA's predicted products from O-glucuronidation (metabolites 1z and 2z) and S-sulfation (metabolites 3z and 4z) revealed the same probability; while this happened in α-ZEL and β-ZEL predicted products from S-sulfation (metabolites 4 ab and 6 ab) (Table 3).

Lastly in terms of toxicity evaluation, probability measured for AMES toxicity oscillated between 60.79% and 85% of no-AMES toxicity and carcinogenicity from 62.12 to 88.57%. Rat acute toxicity oscillated from 1.94 to 2.77 mol/kg.

3.3. Prediction of toxic effects by PASS online

Mycotoxins and products from metabolomics profile were studied by PASS online (Workflow 1). To validate them as suitable inducers/activator candidates, PASS online server was used which predicts possible effects of a compound based on its structural information. This tool compares more than 300 effects and biochemical mechanisms of compounds and gives the probability of activity (Pa) and inactivity (Pi) (Hasan et al., 2019).

Figure 2 shows the probability for seven different toxic effects: carcinogenicity, endocrine disruptor, nephrotoxic, mutagenicity (and AMES

test), genotoxicity and hepatotoxicity. It can be observed that ZEA had the highest probability in reporting carcinogenicity (78.2%); while α-ZEL and β-ZEL in genotoxicity (88.4%) (Figure 2A). Among toxic effects studied, for all metabolite products (5 from ZEA and 7 from α-ZEL and β-ZEL), carcinogenicity reported the highest probability for all three mycotoxins followed by nephrotoxic > hepatotoxic > endocrine disruptor > mutagenic (AMES TEST) > genotoxic (Figure 2B). Nonetheless, metabolite products from ZEA mycotoxin had the broadest range of probability in all toxic effects studied. Details of toxic effects per metabolite product from Phase I and II reactions are reported in Supplementary 1. Regarding the carcinogenicity effect predictions in rat and mouse (male and female), and the IARC classification is reported in Supplementary 2.

3.4. Prediction of biological activities by PASS online

Biological activities predicted by PASS online are reported in Figure 3 and Figure 4. It has been divided in one hand the most common isoforms of cytochrome P450 involved in metabolizing toxic compounds (Figure 3); and in the other hand, cysteine proteases enzymes which are primary effectors in cell death: caspase 3 and caspase 8 (Figure 4).

3.4.1. Cytochrome P450

Prediction effects on isoforms of Cytochrome P450 (CYP1A1, CYP1A2, CYP2C9 and CYP3A4) are reported in Figure 3 for all three mycotoxins and compounds defined in the metabolomics profile (from Phase I and II reactions). Effects are reported for each compounds acting as substrate, inducer or inhibitor. For all CYP450 isoforms all three mycotoxins reported effect as substrates, inducers and inhibitors; however, α-ZEL and β-ZEL reported higher

probability prediction than ZEA in all of them independently of its mode of action (Figure 3).

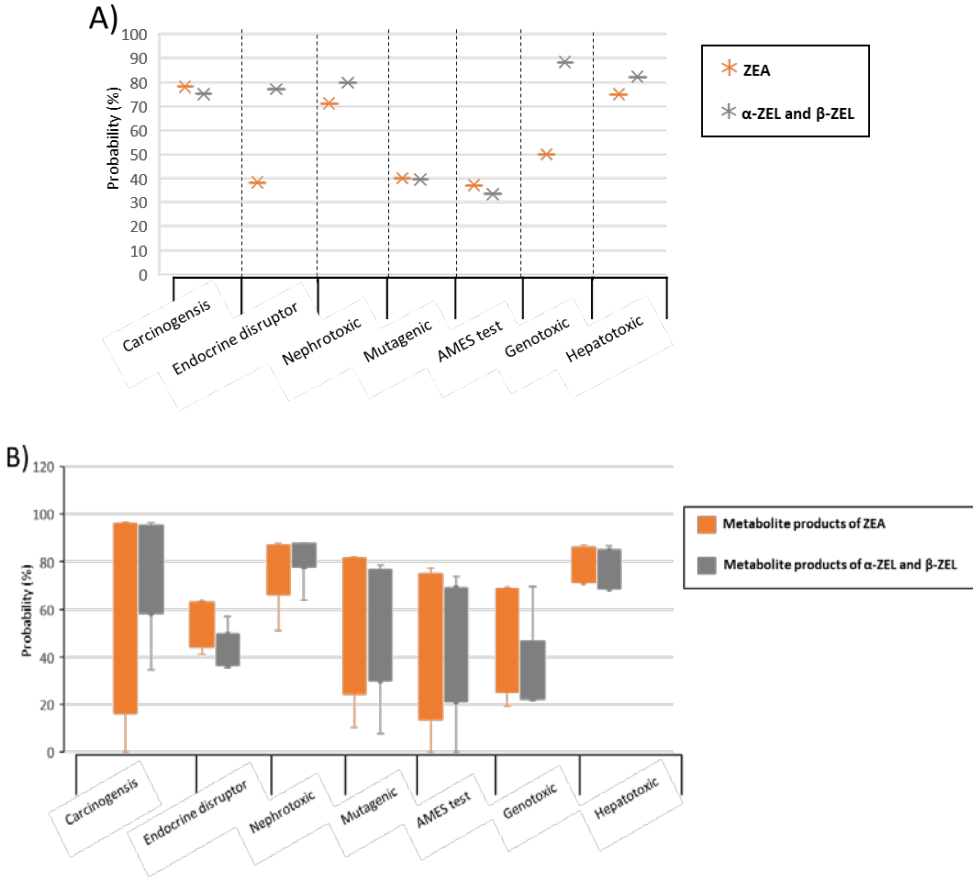

Figure 2. Prediction of toxic effects (probability, %) for ZEA (orange star), α-ZEL and β-ZEL (grey star) (A) and all metabolite products (B, box diagram) of Phase I and II reactions obtained from those mycotoxins: ZEA (orange box) and ZEA's metabolites (grey box). Bars in (B) report the maximum and minimum value of prediction out of the box. (For interpretation of the references to colour in this figure legend, the reader is referred to the Web version of this article.)

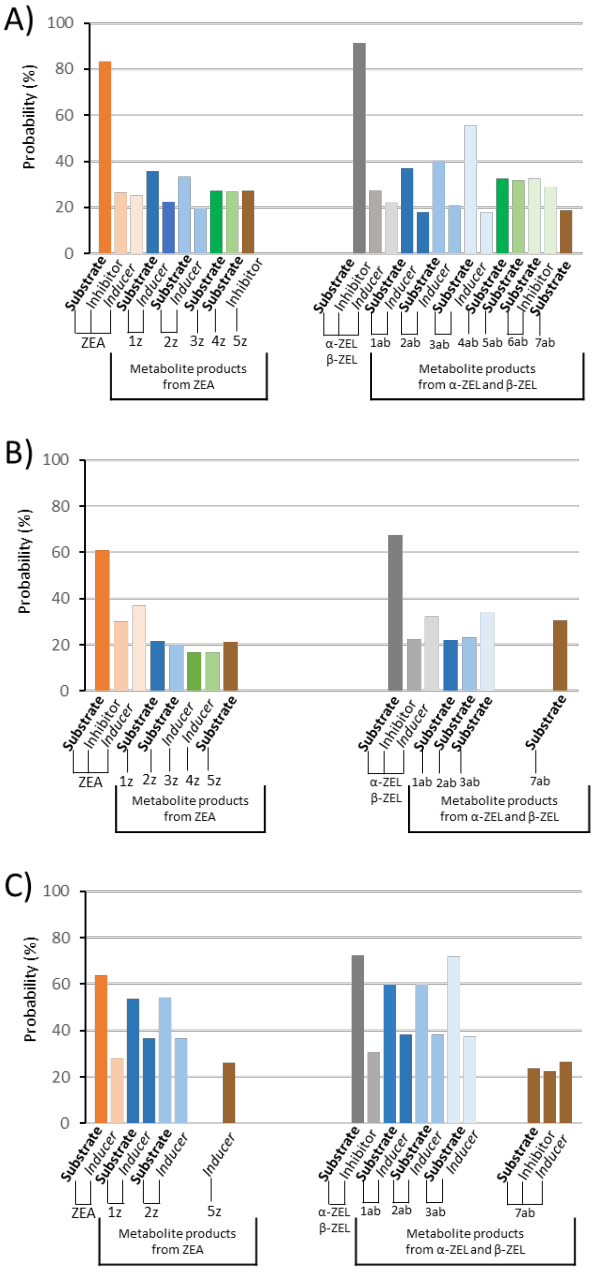
A)
Probability (%)
100
80
60
40
20
0
Substrate
Inhibitor
Inducer
ZEA
1z
2z
3z
4z
5z
α-ZEL
β-ZEL
1ab
2ab
3ab
4ab
5ab
6ab
7ab
Metabolite products from ZEA
Metabolite products from α-ZEL and β-ZEL
B)
Probability (%)
Substrate
Inhibitor
Inducer
ZEA
1z
2z
3z
4z
5z
α-ZEL
β-ZEL
1ab
2ab
3ab
7ab
Metabolite products from ZEA
Metabolite products from α-ZEL and β-ZEL
C)
Probability (%)
Substrate
Inducer
ZEA
1z
2z
5z
α-ZEL
β-ZEL
1ab
2ab
3ab
7ab
Metabolite products from ZEA
Metabolite products from α-ZEL and β-ZEL

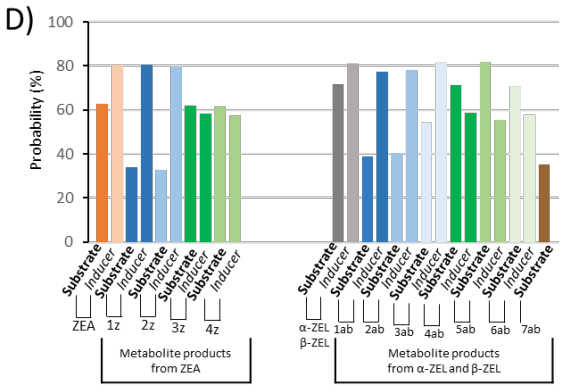

Figure 3. Prediction of inhibition, induction and substrate function of different isoforms of Cytochrome P450 (probability, %) that metabolize the majority of xenobiotics: CYP1A1 (A); CYP1A2 (B); CYP2C9 (C) and CYP3A4 (D). Prediction is reported for each metabolite product from ZEA (from dark to light orange), α-ZEL and β-ZEL (from dark to light grey). O-glucuronidation products (from dark to light blue), S-sulfation products (from dark to light green) and hydrolysis products (in brown). (For interpretation of the references to colour in this figure legend, the reader is referred to the Web version of this article.)

In detail, for isoform CYP1A1, all compounds had effects on it (Fig. 3A). Metabolite products coming from α-ZEL and β-ZEL had slightly higher probability prediction as substrate (>37%) than ZEA (>35%) for all O-glucuronidation, S-sulfation and hydrolysis products; as inducers, only metabolite products coming from O-glucuronidation reported this prediction effects. Finally, as inhibitor, only metabolite 5z from hydrolysis of ZEA and 6 ab from S-sulfation of α-ZEL and β-ZEL presented such prediction both in 30% (Fig. 3A).

For isoform CYP1A2, ZEA metabolite products had effects on it as substrate, except those coming from S-sulfation; and products of S-sulfation from α-ZEL and β-ZEL had no-effect (Figure 3B). As inducers of this isoform

(CYP1A2), only metabolite products of S-sulfation from ZEA (3z and 4z) were predicted in 16%. As inhibitor none of the compounds reported prediction in this direction (Figure 3B).

For isoform CYP2C9, ZEA, α-ZEL and β-ZEL were predicted as substrate; while only ZEA as inducer and α-ZEL and β-ZEL as inhibitor (Figure 3C). For metabolite products coming from O-glucuronidation of these mycotoxins all were predicted as i) substrate: 54% for those coming from ZEA and >60% for those coming from α-ZEL and β-ZEL; and as ii) inducers: >38% for all those coming from ZEA and from α-ZEL and β-ZEL. Metabolite product of hydrolysis coming from ZEA (5z) was predicted only as inducer (26%); while that coming from α-ZEL and β-ZEL (7 ab) was predicted as substrate (22%), inhibitor (23%) and inducer (26%). However, no-effect was predicted for S-sulfation compounds (neither as substrate, inhibitor or inducer).

Finally, ZEA, α-ZEL and β-ZEL were predicted as substrate and inducers with probabilities >60% for isoform CYP3A4 (Figure 3D). All metabolite products from ZEA of O-glucuronidation and S-sulfation were predicted as substrate ranging from 32% (2z) to 61% (4z); and inducers ranging from 57% (4z) to 80% (1z). No effect was predicted for its hydrolysis product (5z). Similar prediction effect was observed for metabolite products from α-ZEL and β-ZEL as substrates ranging from 38% (1 ab) to 81% (5 ab) and as inducers ranging from 58% (6 ab) to 81% (3 ab). The hydrolysis product 7 ab, was only predicted as substrate (35%) (Figure 3D).

3.4.2. Caspases 3 and 8

Caspases are involved in cascade activation of cell death, occurring either naturally or by exposure to toxic compounds. Prediction for caspases 3 and 8 activation (stimulation) is reported in Figure 4A and B, respectively of all 15

compounds. Prediction of activation of both caspases, 3 and 8, was higher for α-ZEL and β-ZEL (86% and 49% for caspase 3 and 8, respectively) than for ZEA (73% and 43% for caspase 3 and 8, respectively).

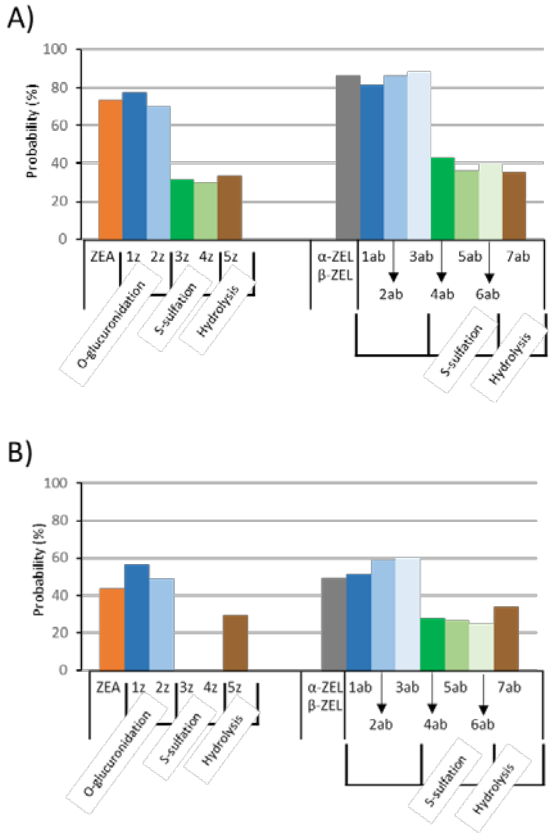

Figure 4. Prediction of caspases activation (probability, %) implicated in cell death pathway: caspase 3 (A) and caspase 8 (B). Graphics are reported for ZEA, α-ZEL, β-ZEL and metabolites products of those generated during Phase I and II reactions: Oglucuronidation (in blue): 1z and 2z from ZEA, and 1 ab, 2 ab and 3 ab from ZEA's metabolites; S-sufation (in green): 3z and 4z from ZEA, and 4 ab, 5 ab and 6 ab from ZEA's metabolites; and hydrolysis (in brown): 5z from ZEA and 7 ab from ZEA's metabolites. (For interpretation of the references to colour in this figure legend, the reader is referred to the Web version of this article.)

Caspase 3 was activated for all compounds studied and for metabolite predicted from α-ZEL and β-ZEL probability was higher than those from ZEA (Fig. 4A). Metabolite products of i) O-glucuronidation from α-ZEL and β-ZEL reported caspase activation >80% while those from ZEA <77%; ii) S-sulfation from α-ZEL and β-ZEL reported caspase activation >36% while those from ZEA <30% and iii) hydrolysis from α-ZEL and β-ZEL reported caspase activation 33% while those from ZEA 35% (Figure 4A).

For caspase 8, ZEA metabolite products reported prediction of activation only from those coming from O-glucuronidation and hydrolysis, from 56% to 29%, respectively (Figure 4B); while those metabolites products coming from α-ZEL and β-ZEL reported activation of caspases from 51% (1 ab) to 60% (3 ab) for O-glucuronidation products, from 25% (6 ab) to 27% (4 ab) for S-sulfation products and 34% (7 ab) for the hydrolysis product (Figure 4B).

4. Discussion

The present study explores the prediction of toxicity of three mycotoxins (ZEA, α-ZEL and β-ZEL) and products defining its metabolomics profile by proposing an *in silico* workflow and by using three software of computational toxicology: MetaTox, SwissADME and PASS online. All three mycotoxins are well-known to be copresent in food and feed not following good manufacture/agricultural practices, generating a public health concern as well as agricultural economic losses. Its effect as endocrine disruptor has been widely reported although the implications of its metabolite products regarding that toxic effects (or others) are unknown.

The workflow proposed, uses MetaTox to obtain the metabolite products formed during Phase I and II reactions, contributing to describe the metabolomics profile (Rudik et al., 2017); SwissADME (Daina et al., 2017) here

it has been used for assessing the ADMET processes suffered by three mycotoxins (ZEA, α-ZEL and β-ZEL) and its metabolites products (1z-5z for ZEA and 1 ab-7ab for α-ZEL and β-ZEL); and PASS online, predicted the toxic effect of activation and the biological activities with probability values (Pa, probability of activation). Different parameters are used for each software program which help in predictions, but as it occurs with in vitro or in vivo studies, they must be prudently assessed (Workflow 1).

Metabolites products predicted through MetaTox for the mycotoxins studied came from two Phase II reactions: O-glucuronidation and S-sulfation. Both are detoxication reactions of first line facilitating excretion. ZEA was predicted to generate two metabolites for each type of reaction (from 1z to 4z); while for α-ZEL and β-ZEL three metabolites (from 1 ab to 6 ab) (Figure 1 and Table 1). For Phase I reaction, only hydrolysis reaction was predicted to take place from ZEA, α-ZEL and β-ZEL, generating only one metabolite product, 7z and 7 ab for ZEA and ZEA's metabolites, respectively. In summary a total of 12 compounds defined the metabolomic profile of ZEA, α-ZEL and β-ZEL (Figure 1 and Table 1). Coinciding with other studies, these reactions take place and generate these compounds; however, their effects are unknown; in fact, the use of these metabolite products as biomarkers have been found in the literature in biomonitoring studies (Lorenz et al., 2019; Follmann et al., 2016; Shephard et al., 2013; Wallin et al., 2015; Gerding et al., 2015) or directly detected in food and aromatic plants as masked mycotoxins (Berthiller et al., 2006, 2009; Mannani et al., 2019). However, an analysis of in silico prediction of toxic effects defined by the metabolomics profile is here the first time reported. EFSA has dealt in assessing the risk of ZEA, α-ZEL and β-ZEL and has indicated that metabolites

products coming from them (also reported as modified forms) might have effects (oestrogenic effect, genotoxicity, endocrine receptor, …) (EFSA, 2011 and 2014) and contribute to the exposure evaluation but the uncertainty exists as there is a lack of data which entails difficulties in defining its toxic effects (EFSA et al., 2014, 2016, 2017). Not to mention the gap in effects of its mixtures or with other mycotoxins or contaminants.

In silico analysis show that ZEA, α-ZEL and β-ZEL are poorly achieving the BBB, have good distribution and are highly favored to be absorbed gastrointestinally (Table 2). The interesting point noticed with the analysis of metabolites products of these mycotoxins, obtained from O-glucuronidation, S-sulfation and hydrolysis reactions, is that these properties change inversely, especially for achieving the BBB (see values from Table 2, Table 3) from low values to high values. There are studies coinciding and others opposite to the results predicted in here when compared with those reported by in vitro and in vivo studies. For all three mycotoxins it has been reported a good gastrointestinal absorption (rapid and extensive) as well as the formation of metabolites from hydrolysis, sulfation and glurcuronidation (Biehl et al., 1993; Frizzell et al., 2015; Pfeiffer et al., 2011; Plasencia et al., 1991); in fact, several strategies and recommendations have been also considered for the entire risk assessment (EFSA 2017; Lorenz et al., 2019). Optimal gastrointestinal absorption predicted by Lipinsky RO5 is reported in Table 1 for the metabolomics profile. It also indicates that the probability of one compound to be absorbed orally is directly related to the ADMET and toxic effects. Only metabolites coming from O-glucuronidation were not following the Lipinsky's RO5 (HBA>10), because of not passing the gastrointestinal barrier; however,

mycotoxins, and metabolites from S-sulfation and hydrolysis reactions did which indicates their good distribution.

Toxic effects associated to compounds from metabolomics profile and mycotoxins seem to contribute one to another. Related to this, EFSA has indicated to assume the toxic effects of one compound as the sum of all metabolites coming from that compound (EFSA, 2011; Lorenz et al., 2019). Nonetheless, it is possible to analyze individual predictions in silico. The most common effect associated to ZEA as well as ZEA's metabolites is as endocrine disruptors with a ranking of oestrogenic potential effect established by EFSA as follows: α- ZEL > ZEN > β-ZEL (EFSA 2011). Besides this common and demonstrated toxic effect through in vitro and in vivo assays (EFSA 2017; Eze et al., 2019), other effects according to several parameters can be predicted (Figure 2A) as well as for its metabolite products (Figure 2B). According to the analysis of main effects predicted in silico for ZEA, α- ZEL, β-ZEL and its metabolite product defining the metabolomic profile, carcinogencity is the toxic effect predicted with high probability; however, IARC has classified ZEA (since 1993) as Group 3 (not classifiable as to their carcinogenicity to humans) based on inadequate evidence in humans and limited evidence in experimental animals (IARC 1993); to mention different behave in mice and mouse with limited evidence reported. This explains the prediction described in Figure 2, which although carcinogenicity indicates high probability (80–90%), the evidence is not coinciding with assays carried out for evaluating such effect. This is not happening with other effects reported in Figure 2 which coincide with studies carried out either in vivo or in vitro (especially for ZEA as it is the most studied): mutagenicity (Abbès et al., 2007; Ben Salah-Abbès et al., 2009); nephrotoxic in

rats (Becci et al., 1982), genotoxic (Ouanes et al., 2003, 2005; El-Makawy et al., 2001). As mentioned before the prediction needs to be confirmed with further assays without forgetting that it is giving a valuable indication to start from.

Cytochrome P450 (CYP450) is an enzymatic complex important as mechanism of defense by the organism when in contact with contaminants. Its main function is to metabolize the majority of toxic compounds through Phase I reactions. It is constituted by several isoforms to highlight the following as the most implicated in defense: CYP3A4, CYP2C9, CYP2C19, CYP1A1 and CYP1A2 (SwissADME). Expression of different isoforms occurs by exposure to contaminants as mycotoxins; which can act as inhibitors, inducers or substrates of this enzymatic complex. Results reported in Fig. 3 reveal that the highest predictions effects were for CYP3A4 (40–80%) (Figure 3D). When analyzing the action of mycotoxins, all three act as substrate, inducers and inhibitors ranging from 60% to 90%, from 21% to 38% and from 23% to 32%, respectively for isoforms CYP1A1 and CYP1A2 (Figure 3); while as substrate (62%–71%) and inducers (89%) for CYP3A4. Finally, for isoform CYP2C9, ZEA act as substrate and inducer and, α- ZEL and β-ZEL as substrate and inhibitor (Figure 3). For metabolite products, probabilities of action were marked for isoform CYP3A4. This isoform jointly CYP1A2 have been reported to play an important role in metabolism of ZEA in humans (Pfeiffer et al., 2009); while jointly with CYP2C8 denotes a high activation hydroxylation of ZEA (Bravin et al., 2009). In summary, different isoforms of CYP seem to contribute in the metabolization of all 15 compounds according to in silico prediction which coincides with the studies performed in vitro (Pfeiffer et al., 2009; Bravin et al., 2009); and more specifically with the isoform CYP3A4 which has the highest values of probability (Figure 3D).

Apoptotic cell death has been studied for ZEA in vitro revealing that activation of caspase 3 and 8 occurs (Banjerdpongchai et al., 2020; Gazzah et al., 2010; Othmen et al., 2008; Agahi et al., 2020 Zhu et al., 2012); as well as for α-ZEL and β-ZEL (Abid-Essefi et al., 2009). Nothing is known nor for its metabolite products defined in the metabolomics profile. Both caspases, implicated in the cascade activation for apoptotic cell death, have been predicted in silico as reported in Figure 4. Results for ZEA coincide with those reported in the literature in vitro denoting a major activation for caspase 3 than caspase-8 (Barjerdpongchai et al., 2010). Among that, similar tendency was observed for all the other 14 compounds studied; and while O-glucuronidates present highest prediction of activation for both caspase-3 and 8 and all compounds, S-sulfation products from ZEA (3z and 4z) do not contribute to activation of cell death through caspase-8 (Figure 4B). The prediction presented in this work in cell death and the in vitro confirmation reported for ZEA, α- ZEL and β-ZEL reveal that the apoptosis pathway of cell death is contributed by its metabolite products, which are generated during its detoxification by Phase I and II reactions.

5. Conclusions

In conclusion, the results obtained in the present study indicate that toxicity of ZEA, α-ZEL and β-ZEL mycotoxins and their metabolomics' profile can be predicted in silico. MetaTox was able to predict a total of 12 metabolites defining the metabolomics profile of each mycotoxin studied (5 from ZEA and 7 from α-ZEL and β-ZEL). SwissADME permitted to analyze each compound by its physicochemical properties and predict the behave of each one according to its absorption, distribution, metabolism and toxicity. Among that it was

possible to assign a HMDB ID according to a score of similarity. Lastly, PASS online provided an entire prediction of all compounds based on its structural information reported in Pa values. The results indicate moderate to high absorption by the gastrointestinal tract, but unlikely to penetrate into the brain on its current form unless metabolized. Slightly better properties to reach blood brain barrier than initial mycotoxins were observed. Toxic effects associated for all compounds revealed that carcinogenicity reported the highest probability for all three mycotoxins followed by nephrotoxic > hepatotoxic > endocrine disruptor > mutagenic (AMES TEST) > genotoxic. Prediction of inhibition, induction and substrate function on different isoforms of Cytochrome P450 varied for each compounds analyzed; similarly, for activation of caspases 3 and 8.

The metabolomics profile of ZEA, α-ZEL and β-ZEL analyzed by in silico programs (MetaTox, SwissADME and PASS online) predicts alteration of systems/pathways/mechanisms that ends up causing several toxic effects, giving an excellent sight and direct studies before starting in vitro or in vivo assays contributing to 3Rs principle by a reduction of animal testing. This innovative proposal in the field of computer toxicology helps (and opens a new window) to investigate the chemical risk assessment, a topic of great interest amongst researchers and safety authorities; nonetheless, it is necessary to continue developing and performing assays that confirm the predictions estimated to achieve solidest conclusions.

Source of funding

This research was supported by the Spanish Ministry of Science and Innovation PID2019-108070RB-100ALI and the Generalitat Valenciana GV2020/020, Generalitat Valenciana GVPROMETEO2018-126.

6. References

Abbès S, Ouanes Z, Salah-Abbès J, Abdel-Wahhab MA, Oueslati R and Bacha H, 2007. Preventive role of aluminosilicate clay against induction of micronuclei and chromosome aberrations in bonemarrow cells of Balb/c mice treated with Zearalenone. Mutation Research-Genetic Toxicology and Environmental Mutagenesis, 631, 85-92.

Abid-Essefi S, Bouaziz C, Golli-Bennour EE, Ouanes Z and Bacha H, 2009. Comparative study of toxic effects of zearalenone and its two major metabolites alpha-zearalenol and beta-zearalenol on cultured human Caco-2 cells. Journal of Biochemical and Molecular Toxicology, 23, 233-243.

Agahi F, Álvarez-Ortega N, Font G, Juan-García A, Juan C, 2020. Oxidative stress, glutathione, and gene expression as key indicators in SH-SY5Y cells exposed to zearalenone metabolites and beauvericin. Toxicology Letters, 334, 44-52.

Agahi, F., Font, G., Juan, C., Juan-García A. 2020. Individual and combined effect of zearalenone derivates and beauvericin mycotoxins on SH-SY5Y cells. Toxins, 12, 212; doi:10.3390/toxins12040212.

Bakker, M.G.; Brown, D.W.; Kelly, A.C.; Kim, H.S.; Kurtzman, C.P.; Mccormick, S.P.; O'Donnell, K.L.; Proctor, R.H.; Vaughan, M.M.; Ward, T.J., 2018. Fusarium mycotoxins: A trans-disciplinary overview. Canadian Journal of Plant Pathology. 40, 161–171.

Banjerdpongchai, R., Kongtawelert, P., Khantamat, O., Srisomsap, C., Chokchaichamnankit, D., Subhasitanont, P., Svasti, J. 2020. Mitochondrial and endoplasmic reticulum stress pathways cooperate in zearalenone-

induced apoptosis of human leukemic cells. J. of Hematology & Oncology 3, 50 http://www.jhoonline.org/content/3/1/50

Becci PJ, Voss KA, Hess FG, Gallo MA, Parent RA, Stevens KR and Taylor JM, 1982. Long-term carcinogenicity and toxicity study of zearalenone in the rat. Journal of Applied Toxicology, 2, 247-254.

Ben Salah-Abbès J, Abbès S, Abdel-Wahhab MA and Oueslati R, 2009. Raphanus sativus extract protects against Zearalenone-induced reproductive toxicity, oxidative stress and mutagenic alterations in male Balb/c mice. Toxicon, 53, 525-533.

Berthiller F, Hametner C, Krenn P, Schweiger W, Ludwig R, Adam G, Krska R and Schuhmacher R, 2009. Preparation and characterization of the conjugated Fusarium mycotoxins zearalenone-4O-beta-Dglucopyranoside, alpha-zearalenol-4O-beta-D-glucopyranoside and beta-zearalenol-4O-beta-D-glucopyranoside by MS/MS and two-dimensional NMR. Food Additives & Contaminants. Part A: Chemistry, Analysis, Control, Exposure & Risk Assessment, 26, 207–213.

Berthiller F, Werner U, Sulyok M, Krska R, Hauser MT and Schuhmacher R, 2006. Liquid chromatography coupled to tandem mass spectrometry (LC-MS/MS) determination of phase II metabolites of the mycotoxin zearalenone in the model plant Arabidopsis thaliana. Food Additives and Contaminants, 23, 1194–1200.

Berthiller, F.; Crews, C.; Dall'Asta, C.; de Saeger, S.; Haesaert, G.; Karlovsky, P.; Oswald, I.P.; Seefelder, W.; Speijers, G.; Stroka, J., 2013. Masked mycotoxins: A review. Molecular Nutrition and Food Research. 57, 165–186.

Biehl ML, Prelusky DB, Koritz GD, Hartin KE, BuckWB, Trenholm HL (1993) Biliary excretion and enterohepatic cycling of zearalenone in immature pigs. Toxicol Appl Pharmacol 121:152–159.

Bravin F, Duca RC, Balaguer P and Delaforge M, 2009. In vitro cytochrome p450 formation of a monohydroxylated metabolite of zearalenone exhibiting estrogenic activities: possible occurrence of this metabolite in vivo. International Journal of Molecular Sciences, 10, 1824-1837.

Cheng F., Li W., Zhou Y., Shen, J., Wu, Z, Liu, G., Lee, P.W., Tang Y. 2012. AdmetSAR: a comprehensive source and free tool for evaluating chemical ADMET properties. J. Chem. Inf. Model., 52: 3099-3105.

Daina A., Michielin O., Zoete V. 2017. SwissADME: a free web tool to evaluate pharmacokinetics, drug-likeness and medicinal chemistry friendliness of small molecules. Scientific Reports, 7:42717. https://doi.org/10.1038/srep42717

EFSA - European Food Safety Authority (2011) Scientific Opinion on the risks for public health related to the presence of zearalenone in food EFSA Journal, 9(6):2197.

EFSA - European Food Safety Authority (2014) Scientific opinion on the risks for human and animal health related to the presence of modified forms of certain mycotoxins in food and feed EFSA J 12:3916. 107pp. https://doi.org/10.2903/j.efsa.2014.3916

EFSA - European Food Safety Authority (2016) Appropriateness to set a group health-based guidance value for ZEN and its modified forms. EFSA J 14:4425. 46pp. https://doi.org/10.2903/j.efsa.2016.4425

EFSA - European Food Safety Authority (2017) Risks to human and animal health related to the presence of DON and its acetylated and modified forms in food and feed. EFSA J 15:4718. 345pp. https://doi.org/10.2903/j.efsa.2017.4718

El-Makawy A, Hassanane MS and Abd Alla ES, 2001. Genotoxic evaluation for the estrogenic mycotoxin zearalenone. Reproduction, Nutrition, Development, 41, 79-89.

Eze, U.A., Huntriss, J., Routledge, M.N., Gong, Y.Y., Connolly, L. 2019. The effect of individual and mixtures of mycotoxins and persistent organochloride pesticides on oestrogen receptor transcriptional activation using in vitro reporter gene assays. Food Chem. Toxicol. 130, 68-78.

Föllmann W, Ali N, Blaszkewicz M, Degen G (2016) Biomonitoring of mycotoxins in urine: pilot study in mill workers. J Toxicol Environ Health A 79:1015–1025.

Frizzell C., Uhlig S., Miles C.O., Verhaegen S., Elliott C.T., Eriksen G.S., Sorlie M., Ropstad E., Connolly L. (2015) Biotransformation of zearalenone and zearalenols to their major glucuronide metabolites reduces estrogenic activity. Toxicol in Vitro 29:575–581.

Frizzell, C., Ndossi, D., Verhaegen, S., Dahl, E., Eriksen, G., Sørlie, M., Connolly, L., 2011. Endocrine disrupting effects of zearalenone, alpha- and beta-zearalenol at the level of nuclear receptor binding and steroidogenesis. Toxicology Letters, 206(2), 210–217.

Gazzah AC, Bennour EE, Bouaziz C, Abid S, Ladjimi M and Bacha H, 2010. Sequential events of apoptosis induced by zearalenone in cultured hepatocarcinoma cells. Mycotoxin Research, 26, 187-197.

Gerding J, Ali N, Schwartzbord J, Cramer B, Brown DL, Degen GH, Humpf HU (2015) A comparative study of the human urinary mycotoxin excretion patterns in Bangladesh, Germany, and Haiti using a rapid and sensitive LC-MS/MS approach. Mycotoxin Res 31:127–136.

Hasan M.N, Bhuiya N.M.M.A, Hossain M.K, 2019. In silico molecular docking, PASS prediction, and ADME/T analysis for finding novel COX-2 inhibitor from Heliotropium indicum. J. Comp. Med. Res., 10, 142-154.

IARC (International Agency for Research on Cancer), 1993. IARC Monographs on the Evaluation of the Carcinogenic Risk of Chemicals to Humans, Vol. 56, Some Naturally Occurring Substances: Heterocyclic Aromatic Amines and Mycotoxins, Lyon. 39-444.

Juan C, Mañes J, Font G, Juan-García A. 2017a. Determination of mycotoxins in fruit berry by-products using QuEChERS extraction method. LWT - Food Science and Technology 86, 344-351.

Juan, C.; Berrada, H.; Mañes, J.; Oueslati, S. 2017b. Multi-mycotoxin determination in barley and derived products from Tunisia and estimation of their dietary intake. Food Chem. Toxicol., 103, 148–156.

Juan C, Mannai A, Ben Salem H, Oueslati S, Berrada H, Juan-García A, Mañes J, 2020. Mycotoxin presence in pre- and post-fermented silage from Tunisia. Arabian Journal of Chemitry, 13, 6753-6761.

Juan-García A, Bind M.A, Engert F, 2020. Larval zebrafish as an in vitro model for evaluating toxicological effects of mycotoxins. Ecotoxicology and Environmental Safety, 202, 110909.

Juan-García, A., Juan, C., Manyes, L., Ruiz M.J. 2016. Binary and tertiary combination of alternariol, 3-acetyl-deoxynivalenol and 15-acetyl-

deoxynivalenol on HepG2 cells: Toxic effects and evaluation of degradation products Toxicology in Vitro 34, 264–273.

Juan-García, A., Tolosa, J., Juan, C., Ruiz, M.J., 2019a. Cytotoxicity, genotoxicity and disturbance of cell cycle in HepG2 cells exposed to OTA and BEA: single and combined actions. Toxins 11(6): 341.

Juan-García, A., Tolosa, J., Juan, C., Ruiz, M.J., 2019b. Cytotoxicity, genotoxicity and disturbance of cell cycle in HepG2 cells exposed to OTA and BEA: single and combined actions. Toxins 11, 341. https://doi.org/10.3390/toxins11060341

Kifer D., Jakši D., Klari M.S. 2020. Assessing the Effect of Mycotoxin Combinations: Which Mathematical Model Is (the Most) Appropriate? Toxins, 12, 153; https://doi.org/10.3390/toxins12030153

Lagunin A., Stepanchikova A., Filimonov D., Poroikov V. 2000. PASS: prediction of activity spectra for biologically active substances. Bioinformatics, 16 (8), 747-748.

Lorenz N., Dänicke, s., Edler, L., Gottschalk, C., Lassek, E., Marko, D., Rychlik, M., Mally, A. 2019. A critical evaluation of health risk assessment of modified mycotoxins with a special focus on zearalenone. Mycotoxin Research, 35, 27–46. https://doi.org/10.1007/s12550-018-0328-z

Mannani, N., Tabarani, A., Abdennebi, E. H., and Zinedine, A. (2019). Assessment of aflatoxin levels in herbal green tea available on the Moroccan market. Food Control 108:e106882. https://doi.org/10.1016/j.foodcont.2019.106882

Othmen ZO, Golli EE, Abid-Essefi S, Bacha H. 2008 Cytotoxicity effects induced by Zearalenone metabolites, alpha Zearalenol and beta Zearalenol, on cultured Vero cells. Toxicology, 252, 72-77.

Ouanes Z, Abid S, Ayed I, Anane R, Mobio T, Creppy EE and Bacha H, 2003. Induction of micronuclei by Zearalenone in Vero monkey kidney cells and in bone marrow cells of mice: protective effect of Vitamin E. Mutation Research, 538, 63-70.

Ouanes Z, Ayed-Boussema I, Baati T, Creppy EE and Bacha H, 2005. Zearalenone induces chromosome aberrations in mouse bone marrow: preventive effect of 17beta-estradiol, progesterone and Vitamin E. Mutation Research, 565, 139-149.

Oueslati, S., Berrada H., Juan-García A., Mañes J. Juan C. 2020. Multiple mycotoxin determination on Tunisian cereals-based food and evaluation of the population exposure. Food Analytical Methods, https://doi.org/10.1007/s12161-020-01737-z

Pfeiffer E, Kommer A, Dempe JS, Hildebrand AA, Metzler M. 2011 Absorption and metabolism of the mycotoxin zearalenone and the growth promotor zeranol in Caco-2 cells in vitro. Mol Nutr Food Res 55:560–567.

Pascari X, Rodriguez-Carrasco Y, Juan C, Mañes J, Marin S, Ramos A.J, Sanchis V, 2019. Transfer of Fusarium mycotoxins from malt to boiled wort. Food Chemistry, 278, 700-710.

Pfeiffer E, Herrmann C, Altem_ller M, Podlech J, Metzler M, 2009. Oxidative in vitro metabolism of the Alternaria toxins altenuene and isoaltenuene. Mol. Nutr. Food Res., 53, 452-459.

Plasencia J, Mirocha CJ. 1991 Isolation and characterization of zearalenone sulfate produced by Fusarium spp. Appl Environ Microbiol 57, 146–150.

Rudik, A.V., Bezhentsev, V.M., Dmitriev, A. V., Druzhilovskiy, D.S., Lagunin, A.A, Filimonov, D.A., Poroikov V.V.2017. MetaTox: Web Application

for Predicting Structure and Toxicity of Xenobiotics' Metabolites. J. Chem. Inf. Model. 57, 638−642.

Shephard GS, Burger HM, Gambacorta L, Gong YY, Krska R, Rheeder JP, Solfrizzo M, Srey C, Sulyok M, Visconti A, Warth B, van der Westhuizen L (2013) Multiple mycotoxin exposure determined by urinary biomarkers in rural subsistence farmers in the former Transkei, South Africa. Food Chem Toxicol 62:217–225

Stanciu, O., Juan, C., Miere, D., Loghin, F., Mañes, J. 2017. Occurrence and co-occurrence of Fusarium mycotoxins in wheat grains and wheat flour from Romania. Food Control. 73, 147–155.

Wallin S, Gambacorta L, Kotova N, Lemming EW, Nalsen C, Solfrizzo M, Olsen M (2015) Biomonitoring of concurrent mycotoxin exposure among adults in Sweden through urinary multi-biomarker analysis. Food Chem Toxicol 83, 133–139

Yang, H., Lou C., Sun, L., Li, J., Cai, Y., Wang, Z., Li, W., Liu, G., Tang, Y. 2018. AdmetSAR 2.0: web-service for prediction and optimization of chemical ADMET properties. Bioinformatics, bty707.

Zhu, L., Yuan, H., Guo, C., Lu, Y., Deng, S., Yang, Y., Wei, Q., Wen, L., He Z., 2012. Zearalenone induces apoptosis and necrosis in porcine granulosa cells via a caspase-3- and caspase-9-dependent mitochondrial signaling pathway. Journal of Cellular Physiology. 227, 1814-1820.

Zoete, V., Daina, A., Bovigny, C., & Michielin, O. SwissSimilarity: A Web Tool for Low to Ultra High Throughput Ligand-Based Virtual Screening., J. Chem. Inf. Model., 2016, 56(8), 1399-1404.

Study 2

Individual and Combined Effect of Zearalenone Derivates and Beauvericin Mycotoxins on SH-SY5Y Cells

Fojan Agahi, Guillermina Font, Cristina Juan* and Ana Juan-García

Laboratory of Toxicology and Food Chemistry, Faculty of Pharmacy, University of Valencia, Burjassot 46100, Valencia, Spain

Agahi et al., 2020, Toxins, 12, 212

Abstract

Beauvericin (BEA) and zearalenone derivatives, α-zearalenol (α-ZEL), and β-zearalenol (β-ZEL), are produced by several *Fusarium* species. Considering the impact of various mycotoxins on human's health, this study determined and evaluated the cytotoxic effect of individual, binary, and tertiary mycotoxin treatments consisting of α-ZEL, β-ZEL, and BEA at different concentrations over 24, 48, and 72 h on SH-SY5Y neuronal cells, by using the MTT assay (3-(4,5-dimethylthiazol-2-yl)-2,5diphenyltetrazoliumbromide). Subsequently, the isobologram method was applied to elucidate if the mixtures produced synergism, antagonism, or additive effects. Ultimately, we determined the amount of mycotoxin recovered from the media after treatment using liquid chromatography coupled with electrospray ionization-quadrupole time-of-flight mass spectrometry (LC-ESI-qTOF-MS). The IC50 values detected at all assayed times ranged from 95 to 0.2 μM for the individual treatments. The result indicated that β-ZEL was the most cytotoxic mycotoxin when tested individually. The major effect detected for all combinations assayed was synergism. Among the combinations assayed, α-ZEL + β-ZEL + BEA and α-ZEL + BEA presented the highest cytotoxic potential with respect to the IC value. At all assayed times, BEA was the mycotoxin recovered at the highest concentration in individual form, and β-ZEL + BEA was the combination recovered at the highest concentration.

Keywords: MTT; SH-SY5Y cells; beauvericin; qTOF–MS/MS; zearalenone derivates.

1. Introduction

Mycotoxins represent one of the most important categories of biologically produced natural toxins with potential effects on human and animal health. The worldwide contamination by these natural products of food, feed, and environment, represents a health risk for animals and humans [1].

Several *Fusarium* species produce toxic substances of considerable concern to livestock and poultry producers. The mycotoxins beauvericin (BEA) and zearalenone (ZEA) and their derivatives (α-zearalenol (α-ZEL), β-zearalenol (β-ZEL), zeranol, taleranol, and zearalanone) can be produced by several *Fusarium* species (mainly *Fusarium graminearum*, but also *Fusarium culmorum*, *Fusarium cerealis*, *Fusarium equiseti*, and *Fusarium semitectum*) that grow on crops in temperate and warm-climate zones [2]. These fungi are present in almost all continents, can grow under poor storage conditions, and mainly contaminate cereal grains, such as maize, wheat, oats, soybeans, and their derived food products [3,4].

It has been proved that ZEA and α-ZEL bind to human estrogen receptors and elicit permanent reproductive tract alterations, and consequently, chronical exposure to ZEA present contaminated food can be a cause of female reproductive changes as a result of its powerful estrogenic activity [5,6,7,8]. It has been also reported that ZEA induces genotoxic effects by induction of DNA adducts, DNA fragmentation, and apoptosis [9,10]. As reported by Dong et al. (2010) [5], metabolic conversion of ZEA mycotoxin to α-ZEL and β-ZEL was found in almost all tissues and occurred more efficiently to α-ZEL than to β-ZEL; these mycotoxins are endocrine disruptors which affect steroid hormones such as progesterone [7]. In 2016, EFSA (European food Safety Authorities) indicated that there is a high uncertainty associated with the exposure to ZEA

and its modified forms and so that it would rather overestimate than underestimate any risk associated with exposure to modified ZEA [8]. Also, recent studies have indicated that ZEA is immunotoxic [4,11,12] and cytotoxic in various cell lines by inhibiting cell proliferation and increasing ROS (reactive oxygen species) generation [13,14,15].

On the other hand, BEA causes cytotoxic effects by reducing cell proliferation in a time- and concentration-dependent manner [16,17]. Moreover, it can increase ROS generation and lipid peroxidation and produces oxidative stress and depletion of antioxidant cellular mechanisms [14,18,19].

Neurotoxicological testing is mainly based on experimental animal models, but several cell lines and tissue culture models have been developed to study the mechanism of neurotoxicity. In general, cells of human origin are attractive alternatives to animal models for the exploration of toxicity to humans. Nonetheless, there are few studies about the effect of mycotoxins at the neuronal level [6,20,21,22].

Regarding the important role of the food industry in human health, studying the impact of mycotoxins and their combinations in feed and food commodities has gained attention over the last few years, due to the ability of most *Fusarium spp.* to simultaneously produce different mycotoxins [23,24,25]. Hence, EFSA has recently published a draft guidance document where a harmonized risk assessment methodology for combined exposure to multiple chemicals in all relevant areas is described [26].

Due to the importance of dietetic exposure to various mycotoxins and their impacts on human's health, there is an increasing concern about the hazard of co-occurrence of mycotoxins produced by *Fusarium* and of co-exposure to them through diet. Many studies have been conducted on the toxicity of

individual mycotoxins; however, few studies have been dedicated to the toxicological interaction of mycotoxins when present in double and triple combinations on different cell lines [16,17,18,27,28,29].

The objective of the present study was to investigate the cytotoxicological interactions between α-ZEL, β-ZEL, and BEA mycotoxins in human neuroblastoma SH-SY5Y cells, via the MTT assay. The effects of combinations of two and three mycotoxins were evaluated by isobologram analysis [30] to determine whether their interaction was synergistic, additive, or antagonistic, as well as to understand how mycotoxins can act at the cellular level.

2. Materials and methods

2.1. Reagents

The reagent-grade chemicals and cell culture components used, Dulbecco's Modified Eagle's Medium- F12 (DMEM/F-12), fetal bovine serum (FBS), and phosphate-buffered saline (PBS) were supplied by Thermofisher, Gibco ™ (Paisley, UK). Methanol (MeOH, HPLC LS/MS grade), was obtained from VWR International (Fontenay-sous-Bois, France). Dimethyl sulfoxide was obtained from Fisher Scientific Co, Fisher BioReagnts ™ (Geel, Belgium). The compound (3-(4,5-dimethylthiazol-2-yl)-2,5-diphenyltetrazolium bromide) (MTT) for the MTT assay, penicillin, streptomycin, and Trypsin–EDTA were purchased from SigmaAldrich (St. Louis, MO, USA). Deionized water (<18, MΩcm resistivity) was obtained in the laboratory using a Milli-QSP® Reagent Water System (Millipore, Beadford, MA, USA). Standard BEA (MW: 783.95 g/mol), α-ZEL, and β-ZEL (MW: 320.38 g/mol) were purchased from SigmaAldrich (St. Louis Mo. USA) (Figure 6). Stock solutions of mycotoxins

were prepared in MeOH (α-ZEL and β-ZEL) and DMSO (BEA) and maintained at −20 °C in the dark. The final concentration of either methanol or DMSO in the medium was ≤1% (v/v) as previously established. All other reagents were of standard laboratory grade.

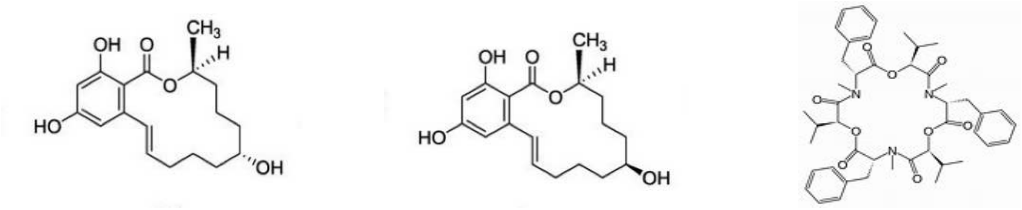

(a) (b) (c)

Figure 6. Chemical structures of the mycotoxins (a) α-ZEL, (b) β-ZEL, and (c) BEA.

2.2. Cell culture

The human neuroblastoma cell line SH-SY5Y was obtained from the American Type Culture Collection (ATCC, Manassas, VA, USA) and cultured in Dulbecco's Modified Eagle's Medium/F12 (DMEM/F-12), supplemented with 10% FBS, 100 U/mL penicillin, and 100 mg/mL streptomycin. The cells were sub-cultivated after trypsinization once or twice a week and suspended in complete medium in a 1:3 split ratio. The cells were maintained as monolayers in 150 cm^2 cell culture flasks with filter screw caps (TPP, Trasadingen, Switzerland). Cell cultures were incubated at 37 °C, 5% CO_2 atmosphere.

2.3. Mycotoxin exposure

Concentration of the mycotoxins and exposure time are two factors that were considered to in this study. The cells were exposed to α-ZEL, β-ZEL, and

BEA mycotoxins individually for 24, 48, and 72 h at a concentration in the ranges of 0.39 to 100 μM for α-ZEL and β-ZEL and 0.009 to 25 μM for BEA, all with 1:2 dilution (Table 3). Also, the mycotoxins were assayed in combination in the following mixtures: α-ZEL + BEA, β-ZEL + BEA, α-ZEL + β-ZEL, and α-ZEL + β-ZEL + BEA at three exposure times 24, 48, and 72 h. The concentrations ranged from 1.87 to 25 μM for the binary combinations were studied and from 3.43 to 27.5 μM for the tertiary combination, including four dilutions of each mycotoxin: BEA (0.31, 0.62, 1.25, and 2.5 μM), α-ZEL and β-ZEL (1.56, 3.12, 6.25 and 12.5 μM) (Table 3). The dilution ratios of the concentrations for the binary combinations were 5:1 for α-ZEL + BEA and β-ZEL + BEA, 1:1 for α-ZEL + β-ZEL, and 5:5:1 for the tertiary combination (β-ZEL + α-ZEL + BEA) (Table 3).

Table 3. Concentration range (μM) of mycotoxins studied individually and in combinations. The dilution ratios were 5:1 for the combinations α-ZEL + BEA and β-ZEL + BEA, 1:1 for α-ZEL + β-ZEL, and 5:5:1 for α-ZEL + β-ZEL + BEA.

Combination tested	Concentration range (μM)
α-ZEL	[0.39 – 100]
β-ZEL	[0.39 – 100]
BEA	[0.009 – 2.5]
α-ZEL + BEA	[1.56 – 12.5] + [0.31 – 2.5]
β-ZEL + BEA	[1.56 – 12.5] + [0.31 – 2.5]
α-ZEL + β-ZEL	[1.56 – 12.5] + [1.56 – 12.5]
α-ZEL + β-ZEL + BEA	[1.56 – 12.5] + [1.56 – 12.5] + [0.31 – 2.5]

2.4. MTT assay

Cytotoxicity was examined by the MTT assay, performed as described by Ruiz et al. (2006) [37], with few modifications. The assay consists in measuring the viability of cells by determining the reduction of the yellow soluble tetrazolium salt only in cells that are metabolically active via a mitochondrial reaction to an insoluble purple formazan crystal. Cells were seeded in 96-well culture plates at 2×10^6 cells/well and allowed to adhere for 18–24 h before mycotoxin additions. Serial dilutions of α-ZEL, β-ZEL, and BEA at 1:2 dilutions were prepared with supplemented medium and added to the respective plates (Table 3). Culture medium without mycotoxins and with 1% MeOH or DMSO was used as a control. After treatment, the medium was removed, and each well received 200 µL of fresh medium containing 50 µL of MTT solution (5 mg/mL; MTT powder dissolved in phosphate-buffered saline). After an incubation time of 4 h at 37 °C in the darkness, the MTT-containing medium was removed, and 200 µL of DMSO and 25 µL of Sorensen's solution were added to each well before reading the optical density at 620 nm with the ELISA plate reader Multiskan EX (Thermo Scientific, MA, USA). Each mycotoxin combination plus a control were tested in three independent experiments. Mean inhibition concentration (IC_{50}) values were calculated from full dose–response curves.

2.5. Experimental design and combination index

The isobologram analysis (Chou–Talalay model) was used to determine the type of interaction (synergism, additive effect, and antagonism) that occurred when the mycotoxins studied were in combination. This model allows characterizing the interactions induced by combinations of mycotoxins in different cell lines and with different mycotoxins but it does not allow the

elucidation of the mechanisms by which these types of interaction are produced. The median effect/combination index (CI) isobologram equation by Chou (2006) [31] and Chou and Talalay (1984) [30] permitted analyzing drug combination effects. The isobologram analysis involves plotting the dose–effect curves for each compound and its combinations in multiple diluted concentrations. Parameters such as *Dm* (median effect dose), *fa* (fraction affected by concentration), and *m* (coefficient signifying the shape of the dose–effect relationship) are relevant in the equation [30]. Therefore, the method considers both potency (*Dm*) and shape (*m*) parameters.

Chou and Talalay (1984) [30] introduced the term combination index (CI). CI values <1, =1, and >1 indicate synergism, additive effects, and antagonism of the combination, respectively. CalcuSyn software version 2.1. (Biosoft, Cambridge, UK, 1996–2007) was used to study the types of interactions assessed by the isobologram analysis. The IC_{25}, IC_{50}, IC_{75}, and IC_{90} are the doses required to produce toxicity at 25%, 50%, 75%, and 90%, respectively.

2.6. Extraction of α-ZEL, β-ZEL, and BEA from the culture media

To determine the intracellular accumulation of the mycotoxins studied, an extraction procedure of the culture media was carried out following the method described by Juan-García et al. (2015 and 2016) [27,28], with several modifications. Briefly, 0.8 mL of culture medium was collected and transferred into a polypropylene tube, 1.5 mL of ethyl acetate was added, and the mixture was shaken for 2 min with an Ultra-Turrax Ika T18 basic (Staufen, Germany). Afterwards, the mixture as sonicated in an ultrasound cleaning bath (VWR, USC1700TH) for 10 min. Finally, the mixture was centrifuged at ~5600× g for

5 min at 22 °C (Centrifuge 5810R, Eppendorf, Germany). The supernatant phase was collected. The liquid–liquid extraction process was repeated three times. Finally, the total volume obtained (approx. 4.5 mL) was evaporated to dryness at 45 °C in an N2 stream with a TurboVap-LV (Zymark, Allschwil, Switzerland) and then re-dissolved in 0.25 mL of a mixture of methanol and water (70:30, v/v) by vortexing vigorously (15 s), before being transferred into a vial for LC–ESI–qTOF-MS injection.

2.7. Determination of BEA, β-ZEL, and α-ZEL by LC–ESI–qTOF-MS

The analysis was performed using an LC–ESI–qTOF-MS system, consisting of an LC Agilent 1200-LC system (Agilent Technologies, Palo Alto, CA, USA) equipped with a vacuum degasser, an autosampler, and a binary pump. The columns were a Gemini NX-C18 column (150 × 2 mm, i.d. 3 μm, Phenomenex, Torrance, California) and a guard column C18 (4 × 2 mm, i.d. 3 μM).

Mobile phases consisted of milli-Q water with 0.1% of formic acid as solvent system A and acetonitrile and 0.1% of formic acid as solvent system B, with the following gradient elution: 3 min, 70% B; in 2 min 70–80% B; in 1 min get 90% of B, maintained 4 min; 90–100% B 4 min and maintained 2 min; in 2 min decrease to 50% B; in 2 min 90% B, maintained 2 min. The flow rate used was 0.250 mL min^{-1}, and the total run time was 22 min. The sample volume injected was 20 μL.

MS analysis was carried out using a 6540 Agilent Ultra- High-Definition Accurate-Mass q-TOF-MS, equipped with an Agilent Dual Jet Stream electrospray ionization (Dual AJS ESI) interface in negative and positive

ionization modes. Operation conditions were as follows: sheath gas temperature 350 °C at a flow rate of 8 L/min, capillary voltage 3500 V, nebulizer pressure 45 psig, drying gas 10 L/min, gas temperature 300 °C, skimmer voltage 65 V, octopole RF peak 750 V, and fragmentor voltage 130 V. Analyses were performed using AutoMS/MS mode with fixed collision energy (10, 20 and 30) and in mass range of 50–1700 m/z. Acquisition rate was 3 spectra/second. Acquisition data were processed with Agilent MassHunter Workstation software.

2.8. Statistical analysis

Statistical analysis of data was carried out using IBM SPSS Statistic version 23.0 (SPSS, Chicago, Il, USA) statistical software package. Data are expressed as mean ± SD of three independent experiments. The statistical analysis of the results was performed by student's T-test for paired samples. Difference between groups were analyzed statistically with ANOVA followed by the Tukey HDS post-hoc test for multiple comparisons. The level of $p \leq 0.05$ was considered statistically significant.

3. Results

3.1. Cytotoxicity assay of individual and combined mycotoxins

The cytotoxicity effects of α-ZEL, β-ZEL, and BEA mycotoxins on SH-SY5Y cells were evaluated by the MTT assays over 24, 48, and 72 h. Figure 1 shows the time- and concentration-dependent decrease in cell viability after exposure to each mycotoxin individually, while IC_{50} values are shown in Table 1. After 24 h, the IC_{50} value could be calculated only for β-ZEL and was 94.3 ± 2.0 μM; after 48 h of exposure, the IC_{50} values were 20.8 ± 0.5 μM for α-ZEL and 9.1 ± 1.8 μM for β-ZEL. After 72 h of exposure, the IC_{50} values were 14.0

± 1.8 µM, 7.5 ± 1.2 µM. and 2.5 ± 0.2 µM for α-ZEL, β-ZEL, and BEA, respectively. According to the IC_{50} values obtained at 72 h, BEA showed the highest cytotoxic effect on SH-S5Y5 cells (Table 1).

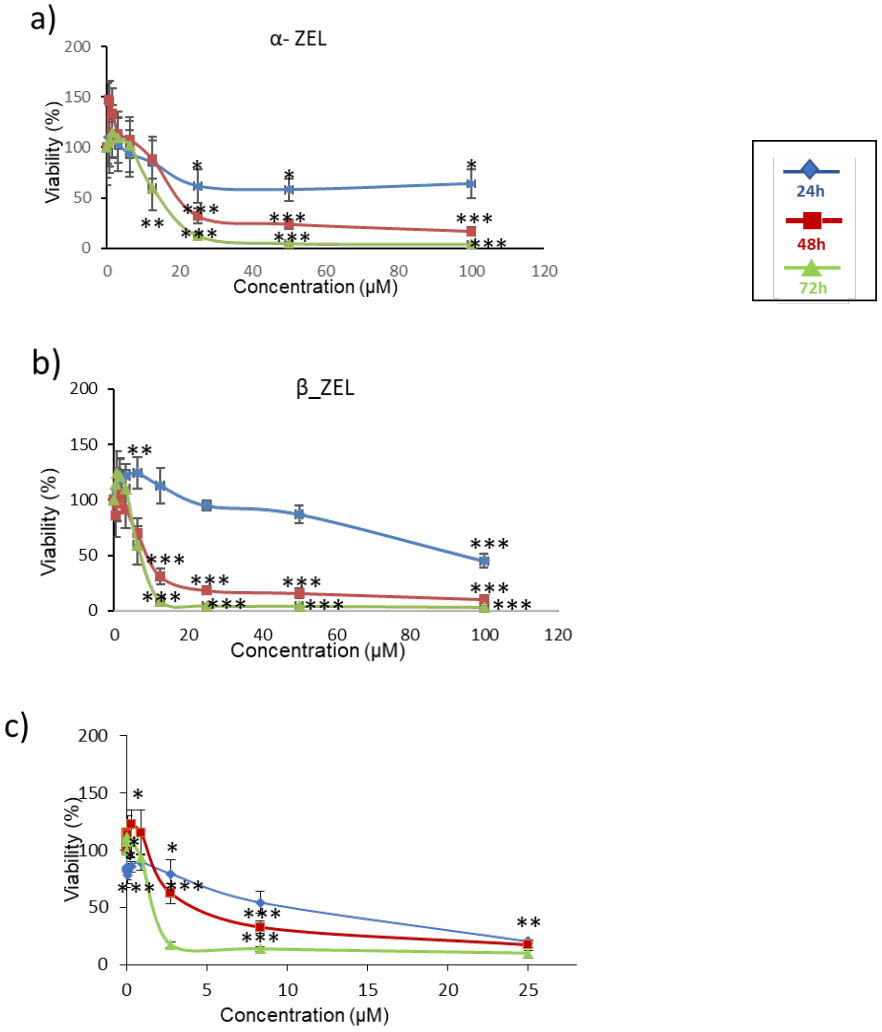

Figure 1. Cytotoxicity of the mycotoxins α-ZEL (a), β-ZEL (b), and BEA (c) individually at 24 h, 48 h, and 72 h. All values are the results of three independent experiments with eight replicates and are expressed as mean ± SD; $p \leq 0.05$ (*), $p \leq 0.01$ (**), $p \leq 0.001$ (***).

Table 1. Medium inhibitory concentration (IC_{50} ± SD) of α-zearalenol (α-ZEL), β-zearalenol (β-ZEL), and beauvericin (BEA) for SH-SY5Y cells after 24, 48, and 72 h of exposure, determined by the MTT assay. Three independent experiments were performed with eight replicates each.

	IC_{50} (μM) ± SD		
Mycotoxin	24 h	48 h	72 h
α-ZEL	n.a	20.8 ± 0.5	14.0 ± 1.8
β-ZEL	94.3 ± 2.0	9.1 ± 1.8	7.5 ± 1.2
BEA	n.a	n.a	2.5 ± 0.2

n.a: not available.

The cytotoxic effect of binary and tertiary combinations of α-ZEL, β-ZEL, and BEA on SH-SY5Y cells was evaluated by the MTT assays over 24, 48, and 72 h. The dose–response curves of the two- and three-mycotoxin combinations are shown in Figure 2 and Figure 3, which demonstrate higher cytotoxicity of the combinations compared with individual mycotoxin. Figure 2 shows the concentration-dependent decrease in SH-SY5Y cell viability upon combined treatment with α-ZEL + BEA (5:1) (Figure 2a), β-ZEL + BEA (5:1) (Figure 2b), α-ZEL + β-ZEL (1:1) (Figure 2c); Figure 3 shows the results for α-ZEL + β-ZEL + BEA (5:5:1).

The α-ZEL + BEA combination at the highest concentration induced a decrease in cell proliferation at 24 h of exposure (Figure 2a) of 35% with respect to the effect α-ZEL tested individually and of 37% with respect to the effect BEA. After 48 h of exposure, the decrease in cell proliferation was 67% with respect to that measured for α-ZEL and 36% with respect to that measured for

BEA. After 72 h of exposure, the viability decreased 53% with respect to α-ZEL and 43% with respect to BEA. After 24 h of exposure, the β-ZEL + BEA combination (Figure 2b) decreased cell proliferation by about 55% and 29% at the highest concentration with respect to β-ZEL and BEA tested individually, respectively. After 48 h of exposure, the highest concentration of the combination reduced cell proliferation by 11% with respect to BEA tested individually. Also, at 72 h of exposure, the combination decreased cell proliferation by approximately 36% with respect to BEA individually tested. Such effect was not noticed after 48 and 72 h with respect to b-ZEL. In Figure 2c, the α-ZEL + β-ZEL combination after 24 h of exposure showed 17% of decrease in cell proliferation compared to β-ZEL individually assayed. After 48 and 72 h of exposure, the highest concentration of the combination reduced cell proliferation by 60% and 50%, respectively, compared to α-ZEL tested alone, whereas, this did not happen with respect to β-ZEL after 48 and 72 h of exposure. Figure 3 shows the dose–response curves for the tertiary combination of α-ZEL, β-ZEL, and BEA at 24, 48, and 72 h of exposure in SH-SY5Y cells. At 24 h of exposure, cell proliferation decreased by 16%, 44%, and 18% compared to cells exposed to α-ZEL, β-ZEL, and BEA alone. After 48 and 72 h of exposure, a significant reduction in cell proliferation, corresponding to 57% and 51%, was observed with respect to α-ZEL alone, and a reduction of 26% and 41% was observed with respect to BEA alone, while such effect was not observed with respect to β-ZEL alone.

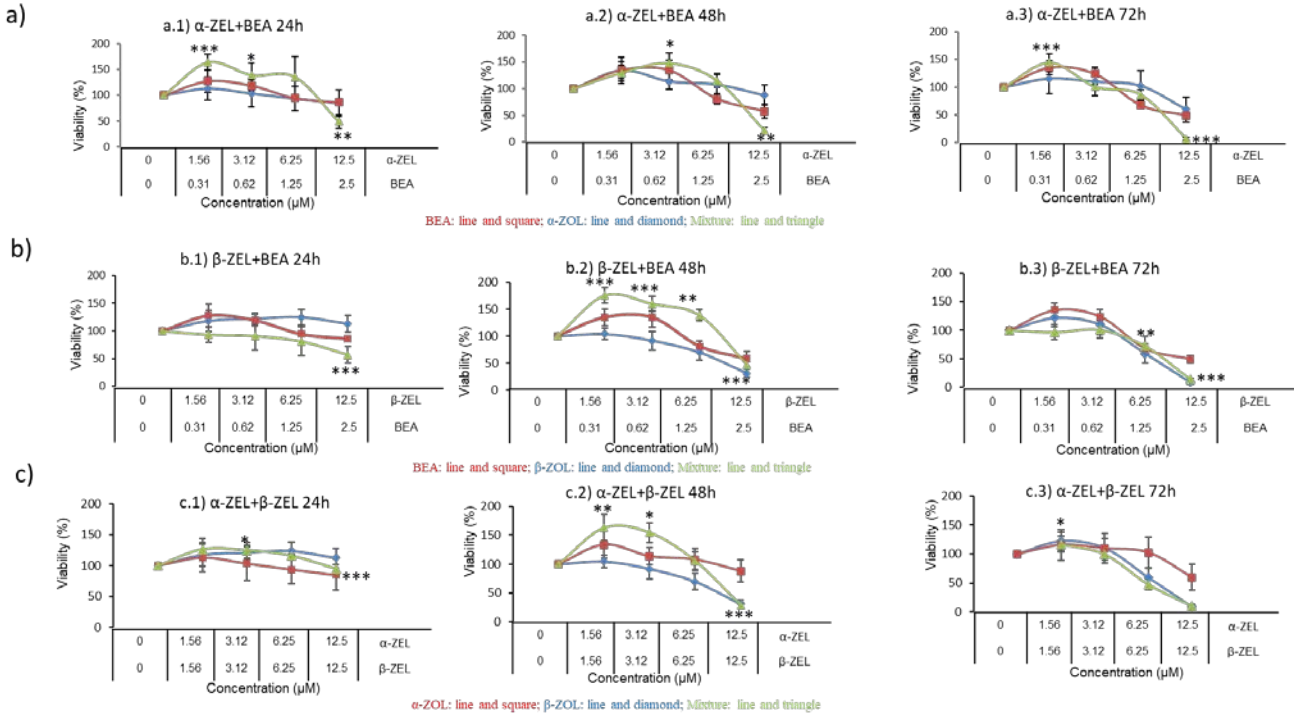

Figure 2. Cytotoxicity of the mycotoxin combinations of α-ZEL + BEA (5:1) (a), β-ZEL + BEA (5:1) (b), and α-ZEL + β-ZEL (1:1) (c) at 24 h (a.1, b.1, and c.1), 48 h (a.2, b.2, and c.2) and 72 h (a.3, b.3, and c.3). All values are the results of three independent experiments with eight replicates and are expressed as mean ± SD; $p \leq 0.05$ (*), $p \leq 0.01$ (**), $p \leq 0.001$ (***).

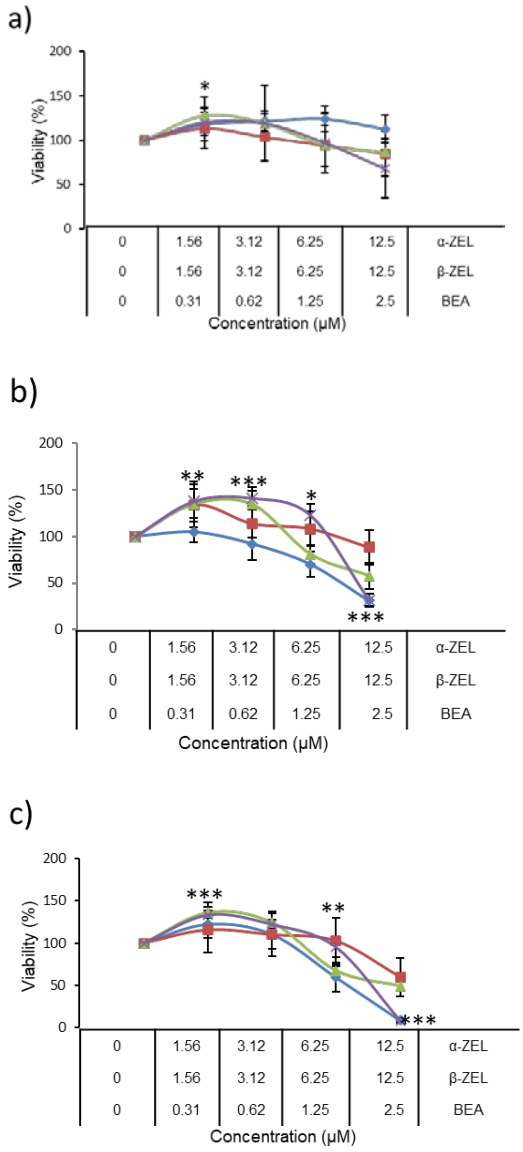

Figure 3. Cytotoxicity of the mycotoxin combination of α-ZEL + β-ZEL + BEA (5:5:1) at 24 h (a), 48 h, (b) and 72 h (c). All values are the results of three independent experiments with eight replicates and are expressed as mean ± SD; $p \leq 0.05$ (*), $p \leq 0.01$ (**), $p \leq 0.001$ (***). BEA: line and square; β-ZEL: line and diamond; α-ZEL: line and triangle; Mixture: line and ×.

The isobologram analysis was used to determine the type of interaction between α-ZEL, β-ZEL, and BEA. The values of the parameters *Dm*, *m*, and *r* of the double and triple combinations, as well as of the mean combination index (CI) are shown in Table 2. The IC_{50}, IC_{75}, and IC_{90} are the doses required to inhibit proliferation at 25%, 50%, 75%, and 90%, respectively. These CI values were calculated automatically by the computer software CalcuSyn. The CI fractional effect (fa) curves for α-ZEL, β-ZEL, and BEA combinations in SH-SY5Y cells are shown in Figure 4. Synergism for all concentration of the α-ZEL + BEA (5:1) mixture after 24 and 48 h of exposure was demonstrated; however, after 72 h of exposure, an additive effect for the α-ZEL + BEA combination was observed (Figure 4a, Table 2). The β-ZEL + BEA (5:1) mixture showed synergism after 24 h of exposure; however, after 48 and 72 h it showed antagonism at high concentrations and moderate synergism at low concentrations (Figure 4b, Table 2). The mixture of α-ZEL + β-ZEL showed antagonism after 24 h of exposure at all concentrations assayed but at 48 and 72 h, it showed antagonism at high concentration and a moderate synergism at low concentration (Figure 4c, Table 2). The tertiary mixture, after 24 h of exposure, showed antagonism at high concentration and synergism at low concentration, while after 48 h, it showed synergism and after 72 h, antagonism at all concentrations assayed (Figure 4d, Table 2).

Cytotoxicity after 24 h of incubation decreased in this order: α-ZEL + BEA > β-ZEL + BEA > α-ZEL + β-ZEL + BEA > α-ZEL + β-ZEL. After 48 and 72 h of incubation, the ranking was α-ZEL + BEA > β-ZEL + BEA >α-ZEL + β-ZEL > α-ZEL + β-ZEL + BEA.

Table 2. The parameters Dm, m, and r are the antilog of x-intercept, the slope, and the linear correlation of the median-effect plot, which means the shape of the dose–effect curve, the potency (IC_{50}), and the conformity of the data to the mass action law, respectively [30,31]. Dm and m values are used for calculating the combination index (CI) value (CI < 1, =1, and >1 indicate synergism (Syn), additive (Add) effect, and antagonism (Ant), respectively. IC_{50}, IC_{75}, and IC_{90} are the doses required to inhibit proliferation at 50%, 75%, and 90%, respectively. CalcuSyn software automatically provided theses values.

Mycotoxin	Time (h)	*Dm* (μM)	*m*	*r*	CI values					
					CI_{50}		CI_{75}		CI_{90}	
α-ZEL	24	66.10	1.36	0.9679						
	48	31.59	1.82	0.9726						
	72	15.24	2.02	0.9873						
β-ZEL	24	171.33	1.28	0.9709						
	48	12.46	1.26	0.9715						
	72	11.65	2.28	0.9464						
BEA	24	21.65	0.98	0.9763						
	48	3.68	1.24	0.9945						
	72	25.92	1.40	0.9805						
α-ZEL + BEA	24	3.05	1.36	0.9736	0.37 ± 0.33	Syn	0.34 ± 0.35	Syn	0.31 ± 0.38	Syn
	48	1.16	1.56	0.9933	0.50 ± 0.24	Syn	0.47 ± 0.26	Syn	0.44 ± 0.29	Syn
	72	1.34	1.54	0.94708	0.96 ± 0.86	Add	1.00 ± 0.51	Add	1.20 ± 1.30	Ant
β-ZEL + BEA	24	3.78	1.20	0.9698	0.29 ± 0.19	Syn	0.26 ± 0.21	Syn	0.24 ± 0.24	Syn
	48	4.81	3.04	0.7744	3.24 ± 0.42	Ant	1.94 ± 0.32	Ant	1.00 ± 0.14	Add
	72	1.89	3.14	0.7585	1.35 ± 0.51	Ant	1.00 ± 0.12	Add	0.60 ± 0.52	Syn
α-ZEL + β-ZEL	24	133.46	1.73	0.7782	2.80 ± 1.01	Ant	2.32 ± 0.51	Ant	1.92 ± 0.62	Ant
	48	19.12	3.40	0.7782	2.14 ± 0.23	Ant	1.35 ± 0.18	Ant	0.30 ± 0.14	Syn
	72	7.89	5.01	0.9409	2.60 ± 0.90	Ant	1.42 ± 0.63	Ant	0.45 ± 0.42	Syn
α-ZEL + β-ZEL + BEA	24	3.74	3.14	0.9478	0.57 ± 0.30	Syn	0.32 ± 0.20	Syn	0.19 ± 0.14	Syn
	48	0.01	0.43	0.7465	0.23 ± 0.06	Syn	0.15 ± 0.07	Syn	0.18 ± 0.10	Syn
	72	7.47	2.30	0.8966	8.54 ± 0.77	Ant	7.60 ± 0.85	Ant	6.88 ± 0.95	Ant

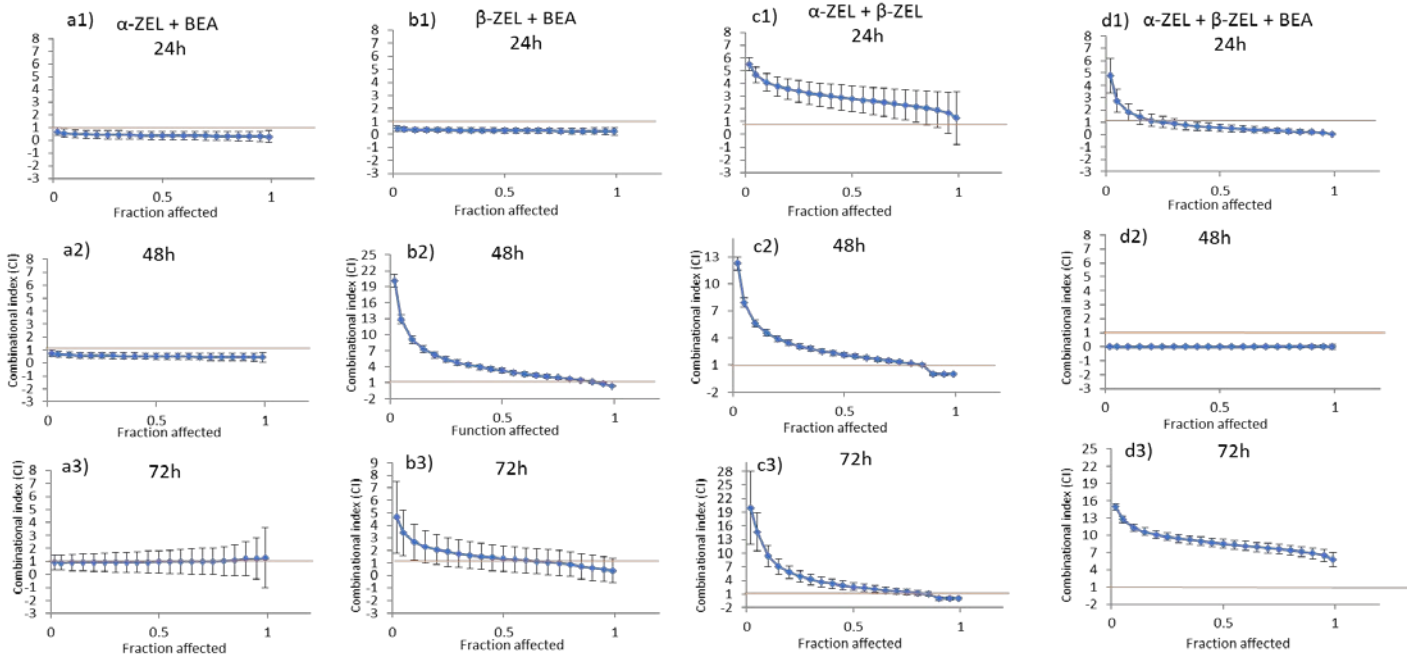

Figure 4. CI vs. fractional effect curve, as described by Chou and Talalay, for SH-SY5Y cells exposed to α-ZEL, β-ZEL, and BEA in binary and tertiary combinations. Each point represents the CI ± SD at a fractional effect as determined in our experiments. The line (CI = 1) indicates additivity, the area under this line indicates synergism, and the area above the line indicates antagonism. SH-SY5Y cells were exposed for 24, 48, and 72 h to α-ZEL + BEA and β-ZEL + BEA at a molar ratio of 5:1 (equimolar proportion), to α-ZEL + β-ZEL at a molar ratio of 1:1, and to α-ZEL + β-ZEL + BEA at a molar ratio of 5:5:1.

3.2. α-ZEL, β-ZEL, and BEA present in cell medium after treatment in binary and tertiary combination

The medium of SH-SY5Y cells containing α-ZEL, β-ZEL, and BEA after treatments (individual and combined after 24, 48, and 72h) was collected from each well. The amount of each mycotoxin remaining in the medium was calculated as a percentage with respect to the respective amount used in the exposure assays. In this sense, we determined whether the amounts were above or below 50% of those used for treatment (Figure 5). In individual exposures, the amounts of BEA and β-ZEL in the medium were below 50% at 48 and 72 h (Figure 5b,c), while, at 24 h, their concentrations tended to be higher and >50% for both mycotoxins. For α-ZEL, the concentration in the medium was maintained above 50% at all times studied (Figure 5a). This evidenced that a lower amount of α-ZEL exerted the examined effect compared to the amount necessary for BEA and β-ZEL, as higher amounts of α-ZEL were detectable in the medium at all times and concentrations.

In the binary combination α-ZEL + BEA (5:1), the amounts of each mycotoxin after 24 and 48 h were below 50% (Figure 5d.1,d.2), although the amount of BEA was higher than that of α-ZEL once the concentration assayed overpassed 0.62 μM for BEA and 3.12 μM for α-ZEL, revealing that the effects exerted by this mixture in neuroblastoma cells depended on both mycotoxins and were due more to α-ZEL than to BEA. This tendency at 72 h was more accentuated, as the amount of BEA in the medium was above 50% for all concentrations, while that of α-ZEL was below 50% (Figure 5d.3).

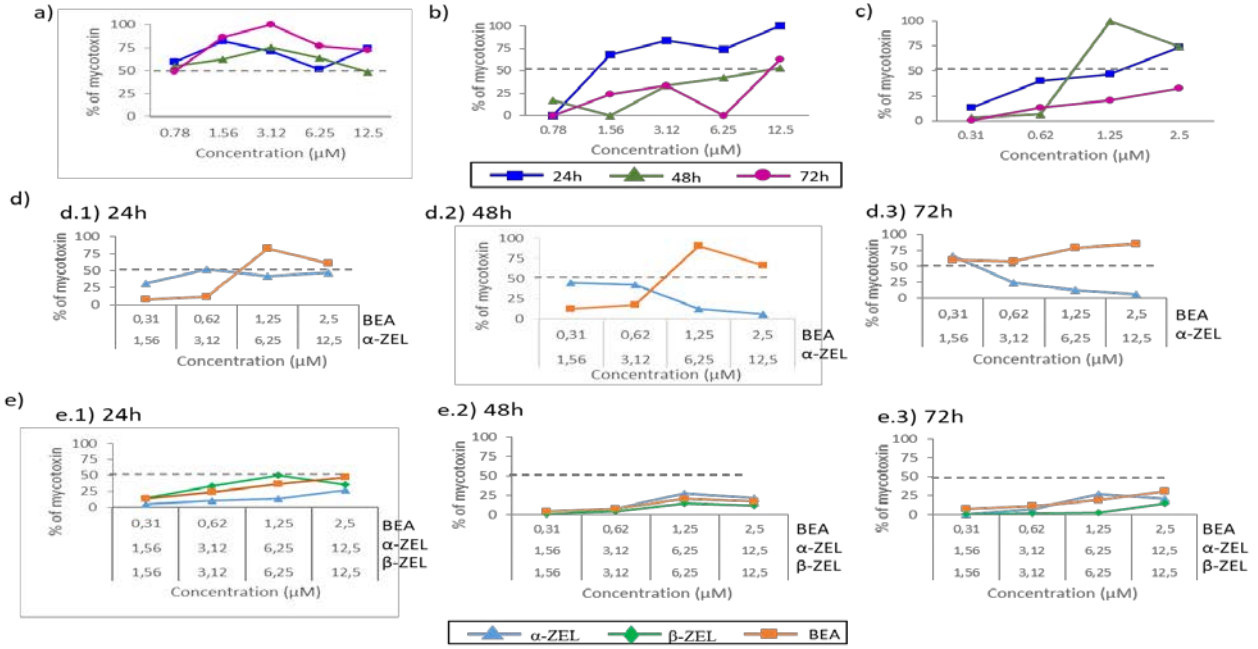

Figure 5. Percentage of α-ZEL, β-ZEL, and BEA remaining in the medium of SH-SY5Y cells after treatment for 24, 48, and 72 h at different concentrations individually or in combination by LC–ESI–qTOF-MS. (a) α-ZEL; (b) β-ZEL; (c) BEA; (d) α-ZEL + BEA and (e) α-ZEL + β-ZEL + BEA.

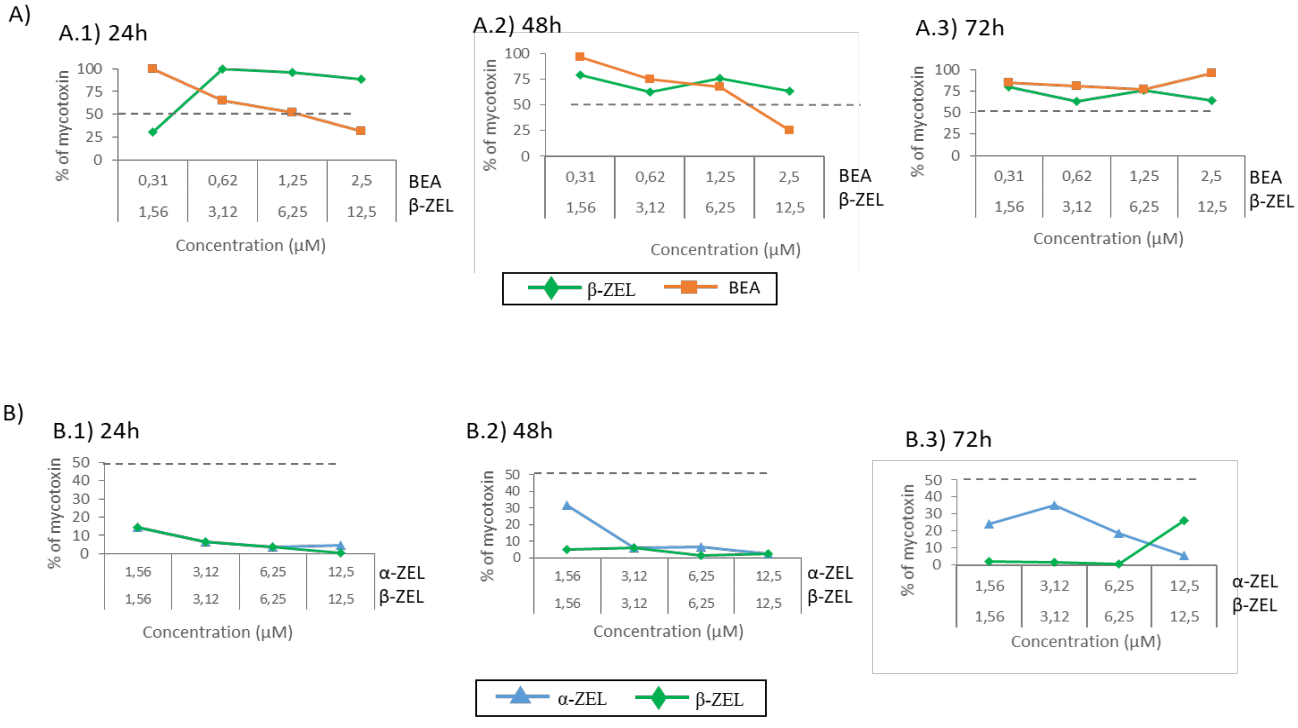

Figure S1. Percentage of α-ZEL, β-ZEL, and BEA remaining in the medium of SH-SY5Y cells after treatment during 24, 48, and 72 h at different concentrations and combinations by LC–ESI–qTOF-MS. (A) β-ZEL+ BEA and (B) α-ZEL + β-ZEL.

Also, for the combination β-ZEL + BEA (5:1), the mycotoxin's percentage remaining in the media was the same as that found for α-ZEL + BEA; however, β-ZEL was detected in higher amount than BEA in all scenarios, revealing that the effect of this mixture and was due more to BEA than to β-ZEL (Supplementary Figure S1A). On the other hand, for the binary combination of ZEA metabolites, α-ZEL + β-ZEL (1:1), the amounts of mycotoxins recovered were below 50%, and slightly superior for α-ZEL than for β-ZEL. This revealed that both mycotoxins contributed to the effect of this mixture in SH-SY5Y cell line (Supplementary Figure S1B). For the tertiary combination (α-ZEL + β-ZEL + BEA, (5:5:1)), the mycotoxins' percentages detected were also below 50% of the administered concentration, and this percentage was higher for higher concentrations administered and lower time of exposure (Figure 5e). This revealed that high amounts of α-ZEL and β-ZEL accessed the neuroblastoma cells, and the effect was due more to β-ZEL at 48 and 72 h, according to the results in Figure 3 and Figure 5.

4. Discussion

Several studies have discussed the cytotoxic and an anti-proliferative effect of ZEA mycotoxin and its metabolites in various cell lines, such as Caco-2 [11], HepG2 cells [13], CHO-K1 cells [32], and SH-SY5Y [6], and hose of BEA mycotoxin in Caco-2 [14], CHO-K1 [19], and HepG2 cells [17]. However, there are no reports on the effect of ZEA metabolites and BEA in neuronal cells. In the present study, we proved the toxicity of ZEA metabolites (α-ZEL and β-ZEL) and BEA in human neuroblastoma SH-SY5Y cells in relation to exposure time, mycotoxin concentration, and mixture of mycotoxins.

According to the IC_{50} values of single mycotoxins, β-ZEL was the most cytotoxic mycotoxin compared to the other mycotoxins assayed individually, which is in accordance with Marin et al. (2019) [33] who studied the cytotoxicity of ZEA and its metabolites in HepG2 cells, individually and in double combinations. On the contrary, Tatay et al. (2014) [32] demonstrated that α-ZEL was the most cytotoxic among three mycotoxins tested (α-ZEL, β-ZEL, and ZEN) in CHO-K1 cells. Regarding to double combinations, it was revealed that presence of two mycotoxins increased the cytotoxic potential in SH-SY5Y cells, as shown by the lower IC_{50} values. According to Figure 2a, IC_{50} for α-ZEL and BEA was not reached in individual treatment however, binary combination α-ZEL + BEA (5:1) inhibited cell proliferation from up to 50 to 90% for all times studied. For the β-ZEL + BEA (5:1) binary combination, as it can be observed in Figure 2b, the IC_{50} values at 48 and 72 h were lower than that of β-ZEL. This was also observed when β-ZEL was combined with α-ZEL, for which combination (α-ZEL + β-ZEL (1:1)), the IC_{50} value was the same as that found for β-ZEL alone. This result was not achieved by Tatay et al. (2014) [31] in CHO-K1 cells, although the mycotoxin concentrations studied in binary assays in that work were two times higher than the concentrations assayed in our study. The proliferation of CHO-K1 cells treated with the α-ZEL + β-ZEL mixture at the highest concentration decreased only by 20% with respect to the values found when each mycotoxin was tested alone. In addition, in that study, the IC50 value was never reached for binary mixtures, whereas in our study in SH-SY5Y cells, after 48 and 72 h, the α-ZEL + β-ZEL combination inhibited cell proliferation up to 70% and 90%, respectively (Figure 2c). For the triple combination (α-ZEL + β-ZEL + BEA, (5:5:1)), cell proliferation inhibition was lower than when β-ZEL was assayed individually, and the same result was found

for β-ZEL + BEA after 48 and 72 h and for α-ZEL + β-ZEL after 48 h in SH-SY5Y cells. This is in contrast with the results obtained for the tertiary combination of α-ZEL + β-ZEL + ZEA in CHO-K1 cells, as this combination was more cytotoxic than each mycotoxin tested alone [30].

As the co-occurrence of mycotoxins in food and feed is very common, some studies evaluated the toxicity and cytotoxicity of several mycotoxins, both individually and in combination, in different cell lines, using the isobologram model. In these experiments, HepG2 cells were exposed to ochratoxin A (OTA) and BEA [16], to double and triple combinations of alternariol, 3-acetyl-deoxynivalenol, and 15-acetyl-deoxynivalenol [28], and to combinations of ZEA and OTA or α-ZEL (tested also individually) [33], CHO-K1 cells in vitro were used to examine the interactions between the mycotoxins beauvericin, deoxynivalenol (DON), and T-2 toxin [26] as well as the combination of BEA, patulin, and ZEA [17], whereas Caco-2 cells were exposed to DON, ZEN, and Aflatoxin B1 [34]. It is important to understand whether the interaction between mycotoxins shows synergism, additive effects, and/or antagonism concerning cell viability.

In SH-SY5Y cells, almost all the combinations tested reduced cell viability more than the individual mycotoxins, except the β-ZEL + BEA (5:1), α-ZEL + β-ZEL (1:1), and α-ZEL + β-ZEL + BEA (5:5:1) combinations, for which the reduction in cell viability was not significantly different from that obtained when β-ZEL was assayed individually. According to Dong et al. (2010) [5], ZEA is degraded more efficiently to α-ZEL than to β-ZEL in almost all tissues, whereas it is converted more efficiently to β-ZEL than to α-ZEL in liver and lungs. Some studies demonstrated that β-ZEL is more cytotoxic than α-ZEL [31,35,36],

whereas other studies found that α-ZEL is more cytotoxic [30,35]. Hence, there is a necessity to clarify the cytotoxicity of these two mycotoxins with studies of the toxicity mechanisms involved.

The IC_{50} values obtained by the MTT assay and the amount of mycotoxin detected in the media by LC–ESI–qTOF-MS were determined and translated into percentage values as an attempt to calculate the amount of each mycotoxin involved in the cytotoxic effect and in the type of interaction effect. Hence, the percentage of mycotoxin present in the media was considered in accordance to the IC_{50} value obtained from the MTT assay (Table 1). The results showed that among the individual mycotoxins assayed, the amount of α-ZEL that remained in the culture medium was above 50% of the administered quantity at all times assayed (Figure 5a). This can be related to the effect in Figure 1a, which shows that the viability was above 100% for the doses reported in Figure 5. This can be justified by the chemical structure of this compound, which might impede its access in the cell. Our results suggest that the availability and capacity of the tested mycotoxins to get into cells were greater than those of α-ZEL, and as a consequence, the amounts of these mycotoxins detected in the media were lower than that of α-ZEL. To notice that the higher the amount of mycotoxin in the medium (at 24 h), the higher the cell viability, which might be related to the lower amount of mycotoxin affecting the live cells. On the contrary, BEA seemed to have easier access the cells, as its percentage in the medium was generally below 50%, but cell viability was maintained above 50% for the doses assayed, indicating the lower potential toxicity of BEA in SH-SY5Y cells compared to ZEA metabolites. In fact, among all three mycotoxins tested, BEA reached the IC_{50} values after long exposures times (72 h) (Table 1 and Figure

1c), highlighting again the mild toxic effect of BEA in SHY-SY5Y cells compared to ZEA metabolites.

According to this and when analyzing combinations, the amounts of ZEA metabolites found in the medium were in most cases below BEA's amounts, indicating easier access of these compounds in SH-SY5Y compared to BEA. In detail, for the α-ZEL + BEA combination (Figure 2a), it can be observed that the lower the amount of α-ZEL in the medium over time (Figure 5d), the lower the viability of SH-SY5Y cells, in particular at 72h. For triple mixtures, the cytotoxic effect was weaker at all times and for all mixtures compared with that of binary combinations; however, the amounts of each mycotoxin detected were all below 50%, and the cytotoxic effect seemed to be bearable for SH-SY5Y cells for doses administered in the first and second mixture but not for those of the third mixture (6.25 + 6.26 + 1.25) μM (α-ZEL + β-ZEL + BEA, 5:5:1), specifically at 48 and 72 h. We suggest that cytotoxicity is due to the stimulation of different biochemical mechanisms that, after a certain level of stimulation, cannot be controlled and cause cell death. Therefore, it is necessary to study in detail the mechanisms of action implicated in the cytotoxic effects that occur when several mycotoxins are present in the same food or diet.

5. Conclusion

In conclusion, the treatment with β-ZEL alone presented the highest cytotoxicological potency compared to treatments with the other mycotoxins assayed (α-ZEL and BEA). The main type of interaction detected between mycotoxins for all combinations assayed was synergism. The potential interaction effects between combinations in this study are difficult to explain since α-ZEL + BEA for binary and α-ZEL + β-ZEL + BEA for tertiary

combination were found more in favor of synergic effect respect to CI value, compared with other combinations, which could be related to the concentration range studied, ratio in each mixture, exposure time assayed and cell line studied. Moreover, among all mycotoxins assayed, α-ZEL appeared to remain in the culture medium and was less able to get into SH-SY5Y cells compared to BEA and β-ZEL. In combinations, such effect was observed for BEA reaching the highest in α-ZEL + BEA.

Supplementary materials: The following are available online at https://www.mdpi.com/2072-6651/12/4/212/s1, Figure S1. Percentage of α-ZEL, β-ZEL, and BEA remaining in the medium of SH-SY5Y cells after treatment during 24, 48, and 72 h at different concentrations and combinations by LC–ESI–qTOF-MS. (A) β-ZEL+ BEA and (B) α-ZEL + β-ZEL.

Key contribution: Individual exposure of β-ZEL in SH-SY5Y cells presented the highest cytotoxicological potency compared to α-ZEL and BEA; while in combination, α-ZEL + β-ZEL + BEA and α-ZEL + BEA presented the highest cytotoxic potential with respect to the IC50 value obtained. Recoveries were the highest for α-ZEL in individual treatment in SH-SY5Y; while, this high recovery was observed for BEA in binary combination α-ZEL + BEA.

Author contributions: Data curation, F.A.; Formal analysis, C.J. and A.J.-G.; Funding acquisition, G.F., C.J., and A.J.-G.; Investigation, F.A., C.J., and A.J.-G.; Methodology, A.J.-G.; Supervision, C.J. and A.J.-G.; Writing—original draft, F.A, C.J. and A.J.-G.; Writing—review & editing, C.J. and A.J.-G. All authors have read and agreed to the published version of the manuscript.

Funding: This research was supported by the Spanish Ministry of Economy and Competitiveness AGL2016-77610-R and the Generalitat Valenciana GVPROMETEO2018-126.

Conflicts of interest: The authors declare no conflict of interest.

6. Refences

1. Zain M.E. Impact of mycotoxins on humans and animals. J. Saudi Chem. Soc. 2011;15:129–144. doi: 10.1016/j.jscs.2010.06.006.
2. Mally A., Solfrizzo M., Degen G.H. Volume Biomonitoring of the mycotoxin Zearalenone: Current state-of-the art and application to human exposure assessment. Arch. Toxicol. 2016;90:1281–1292. doi: 10.1007/s00204-016-1704-0.
3. Richard J.L. Some major mycotoxins and their mycotoxicoses—An overview. Int. J. Food Microbiol. 2007;119:3–10. doi: 10.1016/j.ijfoodmicro.2007.07.019.
4. Hueza I.M., Raspantini P.C., Raspantini L.E., Latorre A.O., Górniak S.L. Zearalenone, an estrogenic mycotoxin, is an immunotoxic compound. Toxins. 2014;6:1080–1095. doi: 10.3390/toxins6031080.
5. Dong M., Tulayakul P., Li J.-Y., Dong K.-S., Manabe N., Kumagai S. Metabolic Conversion of Zearalenone to α-Zearalenol by Goat Tissues. J. Vet. Med. Sci. 2010;72:307–312. doi: 10.1292/jvms.09-0122.
6. Venkataramana M., Chandra Nayaka S., Anand T., Rajesh R., Aiyaz M., Divakara S.T., Murali H.S., Prakash H.S., Lakshmana Rao P.V. Zearalenone induced toxicity in SHSY-5Y cells: The role of oxidative stress evidenced by N-acetyl cysteine. Food Chem. Toxicol. 2014;65:335–342. doi: 10.1016/j.fct.2013.12.042.

7. Gajecka M., Zielonka L., Gajecki M. The effect of low monotonic doses of zearalenone on selected reproductive tissues in pre-pubertal female dogs- a review. Molecules. 2015;20:20669–20687. doi: 10.3390/molecules201119726.

8. EFSA CONTAM Panel (EFSA Panel on Contaminants in the Food Chain) Scientific opinion on the appropriateness to set a group health-based guidance value for zearalenone and its modified forms. EFSA J. 2016;14:4425.

9. Wang J.J., Wei Z.K., Han Z., Liu Z.Y., Zhu X.Y., Li X.W., Wang K., Yang Z.T. Zearalenone Induces Estrogen-Receptor-Independent Neutrophil Extracellular Trap Release in Vitro. J. Agric. Food Chem. 2019;67:4588–4594. doi: 10.1021/acs.jafc.8b05948.

10. El-Makawy A., Hassanane M.S., Abd Alla E.S.A.M. Genotoxic evaluation for the estrogenic mycotoxin zearalenone. Reprod. Nutr. Dev. 2001;41:79–89. doi: 10.1051/rnd:2001114.

11. Abid-Essefi S., Baudrimont I., Hassen W., Ouanes Z., Mobio T.A., Anane R., Creppy E.E., Bacha H. DNA fragmentation, apoptosis and cell cycle arrest induced by zearalenone in cultured DOK, Vero and Caco-2 cells: Prevention by Vitamin E. Toxicology. 2003;192:237–248. doi: 10.1016/S0300-483X(03)00329-9.

12. Cai G., Pan S., Feng N., Zou H., Gu J., Yuan Y., Liu X., Liu Z., Bian J. Zearalenone inhibits T cell chemotaxis by inhibiting cell adhesion and migration related proteins. Ecotox. Environ. Safe. 2019;175:263–271. doi: 10.1016/j.ecoenv.2019.03.045.

13. Hassen W., El Golli E., Baudrimont I., Mobio A.T., Ladjimi M.M., Creppy E.E., Bacha H. Cytotoxicity and Hsp70 induction in HepG2 cells in

response to zearalenone and cytoprotection by sub-lethal heat shock. Toxicology. 2005;207:293–301. doi: 10.1016/j.tox.2004.10.001.

14. Prosperini A., Juan-García A., Font G., Ruiz M.J. Beauvericin induced cytotoxicity via ROS production and mitochondrial damage in Caco-2 cells. Toxicol. Lett. 2013;222:204–211. doi: 10.1016/j.toxlet.2013.07.005.
15. Zhang K., Tan X., Li Y., Liang G., Ning Z., Ma Y., Li Y. Transcriptional profiling analysis of Zearalenone-induced inhibition proliferation on mouse thymic epithelial cell line 1. Ecotox. Environ. Safe. 2018;153:135–141. doi: 10.1016/j.ecoenv.2018.01.005.
16. Zouaoui N., Mallebrera B., Berrada H., Abid-Essefi S., Bacha H., Ruiz M.J. Cytotoxic effects induced by patulin, sterigmatocystin and beauvericin on CHO–K1 cells. Food Chem. Toxicol. 2016;89:92–103. doi: 10.1016/j.fct.2016.01.010.
17. Juan-García A., Tolosa J., Juan C., Ruiz M.J. Cytotoxicity, Genotoxicity and Disturbance of Cell Cycle in HepG2 Cells Exposed to OTA and BEA: Single and Combined Actions. Toxins. 2019;11:341. doi: 10.3390/toxins11060341.
18. Ferrer E., Juan-García A., Font G., Ruiz M.J. Reactive oxygen species induced by beauvericin, patulin and zearalenone in CHO-K1 cells. Toxicol. In Vitro. 2009;23:1504–1509. doi: 10.1016/j.tiv.2009.07.009.
19. Mallebrera B., Font G., Ruiz M.J. Disturbance of antioxidant capacity produced by beauvericin in CHO-K1 cells. Toxicol. Lett. 2014;226:337–342. doi: 10.1016/j.toxlet.2014.02.023.
20. Stockmann-Juvala H., Mikkola J., Naarala J., Loikkanen J., Elovaara E., Savolainen K. Oxidative stress induced by fumonisin B1 in continuous

human and rodent neural cell cultures. Free Radic. Res. 2004;38:933–942. doi: 10.1080/10715760412331273205.

21. Zhang X., Boesch-Saadatmandi C., Lou Y., Wolffram S., Huebbe P., Rimbach G. Ochratoxin A induces apoptosis in neuronal cells. Genes Nutr. 2009;4:41–48. doi: 10.1007/s12263-008-0109-y.
22. Zingales V., Fernández-Franzón M., Ruiz M.J. Sterigmatocystin-induced cytotoxicity via oxidative stress induction in human neuroblastoma cells. Food Chem. Toxicol. 2020;136:110956. doi: 10.1016/j.fct.2019.110956.
23. Stanciu O., Juan C., Miere D., Loghin F., Mañes J. Occurrence and co-occurrence of Fusarium mycotoxins in wheat grains and wheat flour from Romania. Food Control. 2017;73:147–155. doi: 10.1016/j.foodcont.2016.07.042.
24. Juan C., Berrada H., Mañes J., Oueslati S. Multi-mycotoxin determination in barley and derived products from Tunisia and estimation of their dietary intake. Food Chem. Toxicol. 2017;103:148–156. doi: 10.1016/j.fct.2017.02.037.
25. Oueslati S., Berrada H., Mañes J., Juan C. Presence of mycotoxins in Tunisian infant foods samples and subsequent risk assessment. Food Control. 2017;84:362–369. doi: 10.1016/j.foodcont.2017.08.021.
26. EFSA Guidance on harmonised methodologies for human health, animal health and ecological risk assessment of combined exposure to multiple chemicals. EFSA J. 2019;17:5634. doi: 10.2903/j.efsa.2019.5634.
27. Ruiz M.J., Franzova P., Juan-García A., Font G. Toxicological interactions between the mycotoxins beauvericin, deoxynivalenol and T-2 toxin in CHO-K1 cells in vitro. Toxicon. 2011;58:315–326. doi: 10.1016/j.toxicon.2011.07.015.

28. Juan-García A., Juan C., König S., Ruiz M.J. Cytotoxic effects and degradation products of three mycotoxins: Alternariol, 3-acetyl-deoxynivalenol and 15-acetyl-deoxynivalenol in liver hepatocelular carcinoma cells. Toxicol. Lett. 2015;235:8–16. doi: 10.1016/j.toxlet.2015.03.003.

29. Juan-García A., Juan C., Manyes L., Ruiz M.J. Binary and tertiary combination of alternariol, 3-acetyl-deoxynivalenol and 15-acetyl-deoxynivalenol on HepG2 cells: Toxic effects and evaluation of degradation products. Toxicol. In Vitro. 2016;34:264–273. doi: 10.1016/j.tiv.2016.04.016.

30. Chou T.C., Talalay P. Quantitative analysis of dose-effect relationships: The combined effects of multiple drugs or enzyme inhibitors. Adv. Enzyme Regul. 1984;22:27–55. doi: 10.1016/0065-2571(84)90007-4.

31. Chou T.C. Theoretical basis, experimental design, and computerized simulation of synergism and antagonism in drug combination studies. Pharmacol. Rev. 2006;58:621–681. doi: 10.1124/pr.58.3.10.

32. Tatay E., Meca G., Font G., Ruiz M.J. Interactive effects of zearalenone and its metabolites on cytotoxicity and metabolization in ovarian CHO-K1 cells. Toxicol. In Vitro. 2014; 28:95–103. doi: 10.1016/j.tiv.2013.06.025.

33. Marin D.E., Pistol G.C., Bulgaru C.V., Taranu I. Cytotoxic and inflammatory effects of individual and combined exposure of HepG2 cells to zearalenone and its metabolites. N-S. Arch. Pharmacol. 2019;392:937–947. doi: 10.1007/s00210-019-01644-z.

34. Zheng N., Gao Y.N., Liu J., Wang H.W., Wang J.Q. Individual and combined cytotoxicity assessment of zearalenone with ochratoxin A or α-

zearalenol by full factorial design. Food Sci. Biotechnol. 2018;27:251–259. doi: 10.1007/s10068-017-0197-9.

35. Jia J., Wang Q., Wud H., Xiaa S., Guoa H., Blaženovićc I., Zhanga Y., Suna X. Insights into cellular metabolic pathways of the combined toxicity responses of Caco-2 cells exposed to deoxynivalenol, zearalenone and Aflatoxin B1. Food Chem. Toxicol. 2019;126:106–112. doi: 10.1016/j.fct.2018.12.052.
36. Abid S., Bouaziz C.E., Golli-Bennour E., Ouanes Ben Othmen Z., Bacha H. Comparative study of toxic effects of zearalenone and its two major metabolites α-zearalenol and β-zearalenol on cultured human Caco-2 cells. J. Biochem. Mol. Toxic. 2009;23:233–243. doi: 10.1002/jbt.20284.
37. Ruiz M.J., Festila L.E., Fernandez M. Comparison of basal cytotoxicity of seven carbamates in CHO-K1 cells. Environ. Toxicol. Chem. 2006;88:345–354. doi: 10.1080/02772240600630622.

Study 3

Oxidative stress, glutathione, and gene expression key indicators in SH-SY5Y cells exposed to zearalenone metabolites and beauvericin

Fojan Agahi, Neda Álvarez-Ortega, Guillermina Font, Ana Juan-García* and Cristina Juan

Laboratory of Toxicology and Food Chemistry, Faculty of Pharmacy, University of Valencia, Burjassot 46100, Valencia, Spain

Agahi et al., 2020. Toxicology Letters 334, 44–52

Abstract

The co-presence of mycotoxins from fungi of the genus *Fusarium* is a common fact in raw food and food products, as trace levels of them or their metabolites can be detected, unless safety practices during manufacturing are carried out. Zearalenone (ZEA), its metabolites α-zearalenol (α-ZEL) and β-zearalenol (β-ZEL) and, beauvericin (BEA) are co/present in cereals, fruits or their products which is a mixture that consumer are exposed and never evaluated in neuronal cells. In this study the role of oxidative stress and intracellular defense systems was assessed by evaluating reactive oxygen species (ROS) generation and glutathione (GSH) ratio activity in a human neuroblastoma cell line, SH-SY5Y cells, treated individually and combined with α-ZEL, β-ZEL and BEA. It was further examined the expression of genes involved in cell apoptosis (*CASP3, BAX, BCL2*) and receptors of (endogenous or exogenous) estrogens (*ERβ* and *GPER1*), by RT-PCR in those same conditions. These results demonstrated elevated ROS levels in combinations where α-ZEL was involved (2.8- to 8-fold compared to control); however, no significant difference in ROS levels were detected when single mycotoxin was tested. Also, the results revealed a significant increase in GSH/GSSG ratio at all concentrations after 24 h. Expression levels of *CASP3* and *BAX* were up regulated by α-ZEL while *CASP3* and *BCL2* were down regulated by β-ZEL, revealing how ZEA´s metabolites can induce the expression of cell apoptosis genes. However, BEA down-regulated the expression of *BCL2*. Moreover, β-ZEL + BEA was the only combination treatment which was able to down regulate the levels of cell apoptosis gene expression. Relying to our findings, α-ZEL, β-ZEL and BEA, induce injury in SH-SY5Y cells elevating oxidative stress levels, disturbing the antioxidant activity role of glutathione system and finally, causing disorder in the expressions and activities of the related apoptotic cell death genes.

Keywords: α-ZEL, β-ZEL, BEA, ROS, GSH/GSSG, apoptosis, endocrine disruptor

1. Introduction

Mycotoxins are low-molecular-weight toxic compounds synthetized by different types of molds belonging mainly to the genera *Aspergillus, Penicillium*, *Fusarium* and *Alternaria* (Berthiller et al., 2013). The management of the *Fusarium* phytopathogens has been proven to be difficult due to their high genetic variability and broad host specificity (Ploetz et al., 2015). Mycotoxin-producing *Fusarium* species are major pathogens in cereals like wheat, oats, barley, and maize (Nganje et al., 2004; Stanciu et al., 2017a; Juan et al., 2017a, 2017b, 2017b; Oueslati et al., 2020).

Among the *Fusarium* mycotoxins, one of the primarily concerned is zearalenone (ZEA), commonly found in cereals like barley, sorghum, oats, wheat, millet, and rice. (Stanciu et al., 2017a; Bakker et al., 2018; Perincherry et al., 2019; Oueslati et al., 2020). The two major metabolites of ZEA are α-zearalenol (α-ZEL) and β-zearalenol (β-ZEL) which are metabolized in various tissues, particularly in the liver (Fig. 1) (EFSA, 2011 and 2017). There are various studies which have determined the effects of ZEA and its metabolites both in vivo and in vitro to characterize their estrogenic effect (Hueza et al., 2014; Tatay et al., 2017a; Zheng et al., 2019). It is also reported that they exert harmful health effect via decreasing fertility, increased fetal resorption, and changes in the weight of endocrine glands and serum hormone levels. However, exposure to these mycotoxins are not only limited to their estrogenic effect, but other mechanisms such as oxidative stress, cytotoxicity and DNA damages might be important mediators involved in their toxicity (Abid et al., 2009; Tatay et al., 2014, 2016, 2017b; Marin et al., 2019; Agahi et al., 2020).

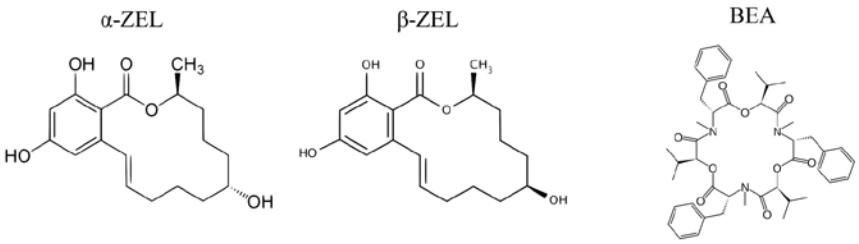

Figure 1. Chemical structures of the mycotoxins: α-ZEL and β-ZEL, BEA.

On the other hand, beauvericin (BEA) also belongs to *Fusarium* species and can cause cytotoxic effects by reducing cell proliferation in time and in concentration dependent manner according to recent publications (Zouaoui et al., 2016; Juan-García et al., 2019a). Moreover, it can increase ROS generation, lipid peroxidation and produce oxidative stress and depletion of antioxidant cellular mechanisms (Ferrer et al., 2009; Prosperini et al., 2013; Mallebrera et al., 2014; Manyes et al., 2018; Juan-García et al., 2019b; and 2020).

Since, in the real scenario, more than one mycotoxin can exist in food products, we dedicated our previous study to investigate the cytotoxic effect of co-presence of all three mentioned compounds on undifferentiated human neuroblastoma cell line (SH-SY5Y cells) and observed how they interfere with the normal functioning of cell proliferation (Agahi et al., 2020). According on our findings, the major effect detected in all combinations was synergism, and the highest cytotoxicity was observed when three mycotoxins were presented together. Therefore, there was a clear need for more comprehensive and reliable toxicology data to determine the reasons which lead to cytotoxicity and reduction of cell proliferation.

Undifferentiated SH-SY5Y cells endogenously express estrogen receptors (Grassi et al., 2013), which function as ligand-activated transcription factors to

regulate gene transcription (Ding et al., 2019). The potential of ZEA´s metabolites in such direction plus mixtures with BEA add insights in elucidating that effect and not only through the most susceptible cells (Ventakarama et al., 2014). BEA reaches the blood brain barrier (BBB) if it passes to the systemic circulation and hence, it is capable of exerting central nervous system effects as demonstrated in a recent in vitro study of BBB transport (with homogenates of mouse brain) (Taevernier et al., 2016). Mycotoxins of the same family (enniatin B and B1) in a porcine BBB model using different cell lines demonstrated to reach the brain parenchyma, highlighting the neurotoxic effect of these mycotoxins (Krug et al., 2018). SH-SY5Y seems to be a good model for studying in vitro effects at neuronal level. A bottleneck is the dose of exposure to study because of the low concentrations of α-ZEL and β-ZEL found in plasma and urine (Föllmann et al., 2016; Shephard et al., 2013; Wallin et al., 2015); so that, to get a good evaluation of toxic effect in vitro, the dose of exposure must be higher than those reported in circulation. In fact, some experiment performed to the BBB transport in vivo in mice used non-real exposure routes (intravenously and intracerebroventriculary) to ensure its experiments (Taevernier et al., 2016) as well as for bioavailability and toxicokinetic studies in pigs (Catteuw et al., 2019).

Cells have cellular protection mechanisms against biological reactive intermediates, xenobiotics (including mycotoxins) and metabolic products. When there is an imbalance between the production of oxidizing molecular species or ROS and the co-presence of cellular antioxidant agents in favor of the pro-oxidants, it can initiate events that contribute to production of oxidative stress and afterwards can damage mainly lipids, proteins and DNA (Hassen et

al., 2007; Tatay et al., 2016; Juan-García et al., 2019b; and 2020). Moreover, the reduced glutathione (GSH)/glutathione disulfide (GSSG) redox couple is an important marker of oxidative stress due to its antioxidative role and high concentrations in cells.

In accordance with several studies, it has been shown that ZEA and its metabolites are generally hypothesized to mimic estrogen-like actions and compete with estrogens in binding to estrogen receptors (*ERs*) which is including the classical estrogen receptor alpha (*ERα*), estrogen receptor beta (*ERβ*) and G protein-coupled estrogen receptor (*GPER1*); these mycotoxins also decreased follicle stimulant hormone (FSH) synthesis and secretion through non-classical estrogen membrane receptor *GPR30* which it is also called *GPER1* (He et al., 2018; Kuiper-Goodman et al., 1987). Due to the structural similarity of these compounds to the endogenous estrogens (Parveen et al., 2009), their ability to activate the *ERs* leading to transcription of estrogen-responsive genes is a keypoint in this report.

Moreover, the *Bcl-2* family members are involved in the regulation of apoptosis by either inhibiting or promoting apoptosis (Martin et al., 1995). Other proteins, including the caspase family, play an additional role in the apoptotic process (Zamai et al., 1996). Several mycotoxins are able to activate caspases and *Bcl-2* family by triggering the apoptosis-inducing factor from the mitochondria. Accumulating evidence has indicated that ZEA induce apoptosis in bovine mammary epithelial cells via *CASP3, BAX, BCL2* genes (Fu et al., 2019); also in porcine granulosa cells via the caspase-3- and caspase-9-dependent mitochondrial signaling pathway (Liu et al., 2018; Zhu et al., 2012).

Hence, the objective of this study was to evaluate the effects of α-ZEL, β-ZEL and BEA, mycotoxins on production of reactive oxygen species (ROS) by using the H2-DCFDA probe on undifferentiated human neuroblastoma cell line (SH-SY5Y) during 120 min. It was also studied the GSH/GSSG ratio in these cells affected by all three mycotoxins individually and in combination. Because of the association of ZEA as endocrine disruptor, the expression of genes that code for estrogen receptors (*ER2* (specifically *ERβ*) and *GPER1*) by all three mycotoxins were examined. Furthermore, to obtain more insight into the factors playing a role in the apoptotic process, and since there are few studies about the ability of ZEA derivates and BEA on cell apoptosis, individually or in two or three combinations, the relative mRNA expression levels of *CASP3, BAX* and *BCL2* were evaluated in SH-SY5Y cell line, through RT-PCR.

2. Materials and methods

2.1. Reagents

The reagent grade chemicals and cell culture components used, Dulbecco's Modified Eagle's Medium- F12 (DMEM/F-12), fetal bovine serum (FBS) and phosphate buffer saline (PBS) were supplied by Thermofisher, Gibco ™ (Paisley, UK). Methanol (MeOH, HPLC LS/MS grade), was obtained from VWR International (Fontenay-sous-Bois, France). Dimethyl sulfoxide was obtained from Fisher Scientific Co, Fisher BioReagnts ™ (Geel, Belgium). [3-(4,5-dimethylthiazol- 2-yl)-2,5-diphenyltetrazolium bromide] (MTT) for MTT assay, penicillin, streptomycin, and Trypsin–EDTA was purchased from SigmaAldrich (St. Louis, MO, USA). Deionized water (<18, MΩcm resistivity) was obtained in the laboratory using a Milli-QSP® Reagent Water System

(Millipore, Beadford, MA, USA). The standard of BEA (MW: 783.95 g/mol), α-ZEL and β-ZEL (MW: 320,38 g/mol) were purchased from SigmaAldrich (St. Louis Mo. USA). Stock solutions of mycotoxins were prepared in MeOH (α-ZEL and β-ZEL) and DMSO (BEA) and maintained at −20 °C in the dark. The final concentration of either MeOH or DMSO in the medium was ≤1% (v/v) as per established. All other standards were of standard laboratory grade.

2.2. Cell culture

Human neuroblastoma cell line, SH-SY5Y, was obtained from American Type Culture Collection (ATCC, Manassas, VA, USA), and cultured in Dulbecco's Modified Eagle's Medium- F12 (DMEM/F-12), supplemented with 10% fetal bovine serum (FBS), 100 U/ml penicillin, and 100 mg/ml streptomycin. The cells were sub-cultivated after trypsinization once or twice a week and suspended in complete medium in a 1:3 split ratio. Cells were maintained as monolayer in 150 cm2 cell culture flasks with filter screw caps (TPP, Trasadingen, Switzerland). Cell cultures were incubated at 37 °C, 5% CO_2 atmosphere.

2.3. Intracellular ROS generation

Early intracellular ROS production was monitored in SH-SY5Y cells by using the H2-DCFDA probe. DCFH-DA is taken up by the cells, and then deacetylated by intracellular esterase's and the resulting H2-DCFDA is oxidized by ROS to the highly fluorescent DCF. Briefly, 2×10^4 cells/well were seeded in a 96-well black culture microplate. After reaching confluence, cells were loaded with 20 μM H2-DCFDA in fresh medium for 20 min. Subsequently, H2-DCFDA was removed and cells were washed with PBS and then exposed to α-

ZEL and β-ZEL (25, 12.5, 6.25 and 3.12 μM), and BEA (2.5, 1.25, 0.78 and 0.39 μM) as an individual treatment. Afterwards, they were assayed in combination through the following mixtures: α-ZEL + BEA, β-ZEL + BEA, α-ZEL + β-ZEL and α-ZEL + β-ZEL + BEA with concentrations ranged from 25 to 1.87 μM for binary combinations, and from 27.5 to 3.43 μM for tertiary combination. The dilution ratio of concentration ranges in binary combinations was (1:1) for α-ZEL + β-ZEL, (5:1) for α-ZEL + BEA and β-ZEL + BEA, and (5:5:1) in tertiary combinations (α-ZEL + β-ZEL + BEA) (Table 1).

Table 1. Sequence of the specific primers used in the analysis of the expression.

Gene Symbol	Forward (5' - 3')	Reverse (5' - 3')
CASP3	GGAGGCCGACTTCTTGTATG	GCCATCCTTTGAATTTCGCC
BAX	ATGCGTTTTCCTTACGTGTCT	GAGGTCAGCAGGGTAGATGA
BCL2	CTTCTTTGAGTTCGGTGGGG	AAATCAAACAGAGGCCGCAT
ER2	AATGCCGATGCCTATCCTCT	ATGGCAAATGAACAGGCAAAG
GPER1	CTCAGCGGACAAAGGATCAC	ACTTCAGCGAATCTCACTCC

Data of single and combination treatments were obtained by considering the cytotoxicity assays for ZEA metabolites and BEA reported in our previous study (Agahi et al., 2020).

Increases in fluorescence were measured on a Perkin Elmer Wallac 1420 VICTOR2™ Multilabel Counter (Turku, Finland), at intervals up to 2 h at excitation/emission wavelengths of 485/535 nm, respectively. Results are expressed as increase in fluorescence in respect to control (untreated cells). Three independent experiments were performed with eight replicates each.

2.4. GSH determination

Determination of GSH and GSSG was assayed according to Maran et al (2009). Briefly, 7×10^5 cells/well were seeded in six-well plates. Once the cells reached 90% confluence, the culture medium was replaced with fresh medium containing different concentrations of: α-ZEL and β-ZEL (1.56, 3.12, 6.25 and 12.5 μM) BEA (0.31, 0.62, 1.25, and 2.5 μM), individually and in combination for 24 and 48 h of incubation. Afterwards, the medium was removed, and cells were washed with PBS and then homogenized in 0.25 ml of 20 mM Tris and 0.1% Triton.

For GSH determination, 10 μL of each homogenized cell sample was placed in 96 well black tissue culture plate, with 200 μL GSH buffer (pH 8.0) and 10 μL of OPT solution, mixed and incubated in darkness at room temperature for 15 min. For GSSG determination, 25 μL of each homogenized cell sample and 25 μL NEM (N-ethylmaleimide, 0.005 g/mL in deionized water) were placed in a 1.5 ml eppendorf, mixed and incubated at room temperature for 20 min. Afterwards, 50 μL of NaOH 0.1 N were added to achieve the correct pH to develop the GSSG assay. 10 μL of the mixture prepared was placed with 200 μL NaOH 1 N and 10 μL of the OPT (O-phthalaldehyde, 0.001 g/mL of in MeOH) solution in 96 well black tissue culture plate, mixed and incubated in darkness at room temperature for 15 min.

Concentrations of GSH and GSSG (prepared in plates described above) were determined using the microplate reader Wallace Victor2, model 1420 multilabel counter (Perkin Elmer, Turku, Finland) with excitation and emission wavelength of 345 and 424 nm, respectively. The GSH and GSSG levels were

expressed in μg/mg proteins. Determinations were performed in two independent experiments with 4 replicates each.

2.5. Gene expression assay by RT-PCR

The real-time polymerase chain reaction (RT-PCR) was applied to do the gene expression assay on SH-SY5Y cells, which were counted and placed (7 × 105 cells/well) in 6-well tissue culture plates. After 24 h, the cells were exposed individually to α-ZEL (12.5 and 25 μM), β-ZEL (12.5 and 25 μM), and BEA (2.5 μM). In addition, the potential effects were evaluated using the following mixtures: α-ZEL + β-ZEL (12.5μM), α-ZEL + BEA (12.5 + 2.5μM), β-ZEL + BEA (12.5 + 2.5μM) and α-ZEL + β-ZEL + BEA (12.5 + 12.5 + 2.5μM), employing DMSO (1%) as vehicle control.

Total RNA was isolated from cell samples using the ReliaPrep™ RNA Cell Miniprep System kit (Promega, Madison, WI, USA) following the manufacturers' instructions. The RNA concentration was measured using a NanoDrop 2000 spectrophotometer (Thermo Scientific, Wilmington, USA), and its purity was evaluated by the absorbance ratios A260/A280 and A260/A230. Agarose gel electrophoresis (1.0%) was used to verify the RNA integrity (Alvarez-Álvarez-Ortega et al., 2017). Subsequently, the cDNA was synthesized from 500 ng of mRNA extracted using the TaqMan reverse transcription reagents kit (Applied Biosystems, Foster City, CA, USA) (Escrivá et al., 2019).

RT-PCR procedure was carried out as described previously by Álvarez-Ortega et al (2019) with some modifications. Briefly, RT-PCR amplification was

performed and monitored using a StepOne Plus thermocycler (Applied Biosystems, Foster City, CA, USA). The reactions were performed in MicroAmp optical 96-well reaction plates (Applied Biosystems). Each 10 μL reaction mixture contained 5 μL of template cDNA, 5 μL of PowerUp SYBR Green Master Mix (Thermo Fisher Scientific Inc.), and 3 μL of forward and reverse primers (2.5 μM). In total, 5 genes were analyzed, the expression of three genes involved in cell apoptosis (*CASP3, BAX, BCL2*) and two genes that code for estrogen receptors (*ER2* (specifically *ERβ*) and *GPER1*) (Table 1). Changes in gene expression were determined using 18S as the reference gene (housekeeping), and the comparative delta delta CT (ΔΔCT) method was utilized to estimate the relative mRNA amount of the target genes. Three experiments with two replicates were carried out. All experiments were run by duplicates and negative controls contained no cDNA.

2.6. Statistical analysis

Statistical analysis of data was carried out using IBM SPSS Statistic version 23.0 (SPSS, Chicago, Il, USA) statistical software package and GraphPad Prism 8.0 (GraphPad Prisma Software, Inc., San Diego, USA). Data were expressed as mean ± SD of three independent experiments. The statistical analysis of the results was performed by student's T-test for paired samples. Difference between groups were analyzed statistically with ANOVA followed by the Tukey HDS post hoc test for multiple comparisons. The level of $p \leq 0.05$ was considered statistically significant.

3. Results

3.1. Intracellular ROS generation of individual and combined mycotoxins

Changes in ROS generation inside SH-SY5Y cells in response to α-ZEL, β-ZEL and BEA (individually and in combinations) were determined. The production of ROS was determined by DCFH-DA assay. A treatment with all mycotoxins alone revealed a moderate change of ROS generation respect to the initial time (Figure 2).

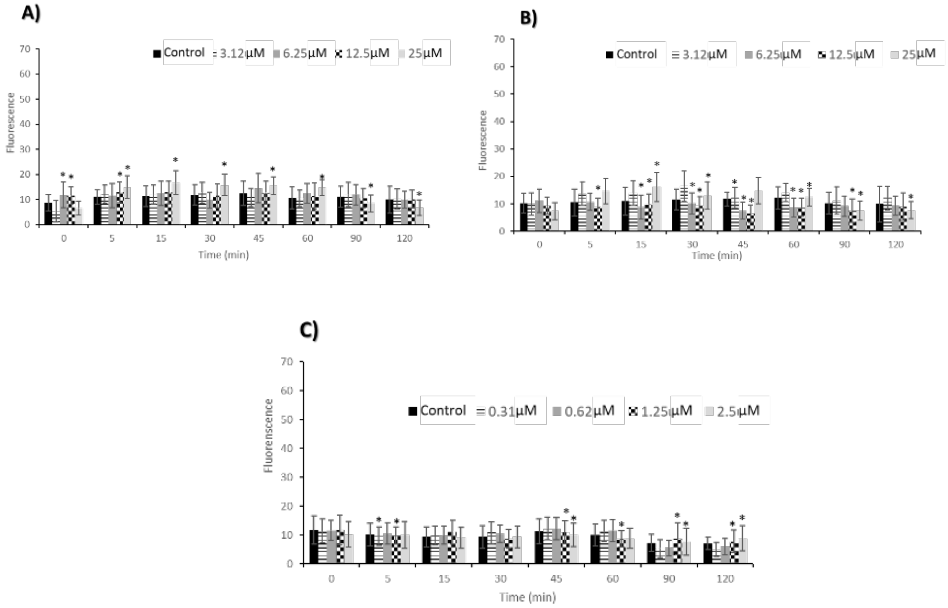

Figure 2. Time dependence of ROS-induced fluorescence in SH-SY5Y cells exposed to α-ZEL (A), β-ZEL (B) and BEA (C), for 120 min at several concentrations (μM). Results are expressed as mean ± SEM (n = 3). (*) Represents significant differences ($p \leq 0.05$) versus control.

According to α-ZEL tested alone, at 25 μM there is slight increase from 5 to 60 min and from 90 to 120 min decline moderately respect to their control (p

≤ 0.05) (Figure 2A). For individual test of β-ZEL, there is total decrease for 12.5 μM from 5 to 90 min and in addition, at 25 μM after 15 and 30 min and from 60 to 120 min it can be observed a moderate decrease compared to their control ($p \leq 0.05$) (Figure 2B). Finally, for BEA, there is a slight decrease at 1.25 and 2.5 μM, from 45 to 120 min respect to control ($p \leq 0.05$) (Figure 2C).

The mycotoxin mixture of α-ZEL + BEA increased ROS generation compared with control, after 45 and 120 min, at [1.56 + 0.31] μM ($p \leq 0.05$), while a gradual decrease at [6.25 + 1.25] μM and [12.5 + 2.5] μM at all times was obtained ($p \leq 0.05$) (Figure 3A). For a combination of β-ZEL + BEA, a decrease of ROS generation with respect to control was observed (Figure 3B) at [6.25 + 1.25] μM and [12.5 + 2.5] μM after 15 to 120 min ($p \leq 0.05$). For α-ZEL + β-ZEL, a statistically significant increase in ROS with respect to the control was obtained at the highest concentration assayed [12.5 + 12.5] μM from 15 to 120 min ($p \leq 0.05$), additionally, for [6.25 + 6.25] μM from 15 to 90 min (Fig. 3C). For the mixture containing all three compounds [α-ZEL + β-ZEL + BEA], as can be seen in Figure 3, at [6.25 + 6.25 + 1.25] μM after 15 min and from 45 to 120 min ($p \leq 0.05$), decrease ROS generation slightly, also, at highest concentration [12.5 + 12.5 + 2.5] μM from 45 to 120 min ($p \leq 0.05$), there is a moderate decrease compared with control (Figure 3D).

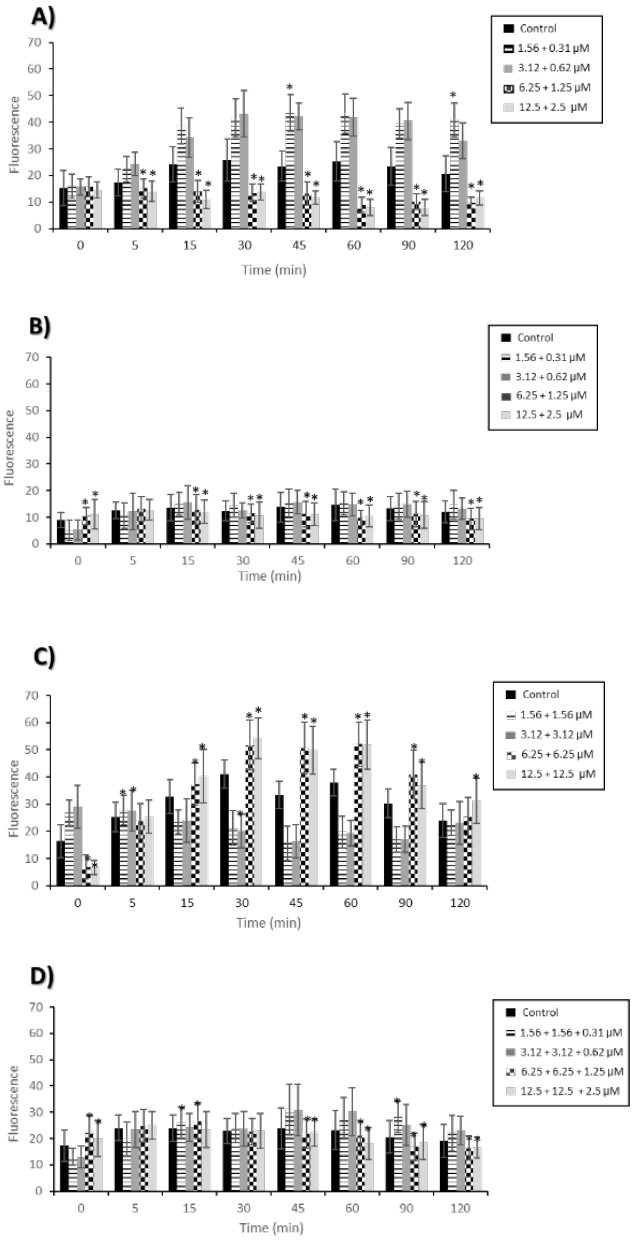

Figure 3. Time dependence of ROS-induced fluorescence in SH-SY5Y cells exposed to mixtures of α-ZEL + BEA (A), β-ZEL + BEA (B) and α-ZEL+β-ZEL (C)

and α-ZEL+β-ZEL + BEA (D) for 120 min at several concentrations (μM). Results are expressed as mean ± SEM (n = 3). (*) Represents significant differences ($p \leq 0.05$) versus control.

3.2. GSH determination

The alteration on GSH, GSSG and GSH/GSSG ratio was measured after 24 and 48 h of exposure to α-ZEL, β-ZEL (1.56, 3.12, 6.25 and 12.5 μM) and BEA (0.31, 0.62, 1.25, and 2.5 μM), individually and in combination in SH-SY5Y cells grown in fresh medium (Figure 4 and Figure 5).

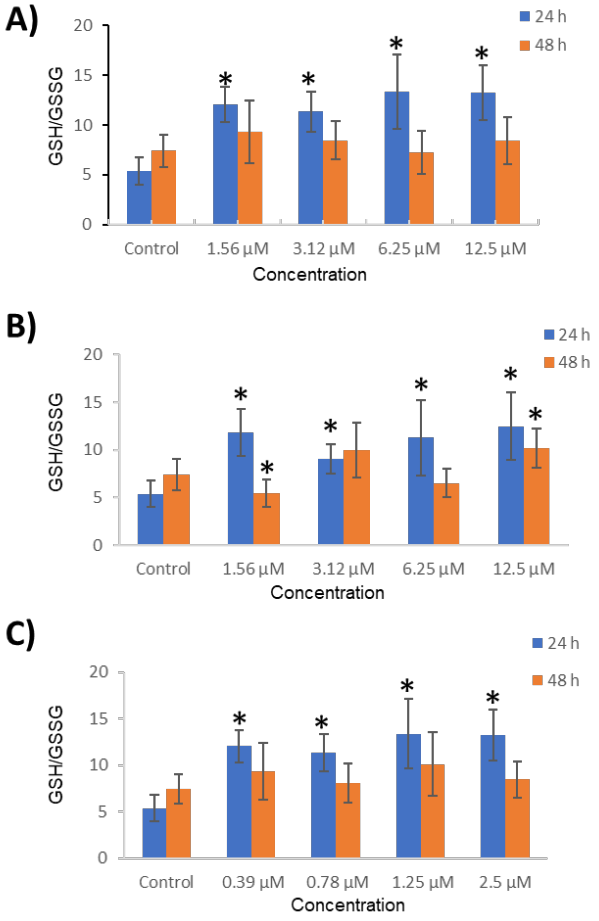

Figure 4. Effect of zearalenone metabolites α-ZEL (A) and β-ZEL (B) (1.56, 3.12, 6.25 and 12.5 µM) and BEA (C) (0.39, 0.78, 1.25 and 2.5 µM) on the GSH/GSSG ratio after 24 h and 48 h of exposure. Data are expressed as mean values ± SEM of two independent experiments with 4 replicates each. *$p \leq 0.05$ indicates a significant difference from the respective control (fresh medium).

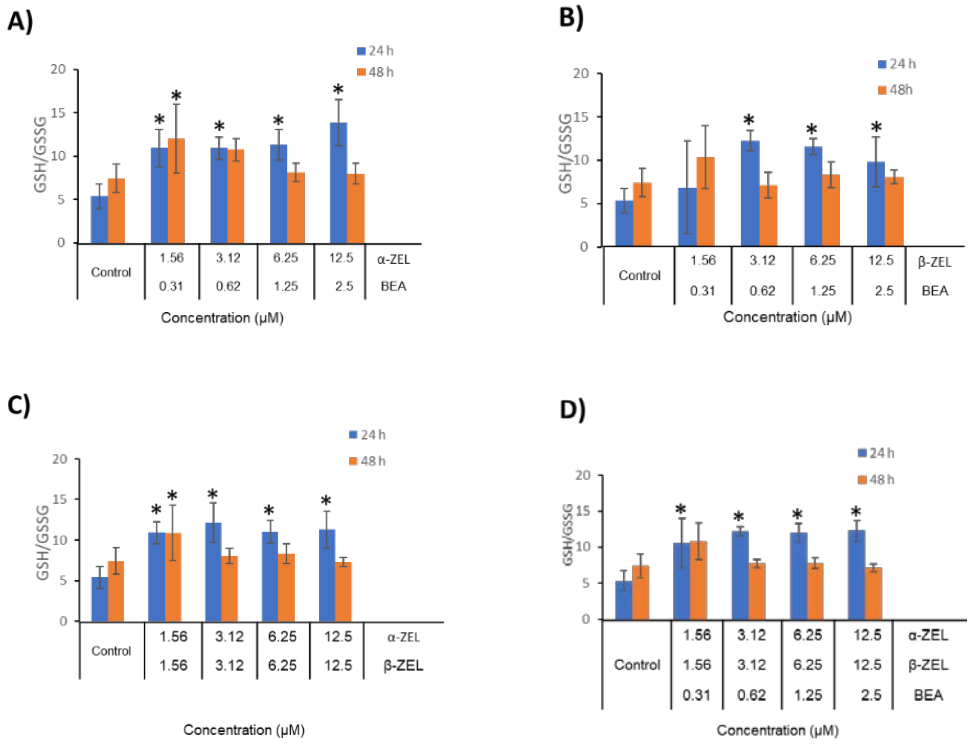

Figure 5. Effect of mycotoxins mixtures α-ZEL + BEA (A), β-ZEL + BEA (B), α-ZEL + β-ZEL (C), and α-ZEL + β-ZEL + BEA (D) on the GSH/GSSG ratio after 24 h and 48 h of exposure. Data are expressed as mean values ± SEM of two independent experiments with 4 replicates each. *p ≤ 0.05 indicates a significant difference from the respective control (fresh medium).

In individual treatments, as shown in Figure 4, GSH/GSSG ratio significantly increased after 24 h in cells exposed to mycotoxins in fresh medium at all concentrations from 111% to 148%, from 68% to 131% and from 103% to 142% for α-ZEL (Figure 4A), β-ZEL (Figure 4B) and BEA (Figure 4C), respectively. However, after 48 h of exposure, GSH/GSSG ratio had a significant increase only after β-ZEL exposure of 12.5 μM by 37% and for the rest was not observed any considerable increase (Figure 4B).

On the other hand, in combination treatments, GSH/GSSG ratio (Figure 5) showed a significant increase in all cases for binary and tertiary mixtures respect to their controls; accordingly, from concentrations tested, percentages reached went from 102% to 157% for α-ZEL + BEA (Figure 5A), from 102% to125% for α-ZEL + β-ZEL (Figure 5C) and sequently, for β-ZEL + BEA binary combination it was observed a considerable increase in all concentrations assayed (from 81% to 127%) except for the lowest concentration assayed [1.56 + 0.31] μM) (Figure 5B). Ultimately, in tertiary mixture GSH/GSSG ratio raised from 95% to 128% for the lowest and the highest concentration respect to control cells after 24 h of exposure (Figure 5D).

After 48 h, in combination treatments GSH/GSSG ratio was not affected by any treatment except for binary mixtures α-ZEL + BEA (Figure 5A) and α-ZEL + β-ZEL (Figure 5C) in their respective lowest concentrations assayed ([1.56 + 031] μM and [1.56 + 1.56] μM) which increased significantly ($p \leq 0.05$) by 61% and 46%, respectively and respect to their control.

3.3. Gene expression assay in individual and combination

Findings in gene expression assay demonstrate that among all mycotoxins assayed individually. Compared to vehicle control, mRNA of *CASP3* and *BAX* mRNA were significantly overexpressed (up to 1.5-fold compared to the reference gene (18S)) for α-ZEL at concentrations of 12.5 and 25 μM ($p \leq 0.05$) (Figure 6A). On the other hand, β-ZEL up-regulated *ERβ* mRNA significantly up to 2.7-fold at 12.5 μM while down-regulated expression of *CASP3* and *BCL2* considerably (Figure 6B). Additionally, BEA up-regulated

only *BCL2* mRNA significantly while it was not able to induce the expression of other studied genes (Figure 6C).

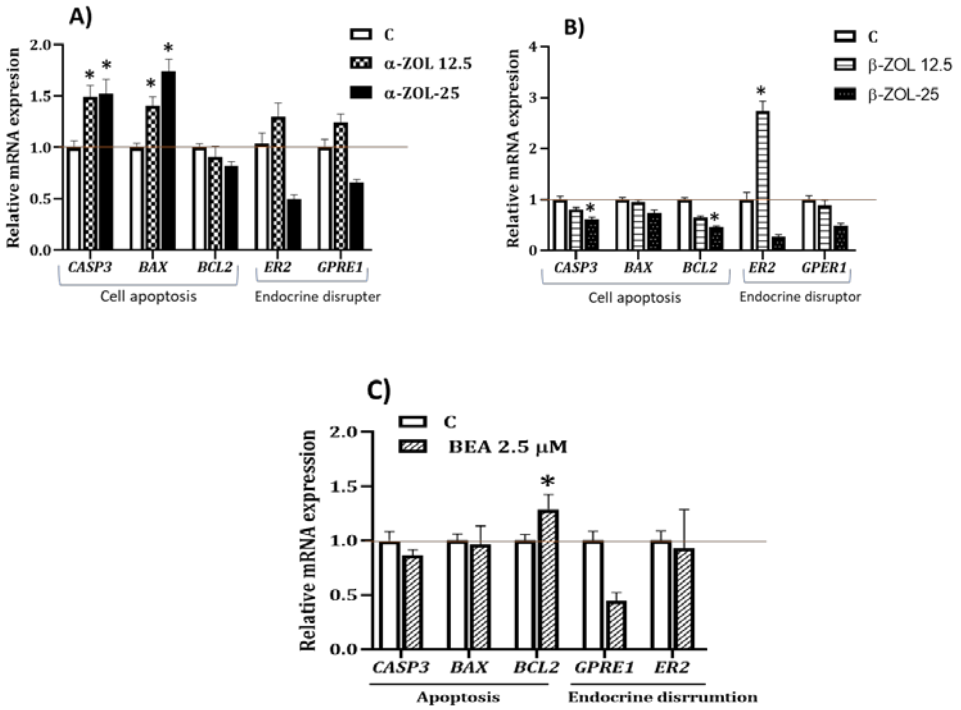

Figure 6. Gene expression patterns of *CASP3, BAX, BCL, ERβ* and *GPER1* under different treatments in SH-SY5Y during 24 h by qRT-PCR. (A) for α-ZEL treatment, (B) for β-ZEL treatment and (C) for BEA treatment. *CASP3, BAX* and *Bcl2* are marker gene for cell apoptosis and *ERβ* and *GPER1* are markers of estrogen receptors. Three experiments with two replicates were carried out. Error bars represent standard deviations. Asterisks indicate significant ($p < 0.05$) differences in treated plants compared to mock-treated plants or to the time point before treatment.

Among all combination treatments, β-ZEL + BEA was able to up-regulate the expression of all genes involved in cell apoptosis up to 1.5-fold (Figure 7). Also, the expression of *BCL2* mRNA down-regulated significantly when cells were exposed to α-ZEL + β-ZEL combination (Figure 7).

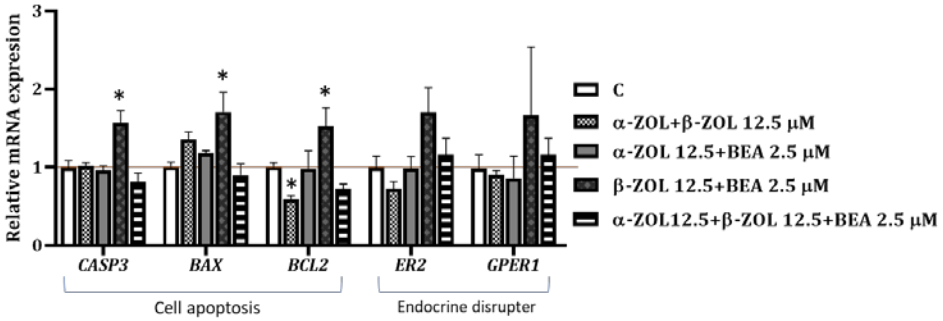

Figure 7. Gene expression patterns of *CASP3, BAX, BCL, ERβ* and *GPER1* under different combination treatments in SH-SY5Y during 24 h by qRT-PCR. *CASP3, BAX* and *BCL* are marker gene for cell apoptosis and *ERβ* and *GPER1* are markers of estrogen receptors. Three experiments with two replicates were carried out. Error bars represent standard deviations. Asterisks indicate significant ($p < 0.05$) differences in treated plants compared to mock-treated plants or to the time point before treatment.

4. Discussion

Oxidative stress induced by mycotoxins has been explained by their ability to provoke generation of ROS in most of the cases. ZEA´s metabolites and BEA are known to be a common contaminant of important cereal and cereal-based products, such as corn, rice, wheat, barley and oats, throughout the world (Bertero et al., 2018); however, there are limited studies to demonstrate the effects of these mycotoxins on cells cytotoxicity according to their relationship on different factors such as oxidative stress and regulation of gene expression, individually and in combination (Ferrer et al., 2009; Tatay et al., 2016, 2017b; Marin et al., 2019; Fu et al., 2019).

In a previous study conducted in our laboratory, ZEA´s metabolites (α-ZEL and β-ZEL) and BEA were examined individually and in combination and

it was observed that all caused cytotoxic effect on SH-SY5Y cells (Agahi et al., 2020). Accordingly, the present study aimed to determine the mechanism whereby α-ZEL, β-ZEL and BEA induce oxidative stress in the same cell line and its possible effect on alteration of GSH and GSSG levels. Also, to evaluate the effects of these three mycotoxins on expression of cell apoptosis and genes that code for estrogen receptors.

ZEA and its derivatives are known to be potent inducers of ROS in mammalian systems (Ben-Salem et al., 2015; Tatay et al., 2017b; Ben-Salem et al., 2017), also the studies of Ferrer et al. (2009), Prosperini et al. (2013) and Mallebrera et al. (2014) showed elevated level of ROS production by BEA when exposed to different cell lines (CHO-K1 and Caco-2 cells). Regarding to our results obtained from evaluating ROS generation, elevated ROS levels in combinations where α-ZEL was involved, were observed with increases of 2.8- to 8-fold compared to control (Figure 3), coinciding with that obtained by Tatay et al. (2017b) on HepG2 cells that α-ZEL was the major contributor to ROS production. However, no significant difference in ROS levels were detected when each mycotoxins was tested alone (Figure 2).

On the other hand, opposite to results previously published for SH-SY5Y cells, HepG2 cells and CHO-K1 cells (Venkataramana et al., 2014; Zingales et al., 2020; Tatay et al., 2016, 2017b) it was not observed any relationship between increasing time or concentration and the amount of ROS production in cells. The increased ROS generation in cells exposed to ZEA´s metabolites and BEA could be a consequent contribution to cell injury or oxidative stress. When the disruption occurred between the balance of antioxidant defense and ROS production, the cells try to survive so cellular

antioxidant enzymes play their major role which is protecting cells from oxidative stress and damage. Regarding this fact, the first non-enzymatic antioxidant defense system in cells is GSH which plays a basic role in binding with ROS. Hence, with considering that the levels of GSH determine the balance in the antioxidant defense system, the impact on cellular GSH content present in two redox form (glutathione reduced (GSH) and glutathione disulfide (GSSG)), was evaluated after 24 h and 48 h in SH-SY5Y cells for α-ZEL, β-ZEL and BEA individually and combined, as all three have toxicological interest due to their potential to cause oxidative stress and damage (Figure 2 and Figure 3).

The obtained data suggested that α-ZEL, β-ZEL and BEA, in individual and combination treatment after 24 h had induced GSH/GSSG in the SH-SY5Y cells, since the ratio was significantly elevated (Figure 4 and Figure 5); whereas, after 48 h of exposure the same result was only observed for α-ZEL + BEA and α-ZEL + β-ZEL combination at the lowest concentration assayed (Figure 5). The contrary effect was obtained by Zingales et al. (2020) when exposed to sterigmatocystin in the same cell line (SH-SY5Y cells), by depleting the GSH/GSSG ratio at the highest concentrations assayed.

Due to the increase in ROS levels and alteration in GSH/GSSG ratio, it was examined if such effects could be altering in SH-SY5Y cells the expression of genes involved in cell damage as apoptosis-related genes (*CASP3, BAX*, *BCL2*) and genes that code for estrogen receptors (*ERβ* and *GPER1*).

According to the OECD (Organization for Economic Cooperation and Development) EDTA (Endocrine Disrupter Testing and Assessment) meeting in April 2011, a possible endocrine disrupter is a chemical that is able to alter the

functioning of the endocrine system but for which information about possible adverse consequences of that alteration in an intact organism is uncertain (Organisation for Economic Co-operation and Development (OECD, 2011). In the light of this fact, the research carried out by Ranzenigo et al. (2008) and Frizzell et al. (2011) had shown that ZEA and its metabolites, α-ZEL and β-ZEL, act as potential endocrine disruptors by interfering with nuclear receptor signaling and also by altering hormone production. Moreover, Le Guevel and Pakdel, 2001 have shown that ZEA and its derivates can exert their estrogenic effects through their ability to bind to the estrogen receptor (ER) since the expression of *ERβ* mRNA in SH-SY5Y cells has been shown in other studies (Bang et al., 2004; Grassi et al., 2013; Xiao et al., 2013). Hence, we examined *GPER1* and *ERβ*. In our study as it is indicated in Figure 6 and Figure 7, among all three mycotoxins assayed in individual and combination forms, only β-ZEL up-regulated the expression of *ERβ* mRNA significantly up to 2.7-fold at 12.5 μM compared to the reference gene (*18S*); while for *GPER1*, any significant regulation was observed (Figure 6B).

Studies have shown that the *BCL2* and *BAX* pathways are involved in ZEA-induced apoptosis in primary rat cells (Li et al., 2011); also, the caspase family of proteins plays an important role in the initiation of apoptosis, of which caspase-3 is the primary initiator (Riedl and Salvesen, 2007). Nevertheless, there are no sufficient data about the two major metabolites of ZEA (α-ZEL and β-ZEL), since it is proved that it breaks down into their main metabolites during phase I metabolism (Metzler et al., 2010). The results of our study for individual treatments demonstrated that, while α-ZEL up-regulated the expression of cell apoptosis genes (Figure 6A), β-ZEL shows an adverse effect which was down-regulating of these genes (Figure 6B). Additionally, BEA only up-regulated the

expression of *BCL2* significantly (Figure 6C). Moreover, as it can be observed in Fig. 7, β-ZEL + BEA was the only combination that elevated the expression of cell apoptosis genes.

Then α-ZEL presented effect on gene expression, either cell apoptosis and estrogen receptors. However, in the combination, β-ZEL + BEA at [12.5 + 2.5] μM it was up-regulated the expression of all five studied gene expression involved in cell apoptosis (*CASP3, BAX, BCL2*) and estrogen receptors (*ERβ* and *GPER1*).

5. Conclusion

In conclusion, the results obtained in the present study indicate that α-ZEL, β-ZEL and BEA mycotoxins in SH-SY5Y cells, enhanced the oxidative damage by increasing ROS generation and GSH/GSSG ratio. In accordance to our findings, α-ZEL is more likely to induce oxidative stress in both individual and combination studies, also, this mycotoxin was found to be the most effective factor to enhance GSH/GSSG ratio in individual treatment and when it was involved in α-ZEL + BEA combination, which this can have consequences on initiation of oxidative damage. Regarding to expression genes effect, it is an unexplored area to investigate the endocrine-disruptive and cell apoptosis effects by up/down-regulation of implicated genes on SH-SY5Y cells exposed to mycotoxins and presented here for the first time. Our results show that β-ZEL might be considered a mycotoxin that induces apoptotic effect, individually and in combination while this happens for α-ZEL in individual exposure in SH-SY5Y cells. Nonetheless, there is no evidence how these genes can have further

effects in more developed and complex cell systems closer to human or animal body exposed to α-ZEL, β-ZEL and BEA so that further studies are necessary.

Declaration of Competing Interest

The authors declare that they have no known competing financial interests or personal relationships that could have appeared to influence the work reported in this paper.

Acknowledgements

This research has been supported by Spanish Ministry of Science and Innovation PID2019-108070RB-I00ALI, Generalitat Valenciana GVPROMETEO2018-126 and Generalitat Valenciana GV/2020/020. N.A.O. would like to thank Program for Doctoral Studies in Colombia (COLCIENCIAS 727.2015).

6. References

Abid, S., Bouaziz, C,El., Golli-Bennour, E., Ouanes Ben Othmen, Z., Bacha, H., 2009. Comparative study of toxic effects of zearalenone and its two major metabolites α-zearalenol and β-zearalenol on cultured human Caco-2 cells. Journal of Biochemical and Molecular Toxicology. 23, 233–243.

Alvarez-Ortega, N., Caballero-Gallardo, K and Olivero-Verbel, J., 2019. Toxicological effects in children exposed to lead: A cross-sectional study at the Colombian Caribbean coast. Environment international 130, 104809.

Alvarez-Ortega, N., Caballero-Gallardo, K., and Olivero-Verbel, J., 2017. Low blood lead levels impair intellectual and hematological function in children

from Cartagena, Caribbean coast of Colombia. Journal of Trace Elements in Medicine and Biology, 44, 233-240.

Bakker, M.G.; Brown, D.W.; Kelly, A.C.; Kim, H.S.; Kurtzman, C.P.; Mccormick, S.P.; O'Donnell, K.L.; Proctor, R.H.; Vaughan, M.M.; Ward, T.J., 2018. Fusarium mycotoxins: A trans-disciplinary overview. Canadian Journal of Plant Pathology. 40, 161–171.

Ben-Salem, I., Boussabbeh, M., Da-Silva, J.P., Guilbert, A., Bacha, H., Abid-Essefi, S., Lemaire, Ch., 2017. SIRT1 protects cardiac cells against apoptosis induced by zearalenone or its metabolites α- and β-zearalenol through an autophagy-dependent pathway. Toxicology and Applied Pharmacology. 314, 82-90.

Ben-Salem, I., Prola, A., Boussabbeh, M., Guilbert, A., Bacha, H., Lemaire, C., Abid-Essefi, S., 2015. Activation of ER stress and apoptosis by a- and b-zearalenol in HCT116 cells, protective role of Quercetin. NeuroToxicology. 53, 334-342.

Bertero, A., Spicer, L.J., Calonia, F., 2018. Fusarium mycotoxins and in vitro species-specific approach with porcine intestinal and brain in vitro barriers: A review. Food Chemical and Toxicology. 121, 666-675.

Berthiller, F.; Crews, C.; Dall'Asta, C.; de Saeger, S.; Haesaert, G.; Karlovsky, P.; Oswald, I.P.; Seefelder, W.; Speijers, G.; Stroka, J., 2013. Masked mycotoxins: A review. Molecular Nutrition and Food Research. 57, 165–186.

Biswas, S.K., & Rahman, I., 2009. Environmental toxicity, redox signaling and lung inflammation: The role of glutathione. Molecular Aspects of Medicine, 30(1-2), 60–76.

Di Monte, D., Bellomo, G., Thor, H., Nicotera, P., Orrenius, S., 1984. Menadione-induced cytotoxicity is associated with protein thiol oxidation and alteration in intracellular Ca2+ homeostasis. Archives of Biochemistry and Biophysics. 235(2):343-50.

Dong, M., Tulayakul, P., Li, J-Y., Dong, K-S., Manabe, N., Kumagai, S., 2010. Metabolic Conversion of Zearalenone to α-Zearalenol by Goat Tissues. Journal of Veterinary Medical Science. 72, 307-312.

Escrivá, L., Alonso-Garrido, M., Font, G., and Manyes, L., 2019. Transcriptional study after Beauvericin and Enniatin B combined exposure in Jurkat T cells. Food and Chemical Toxicology, 130, 122-129.

Ferrer, E., Juan-García, A., Font, G., Ruiz, M.J., 2009. Reactive oxygen species induced by beauvericin, patulin and zearalenone in CHO-K1 cells. Toxicology In Vitro. 23, 1504–1509.

Frizzell, C., Ndossi, D., Verhaegen, S., Dahl, E., Eriksen, G., Sørlie, M., Connolly, L., 2011. Endocrine disrupting effects of zearalenone, alpha- and beta-zearalenol at the level of nuclear receptor binding and steroidogenesis. Toxicology Letters, 206(2), 210–217.

Fu, Y., Jin, Y., Y.Z., Shan, A., Fang, H., Shen, J., Zhou, C., Yu, H., Zhou, Y.F., Wang, X., Wang, J., Li, R., Wang, R., Zhang, J., 2019. Zearalenone induces apoptosis in bovine mammary epithelial cells by activating endoplasmic reticulum stress. Journal of Dairy Science. 102, 10543-10553.

Hassen, W., Ayed-Boussema., I., Oscoz, A.A., De Cerain Lopez, A., Bacha, H., 2007. The role of oxidative stress in zearalenone-mediated toxicity in Hep G2 cells: oxidative DNA damage, glutathione depletion and stress proteins induction Toxicology. 232, 294-302.

He, J., Wei, Ch., Li, Y., Liu, Y., Wang, Y., Pan, J., Liu, J., Wu, Y., Sheng Cui, Sh., 2018. Zearalenone and alpha-zearalenol inhibit the synthesis and secretion of pig follicle stimulating hormone via the non-classical estrogen membrane receptor GPR30. Molecular and Cellular Endocrinology. 461, 43-54.

Hueza, I.M., Raspantini, P.C., Raspantini, L.E., Latorre, A.O., Górniak, S.L., 2014. Zearalenone, an estrogenic mycotoxin, is an immunotoxic compound. Toxins. 6(3), 1080–1095.

Juan-García, A., Tolosa, J., Juan, C., Ruiz, M.J., 2019. Cytotoxicity, Genotoxicity and Disturbance of Cell Cycle in HepG2 Cells Exposed to OTA and BEA: Single and Combined Actions. Toxins (Basel). 11(6): 341.

Kuiper-Goodman, T., Scott, P.M., Watanabe, H., 1987. Risk assessment of the mycotoxin zearalenone. Regulatory Toxicology and Pharmacology. 7 (3), 253-306.

Le Guevel, R., Pakdel, F., 2001. Assessment of oestrogenic potency of chemicals used as growth promoter by in-vitro methods. Human Reproduction. 16, 1030–1036.

Li, G.Y., Xie, P., Li, H.Y., Hao, L., Xiong, Q., Qiu, T., 2011. Involment of p53, Bax, and Bcl-2 pathway in microcystins-induced apoptosis in rat testis. Environmental Toxicology. 26,111–117.

Liu, X.L., Wu, R.Y., Sun, X.F., Cheng, S.F., Zhang, R.Q., Zhang, T.Y., Zhang, X.F., Zhao, Y., Shen, W., Li, L., 2018. Mycotoxin zearalenone exposure impairs genomic stability of swine follicular granulosa cells in vitro. Int. J. Biol. Sci., 14, 294-305.

Mallebrera, B., Font, G., Ruiz, M.J., 2014. Disturbance of antioxidant capacity produced by beauvericin in CHO-K1 cells. Toxicology Letters. 226, 337-342.

Marin, D. E., Pistol, G. C., Bulgaru, C. V., Taranu, I., 2019. Cytotoxic and inflammatory effects of individual and combined exposure of HepG2 cells to zearalenone and its metabolites. Naunyn-Schmiedeberg's Archives of Pharmacology. 392, 937–947.

Martin, SJ., Reutelingsperger, CP., McGahon, AJ., Rader, JA., van Schie, RC., LaFace, DM., Green, DR., 1995. Early redistribution of plasma membrane phosphatidylserine is a general feature of apoptosis regardless of the initiating stimulus: inhibition by overexpression of Bcl-2 and Abl. Journal of Experimental Medicine. 182:1545–1556.

Metzler, M., Pfeiffer, E., Hildebrand, A.A., 2010. Zearalenone and its metabolites as endocrine disrupting chemicals. World Mycotoxin Journal. 3, 385-401.

Nganje, W.E.; Bangsund, D.A.; Leistritz, F.L.; Wilson, W.W.; Tiapo, N.M., 2004. Regional economic impacts of Fusarium head blight in wheat and barley. Review of Agricultural Economics. 26, 332–347.

Organisation for Economic Co-operation and Development (OECD). 2011. In Environment, Health and Safety News: The OECD Environment, Health and Safety Programme: Achievements, no. 27 on December 2011, [online: http://www.oecd.org/env/chemicalsafetyandbiosafety/49171557.pdf]

Parveen, M., Zhu, Y., Kiyama, R., 2009. Expression profiling of the genes responding to zearalenone and its analogues using estrogen-responsive genes. FEBS Letters. 583, 2377–2384.

Perincherry, L; Lalak-Kanczugowska, J; Stepien, L., 2019. Fusarium-Produced Mycotoxins in Plant-Pathogen Interactions (review). Toxins. 11(11): 664.

Ploetz, R.C., 2015. Fusarium wilt of banana. Phytopathology. 105, 1512-1521.

Prosperini, A., Juan-García, A., Font, G., Ruiz, M. J., 2013. Beauvericin-induced cytotoxicity via ROS production and mitochondrial damage in Caco-2 cells. Toxicology Letters. 222(2), 204–211.

Ranzenigo, G., Caloni, F., Cremonesi, F., Y.Aad, P., J.Spicer, L., 2008. Effects of Fusarium mycotoxins on steroid production by porcine granulosa cells. Animal Reproduction Science. 107, 115-130.

Riedl, S.J., and. Salvesen, G.S., 2007. The apoptosome: Signalling platform of cell death. Nature reviews molecular cell biology. 8, 405–413.

Stanciu, O., Juan, C., Miere, D., Dumitrescu, A., Bodoki, E., Loghin, F., Mañes, J., 2017. Climatic conditions influence emerging mycotoxin presence in wheat grown in Romania – A 2-year survey. Crop Protection. 100, 124-133.

Tatay, E., Espín, S., García-Fernández, A.J., Ruiz, M.J., 2017a. Estrogenic activity of zearalenone, α-zearalenol and β-zearalenol assessed using the E-Screen assay in MCF-7 cells. Toxicology Mechanisms and Methods. 1537-6524.

Tatay, E., Espín, S., García-Fernández, A.J., Ruiz, M.J., 2017b. Oxidative damage and disturbance of antioxidant capacity by zearalenone and its metabolites in human cells. Toxicology in Vitro. 45, 334-339.

Tatay, E., Font, G and Ruiz, M.J., 2016. Cytotoxic effects of zearalenone and its metabolites and antioxidant cell defense in CHO-K1 cells. Food and Chemical Toxicology. 96, 43-49.

Tatay, E., Meca, G., Font, G., Ruiz, M.J., 2014. Interactive effects of zearalenone and its metabolites on cytotoxicity and metabolization in ovarian CHO-K1 cells. Toxicology in Vitro. 28, 95-103.

Venkataramana, M., Chandra Nayaka, S., Anand, T., Rajesh, R., Aiyaz, M., Divakara, S.T., Murali, H.S., Prakash, H.S., Lakshmana Rao, P.V., 2014. Zearalenone induced toxicity in SHSY-5Y cells: The role of oxidative stress evidenced by N-acetyl cysteine. Food and Chemical Toxicology. 65, 335-342.

Zamai, L., Falcieri, E., Marhefka, G., Vitale, M., 1996. Supravital exposure to propidium iodide identifies apoptotic cells in the absence of nucleosomal DNA fragmentation. Cytometry 23:303–311.

Zheng, W., Feng, N., Wang, Y., Noll, L., Xu, Sh., Liu, X., Lu, N., Zou, H., Gu, J., Yuan, Y., Liu, X., Zhu, G., Bian, J., Bai, J., Liu, Z., 2019. Effects of zearalenone and its derivatives on the synthesis and secretion of mammalian sex steroid hormones: A review. Food and Toxicology. 126, 262-276.

Zhu, L., Yuan, H., Guo, C., Lu, Y., Deng, S., Yang, Y., Wei, Q., Wen, L., He Z., 2012. Zearalenone induces apoptosis and necrosis in porcine granulosa cells via a caspase-3- and caspase-9-dependent mitochondrial signaling pathway. Journal of Cellular Physiology. 227, 1814-1820.

Zingales, V., Fernández-Franzón, M., Ruiz, M.J., 2020. Sterigmatocystin-induced cytotoxicity via oxidative stress induction in human neuroblastoma cells. Food and Chemical Toxicology. 136, 110956.

Zouaoui, N., Mallebrera, B., Berrada, H., Abid-Essefi, S., Bacha, H., Ruiz, M.-J., 2016. Cytotoxic effects induced by patulin, sterigmatocystin and beauvericin on CHO–K1 cells. Food and Chemical Toxicology. 89, 92–103.

Study 4

Study of enzymatic activity in human neuroblastoma cells SH-SY5Y exposed to zearalenone's derivates and beauvericin.

Fojan Agahi, Ana Juan-García*, Guillermina Font, Cristina Juan

Laboratory of Toxicology and Food Chemistry, Faculty of Pharmacy, University of Valencia, Burjassot 46100, Valencia, Spain

Agahi et al., 2021. Food and Chemical Toxicology, 152, 112227

Abstract

Beauvericin (BEA), α-zearalenol (α-ZEL) and β-zearalenol (β-ZEL), are produced by several Fusarium species that contaminate cereal grains. These mycotoxins can cause cytotoxicity and neurotoxicity in various cell lines and they are also capable of produce oxidative stress at molecular level. However, mammalian cells are equipped with a protective endogenous antioxidant system formed by no-enzymatic antioxidant and enzymatic protective systems such as glutathione peroxidase (GPx), glutathione S-transferase (GST), catalase (CAT) and superoxide dismutase (SOD). The aim of this study was evaluating the effects of α-ZEL, β-ZEL and BEA, on enzymatic GPx, GST, CAT and SOD activity in human neuroblastoma cells using the SH-SY5Y cell line, over 24h and 48h with different treatments at the following concentration range: from 1.56 to 12.5 μM for α-ZEL and β-ZEL, from 0.39 to 2.5 μM for BEA, from 1.87 to 25 μM for binary combinations and from 3.43 to 27.5 μM for tertiary combination.

SH-SY5Y cells exposed to α-ZEL, β-ZEL and BEA revealed an overall increase in the activity of i) GPx, after 24 h of exposure up to 24-fold in individual treatments and 15-fold in binary combination; ii) GST after 24 h of exposure up to 10-fold (only in combination forms), and iii) SOD up to 3.5- and 5-fold in individual and combined treatment, respectively after 48 h of exposure. On the other hand, CAT activity decreased significantly in all treatments up to 92% after 24 h except for β-ZEL + BEA, which revealed the opposite.

Keywords: Enzymatic antioxidant, Zearalenone's derivates, Beauvericin, Neuronal cells

1. Introduction

Many species of *Fusarium* produce a variety of mycotoxins which are widely distributed in nature and have serious health impacts in both humans and animals (Darwish et al, 2014; Dweba et al, 2017). The mycotoxins beauvericin (BEA) and zearalenone´s (ZEA) derivatives (α-zearalenol (α-ZEL) and β-zearalenol (β-ZEL)), are produced mainly by *Fusarium* species in agricultural crops and can be co-present in the same foodstuffs, feed or in the diet (Oueslati et al., 2020). ZEA is one of the most common mycotoxins in Europe produced by fungi, which has a great agro-economic importance (Wei et al, 2020; Bocianowski et al, 2020). The major pathway for ZEA biotransformation by animals is based on hydroxylation resulting in the formation of α-ZEL and β-ZEL, presumably catalyzed by 3 α- and 3β-hydroxysteroid dehydrogenases (Olsen et al, 1981) which will follow a metabolization process with different effects as recently predicted *in silico* (Agahi et al., 2020c). This conversion has been shown to occur in the liver of various species (Malekinejad et al., 2006a) and in various cells, such as bovine and porcine granulosa cells (Malekinejad et al., 2006b), rat erythrocytes (Chang and Lin, 1984), the intestinal mucosa of swine (Biehl et al., 1993) and human intestinal Caco-2 cells (Pfeiffer et al., 2011, Videmann et al., 2008, 2009). Devreese et al., (2015) have also demonstrated that both α-ZEL and β-ZEL were absorbed equally after intravenous administration of ZEA in broiler chickens, laying hens, and turkey poults; whereas an increased biotransformation to β-ZEL was demonstrated after oral administration (Devreese et al., 2015). Beside this, it has been demonstrated that ZEA, α-ZEL and β-ZEL impaired cell proliferation, steroid production, and gene expression in bovine small-follicle granulosa cells in vitro (Pizzo et al., 2016); more

importantly, it has been proved that α-ZEL and β-ZEL have a higher capacity to induce oxidative stress and damage in HepG2 cells than ZEA itself (Tatay et al, 2017). Brodehl et al. (2014) also showed that α-ZEL was 10-fold higher estrogenic than the parent ZEA, and in other study almost 500-fold stronger in comparison to ZEA, while β-ZEL was 16 times lower than ZEA (Drzymala et al., 2015; Molina-Molina et al., 2014). Moreover, in our previous study on SH-SY5Y cells reactive oxygen species (ROS) levels were higher in those combinations where α-ZEL was involved (2.8- to 8-fold compared to control) (Agahi et al., 2020b). Whereas when cytotoxicity of ZEA's metabolites were studied individually on the same cells line, it was shown that β-ZEL was more cytotoxic compared to α-ZEL (Agahi et al., 2020b). However, there isn´t information about combinations of these both metabolites jointly other mycotoxins that can be present in the same foodstuff.

Regarding beauvericin (BEA), it is characterized by allowing flux of cations on channel cells, (Kouri et al., 2003; Ojcius et al., 1991), thereby increasing the intracellular Ca^{2+} which can ultimately activate several biological pathways leading to cell death. Additionally, BEA was demonstrated to reduce calcium retention in isolated mitochondria (Tonshin et al., 2010). Ca^{2+} influx across the plasma membrane activate mitochondrial permeability transition pore opening and collapse the mitochondrial membrane potential. Moreover, BEA reduced cell viability and induced cytotoxic effects in different human cell lines which has been demonstrated through various in vitro studies (Prosperini et al, 2013; Mallebrera et al, 2014; Juan-García, 2019a and 2019b; Agahi et al, 2020b). Also, features characteristic of necrosis and apoptosis were observed in BEA-treated cells (Agahi et al, 2020a; Manyes et al, 2018; Prosperini et al, 2013; Klarić et al, 2008).

On the other hand, all organisms with a well-developed central nervous system have a blood–brain barrier (BBB) which is created by the endothelial cells that form the walls of the capillaries in the brain and spinal cord of humans (Abbott et al, 2005). It has been shown that BBB function as a protective barrier from neurotoxic substances circulating in the blood which maybe endogenous metabolites or proteins, or xenobiotics ingested in the diet or acquired from the environment. It has been proved by various studies that Fusarium mycotoxins are capable to cross the BBB and cause neuronal cell death (Taevernier et al, 2016; Behrens et al, 2015; Krug et al, 2018). However, there are limited studies about the effects of ZEA´s derivates and BEA mycotoxins on BBB doses of which are studied here in vitro with an undifferentiated human neuroblastome cell line, SH-SY5Y. SH-SY5Y is a cell line commonly used as neuronal model (Xicoy et al., 2017). The implications or evidences of these mycotoxins in trigger brain disorders in humans still remains unclear; while for other mycotoxins as tremortoxins neurotoxic effects in animals have been reported (Reddy et al., 2019).

As it is known, oxidative stress is the answer of disbalance between the production of ROS and a biological system's ability to detoxify or repair the resulting damage, which potentially can cause lipid peroxidation, degradation of cytosolic proteins and damage to DNA, which ultimately may lead to cell death (Dinu et al., 2011; Tatay et al., 2017). Furthermore, excite-toxicity and oxidative stress may cause neuronal cell degeneration and death (Gandhi and Abramov, 2012). Oxidative stress generates negative effects in neurons and astrocytes, a phenomenon that has been associated with the progression of different conditions such as Parkinson's disease and Alzheimer's disease, and cancer

(Albarracin et al., 2012). More recently, there are wide number of studies evidencing on the effects of oxidative stress damage caused by mycotoxins on different cell lines (Juan-García et al, 2020; Taroncher et al, 2020; Zingales et al., 2020, Tatay et al, 2016).

Considering this fact, enzymatic antioxidant function is to compensate the elevated ROS levels as well as non-enzymatic antioxidant system. However, depletion of these defense elements further promotes oxidative stress. In previous study we investigated the effects of α-ZEL, β-ZEL and BEA, mycotoxins on production of ROS on SH-SY5Y cell line (Agahi et al., 2020a). Hence, in the light of this, we further set out the present study to evaluate the enzymatic protective system in the same undifferentiated human neuroblastoma cell line, SH-SY5Y. As mentioned above it has been widely used as a cell model for the pathogenesis studies of neurotoxicity (Cai et al., 2020; Sirin et al., 2020; Lawana et al., 2020; Kim et al., 2020). Due to the lack of information in ZEA´s metabolites jointly other mycotoxins that can be present in the same foodstuffs, SH-SY5Y have been exposed to α-ZEL, β-ZEL and BEA (both individually and combined exposures) establishing the first time to figure out the effect in antioxidant enzymes activities including glutathione peroxidase (GPX), glutathione transferase (GST), catalase (CAT), and superoxide dismutase (SOD) and its implications.

2. Material and methods

2.1. Reagents

The reagent grade chemicals and cell culture components used, Dulbecco's Modified Eagle's Medium- F12 (DMEM/F-12), fetal bovine serum (FBS) and phosphate buffer saline (PBS) were supplied by Thermofisher, Gibco

™ (Paisley, UK). Methanol (MeOH, HPLC LS/MS grade), was obtained from VWR International (Fontenay-sous-Bois, France). Dimethyl sulfoxide (DMSO) was obtained from Fisher Scientific Co, Fisher BioReagnts ™ (Geel, Belgium). Deionized water (<18, MΩcm resistivity) was obtained in the laboratory using a Milli-QSP® Reagent Water System (Millipore, Beadford, MA, USA). Penicillin, streptomycin, and Trypsin–EDTA, β –nicotinamide adenine dinucleotide phosphate (β-NADPH), sodium azide (NaN3), glutathione reductase (GR), o-phtaldialdehyde (OPT), N-ethylmaleimide (NEM), t-octylphenoxypolyethoxyethanol (Triton-X 100), 1-chloro-2,4-dinitrobenzene (CDNB), ethylenediaminetetraacetic acid (EDTA), tris(hydroxymethyl)aminomethane (Tris), 4',6-diamidine-2'-phenylindole dihydrochloride (DAPI), H_2O_2 and the standard of BEA (MW: 783.95 g/mol), α-ZEL and β-ZEL (MW: 320,38 g/mol) were purchased from SigmaAldrich (St. Louis Mo. USA). Stock solutions of mycotoxins were prepared in MeOH (α-ZEL and β-ZEL) and DMSO (BEA) and maintained at −20 °C in the dark. The final concentration of either MeOH or DMSO in the medium was ≤1% (v/v) as per established. All other standards were of standard laboratory grade.

2.2. Cell culture

Human neuroblastoma cell line, SH-SY5Y, was obtained from American Type Culture Collection (ATCC, Manassas, VA, USA), and cultured in Dulbecco's Modified Eagle's Medium- F12 (DMEM/F-12), supplemented with 10% fetal bovine serum (FBS), 100 U/ml penicillin, and 100 mg/ml streptomycin. The cells were sub-cultivated after trypsinization once or twice a week and suspended in complete medium in a 1:3 split ratio. Cells were maintained as monolayer in 150 cm2 cell culture flasks with filter screw caps

(TPP, Trasadingen, Switzerland). Cell cultures were incubated at 37°C, 5% CO_2 atmosphere.

2.3. Determination of enzymatic activities

To determine the scavenging procedures in SH-SY5Y, cells got exposed to α-ZEL and β-ZEL (12.5, 6.25, 3.12 and 1.56 μM), and BEA (2.5, 1.25, 0.78 and 0.39 μM) for individual treatment. Afterwards, they were assayed in combination through the following mixtures: α-ZEL + BEA, β-ZEL + BEA, α-ZEL + β-ZEL and α-ZEL + β-ZEL + BEA with concentrations ranged from 25 to 1.87 μM for binary combinations, and from 27.5 to 3.43 μM for tertiary combination. The dilution ratio of concentration ranges in binary combinations was (1:1) for α-ZEL + β-ZEL, (5:1) for α-ZEL + BEA and β-ZEL + BEA, and (5:5:1) in tertiary combinations (α-ZEL + β-ZEL + BEA)

For these assays, 7×10^5 cells/well were seeded in six-well plates. After cells achieved the 90% confluence, cells were treated with α-ZEL and β-ZEL and BEA at the concentrations above detailed for 24 h and 48h. Then, the medium was removed, and cells were homogenized in 0.1 M phosphate buffer pH 7.5 containing 2 mM EDTA to a final volume of 0.5 mL. Aliquotes for each enzyme activity assay were prepared by disposing 125 μl in individual Eppendorfs.

2.3.1. Glutathione peroxidase activity

The glutathione peroxidase (GPx) activity was assayed spectrophotometrically using H_2O_2 as substrate for Se-dependent peroxidase activity of GPx by following oxidation of NADPH during the first 5 min in a coupled reaction with GR, as described by Maran et al., (2009). In 1 ml final

volume, the reaction mixture contained 500 µl of 0.1 M phosphate buffer, pH 7.5 with 4 mM NaN3 and 2 mM EDTA, 100 µl of 20 mM GSH, 250 µl of ultrapure water, 2 U freshly prepared GR, 20 µl of 10 mM NADPH and 50 µl of 5 mM H2O2. 50 µL of homogenized cell sample was added to the reaction mixture. One unit of GPx will reduce 1 µmol of GSSG per min at pH 7.5. The GPx enzymatic activity was calculated by using a molar absorptivity of NADPH ($6.22\ mM^{-1}\ cm^{-1}$) and expressed as µmol of NADPH oxidized/min/mg of protein. Assays were conducted at 25 °C in a thermocirculator of PerkinElmer UV/vis spectrometer Lambda 2 version 5.1. The absorbance was measured at 340 nm.

2.3.2. Glutathione S-transferase activity

The glutathione S-transferase (GST) activity was determined by following the conjugation of GSH with 1-chloro-2,4-dinitrobenzene (CDNB) during 5 min, according to the method of Maran et al., (2009). The reaction mixture contained in a final volume of 1 ml: 825 µl of 0.1 M Na/K phosphate buffer at pH 6.5, 100 µl of 20 mM GSH, 25 µl of 50 mM CDNB dissolved in ethanol and 50 µl of homogenized cell sample. The GST activity was expressed as mol of product formed/min/mg of protein using a molar absorptivity of CDNB (9.6 mM−1 cm−1). Enzymatic activity was assayed in a thermocirculator of PerkinElmer UV/vis spectrometer Lambda 2 version 5.1. The absorbance was measured at 340 nm.

2.3.3. Catalase activity

The catalase (CAT) activity was measured according to Ueda et al., (1990). Briefly, 100 µl of homogenized cell sample was mixed with 500 µl of 0.5 M potassium phosphate buffer at pH 7.2 and 400 µl of 40 mM H2O2. The rate of enzymatic decomposition of H_2O_2 was determined as absorbance decrements at 240 nm for 3 min at 30 °C with a spectrophotometer (Super Aquarius CECIL 9500 CE). The CAT activity was calculated by using the molar absorptivity of H2O2 (43.6 mM−1 cm−1) and expressed as µmol H_2O_2/min/mg of protein.

2.3.4. Superoxide dismutase activity

The superoxide dismutase (SOD) activity was determined using the Ransod kit (Randox Laboratories, United Kingdom) adapted for 1.5 ml cuvettes. The SOD destroys the free radical superoxide by converting it to peroxide. The SOD activity was monitored at 505 nm during 3 min at 37 °C with a spectrophotometer (PerkinElmer UV/Vis Lambda 2 version 5.1). The SOD results were expressed as units of SOD per mg protein. All the enzyme determinations were performed in duplicate.

2.6. Statistical analysis

Statistical analysis of data was carried out using IBM SPSS Statistic version 23.0 (SPSS, Chicago, Il, USA) statistical software package and GraphPad Prism 8.0 (GraphPad Software, Inc., San Diego, USA). Data were expressed as mean ± SD of three independent experiments. The statistical analysis of the results was performed by student's T-test for paired samples. Difference between groups were analyzed statistically with ANOVA followed by the Tukey HDS post hoc test for multiple comparisons. The level of $p \leq 0.05$ was considered statistically significant.

3. Result

The GPx, GST, CAT and SOD activities measured in undifferentiated SH-SY5Y cells after 24 h and 48 h of incubation with α-ZEL, β-ZEL and BEA in individual and in combination form, are presented in Figures from 1 to 5. Results of enzymes are expressed in folds and correspond to the number of times that increase or decrease respect to untreated cells (control).

3.1. Enzymatic activity of GPx

As shown in Figures 1A and 1B the GPx activity in SH-SY5Y cells exposed to α-ZEL and β-ZEL, increased significantly at all concentrations assayed only after 24 h compared to control. Increases went by 13.5- to 23-fold for α-ZEL and 9- to 17-fold for β-ZEL. This increase was observed after both 24 h and 48 h of exposure at all concentrations in cells exposed to BEA from 9- to 17-fold and from 2- to 9-fold after 24h and 48 h, respectively (Figure 1C).

Similarly, for all binary treatments the level of GPx activity increased significantly after 24 h of exposure, for α-ZEL + BEA at all concentrations assayed from 7.6- to 14.5-fold (Figure 1D)., for β-ZEL + BEA at all concentrations assayed from 4.7- to 10.3-fold (Figure 1E); and for α-ZEL + β-ZEL at all concentrations except at the lowest one from 2.5- to 7.8-fold compared to unexposed cells (Figure 1F). In contrary, the GPx activity in cells exposed to tertiary mixture of α-ZEL + β-ZEL + BEA an increase after 48 h of exposure at all concentrations assayed from 1- to 6-fold compared to control was observed (Figure 5A). In summary, it was observed higher GPx activity in individual exposure than in combinations which could be due to the low concentration level of ROS activity when cells were treated with mycotoxins individually that was observed in the previous study (Agahi et al., 2020a).

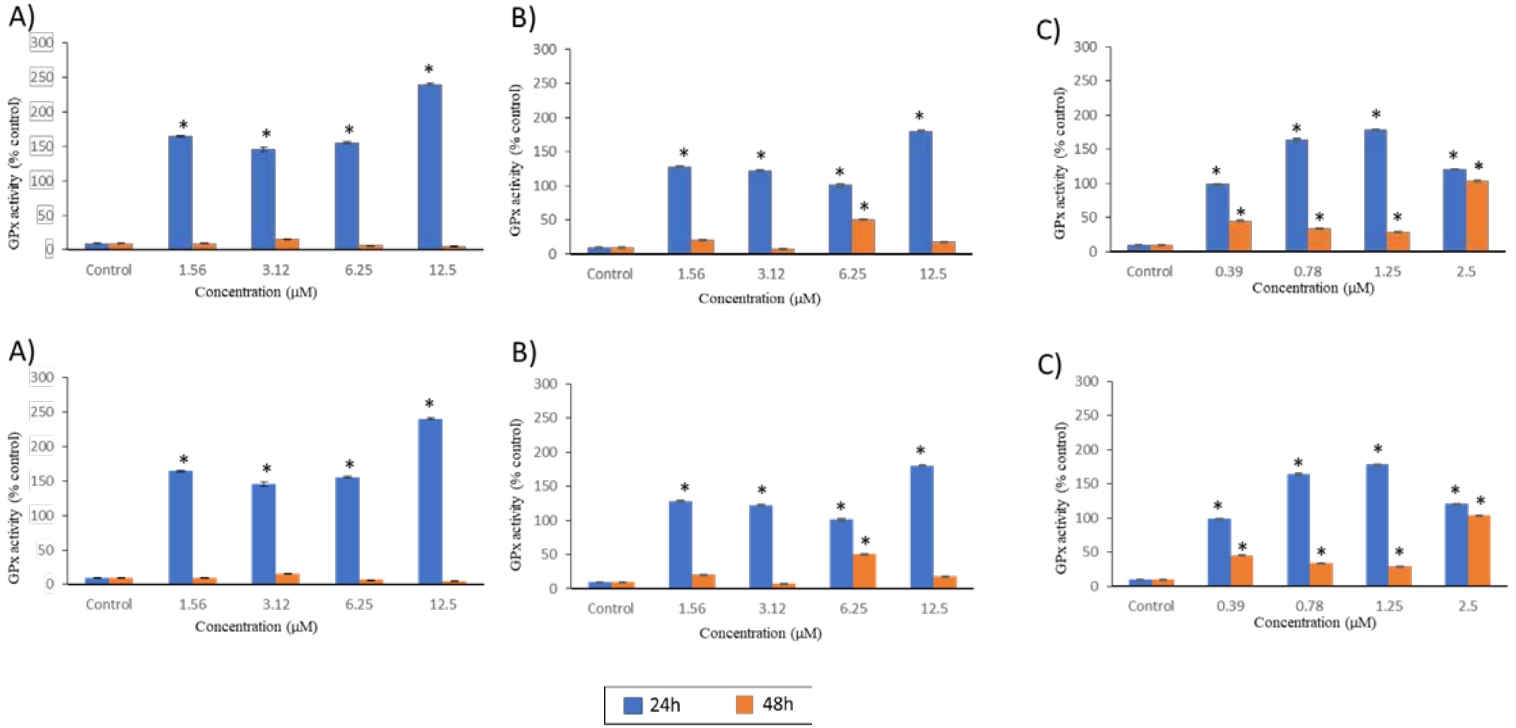

Figure 1. Effect of α-ZEL (A), β-ZEL (B) and BEA (C), α-ZEL + BEA (D), β-ZEL + BEA (E), and α-ZEL + β-ZEL + BEA (F) on glutathione peroxidase (GPx) activity after 24 h and 48 h of exposure in SH-SY5Y cells. Data are expressed in % of the unexposed control. The GPx activity is expressed as µmol of NADPH oxidized/min/mg of protein; mean ± SEM (n = 3). *p ≤ 0.05 indicates a significant difference from the respective solvent control.

3.2. Enzymatic activity of GST

Results for GST activity are described in percentage for individual treatments and compared to untreated cells (control). This enzyme activity increased significantly after 48 h of exposure in SH-SY5Y cells exposed to β-ZEL at 3.12 and 12.5 μM by 22% and 102%, respectively (Figure 2B). Similarly, this happened after being exposed to BEA to doses above 0.78 μM for 48 h of exposure by 4% to 32% (Figure 2C).

In combination treatments, GST activity increased significantly after 24 h of exposure to α-ZEL + BEA at [1.56 + 0.39] μM, [6.25 + 1.25] μM and [12.5 + 2.5] μM from 5.6- to 8- fold compared to control (Figure 2D), also after 48 h of exposure a notable increase at [6.25 + 1.25] was observed (Figure 2D). For β-ZEL + BEA, a significant increase at [6.25 + 1.25] μM and [12.5 + 2.5] μM by 4- and 3- fold compared to untreated cells was observed after 24 h of exposure (Figure 2E). As shown in Figure 2F, GST activity in SH-SY5Y cells exposed to α-ZEL + β-ZEL, increased significantly at all concentrations assayed up to 8.8-fold after 24 h of exposure compared to control. For tertiary mixture, α-ZEL + β-ZEL + BEA, GST activity in SH-SY5Y cells increased significantly from 1- to 7.7-fold compared to control (Figure 5B).

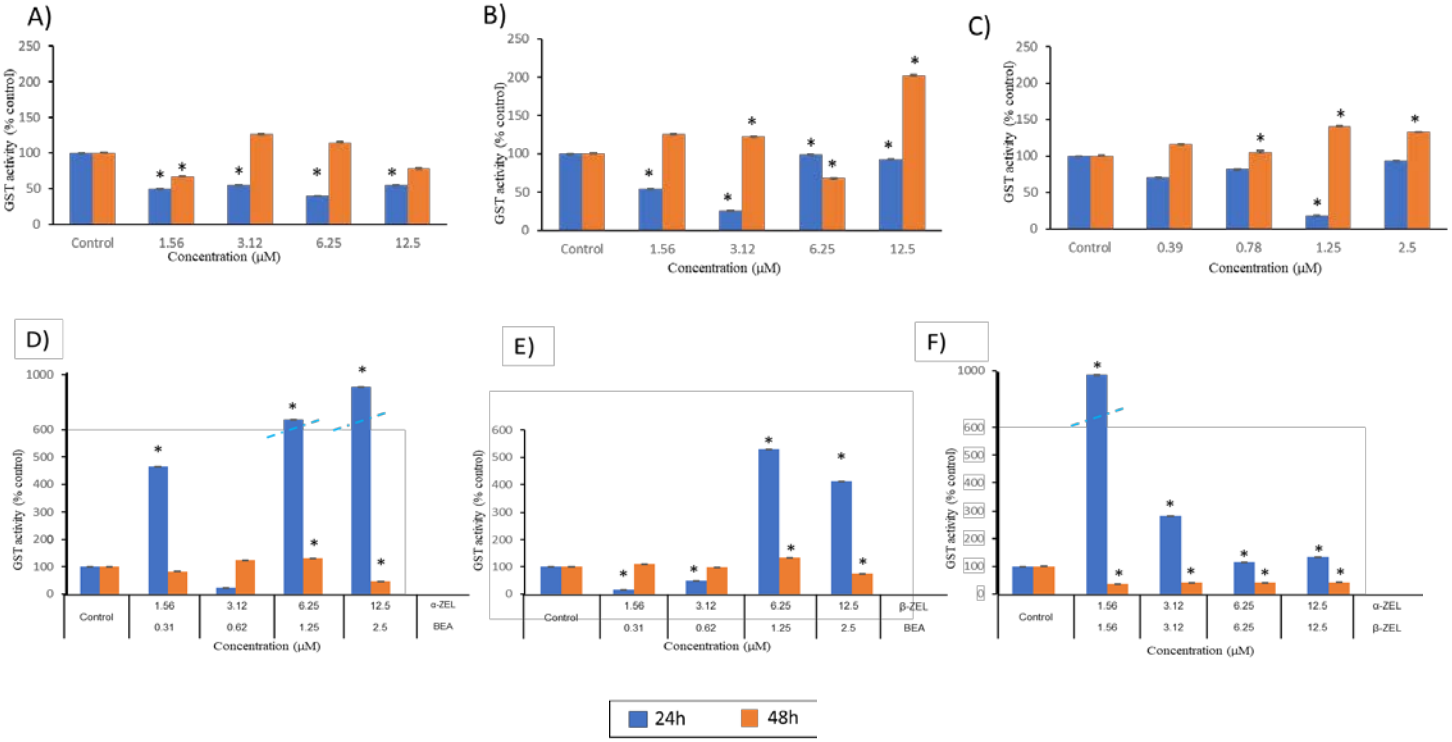

Figure 2. Effect of α-ZEL (A), β-ZEL (B), BEA (C), α-ZEL + BEA (D), β-ZEL + BEA (E) and α-ZEL + β-ZEL (F) on glutathione S-transferase (GST) activity after 24 h and 48 h of exposure in SH-SY5Y cells. Data are expressed in % of the unexposed control. The GST activity is expressed as mol of product formed/min/mg of protein; mean ± SEM (n = 3). *$p \leq 0.05$ indicates a significant difference from the respective solvent control.

190

3.3. Enzymatic activity of CAT

The CAT activity increased significantly in SH-SY5Y cells exposed to α-ZEL and β-ZEL only after 48 h of exposure (from 0.4 to 1.4-fold for α-ZEL and 1 to 4.2-fold for β-ZEL) at all concentrations assayed (Figure 3A and 3B); while this was not observed when cells were exposed to BEA mycotoxin (Figure 3C).

For combination treatments, it was observed a significant increase mostly after 48 h of exposure except for β-ZEL + BEA. Accordingly, in cells exposed to α-ZEL + BEA, at [3.12 + 0.78] μM and [12.5 + 2.5] μM, by 2.1- and 1.5-fold respectively (Figure 3D). for α-ZEL + β-ZEL at [1.56 + 0.39] μM, [6.25 + 1.25] μM and [12.5 + 2.5] μM from 0.8- to 3.5- fold (Figure 3F), and for tertiary mixture at lowest concentration assayed ([1.56 + 1.5 + 0.39] μM by 0.6-fold (Figure 5C), while for β-ZEL + BEA, this happened after 24 of exposure at all concentrations assayed from 0.6- to 3.2- folds, except when cells were exposed to the highest concentration ([12.5 + 2.5] μM) (Figure 3E).

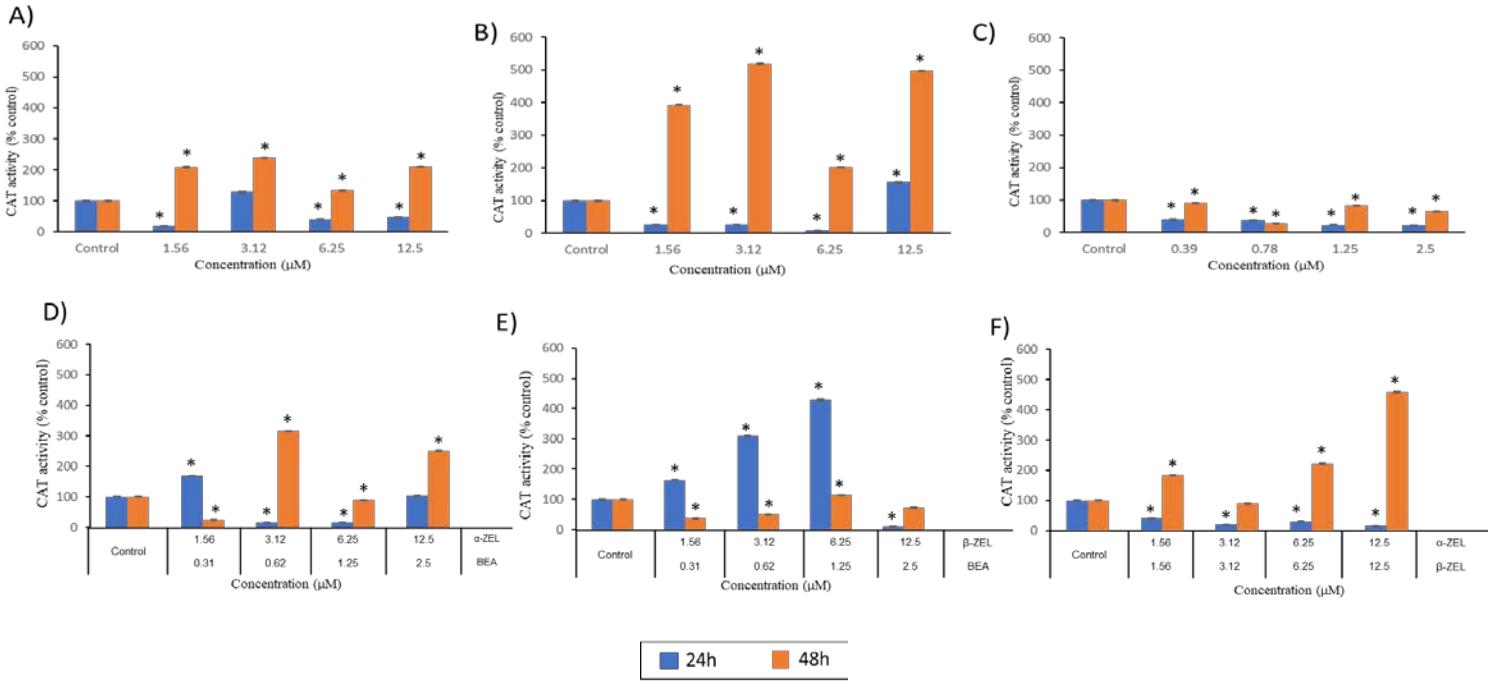

Figure 3. Effect of α-ZEL (A), β-ZEL (B), BEA (C), α-ZEL + BEA (D), β-ZEL + BEA (E) and α-ZEL + β-ZEL (F) on catalase (CAT) activity after 24 h and 48 h of exposure in SH-SY5Y cells. Data are expressed in % of the unexposed control. The CAT activity is expressed as µmol H_2O_2 /min/mg of protein; mean ± SEM (n = 3). *$p \leq 0.05$ indicates a significant difference from the respective solvent control.

192

3.4. Enzymatic activity of SOD

As shown in Figure 4, SOD activity increased significantly after being exposed to all treatments individually and in combination only after 48 h of exposure at all concentrations assayed. Accordingly, for α-ZEL up to 1.4-fold (Figure 4A), for β-ZEL up to 2.5-fold (Figure 4B), for BEA up to 1-fold (Figure 4C), and in binary and tertiary treatments, for α-ZEL + BEA from 2.7- to 3.3-fold (Figure 4D), for β-ZEL + BEA from 2- to 4- fold (Figure 4E), for α-ZEL + β-ZEL a minor increase up to 1-fold (Figure 4F), and ultimately for α-ZEL + β-ZEL + BEA, from 1- to 2.5- fold in comparison to untreated cells (Figure 5D). Therefore, as a result, binary combinations of α-ZEL + BEA and β-ZEL + BEA showed the major increase among other treatments.

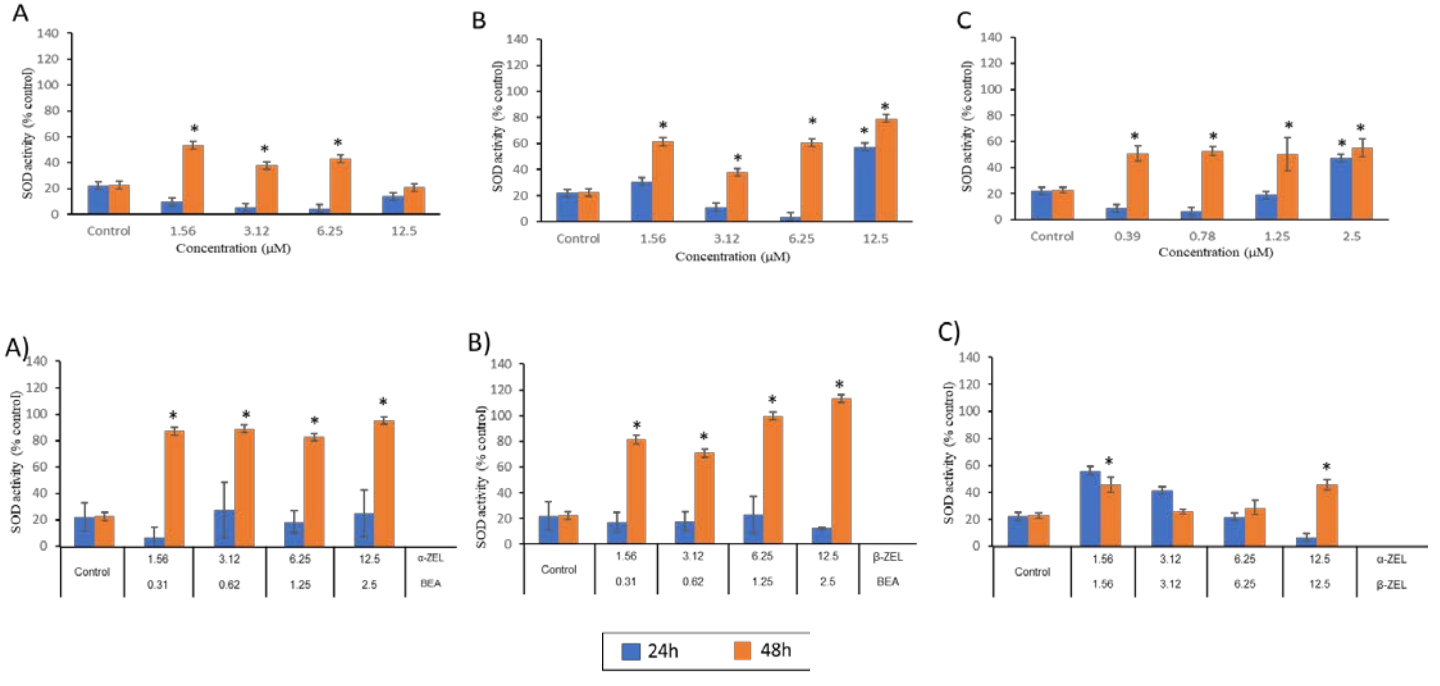

Figure 4. Effect of α-ZEL (A), β-ZEL (B) and BEA (C) on superoxidase dismutase (SOD) activity after 24 h and 48 h of exposure in SH-SY5Y cells. Data are expressed in % of the unexposed control. The SOD activity is expressed as units of SOD/mg of protein; mean ± SEM (n = 3). *$p \leq 0.05$ indicates a significant difference from the respective solvent control.

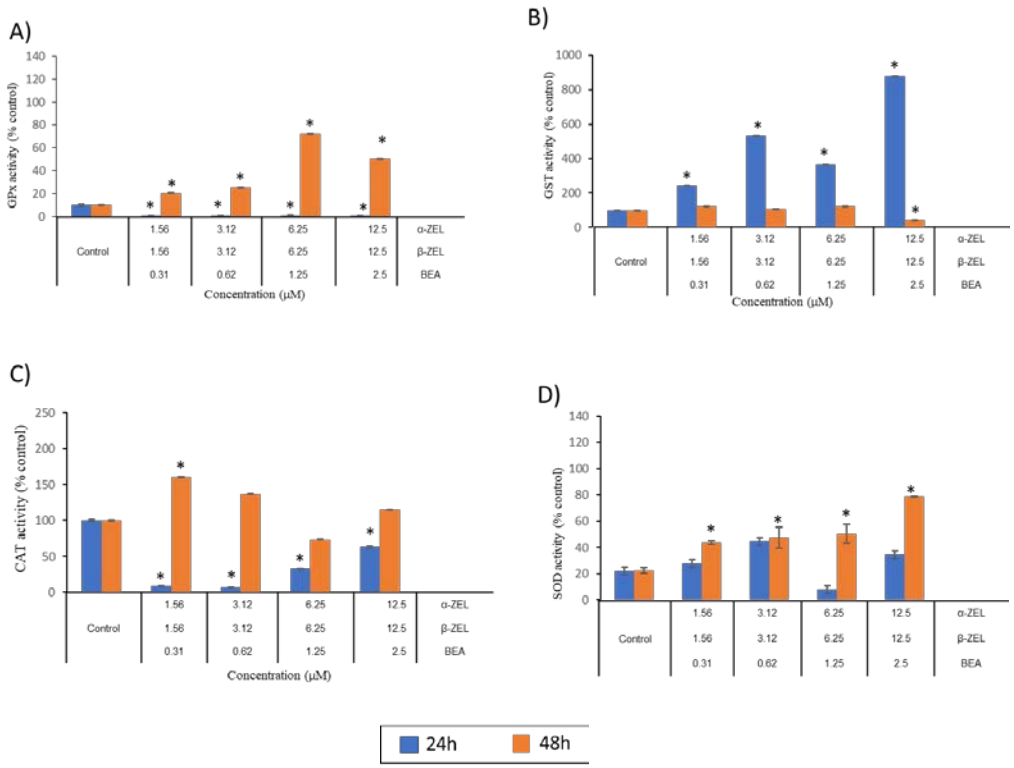

Figure 5. Effect of α-ZEL + β-ZEL + BEA on glutathione peroxidase (GPx) (A), glutathione peroxidase (GPx) (B), catalase (CAT) (C) and superoxidase dismutase (SOD) (D) activity after 24 h and 48 h of exposure in SH-SY5Y cells. Data are expressed in % of the unexposed control. The GPx activity is expressed as μmol of NADPH oxidized/min/mg of protein; mean ± SEM (n = 3). *$p \leq 0.05$ indicates a significant difference from the respective solvent control.

4. Discussion

The study of α-ZEL, β-ZEL and BEA individually and combined for SH-SY5Y cells in enzyme activity for GPx, GST, CAT and SOD are here for the first time presented; however, in these same conditions oxidative stress and glutathione levels in our laboratory had been studied (Agahi et al., 2020a). So that, although results in here are discussed and compared with other studies for

any of the mycotoxins presented, results are mostly correlated with the effects obtained before in the same conditions in our laboratory. Same doses of exposure for individual and combined treatments (included the ratios for the mixtures) have been chosen according to previous results of cytotoxicity in undifferentiated SH-SY5Y cells (Agahi et al., 2020b) as well as not overpassing the levels found in food and the levels reaching the BBB.

Cellular systems are protected against oxidative damage by a multilayer network of mitochondrial anti-oxidant systems, which consist of SOD, CAT, GPx, GST and glutathione reductase (GR) enzymes. A number of low molecular weight antioxidants also intervene, such as α-tocopherol and ubiquinol and those coming from the food intake as zeaxanthin, lutein, polyphenols from goji berries and coffee, among others (Wei et al, 2001; Montesano et al., 2020; Juan-García et al., 2019a; Juan et al. 2020). These molecules are particularly effective in scavenging lipid peroxyl radicals and preventing free radical chain reactions of lipid peroxidation (Szeto et al, 2006).

Mitochondria converts 1–5% of the oxygen in cells to ROS which cannot be fully neutralized by defense systems completely (Wei et al, 2001). This can cause cumulative oxidative injuries to mitochondria, and progressively become less efficient in reducing ROS to end up undermining the mitochondria defense system and its consequences as induce mitochondrial DNA mutations, damage the mitochondrial respiratory chain, membrane permeability, Ca2+ homeostasis and mitochondrial defense systems (Brand et al., 2004). All these aspects are implicated in the development of neurodegenerative diseases as well and mediate or amplify the neuronal dysfunction during the course of neurodegeneration as

previously reported in the literature (Szeto et al, 2006; Moreira et al, 2010; Michael et al, 2006).

The balanced enzymatic system in the mitochondrial matrix runs as follows: enzyme manganese superoxide dismutase (MnSOD or SOD2) or copper/zinc SOD (Cu/ZnSOD or SOD1) in the mitochondrial intermembrane space and cytosol convert O_2•- to hydrogen peroxide (H_2O_2) in the reaction O_2•- + O_2•- + 2H+→ H_2O_2 + O_2 (Fridovich et al, 1995). H_2O_2 is more stable than O2•- and can diffuse from mitochondria into the cytosol and nucleus. Afterward, H_2O_2 is detoxified by GPx in mitochondria and the cytosol by using glutathione (GSH) as a substrate, and by CAT in peroxisomes both by converting it to H_2O (Wei et al, 2001).

The results reported in here for BEA, α-ZEL and β-ZEL in undifferentiated SH-SY5Y cells, showed an increase of SOD activity in all treatments assayed, individually and combined, from 1- to 4- fold after 48 h of exposure compared to unexposed cells; while after 24 h of exposure, this activity remained unchanged (Figure 4 and Figure 5D). According to the connected enzymatic system described above, after accelerating the activity of SOD, the production of H_2O_2 increases, and consequently GPx antioxidant activity which is in charge of detoxifying H_2O_2 molecules, increases as well. Coinciding with this, GPx activity in SH-SY5Y exposed to mycotoxins increased significantly in all treatments individually and in binary combination after 24 h of exposure from 2.5- to 23- fold compared to untreated cells (Figure 1 and Figure 5A). GSH plays an important role in in detoxifying H_2O_2 molecules but no changes in the activity of this antioxidant was observed when previously studied in our lab at

the same conditions and for the same cell line (Agahi et al., 2020a). In fact, there is no GSH lack evidenced nor correlated with ROS levels and GPx activity. So that, results presented in here seem to have a close support to our previous findings (Agahi et al, 2020a).

In tertiary combination, the activity of GPx decreased significantly at 24 h and remained unchanged after 48 h of exposure for almost all treatments (Figure 1 and 5A). In several studies, cells with increased levels of SOD showed to be hypersensitive to oxidative stress rather than protected from it (Michiels et al., 1994; Weydert et al., 2006). Hence, the dysfunctionality of H_2O_2 conversion by an adequate level of CAT and GPx, may be detrimental to the cell, by the consequence that H_2O_2 might accumulate to end up cells dying. In the light of this, the decreased activity level of GPx at 48 h can be justified by the increase of activity in SOD (Figure 4 and 5D) coinciding with cytotoxicity and oxidative stress results reported by Agahi et al., (2020a and 2020b). This suggests that GPx activity in SH-SY5Y cell line is not the major implicated enzyme in detoxifying against cytotoxicity of BEA, α-ZEL and β-ZELIt is possible that GPx inactivates itself by its own substrates (Pigeolet et al., 1990) a fact that could be happening at 48 h in tertiary combination and associated to levels of ROS.

Similar results were obtained for sterigmatocystin (STE) mycotoxins in SH-SY5Y cells exposed during 24 h, where SOD and GPx enzymes decreased suggesting that these enzymes are unable to counteract the oxidative stress produced by STE exposure (Zingales et al., 2020). On the other hand, opposite results were obtained for HepG2 and CHO–K1 cells exposed to α-ZEL and β-ZEL individually for 24 h, where both SOD and GPx activity increased (Tatay et al., 2016 and 2017); also for HT-29 cells exposed to deoxynivalenol (DON)

during 24 h, where it was suggested that SOD and GPx were enzymes primarily involved in combating cellular oxidative (Krishnaswamy et al., 2010); and in CHO–K1 cells exposed to different concentrations of BEA for 24 h revealed an increase in GPx activity (Mallebrera et al., 2014). While in Hek-293 cells exposed to DON mycotoxin between 6 to 24 h of exposure, it was reported a significant increase in SOD activity (Dinu et al., 2011).

CAT enzyme is also involved in catalyze the decomposition of H2O2 along with GPx. CAT enzymes are abundant in the peroxisomes of liver cells while not as much in neuronal cells, and GPx is abundant in mitochondria and cytosol compartment. In this study, according to the results obtained from CAT activity in undifferentiated SH-SY5Y cells treated with α-ZEL, β-ZEL and BEA, it was observed a significant decrease in all individual treatments at 24h (Figure 2A, 2B and 2C) as well as in combinations except in the binary treatment β-ZEL + BEA (Figure 2E). This decrease of CAT activity is probably associated to the competition of GPx with CAT enzyme in detoxifying H2O2 activity in the stage of 24 h of exposure mentioned above; although it is also possible that due to the high concentrations of peroxide, CAT inactivates or it is trying to equilibrate (Williams, 1928). Contrary, in the stage of 48 h of exposure, the activity of CAT in SH-SY5Y cells increased significantly for α-ZEL and β-ZEL mycotoxins in individual and combined treatments up to 4-fold in comparison to control cells (Figure 2 and Figure 5B). Moreover, the excess of H_2O_2 can cross the mitochondrial membrane and can be degraded by CAT; thus, it could be speculated that there is a compensation of CAT activity to reduce H_2O_2 levels, while GPx is inactivated for the same treatments during 48 h of exposure. Coinciding with this, similar results were found by Tatay et al., (2016, 2017) and

Dinu et al., (2011) where CAT activity was reduced in a dose-dependent manner, suggesting that the accumulation of superoxide anion produced by assayed mycotoxins may inhibit CAT activity (Kono and Fridovich, 1982).

Finally, GST is a family of enzymes that catalyze the conjugation of GSH with a multitude of substrates to detoxify the exogenous and endogenous compounds. These enzymes are involved in the detoxification of xenobiotics and protective mechanism against cellular damage, such as oxidative stress. According to our results, a down regulation of the antioxidant defense system by decreasing the activity of GST enzyme only in cells exposed to α-ZEL and β-ZEL individually was observed (Figure 3A and 3B). Inversely, a significant increase was demonstrated in all combination treatments, particularly in the highest concentrations assayed (except in α-ZEL + β-ZEL) (Figure 3). In accordance with Grigutyte et al., (2009) increase in GST activity is considered a chemical stress signal, therefore, this effect can be in consequence of increasing enzymatic activity in combination treatments by augmenting the levels of ROS as previously reported, from 2.8- to 8- fold compared to control (Agahi et al., 2020a). Conversely, the decrease or unchanged GST activity in individual treatments can be as a result of no changing in ROS activity as it was proved previously (Agahi et al, 2020a).

5. Conclusions

In conclusion, the results achieved in the present study suggest that α-ZEL, β-ZEL and BEA mycotoxins in undifferentiated SH-SY5Y cells, individually and combined, increases the GPx activity after 24 h of exposure which can help to reduce the effects associated to these mycotoxins as the production of ROS originated at the same conditions (Agahi et al., 2020b). On

the other hand, due to the balance of the enzymatic system the high activity detected for SOD enzyme after 48 h revealed decreases in the activity of GPx and CAT enzymes. CAT enzyme showed the highest activity for α-ZEL and β-ZEL in SH-SY5Y cells when exposed individually and in combined treatments. When mycotoxins merged together, GST enzyme activity increased which supports the fact that damage associated to oxidative stress by these mycotoxins is trying to be alleviated by GST activity. Ultimately, altogether and from achieved results it can be comprehended that antioxidant enzymatic system in SH-SY5Y cells, provide a strong protector role toward the damage caused by α-ZEL, β-ZEL and BEA mycotoxins in undifferentiated SH-SY5Y cells in individual and combined treatments.

Acknowledgements:

Authors would like to thank Spanish Ministry of Science and Innovation PID2019-108070RB-I00ALI and Generalitat Valenciana GV 2020/020.

6. References

Abbott, N.J. 2005. Dynamics of CNS Barriers: Evolution, Differentiation, and Modulation. Cellular and Molecular Neurobiology. 25, 5–23.

Agahi, F., Álvarez-Ortega, A., Font, G., Juan-García, A., Juan, C., 2020a. Oxidative stress, glutathione, and gene expression as key indicators in SH-SY5Y cells exposed to zearalenone metabolites and beauvericin, Toxicology Letters, 334, 44-52.

Agahi, F., Font, G., Juan, C., Juan-García, A., 2020b. Individual and combined effect of zearalenone derivates and beauvericin mycotoxins on SH-SY5Y cells. Toxins, 12, 212.

Agahi F., Juan C., Font G., Juan-García A. 2020c. In silico methods for metabolomic and toxicity prediction of zearalenone, α-zearalenone and β-zearalenone Food Chem Toxicol 146, 111818.

Albarracin, S.L., Stab B., Casas, Z., Sutachan, J.J., Samudio, I., Gonzalez, J., Gonzalo, L., Capani, F., Morales, L., Barreto, G.E. 2012. Effects of natural antioxidants in neurodegenerative disease. Nutritional Neuroscience, 15, 1-9

Behrens M., Hüwel S., Galla H.J., Humpf H.U. 2015. Blood-brain barrier effects of the Fusarium mycotoxins deoxynivalenol, 3 acetyldeoxynivalenol, and moniliformin and their transfer to the brain. PLoS One, 10 (11), 0143640.

Biehl, M.L., Prelusky, D.B., Koritz, G.D., Hartin, K.E., Buck, W.B., Trenholm, H.L., 1993. Biliary-excretion and enterohepatic cycling of zearalenone in immature pigs. Toxicology and Applied Pharmacology, 121 (1), 152-159.

Bocianowski, J., Szulc, P., Waskiewicz, A., Cyplik, A., 2020. The Effect of Agrotechnical Factors on Fusarium Mycotoxins Level in Maize. Agriculture, 10(11), 528.

Brand, M.D., Affourtit, C., Esteves, T.C., Green, K., 2004. Mitochondrial superoxide: production, biological effects, and activation of uncoupling proteins. Free Radical Biology and Medicine. 37(6): 755-767.

Brodehl, A., Möller, A., Kunte, H.J., Koch, M., Maul, R., 2014. Biotransformation of the mycotoxin zearalenone by fungi of the genera Rhizopus and Aspergillus, FEMS. Microbiology Letters, 359:124–130.

Cai, Y., Shen, H., Weng, H., Wang, Y., Cai, G., Chen, X., Ye, Q., 2020. Overexpression of PGC-1α influences the mitochondrial unfolded protein response (mtUPR) induced by MPP+ in human SH-SY5Y neuroblastoma cells. Scientific Reports, 10, 10444.

Chang, W., Lin, J., 1984. Transformation of zearalenone and zearalenol by rat erythrocytes. Food and Chemical Toxicology, 22 (11), 887-891.

Darwish, W.S., Ikenaka, Y., Nakayama, Sh.M.M., Ishizuka, M., 2014. An Overview on Mycotoxin Contamination of Foods in Africa. Toxicology, 76, 789-797.

Devreese. M., Antonissen. G., Broekaert. N., De Baere. S., Vanhaecke. L., De Backer. P., and Croubels. S., 2015. Comparative Toxicokinetics, Absolute Oral Bioavailability, and Biotransformation of Zearalenone in Different Poultry Species. Agricultural and Food Chemistry. 63, 20, 5092–5098.

Dinu, D., Bodea, G.O., Ceapa, C.D., Munteanu, M.C., Roming, F.I., Serban, A.I., 2011. Adapted response of the antioxidant defense system to oxidative stress induced by deoxynivalenol in Hek-293 cells. Toxicon, 57, 1023-1032.

Drzymala, S.S., Binder, J., Brodehl, A., Penkert, M., Rosowski, M., Garbe, L.A., Koch, M., 2015. Estrogenicity of novel phase I and phase II metabolites of zearalenone and cis-zearalenone. Toxicon, 105, 10−12.

Dweba, C.C., Figlan, S., Shimelis, H.A., Motaung, T.E., Sydenham, S., Mwadzingeni, L., Tsilo, T.J., 2017. Fusarium head blight of wheat: pathogenesis and control strategies. Crop Protection, 91, 114-122.

Follmann, W., Ali, N., Blaszkewicz, M., Degen, G.H., 2016. Biomonitoring of mycotoxins in urine: pilot study in mill workers. Journal of Toxicology and Environmental Health, 79, 1015-1025.

Fridovich, I., 1995. Superoxide radical and superoxide dismutases. Annual Review of Biochemistry. 64, 97–112.

Gandhi, S., Abramov, A.Y., 2012. Mechanism of oxidative stress in neurodegeneration Oxidative Medicine and Cellular Longevity, 2012, 1-11.

Juan-García, A., Carbone, S., Ben-Mahmoud, M., Sagratini, G., Mañes, J., 2020. Beauvericin and ochratoxin A mycotoxins individually and combined in

HepG2 cells alter lipid peroxidation, levels of reactive oxygen species and glutathione. Food and Chemical Toxicology, 139, 111247.

Juan C., de Simone G., Sagratini G., Caprioli G., Mañes J., Juan-García A. 2020. Reducing the effect of beauvericin on neuroblastoma SH-SY5Y cell line by natural products. Toxicon 188, 164–171.Juan-García A., Bind M.A., Engert F. 2020. Larval zebrafish as an in vitro model for evaluating toxicological effects of mycotoxins. Ecotoxicology and Environmental Safety 202, 110909.

Juan-García A., Montesano D., Mañes J., Juan C. 2019a. Cytoprotective effects of carotenoids-rich extract from Lycium barbarum L. on the beauvericin-induced cytotoxicity on Caco-2 cells. Food Chem Toxicol, 133, 110798.

Juan-García, A., Tolosa, J., Juan, C., Ruiz, M.J., 2019b. Cytotoxicity, genotoxicity and disturbance of cell cycle in HepG2 cells exposed to OTA and BEA: single and combined actions. Toxins, 11, 341.

Kim, HB., Yoo, JY., Yoo, SY. Lee, J.H., Chang, W., Kim, H.S., Baik, T.K., Woo, R.S., 2020. Neuregulin-1 inhibits CoCl2-induced upregulation of excitatory amino acid carrier 1 expression and oxidative stress in SH-SY5Y cells and the hippocampus of mice. Molecular Brain, 13, 153.

Klarić, M.Š., Rumora, L., Ljubanović, D. Pepeljnjak, S., 2008. Cytotoxicity and apoptosis induced by fumonisin B1, beauvericin and ochratoxin A in porcine kidney PK15 cells: effects of individual and combined treatment. Archives of Toxicology, 82, 247–255.

Kono, N.S., Fridovich, I., 1982. Superoxide radical inhibits catalase. Journal of Biological Chemistry, 257, 5751-5754.

Kouri, K., Lemmens, M., Lemmens-Gruber, R., 2003. Beauvericin-induced channels in ventricular myocytes and liposomes. Biochimica et Biophysica Acta, 1609, 203-210.

Krishnaswamy, R., Devaraj, S.N., Padma, V.V., 2010. Lutein protects HT-29 cells against Deoxynivalenol-induced oxidative stress and apoptosis: prevention of NF-kappaB nuclear localization and down regulation of NF-κB and Cyclo-Oxygenase - 2 expression. 49(1), 50-60.

Krug I., Behrens M., Esselen M., Humpf H.U. 2018. Transport of enniatin B and enniatin B1 across the blood-brain barrier and hints for neurotoxic effects in cerebral cells. PLoS One, 13 (5) 0197406.

Lawana, V., Um, S.Y., Rochet, J.C., Turesky, R.J., Shannahan, J.H., Cannon, J.R., 2020. Neuromelanin Modulates Heterocyclic Aromatic Amine-Induced Dopaminergic Neurotoxicity. Toxicological Sciences, 173, 171–188.

Lin, M.T. and Beal, M.F., 2006. Mitochondrial dysfunction and oxidative stress in neurodegenerative diseases (review). Nature. 19;443(7113), 787-95.

Malekinejad, H., Colenbrander, B., Fink-Gremmels, J., 2006a. Hydroxysteroid dehydrogenases in bovine and porcine granulosa cells convert zearalenone into its hydroxylated metabolites alpha-zearalenol and beta-zearalenol. Veterinary Research Communications, 30 (4), 445-453.

Malekinejad, H., Maas-Bakker, R., Fink-Gremmels, J., 2006b. Species differences in the hepatic biotransformation of zearalenone. Veterinary Journal., 172 (1), 96-102.

Mallebrera, B., Font, G., Ruiz, M.J., 2014. Disturbance of antioxidant capacity produced by beauvericin in CHO-K1 cells. Toxicology Letters., 226, 337-342.

Manyes, L., Escriva, L., Ruiz, M.J., Juan-García. A., 2018. Beauvericin and enniatin B effects on a human lymphoblastoid Jurkat T-cell model. Food Chemical and Toxicology, 115, 127-135.

Maran, E., Fernandez, M., Barbieri, P., Font, G., Ruiz, M.J. 2009. Effects of four carbamate compounds on antioxidant parameters. Ecotoxicology and Environmental Safety. 72, 922-930.

Michiels, C., Raes, M., Toussaint, O., Remacle, J., 1994. Importance of Se-glutathione peroxidase, catalase and Cu/Zn–SOD for cell survival against oxidative stress. Free Radical Biology and Medicine, 17, 235-248.

Molina-Molina, J.M., Real, M., Jimenez-Diaz, I., Belhassen, H., Hedhili, A., Torne, P., Fernandez, M.F., Olea, N., 2014. Assessment of estrogenic and anti-androgenic activities of the mycotoxin zearalenone and its metabolites using in vitro receptor-specific bioassays. Food and Chemical Toxicology, 74, 233−239.

Montesano D., Juan-García A., Mañes J., Juan C. 2020. Chemoprotective effect of carotenoids from Lycium barbarum L. on SH-SY5Y neuroblastoma cells treated with beauvericin. Food Chem Toxicol 141, 111414.

Moreira, P.I., Zhu, X., Wang, X., Lee, H.G., Nunomura, A., Petersen, R.B., Perry, G., Smith, M.A., 2010. Mitochondria: a therapeutic target in neurodegeneration. Biochimica et Biophysica Acta. 1802(1), 212-220.

Ojcius, D.M., Zychlinsky, A., Zheng, L.M. and Young, J.D., 1991. Ionophore-induced apoptosis: role of DNA fragmentation and calcium fluxes. Experimental Cell Research 197: 43-49.

Olsen, M., Pettersson, H., Kiessling, K.H., 1981. Reduction of zearalenone to zearalenol in female rat liver by 3 alpha-hydroxysteroid dehydrogenase. Toxicology and Applied Pharmacology, 48, 157-161.

Oueslati S., Berrada H., Juan-García A., Mañes J., Juan C. 2020. Multiple mycotoxin determination on Tunisian cereals-based food and evaluation of the population exposure. Food Anal Meth. https://doi.org/10.1007/s12161-020-01737-z.

Pfeiffer, E., Kommer, A., Dempe, J.S., Hildebrand, A.A., Metzler, M., 2011. Absorption and metabolism of the mycotoxin zearalenone and the growth promotor zeranol in caco-2 cells in vitro. Molecular Nutrition & Food Research, 55 (4), 560-567.

Pigeolet, E., Corbisier, P., Houbion, A., Lambert, D., Michiels, C., Raes, M., Zachary, M.D., Remacle, J., 1990. Glutathione peroxidase, superoxide dismutase, and catalase inactivation by peroxide and oxygen derived free radical. Mechanism of Ageing and Development, 51, 283-297.

Pizzo, F., Caloni, F., Schreiber, N.B., Cortinovis, C., Spicer, L.J., 2016. In vitro effects of deoxynivalenol and zearalenone major metabolites alone and combined, on cell proliferation, steroid production and gene expression in bovine small-follicle granulosa cells. Toxicon, 109, 70-83.

Prosperini, A., Juan-García, A., Font, G., Ruiz, M.J., 2013. Beauvericin-induced cytotoxicity via ROS production and mitochondrial damage in Caco-2 cells. Toxicology Letters, 222 (2), 204-211.

Reddy P., Guthridge K., Vassiliadis S., Hemsworth J. Hettiarachchige I., Spangenberg G., Rochfort S. 2019. Tremorgenic mycotoxins: structure diversity and biological activity. Toxins, 11, 302, doi:10.3390/toxins11050302.

Sirin, S., Aslim, B., 2020. Characterization of lactic acid bacteria derived exopolysaccharides for use as a defined neuroprotective agent against amyloid beta1–42-induced apoptosis in SH-SY5Y cells. Scientific Reports, 10, 8124.

Szeto, H.H., 2006. Mitochondria-targeted peptide antioxidants: novel neuroprotective agents. AAPS Journal. 8(3), 521-531.

Taevernier L., Bracke N., Veryser L., Wynendaele E., Gevaert B., Peremans K., Spiegeleer B.D. 2016. Blood-brain barrier transport kinetics of the cyclic

depsipeptide mycotoxins beauvericin and enniatins, Toxicology Letters, 258, 175-184.

Taroncher, M., Pigni, M.Ch., Diana, M.N., Juan-García, A., Ruiz, M.J., 2020. Does low concentration mycotoxin exposure induce toxicity in HepG2 cells through oxidative stress?, Toxicology Mechanisms and Methods, 30:6, 417-426.

Tatay, E., Espin, S., Garcia-Fernandez, A.J., Ruiz, M.J., 2017. Oxidative damage and disturbance of antioxidant capacity by zearalenone and its metabolites in human cells. Toxicology In Vitro, 45, 334-339.

Tatay, E., Font, G., Ruiz, M.J., 2016. Cytotoxic effects of zearalenone and its metabolites and antioxidant cell defense in CHO-K1 cells. Food and Chemical Toxicology, 96, 43-49.

Tonshin, A.A., Teplova, V.V., Andersson, M.A., Salkinoja-Salonen, M.S., 2010. The Fusarium mycotoxins enniatins and beauvericin cause mitochondrial dysfunction by affecting the mitochondrial volume regulation, oxidative phosphorylation and ion homeostasis. Toxicology, 276, 49-57.

Ueda, M., Mozaffar, S., Tanaka, A. 1990. Catalase from Candida boidinii 2201. Methods in Enzymology, 188, 463-467.

Videmann, B., Mazallon, M., Prouillac, C., Delaforge, M., Lecoeur, S., 2009. ABCC1, ABCC2 and ABCC3 are implicated in the transepithelial transport of the myco-estrogen zearalenone and its major metabolites. Toxicology Letter, 190 (2), 215-223.

Videmann, B., Mazallon, M., Tep, J., Lecoeur, S., 2008. Metabolism and transfer of the mycotoxin zearalenone in human intestinal caco-2 cells. Food and Chemical Toxicology, 46 (10), 3279-3286.

Wei, J and Wu, B., 2020. Chemistry and bioactivities of secondary metabolites from the genus Fusarium. Fitoterapia, 146, 104638.

Wei, Y.H., Lu, C.Y., Wei, C.Y., Ma, Y.S., Lee, H.C., 2001. Oxidative stress in human aging and mitochondrial disease? consequences of defective mitochondrial respiration and impaired antioxidant enzyme system. Chinese Journal of Physiology. 44(1):1–11.

Weydert, Ch.J., Waugh, T.A., Ritchie, J.M., Kanchan, S.I., Smith, J.L., Ling, L., Spitz, D.R., Oberley, L.W., 2006. Overexpression of manganese or copper-zinc superoxide dismutase inhibits breast cancer growth. Free Radical Biol. Med., 41, 226-237.

Williams, J., 1928. The decomposition of hydrogen peroxide by liver catalase. Journal of General Physiology, 1, 309-337.

Xicoy H, Wieringa B, Martens GJ. 2017. The SH-SY5Y cell line in Parkinson's disease research: a systematic review. Mol Neurodegener. 12(1):10. PMID: 28118852; DOI: 10.1186/s13024-017-0149-0.

Study 5

Neurotoxicity of zearalenone's metabolites and beauvericin mycotoxins via apoptosis and cell cycle disruption

Fojan Agahi, Cristina Juan*, Guillermina Font, Ana Juan-García

Laboratory of Toxicology and Food Chemistry, Faculty of Pharmacy, University of Valencia, Burjassot 46100, Valencia, Spain

Toxicology, 2021, 456, 152784

Abstract

Cell cycle progression and programmed cell death are imposed by pathological stimuli of extrinsic or intrinsic including the exposure to neurotoxins, oxidative stress and DNA damage. All can cause abrupt or delayed cell death, inactivate normal cell survival or cell death networks. Nevertheless, the mechanisms of the neuronal cell death are unresolved. One of the cell deaths triggers which have been wildly studied, correspond to mycotoxins produced by Fusarium species, which have been demonstrated cytotoxicity and neurotoxicity through impairing cell proliferation, gene expression and induction of oxidative stress. The aim of present study was to analyze the cell cycle progression and cell death pathway by flow cytometry in undifferentiated SH-SY5Y neuronal cells exposed to α-zearalenol (α-ZEL), β-zearalenol (β-ZEL) and beauvericin (BEA) over 24h and 48h individually and combined at the following concentration ranges: from 1.56 to 12.5 μM for α-ZEL and β-ZEL, from 0.39 to 2.5 μM for BEA, from 1.87 to 25 μM for binary combinations and from 3.43 to 27.5 μM for tertiary combination. Alterations in cell cycle were observed remarkably for β-ZEL at the highest concentration in all treatments where engaged (β-ZEL, β-ZEL + BEA and β-ZEL + α-ZEL), for both 24h and 48h. by activating the cell proliferation in G0/G1 phase (up to 43.6%) and causing delays or arrests in S and G2/M phases (up to 19.6%). Tertiary mixtures revealed increases of cell proliferation in subG0 phase by 4-folds versus control. Similarly, for cell death among individual treatments β-ZEL showed a significant growth in early apoptotic cells population at the highest concentration assayed as well as for all combination treatments where β-ZEL was involved, in both early apoptotic and apoptotic/necrotic cell death pathways.

Keywords: cell cycle, cell death, Zearalenone's metabolites, Beauvericin, Neuronal cells

1. Introduction

Cell cycle and cell death are balanced routes that ensure the tissue structure and homeostasis which occurs through many pathways. There are two distinct routs of cell death, called apoptosis and necrosis, as per the structural and biochemical differences. Coupling the process of mitosis with apoptosis seem to be regulated through a specific set of precise factors (Pucci et al., 2000; King et al., 1995). The occurrence of programmed cell death is a highly conserved mechanism in tissue remodeling, which enables an organism to eliminate redundant and malfunctioning cells through a process of cellular disintegration that has the advantage of not inducing an undesirable inflammatory response (Elmore et al., 2007; Thompson et al., 1995). However, unregulatable death events of cells can induce many disorders such as neurodegenerative disorders which can lead to various chronic disease states of amyotrophic lateral sclerosis (ALS) and Alzheimer's disease, and in neurological injury such as cerebral ischemia and trauma. It can also induce defense mechanisms of cancer cells against the apoptotic and necrotic signals where a loss of balance between cell division and cell death occurs (Wong et al., 2011; Okouchi et al., 2007).

The cell cycle is a set of events responsible for cell duplication, by which cells alternate DNA synthesis and mitosis and ensure that each of these processes finishes before the other begins. Such careful control is articulated at the level of checkpoints mechanisms that sense the progress of each cell cycle phase and only upon its completion allow progression into the next; hence, dysfunction of checkpoints can prove fatal for the affected cell (Pucci et al., 2000). Whether or not apoptosis and necrosis occur as a consequence of a

defective cell cycle, it is clear that damage to the cell cycle or to genomic integrity is an extremely efficient trigger of cell death (Manickam et al., 2020; Zingales et al., 2020; Swomley et al., 2014). It has been proved that several cytotoxic agents induce cell death through oxidative stress in the form of increased reactive oxygen species (ROS), which not only triggers cell death but it is also implicated in several disorders (Manickam et al., 2020; Carri et al., 2003; Jenner, 2003; Klein and Ackerman, 2003). ROS are considered to damage cells and ultimately apoptosis by destruction of cellular components including lipids, proteins, and nucleic acids (Kannan and Jain, 2000). In the sight of this fact, various in vitro and in vivo study suggested that ROS generation can be provoked by many toxins including one of the most recent studies as for mycotoxins (Agahi et al., 2020b; Tatay et al., 2017; Mallebrera et al., 2014; Prosperini et al., 2013). We previously demonstrated that α-ZEL, β-ZEL and BEA mycotoxins from fungi of the genus Fusarium, induce injury in human neuroblastoma SH-SY5Y cells by elevating oxidative stress levels which lead to the induction of cytotoxicity, ROS generation, disruption of enzymatic and non-enzymatic activity and more importantly causing disorders through alteration in the expression of genes Casp-3, Bax and Bcl-2; all three involved in cell apoptosis (Agahi et al., 2020a; 2020b). However, little is known about the effects of these mycotoxins or the implication of ROS levels on alterations of cell cycle progression nor in cell death route activation.

It is believed that the human-derived SH-SY5Y cells express a number of human-specific proteins and protein isoforms that would not be inherently present in rodent primary cultures. Both undifferentiated and differentiated SH-SY5Y cells have been utilized for in vitro experiments requiring neuronal-like cells. In the undifferentiated form, SH-SY5Y cells have catecholaminergic

characteristic and recognized morphologically by neuroblast-like (Kovalevich et al., 2013). Hence, we set out the present study to investigate the cell cycle regulation in an undifferentiated SH-SY5Y neuronal cells line exposed by α-ZEL, β-ZEL and BEA mycotoxins individually, in binary and in tertiary combinations during 24 h and 48 h of exposure, and also determine the mechanism of cytotoxicity causing cell death whether is through apoptotic, apoptotic/necrotic or necrotic pathways.

2. Material and methods

2.1. Reagents

The reagent grade chemicals and cell culture components used, Dulbecco's Modified Eagle's Medium- F12 (DMEM/F-12), fetal bovine serum (FBS) and phosphate buffer saline (PBS) were supplied by Thermofisher, Gibco ™ (Paisley, UK). Methanol (MeOH, HPLC LS/MS grade) was obtained from VWR International (Fontenay-sous-Bois, France). Dimethyl sulfoxide was obtained from Fisher Scientific Co, Fisher BioReagnts ™ (Geel, Belgium). Deionized water (<18, MΩcm resistivity) was obtained in the laboratory using a Milli-QSP® Reagent Water System (Millipore, Beadford, MA, USA). HEPES, t-octylphenoxypolyethoxyethanol (Triton-X 100), tris-hydroxymethyl aminomethane (Tris), ribonuclease A from bovine pancreas (RNAase), Annexin V-FITC, propidium iodide (PI), the standard of BEA (MW: 783.95 g/mol), α-ZEL and β-ZEL (MW: 320,38 g/mol) were purchased from SigmaAldrich (St. Louis Mo. USA). Stock solutions of mycotoxins were prepared in MeOH (α-ZEL and β-ZEL) and DMSO (BEA) and maintained at −20 °C in the dark. The

final concentration of either MeOH or DMSO in the medium was ≤1% (v/v) as per established. All other standards were of standard laboratory grade.

2.2. Cell culture

Human neuroblastoma cell line, SH-SY5Y, was obtained from American Type Culture Collection (ATCC, Manassas, VA, USA), and cultured in Dulbecco's Modified Eagle's Medium- F12 (DMEM/F-12), supplemented with 10% fetal bovine serum (FBS), 100 U/ml penicillin, and 100 mg/ml streptomycin. The cells were sub-cultivated after trypsinization once or twice a week and suspended in complete medium in a 1:3 split ratio. Cells were maintained as monolayer in 150 cm^2 cell culture flasks with filter screw caps (TPP, Trasadingen, Switzerland). Cell cultures were incubated at 37°C, 5% CO_2 atmosphere.

2.3. Cell cycle analysis

Cell cycle analysis was performed using Vindelov's PI staining solution as described previously by Juan-García et al., (2013). The PI solution is a fluorescent DNA intercalating agent able to bind and label double-stranded nucleic acids, making it possible to achieve rapid and precise evaluation of cellular DNA content by flow cytometric analysis. The cell cycle is monitored by different key checkpoints or decision points on whether the cell should divide, delay division, or enter a resting stage. 5-Fluorouracil (5-Fu) inhibits thymidylate synthase, which blocks synthesis of the nucleoside thymidine, and thus affects DNA synthesis in the S phase. The etoposide inhibits DNA topoisomerase II and exerts its effects at the G2-M checkpoint. Etoposide and 5-Fu were used as positive control. For this, 7×10^5 cells/well were seeded in

six-well plates. After cells achieved the 90% confluence, cells were treated with α-ZEL and β-ZEL (12.5, 6.25, 3.12 and 1.56 μM), and BEA (2.5, 1.25, 0.78 and 0.39 μM) as an individual treatment. In assays of combinations the following mixtures were tested: α-ZEL + BEA, β-ZEL + BEA, α-ZEL + β-ZEL and α-ZEL + β-ZEL + BEA with concentrations ranged from 25 to 1.87 μM for binary combinations, and from 27.5 to 3.43 μM for tertiary combination. The dilution ratio of concentration ranges in binary combinations was (1:1) for α-ZEL + β-ZEL, (5:1) for α-ZEL + BEA and β-ZEL + BEA, and (5:5:1) in tertiary combinations (α-ZEL + β-ZEL + BEA). Then, cells were trypsinized (0.14 ml) and removed after 3 min and placed on ice for 30 min with 0.36 ml of fresh medium containing 0.5 ml Vindelov's PI staining solution prepared as follows: 40 μg/ml RNAase, 0.1% Triton X-100, 10 mM Tris, 10 mM NaCl and 50 μg/ml of PI in PBS. Fifty thousand cells for each sample were analyzed using BD LSRFortessa (BD Biosciences) flow cytometry. The experiments were carried out in duplicate, and the results were expressed as the mean ± SEM of different independent experiments.

2.4. Measurement of necrosis-apoptosis by Annexin V-FITC/PI

Cell death generally proceeds through two molecular mechanisms: necrosis and apoptosis. One of the characteristics of apoptosis is the externalization of phosphatidylserine (PS) to the outer leaflet of the plasma membrane. The differential of population of apoptotic cells (early or late), necrotic and dead cells was identified by Annexin V-FITC/PI double staining (Vermes et al., 1995). Cells considered as viable are both Annexin V-FITC-/PI− negative; cells in early apoptosis (pro-apoptotic/apoptotic cells) are Annexin V-

FITC+/PI−. Cells stained negative for Annexin V-FITC and positive for PI represented necrotic cells. Cells stained positive for both Annexin V-FITC and PI corresponded to late apoptotic/necrotic cells. The assay was carried out as described by Juan-García et al., (2013). 10,000 cells were acquired and analyzed on a BD FACSCanto flow cytometer with FACSDiva software v 6.1.3 (BD Biosciences). Undifferentiated neuroblastoma SH-SY5Y cells were seeded and exposed to mycotoxins as detailed previously in section 2.3. Green (FL-1, 530 nm) and orange-red fluorescence (FL-2, 585 nm) were detected, emitted by FITC and PI, respectively. Quadrant statistics were performed to determine viable cells (live cells), early apoptotic, apoptotic/necrotic (late apoptotic) and necrotic (dead cells) from the total population of cells.

2.5. Statistical analysis

Statistical analysis of data was carried out using IBM SPSS Statistic version 23.0 (SPSS, Chicago, Il, USA) statistical software package and GraphPad Prism 8.0 (GraphPad Software, Inc., San Diego, USA). Data were expressed as mean ± SD of three independent experiments. The statistical analysis of the results was performed by student's T-test for paired samples. Difference between groups were analyzed statistically with ANOVA followed by the Tukey HDS post hoc test for multiple comparisons. The level of $p \leq 0.05$ was considered statistically significant.

3. Results

3.1. Cell cycle analysis in individual treatments

Flow cytometry was used to determine cell proliferation by cell cycle analysis with PI staining. As it is shown in Figure 1a.1, in individual treatment of

α-ZEL after 24 h of exposure, a significant concentration-dependent increase in G0/G1 phase was observed at 3.12 μM, 6.25 μM and 12.5 μM by 1.5%, 4.5% and 6% respectively, accompanied by a reduction in S phase at all concentrations up to 25.7%, and in G2/M phase up to 32.4% as compared to the control. Conversely, a concentration-dependent reduction in the number of cells in G0/G1 phase was detected after 48 h at 1.56 μM, 6.25 μM and 12.5 μM by 6.9%, 7.6% and 9%, respectively (Fig. 1a.2). For individual treatment of β-ZEL after 24 h of exposure, a significant dose-dependent increase in G0/G1 phase was observed at all concentrations assayed from 4.7% to 34.6% versus the control (Figure 1b.1); which was accompanied by a dose-dependent decline in S phase from 29% to 87%, and also in G2/M phase at the highest concentrations assayed of 6.25 μM and 12.5 μM by 46% and 68%, respectively (Figure 1b.1).However, after 48 h of exposure in G0/G1 phase, this increase was only observed at the highest concentration assayed (12.5 μM) by 7.7%, accompanied by unchanged activity in S phase and a significant decrease in G2/M phase at 3.12 μM and 6.25 μM by 30% and 21%, respectively (Fig. 1b.2). For BEA, after 24 h of exposure, a significant increase was observed in G0/G1 phase at the lowest concentrations assayed (0.39 μM and 0.78 μM,) by 10% to 13.8%, followed by a notable reduction in S phase at the same concentrations from 19.8% to 28.7% (Figure 1c.1). The same increase happened for G2/M phase at 0.39 μM, 0.78 μM and 2.5 μM by 10.2%, 13.2% and 38.3% respectively, in comparison to unexposed cells (Figure 1c.1). Inversely, after 48 h exposure cell population remained unchanged in G0/G1 phase and G2/M phase, while in S phase a significant decrease was detected at 0.78 μM and 2.5 μM by 20% and 42.3%, respectively compared to control cells (Figure 1c.2).

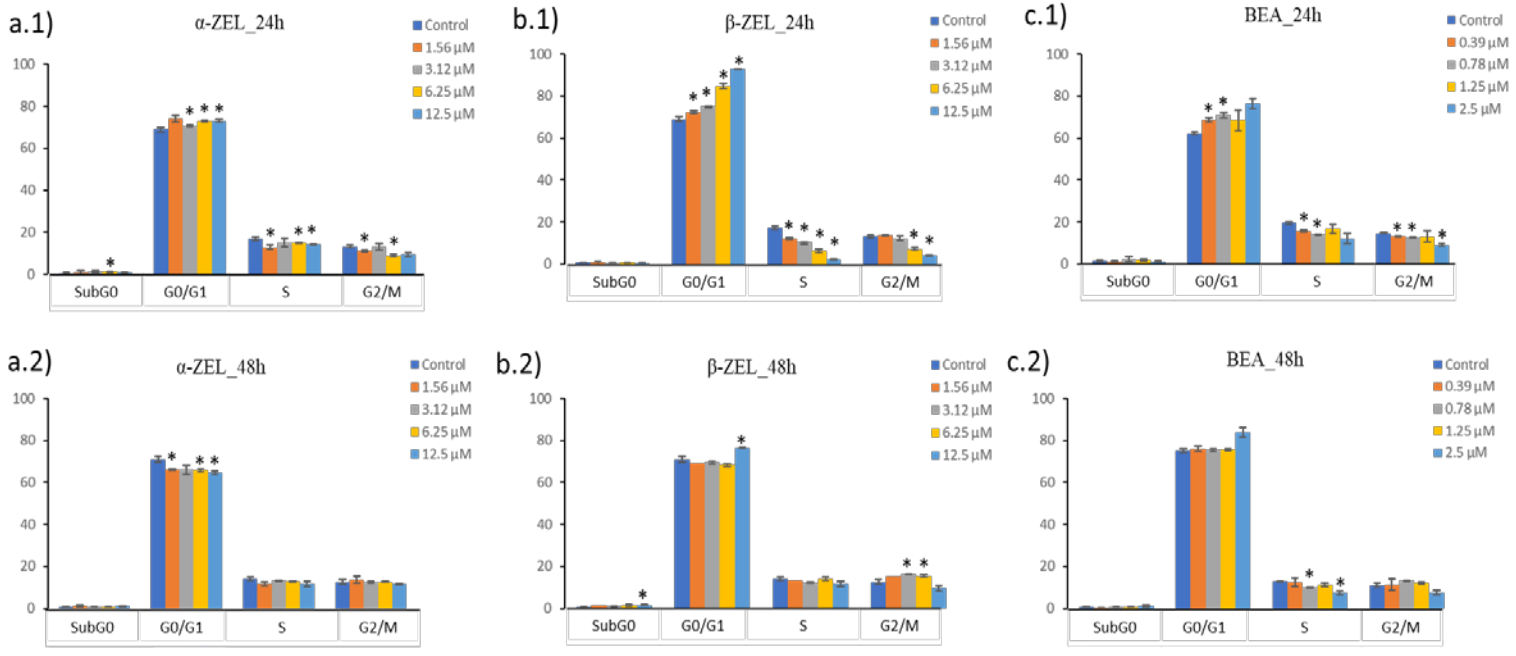

Figure 1. Cell cycle progression of SH-SY5Y cells treated with α-ZEL (a), β-ZEL (b) and BEA (c) after 24h (a.1, b.1, and c.1) and 48 h (a.2, b.2, and c.2) and analyzed by flow cytometry. The values were expressed as the mean ± SD for two replications. Data are expressed in % of the unexposed control. *$p \leq 0.05$ indicates a significant difference from the respective solvent control.

3.2. Cell cycle analysis in combination treatments

Figure 2 reports the results of cell cycle progression for binary combinations. For α-ZEL + BEA (Figure 2a), G0/G1 phase increased significantly at all concentrations assayed up to 15.4% compared to untreated cells after 24 h of exposure (Figure 2a.1). For S phase, a significant decrease was observed at the highest concentration assayed ([12.5 + 2.5] μM) by 31.6% and 55.4%, for 24 h and 48 h, respectively (Figure 2a). For β-ZEL + BEA treatment (Figure 2b), G0/G1 phase revealed a significant increase at [3.12 + 0.78] μM, [6.25 + 1.25] μM and [12.5 + 2.5] μM by 22.9%, 34.3% and 30%, respectively at 24 h, followed by a dose-dependent decrease in S phase at the same concentrations from 37.5% to 66.5%, and in G2/M phase at all concentrations from 36%to 6 compared to unexposed cells (Figure 2b.1).On the other hand, after 48 h of exposure a marked alteration in all phases was observed at the highest concentrations assayed ([12.5 + 2.5] μM): cells in G0/G1 phase increased by 19.6%, followed by a decrease in S and G2/M phases by 44% and 78%, respectively compared to unexposed cells (Figure 2b.2). For α-ZEL + β-ZEL (Figure 2c) cell distribution in G0/G1 phase was significantly high in a dose-dependent manner after 24 h of exposure at [1.56 + 0.39] μM, [6.25 + 1.25] μM and [12.5 + 2.5] μM by 17.9%, 32.8% and 43.6%, respectively compared to control cells (Figure 2c.1); this was accompanied by a significant reduction in cells population in S phase at the highest concentrations assayed [6.25 + 1.25] μM and [12.5 + 2.5] μM by 49% and 84.6%, respectively, and also in G2/M phase at all concentrations assayed in a concentration-dependent manner (from 35.7% to 60%) (Figure 2c.1). Remarkably, after 48 h of exposure a shift in percentage of cells distribution was observed at highest concentrations assayed

at all phases; increase in G0/G1 phase by 15%, and decreased in S and G2/M phases by 38% and 61%, respectively (Figure 2c.2). Ultimately, tertiary combination of α-ZEL + β-ZEL + BEA is shown in Figure 5. After 24 h of exposure a significant increase in cells number of G0/G1 phase was observed at all concentrations assayed, from 16.7% to 34.6% in comparison to unexposed cells (Figure 5a.1). This was followed by a considerable decline in S phase cells population at [3.12 + 3.12 + 0.78] μM, [6.25 +6.25 + 1.25] μM and [12.5 + 12.5 + 2.5] μM by 37%, 59.6% and 55.3%, respectively; and a dose-dependent decrease in G2/M phase at [1.56 + 1.56 + 0.39] μM, [3.12 + 3.12 + 0.78] μM and [6.25 +6.25 + 1.25] μM by 29.2%, 51.9% and 61.2%, respectively (Figure 5a.1).

After 48 h of exposure, the population of cells in G0/G1 and S phases decreased significantly at the highest concentration assayed ([12.5 + 12.5 + 2.5] μM) by 18.8% and 41.4%, respectively, while a significant increase in G2/M phase was observed at the highest concentration by 113%, and lastly, a dramatic growth in cells number in subG0 phase was noticed at [3.12 + 3.12 + 0.78] and [6.25 +6.25 + 1.25] μM by 2- and 3.2-folds respectively compare to control cells (Figure 5a.2) which could be due to the increase in necrotic cells.

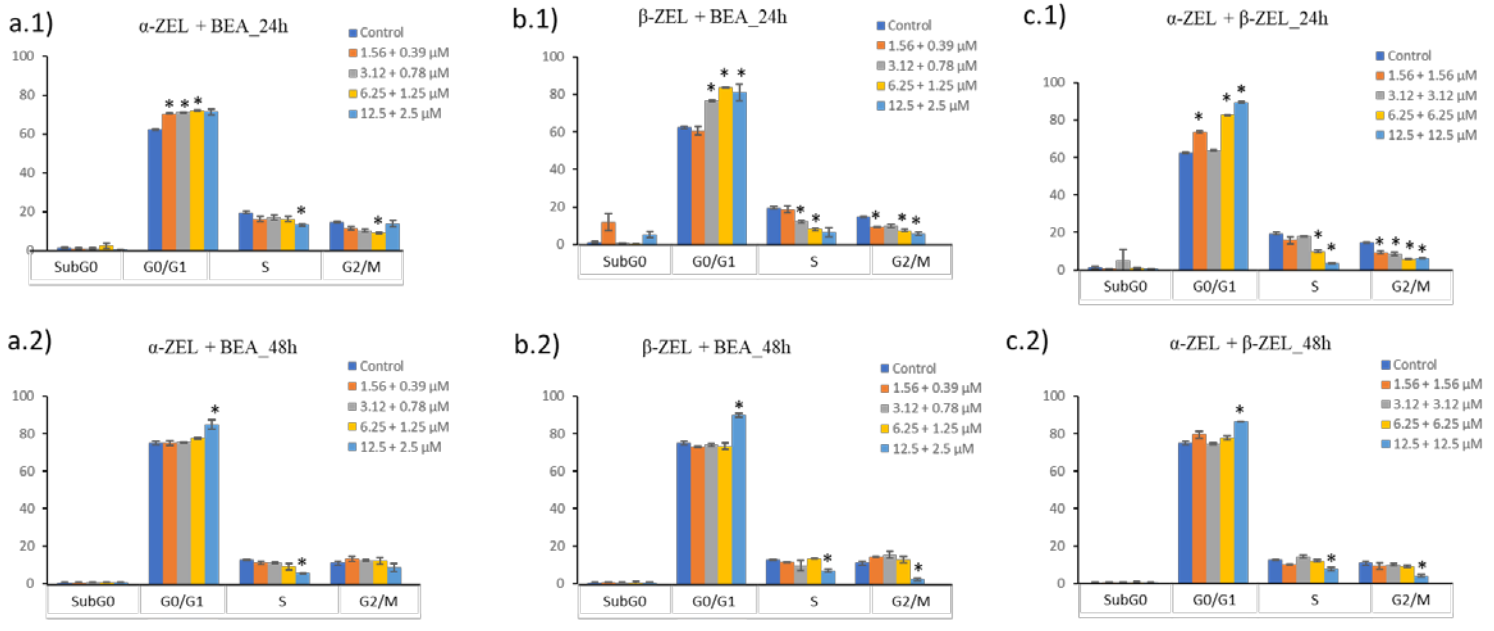

Figure 2. Cell cycle progression of SH-SY5Y cells treated with binary combinations α-ZEL + BEA (a), β-ZEL + BEA (b) and α-ZEL + β-ZEL (c) after 24h (a.1, b.1 and c.1) and 48 h (a.2, b.2 and c.2) and analyzed by flow cytometry. The values were expressed as the mean ± SD for two replications. Data are expressed in % of the unexposed control. *$p \leq 0.05$ indicates a significant difference from the respective solvent control.

3.3. Necrosis-apoptosis analysis in individual treatments

To determine the death pathway underlying the observed decline on cell proliferation found by our previous study on cytotoxicity effect of α-ZEL, β-ZEL and BEA individually and in combinations, the mechanism of induction of cell death was decided to study in SH-SY5Y cells after 24 h and 48 h of exposure (Figures 3, 4 and 5b).

As it is shown in Figure 3a.1, after 24 h of exposure, α-ZEL treated cells increased significantly in apoptotic and apoptotic/necrotic cells by up to 83.3% and 88.7% compared to control, while conversely, after 48 h of exposure it was observed a notable decrease at all concentration assayed in apoptotic cells up to 52.9% and an increase in apoptotic/necrotic cells at [6.25 + 1.25] and [12.5 + 2.5] μM by 23.7% and 48.8% versus control (Figure 3a.2). Moreover, after 48h of exposure it was observed a considerable increase in necrotic cells up to 95% (Figure 3a.2). For β-ZEL, a significant increase was observed in apoptotic cells exposed to the highest concentration assayed (12.5 μM) after both 24 h and 48 h of exposure by 43.9% and 50%, respectively (Figure 3b.1). Also, apoptotic/necrotic cells increased significantly at 6.25 μM by 53% after 24 h and at 1.56, 3.12 and 12.5 μM by 38.8%, 24% and 27.7% respectively after 48 h of exposure compared to control cells (Figure 3b). For BEA, after 48 h exposure a significant decrease was noticed at all concentrations from 8% to 44%, versus control. in apoptotic/necrotic cells increased for both time of exposure, which was up to 89% for 24 h and up to 38.8% for 48 h (Figure 3c). Also, after 48 h of exposure a notable increase was observed in necrotic cells at 0.39 and 0.78 μM by almost 2 times compare to control cells.

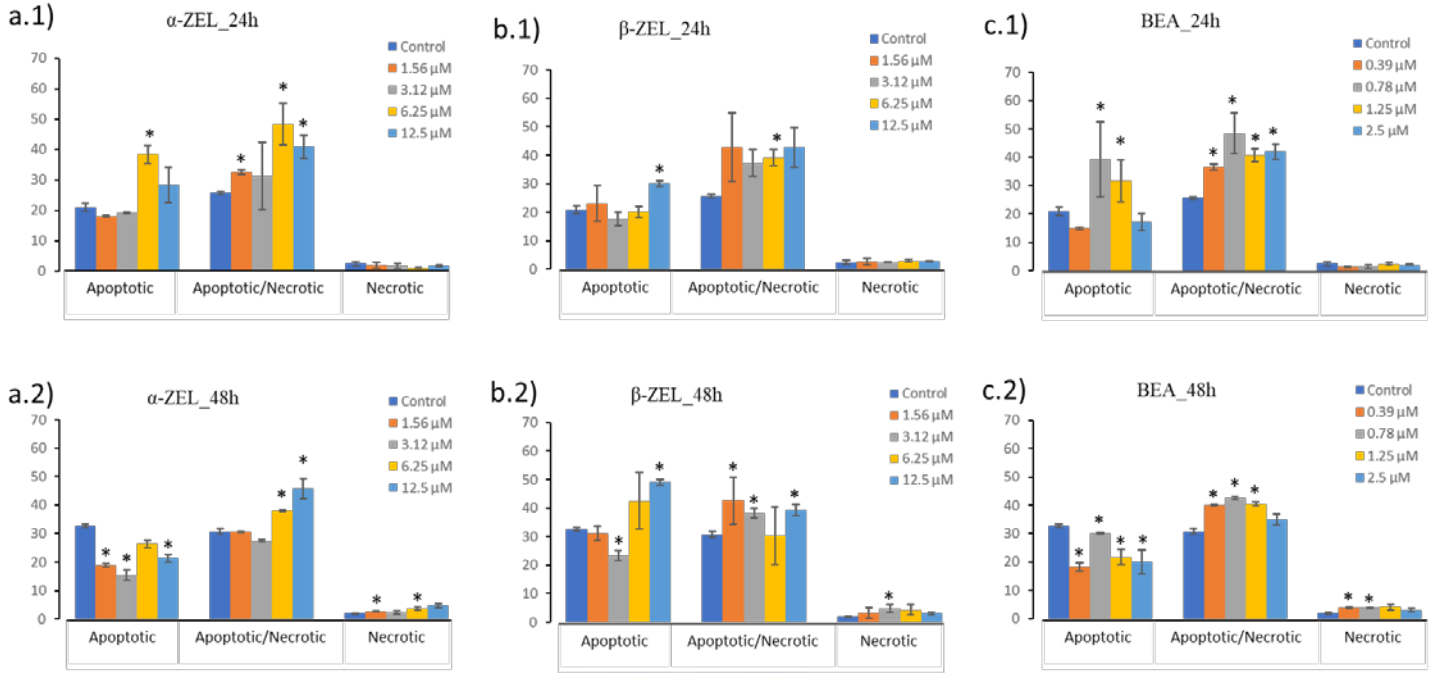

Figure 3. The Apoptosis-Necrosis progression of SH-SY5Y cells treated with α-ZEL (a), β-ZEL (b) and BEA (c) after 24h (a.1, b.1, and c.1) and 48 h (a.2, b.2, and c.2), analysis by flow cytometry. The values were expressed as the mean ± SD for two replications. Data are expressed in % of the unexposed control. *p ≤ 0.05 indicates a significant difference from the respective solvent control.

3.4. Necrosis-apoptosis analysis in combination treatments

The apoptosis-necrosis progression of binary combinations is shown in Figure 4. For α-ZEL + BEA combination, it was observed a significant increase at 2.5 μM in both exposure time (by 57.6% for 24 h and by 40.8% for 48 h), similarly the same happened for apoptotic/necrotic cells at all concentrations assayed from 47.3% to 83% for 24 h and from 37% to 58.7% for 48 h of exposure (Figure 4a). After 24 h (Figure 4b), apoptotic cells increased considerably at the highest concentration of [12.5 + 2.5] μM by 44%, and at [6.25 + 1.25] and [12.5 + 2.5] μM by 28% and 61.8% for 48 h. Also, it was observed a significant increase in apoptotic/necrotic cells at all concentrations assayed for both times of exposure (from 29.7% to 93.8% for 24 h, and from 20.8% to 50% for 48 h), while necrotic cells population remained unchanged (Figure 4b). For α-ZEL + β-ZEL treatments (Figure 4c.1), after 24 h of exposure, a markable increase was observed at the highest concentration assayed ([12.5 + 2.5] μM) in apoptotic/necrotic cells by 128%. On the other hand, after 48 h of exposure, a considerable increase was observed at [6.25 + 1.25] and [12.5 + 2.5] μM in both apoptotic (by 19.9% and 19.8%) and apoptotic/necrotic (by 49.3% and 78.6%) respect to unexposed cells (Figure 4c.2).

Ultimately, for tertiary combination of α-ZEL + β-ZEL + BEA as it is show in Figure 5b, a significant increment was noticed at the highest concentration assayed ([12.5 + 12.5 + 2.5] μM) for apoptotic cells for both exposure time (24 h and 48 h by 126% and 61.6%, respectively), and in the same way for apoptotic/necrotic cells at all concentrations assayed for both time of exposre (from 42.8% to 68.6% for 24 h and from 23.6% to 38.6% for 48 h) in comparison to unexposed cells (Figure 5b).

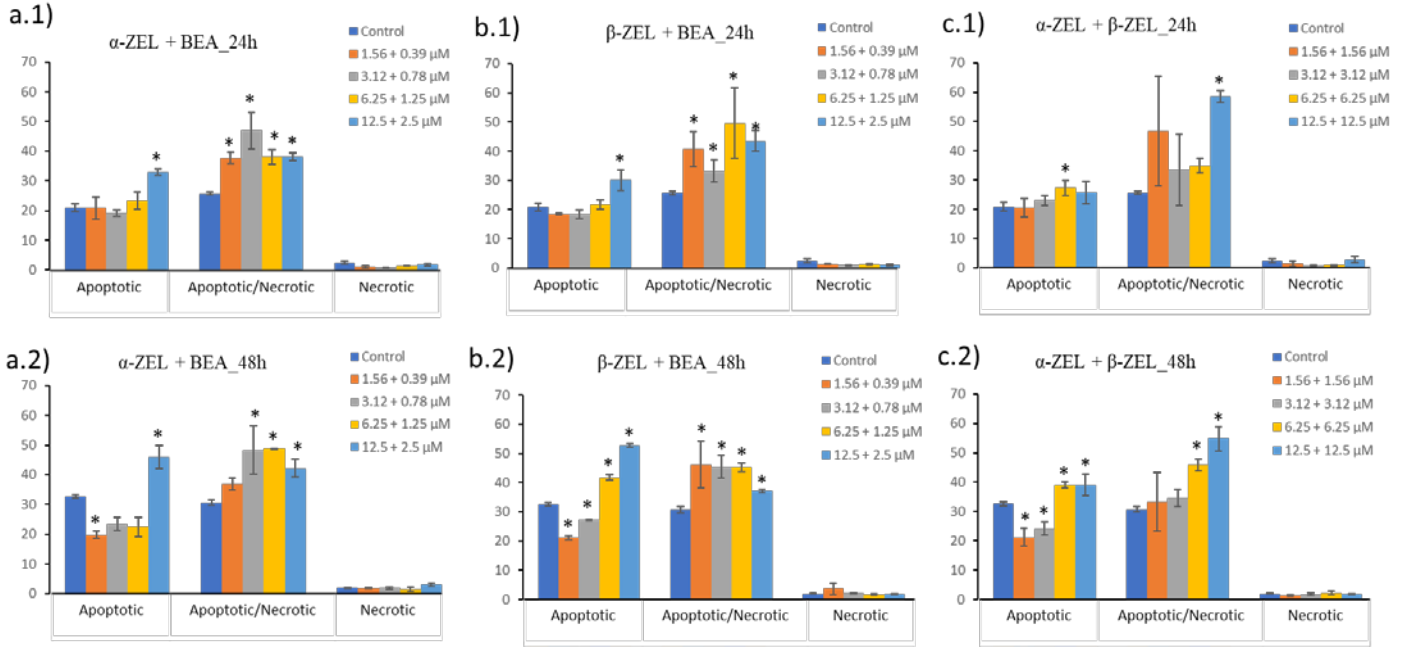

Figure 4. The Apoptosis-Necrosis progression of SH-SY5Y cells treated with α-ZEL + BEA (a), β-ZEL + BEA (b) and α-ZEL + β-ZEL (c) after 24h (a.1, b.1, c.1 and d.1) and 48 h (a.2, b.2, c.2 and d.2), analysis by flow cytometry. The values were expressed as the mean ± SD for two replications. Data are expressed in % of the unexposed control. *$p \leq 0.05$ indicates a significant difference from the respective solvent control.

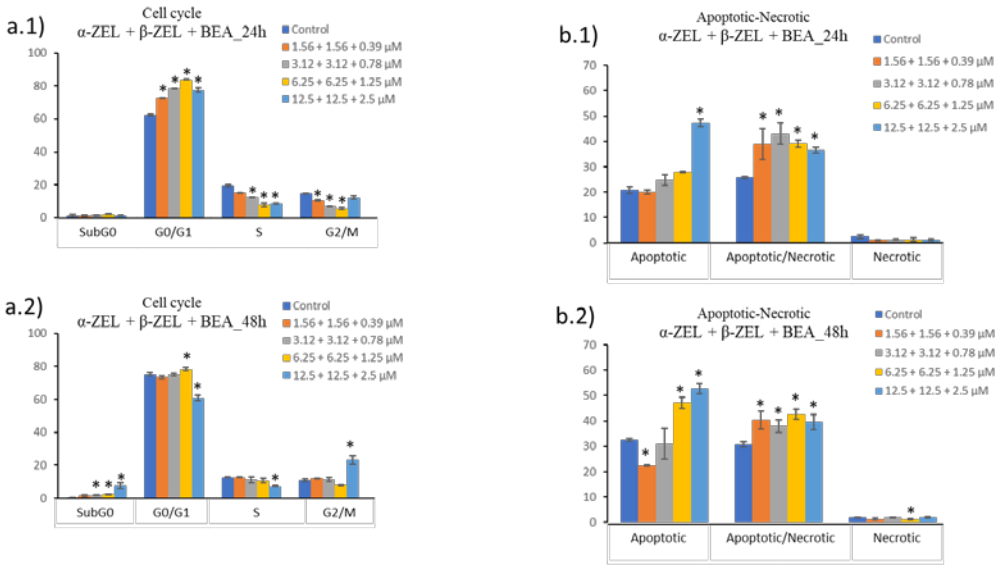

Figure 5. Cell cycle progression (a) and apoptosis-necrosis progression (b) of SH-SY5Y cells treated in tertiary combination α-ZEL + β-ZEL + BEA after 24h (a.1 and b.1) and 48 h (a.2 and b.2) and analyzed by flow cytometry. The values were expressed as the mean ± SD for two replications. Data are expressed in % of the unexposed control. *$p \leq 0.05$ indicates a significant difference from the respective solvent control.

4. Discussion

The cell cycle is typically divided into four phases: G1 (first gap), S (DNA synthesis), G2 (second gap), and M (mitosis) which are responsible for cell duplication (MacLachlan et al., 1995). Transmission of genetic information from one cell generation to the next requires genome replication during the S-phase, and its segregation to the two new daughter cells during mitosis or M-phase. These two phases are crucial events in a cyclic process that allows the correct duplication of the cell without accumulating genetic abnormalities. In a normal cell cycle, M-phase does not occur until S-phase is complete. G1 separates M from S, and G2 is between S and M. The timing and order of cell cycle events are monitored during cell cycle checkpoints that occur at the G1/S boundary, in S-phase, and during the G2/M-phases (MacLachlan et al., 1995). These checkpoints can be activated or arrested by stimulation signals such as growth

factors, DNA damage and by mis-aligned chromosomes at the mitotic spindle (Abid-Essefi et al., 2003; Prosperini et al., 2013). If the damage cannot be repaired, the cell ends up dying by apoptosis or necrosis.

In accordance with the results achieved from cell cycle analysis presented in here for SH-SY5Y cells, after 24 h of exposure, cell proliferation was arrested remarkably in G0/G1 phase by mycotoxins in comparison with non-treated cells. Such effect was mostly highlighted in treatments where β-ZEL was involved (Figures 1b.1, 2b.1 and 2c.1). Conversely, after 48 h of exposure, it was detected unchanged activity and/or decrease in number of cells in G0/G1 phase for all treatments except where β-ZEL engaged, which showed cells cycle arrest at the highest concentrations assayed (Figures 1b.2, Figure 2b.2 and 2c.2). These findings were fortified by the results achieved in our previous study also in SH-SY5Y cells, where β-ZEL was the most cytotoxic mycotoxin when tested individually (Agahi et al., 2020a).

It is detected that growth arrest can be induced when DNA is damaged (Kastan et al., 1991; Linke et al., 1996); additionally, variations in neuronal cells death may arise from the alteration in the expression of several families of genes that regulate apoptosis which are identified in mammals as Bcl-2, Casp-3 and Bax. The Bcl-2 is recognized as anti-apoptotic protein family (Merry et al., 1997); while Bax, member of the Bcl-2 protein family, functions as an apoptotic activator or pro-apoptotic; likewise, Caspase-3 (Casp-3) as a member of caspase family, is believed to activate cell surface death receptors, which is a major commitment step for apoptosis (Wolf et al., 1999). Results of the expression of all three genes in SH-SY5Y cells with these mycotoxins treatments and combinations previously reported (Agahi et al., 2020b) are in accordance with the results obtained here (Figure 1 and 2), as a down regulation of genes Bcl-2 and Casp3 in SH-SY5Y cells was observed when exposed to β-ZEL, and up regulation in all apoptotic genes when exposed to β-ZEL + BEA (Agahi et al., 2020b). It has been also evidenced that the G2/M checkpoint prevents cells from entering mitosis when DNA replication/repair is not complete (He et al., 2020); and coinciding with results from publication mentioned above it was proved that α-ZEL + β-ZEL + BEA down-regulate Bcl-2 gene in SH-SY5Y

cells (Agahi et al., 2020), so it can be concluded that growth arrest in G2/M phase by more than 2 times, might be due to the DNA damage, and consequently this will result in increasing necrotic cells in subG0 phase by 4 times compared to control cells as shown in Figure 5a.2.

Along with SH-SY5Y cells, increment in G0/G1 phase, and decrease in all treatments for S and G2/M phases was observed, mainly at the highest concentration assayed for each treatment, remarkably in β-ZEL, β-ZEL + BEA and β-ZEL + α-ZEL treatments for both phases (Figure 1b, 2b and 2c). This could be due to DNA damage and mitosis impairment. Different studies on the cytotoxic and neurotoxic effects of several chemicals and toxins on the alteration of SH-SY5Y cell cycle have been carried out, but not for mycotoxins. For instance, in a study carried out by Sudo et al., (2019) it was indicated that heavy metals (MeHg, HgCl2, and CdCl2) which are known to induce neurotoxicity, can alter SH-SY5Y cell cycle by arresting them in S and G2/M phases. When looking at studies of the assayed mycotoxins on other cell lines similar results have been revealed for ZEA in inducing G0/G1-phase arrest in hESCs cells and granulosa cells, (Cao et al., 2019; Zhang et al., 2018) but contradictory on prostate cancer (PCa) cells, intestinal epithelial cells (IECs) and sertoli cells, where cell cycle arrest occurred in the G2/M phase at the highest doses assayed (Kowalska et al., 2020; Wang et al., 2019; Zheng et al., 2018). Also, in another study performed on RAW264.7 macrophages cells, accumulation of cells in the sub-G1 phase was significantly higher in the groups exposed to β-ZEL than α-ZEL after 24 h (Lu et al., 2013).

On the other hand, for BEA similar results was observed on CHO-K1 cells where cells were arrested in G0/G1 phase after 24 h and an opposite result after 48 h and 72 h where cell arrest happened through G2/M phase (Mallebrera et al., 2016); also on Caco-2 cells where cells were arrested mainly in G2/M phase (Prosperini et al., 2013). Although there are few studies about the effect of combined mycotoxins on cell cycle alteration, Juan-García et al., (2019) investigated the effect of BEA mycotoxin individually and combined with ochratoxin A (OTA) on HepG2 cells. Results of BEA showed a significant decrease in all phases of cell cycle but only in G0/G1 phase when combined with OTA. Gathering all, it can be concluded that alterations in SH-SY5Y cell

cycle induced by ZEA's metabolites and BEA, differ with other studies; however, depending on the cell line and concentrations assayed, there is no doubt that these mycotoxins can interrupt cell cycle progression and initiate cell death.

The majority of cells that die by "apoptosis", have condensed nuclei and are eliminated by degradation of cell components for nearby cells (Thompson et al., 1995). In contrast, necrosis is a cell death initiated by rapid and severe failure to sustain homeostasis, which it involves damage to the structural and functional integrity of the cell and provokes an inflammatory response (Jacobson et al., 1997; Farber et al., 1994). Toxicological cell culture studies have verified that stimulus intensity influences the mode of cell death (Lennon et al, 1991; Fernandes et al., 1994), although the modes of cell death are still viewed as mechanistically distinct as described above. It has been proposed that cell death occurs as an apoptosis-necrosis continuum, which occurs as hybrids ranging from apoptosis to necrosis (Martin, 2001). Several lines of evidence support a role for apoptosis in the toxicity of ZEA´s metabolites and BEA mycotoxins in different cell models (Agahi et al., 2020b; Juan-García et al., 2019; Ben-Salem et al., 2017; Ayed-Boussema et al., 2008; Bouaziz et al., 2007).

According to our study of apoptosis-necrosis progression on SH-SY5Y cells, in individual treatments of mycotoxins, it was observed a significant tendency of growth in early apoptotic cells population for β-ZEL at the highest concentration assayed (12.5 μM) (Figures 3b.1 and 3b.2); while for α-ZEL and BEA this tendency shifted considerably from apoptotic cells population to apoptotic/necrotic (late apoptotic) cells after 48 h of exposure (Figures 3a.2 and 3c.2). In spite of the fact that there are few studies carried out on ZEA's metabolites on cell death pathway, this could be fortified by results achieved by Lu et al., (2013) on RAW 264.7 macrophages which early apoptotic cells increased significantly when exposed to β-ZEL 50 μM, rather than α-ZEL. Also, in other studies, ZEA caused cell death in apoptotic pathway on pig granulosa cells, and in late apoptotic and necrotic pathways on RAW 264.7 macrophages cells, both studies after 24 h (Li et al., 2015; Zhu et al., 2012). Conversely, for BEA, it was observed an increase in early apoptotic cell death pathway in CHO-

K1 cells (from 1and 5 μM), and in Caco-2 cells (from 1.5 μM and 3.0 μM) (Mallebrera et al., 2016; Prosperini et al., 2013); while an induction in necrotic cell death pathway in CHO-K1 cells (1 and 5 μM), and in C6 cells (1.5 μM) (Mallebrera et al., 2016; Wätjen et al., 2014). Despite the large number of studies about the effects of these mycotoxins on cell death pathway and the variety of results, all of them are focused only on studies performed in individual form.

Among binary and tertiary combinations, a remarkable increase in cell proportion was belonged to both early apoptotic and apoptotic/necrotic cell death pathways after 24 h of exposure (Figures 4, 5b.1 and 5b.2), which was specifically detected at the highest concentration assayed as described in sections 3.4; for tertiary mixture early apoptotic cells increased by 126% (Figure 5b.1) and for binary combination β-ZEL + α-ZEL in apoptotic/necrotic (late apoptotic) cells by 128% both at the highest concentration (Figure 4c.1). However, after 48 h of exposure a significant increase in apoptotic cell population was noticed for tertiary combination and β-ZEL + BEA at the highest concentration assayed by more than 60% compared to control cells (Figures 5b.2 and 4b.2).

The concept of an apoptosis-necrosis cell death progression could be important for understanding neuronal cell death, and thus may be important for the prevention of neuronal loss in human neurological disorder. Although, the death of neurons is not always strictly by apoptosis or necrosis pathways as described by Martin et al., (2001), our results provide further novel information in the mechanisms of neuronal death and the route of dying neurons in an undifferentiated SH-SY5Y neuronal cells when exposed to α-ZEL, β-ZEL and BEA mycotoxins individually and combined. In summary, our results demonstrate that β-ZEL possessed the highest potential in disturbing cell cycle progression by activating and/or arresting cells in G0/G1 phase, and additionally causing cell death mainly in apoptotic pathway at the highest concentration in all treatments where engaged. Thus, these findings offer a better understanding of the cytotoxicity effect of α-ZEL, β-ZEL and BEA mycotoxins when coexist in food and feed, and their effect on the molecular mechanisms of neuronal cell death in nervous system which can lead to new approaches for the prevention of neurodegeneration and neurological disabilities. All this can

expand the field of cell death biology, by regulating new norms in the levels of these mycotoxins in food and feed systems.

Acknowledgements:

Authors would like to thank Spanish Ministry of Science and Innovation PID2019-108070RB-I00ALI and Generalitat Valenciana GV 2020/020.

5. References

Abid-Essefi, S., Baudrimont, I., Hansen, W., Ouanes, Z., Mobio, T.A., Anane, R., Creppy, E.E., Bacha, H., 2003. DNA fragmentation, apoptosis and cell cycle arrest induced by zearalenone in cultured DOK, Vero and Caco-2 cells: prevention by Vitamin E. Toxicology, 192, 237-248.

Agahi, F., Font, G., Juan, C., Juan-García, A., 2020a. Individual and combined effect of zearalenone derivates and beauvericin mycotoxins on SH-SY5Y cells. Toxins, 12, 212.

Agahi, F., Álvarez-Ortega, A., Font, G., Juan-García, A., Juan, C., 2020b. Oxidative stress, glutathione, and gene expression as key indicators in SH-SY5Y cells exposed to zearalenone metabolites and beauvericin, Toxicology Letters, 334, 44-52.

Ayed-Boussema, I., Bouaziz, C., Rjiba, K., Valenti, K., Laporte, F., Bacha, H., Hassen, W., 2008. The mycotoxin Zearalenone induces apoptosis in human hepatocytes (HepG2) via p53-dependent mitochondrial signaling pathway. Toxicology in Vitro, 22, 1671-1680.

Ben-Salem, I., Boussabbeh, M., Da-Silva, J.P., Guilbert, A., Bacha, H., Abid-Essefi, S., Lemaire Ch., 2017. SIRT1 protects cardiac cells against apoptosis induced by zearalenone or its metabolites α- and β-zearalenol through an autophagy-dependent pathway. Toxicology and Applied Pharmacology, 314, 82-90.

Bouaziz, C., Abid-Essefi, S., El Golli, E., Bacha, H., 2007. Cytotoxicity and apoptosis induction by the mycotoxin zearalenone and its metabolites alpha and beta zearalenol in the human Caco-2 cells. Toxicology Letters, 172, 62-71.

Cao, H., Zhi, Y., Xu, H., Fang, H., Jia, X., 2019. Zearalenone causes embryotoxicity and induces oxidative stress and apoptosis in differentiated human embryonic stem cells. Toxicology in Vitro, 54, 243-250.

Carri, M.t., Ferri, A., Cozzolino, M., Calabrese, L., Rotilio, G., 2003. Neurodegeneration in amyotrophic lateral sclerosis: the role of oxidative stress and altered homeostasis of metals. Brain Research Bulletin, 61, 365-374.

Elmore, S., 2007. Apoptosis: a review of programmed cell death. Toxicologic Pathology, 35, 495-516.

Farber, E., 1994. Programmed cell death: necrosis versus apoptosis. Modern Pathology, 7, 605-609.

Fernandes, R.S and Cotter T.G., 1994. Apoptosis or necrosis: intracellular levels of glutathione influence mode of cell death. Biochemical Pharmacology, 48, 675-681.

He, P., Li, Z., Xu, F., Ru, G., Huang, Y., Lin, E., Peng, S., 2020. AMPK Activity Contributes to G2 Arrest and DNA Damage Decrease via p53/p21 Pathways in Oxidatively Damaged Mouse Zygotes. Frontiers in Cell and Developmental Biology. 8:539485.

Jacobson, M.D., Weil, M., and Raff, M.C., 1997. Programmed cell death in animal development. Cell, 88, 347–354.

Jenner, P., 2003. Oxidative stress in Parkinson's disease. Annals of Neurology, 53, 26-36.

Juan-García, A., Manyes, L., Ruiz, M.J., Font, G., 2013. Involvement of enniatins-induced cytotoxicity in human HepG2 cells. Toxicology Letters, 218, 166–173.

Juan-García, A., Tolosa, J., Juan, C., Ruiz, M.J., 2019. Cytotoxicity, genotoxicity and disturbance of cell cycle in HepG2 cells exposed to OTA and BEA: single and combined actions. Toxins, 11, 341.

Kannan, K and Jain, S.K., 2000. Oxidative stress and apoptosis. Pathophysiology, 7, 153-163.

Kastan, M.B., Onyekwere, O., Sidransky, D., Vogelstein, B., Craig, R.W., 1991., Participation of p53 protein in the cellular response to DNA damage. Cancer Research, 51:6304–6311

King, K.L., Cidlowski, J.A., 1995. Cell cycle and apoptosis: common pathways to life and death. Journal of Cellular Biochemistry, 58, 175-180.

Klein, J.A, Ackerman, S.L., 2003. Oxidative stress, cell cycle, and neurodegeneration. Journal of Clinical Investigation, 111, 785-793.

Kovalevich, J., Langford, D., 2013. Considerations for the use of SH-SY5Y neuroblastoma cells in neurobiology. In: Amini S, White MK (eds) Neuronal cell culture: methods and protocols. Humana Press, Totowa, NJ, 9–21.

Kowalska, K., Habrowska-Gorczynska, D.E., Dominska, K., Urbanek, K.A., Piastowska-Ciesielska, A.W., 2020. ER Beta and NF Kappa B-Modulators of Zearalenone-Induced Oxidative Stress in Human Prostate Cancer Cells. Toxins, 12(3), 199.

Lennon, S.V., Martin, S.J., Cotter, T.G., 1991. Dose-dependent induction of apoptosis in human tumour cell lines by widely diverging stimuli. Cell Proliferation, 24: 203-214, 1991.

Linke, S.P., Clarkin, K.C., Di Leonardo, A., Tsou, A., Wahl, G.M., 1996. A reversible, p53-dependent G0/G1 cell cycle arrest induced by ribonucleotide depletion in the absence of detectable DNA damage. Genes & Development, 10:934–947.

Li, Q., Zhang, Zh., Lin, P., Lei, L., 2015. Endoplasmic Reticulum Stress Cooperates in Zearalenone-Induced Cell Death of RAW 264.7 Macrophages. International journal of molecular sciences. 16(8), 19780–19795.

Lu, J., Yu, J.Y., Lim, Sh.S., Son, Y.O., Kim, D.H., Lee, S.A., hi, X., Lee, J.Ch., 2013. Cellular mechanisms of the cytotoxic effects of the zearalenone

metabolites α-zearalenol and β-zearalenol on RAW264.7 macrophages. Toxicology in Vitro, 27(3), 1007-1017.

MacLachlan, T.K., Sang, N., Giordano, A., 1995. Cyclins, cyclin-dependent kinases and cdk inhibitors: implications in cell cycle control and cancer. Critical Reviews in Eukaryotic Gene Expression, 5(2):127-56.

Mallebrera, B., Font, G., Ruiz, M.J., 2014. Disturbance of antioxidant capacity produced by beauvericin in CHO-K1 cells. Toxicology Letters., 226, 337-342.

Mallebrera, B., Juan-Garcia, A., Font, G., Ruiz, M.J., 2016. Mechanisms of beauvericin toxicity and antioxidant cellular defense. Toxicology Letters, 246, 28-34.

Manickam, N., Radhakrishnan, R.K., Andrews, J.F.V., Selvaraj, D.B., Kandasamy, M., 2020. Cell cycle re-entry of neurons and reactive neuroblastosis in Huntington's disease: Possibilities for neural-glial transition in the brain. Life Sciences, 263, 118569.

Martin, L., 2001. Neuronal cell death in nervous system development, disease, and injury (Review). International Journal of Molecular Medicine. 7, 455-478.

Merry, D.E and Korsmeyer, S.J., 1997. Bcl-2 gene family in the nervous system. Annual Review of Neuroscience, 20: 245-267.

Okouchi, M.., Ekshyyan, O., Maracine, M., Aw, T.Y., 2007. Neuronal apoptosis in neurodegeneration. Antioxidants & Redox Signaling, 9, 1059-1096.

Prosperini, A., Juan-García, A., Font, G., Ruiz, M.J., 2013. Beauvericin-induced cytotoxicity via ROS production and mitochondrial damage in Caco-2 cells. Toxicology Letters, 222 (2), 204-211.

Pucci, B., Kasten, M., Giordano, A., 2000. Cell cycle and apoptosis. Neoplasia, 2, 291-299.

Sudo, K., Dao, C.V., Atsushi, M., Mitsuya, Sh., 2019. Comparative analysis of in vitro neurotoxicity of methylmercury, mercury, cadmium, and hydrogen peroxide on SH-SY5Y cells. Journal of Veterinary Medical Science, 81(6) 828-837.

Swomley, A. M., Förster, S., Keeney, J. T., Triplett, J., Zhang, Z., Sultana, R., Butterfield, D. A., 2014. Abeta, oxidative stress in Alzheimer disease: evidence based on proteomics studies. Biochimica et biophysica acta, 1842(8), 1248–1257.

Tatay, E., Espin, S., Garcia-Fernandez, A.J., Ruiz, M.J., 2017. Oxidative damage and disturbance of antioxidant capacity by zearalenone and its metabolites in human cells. Toxicology In Vitro, 45, 334-339.

Thompson, C.B., 1995. Apoptosis in the pathogenesis and treatment of disease. Science, 267, 1456-1462.

Vermes, I., Haanen, C., Steffens-Nakken, H., Reutellingsperger, C., 1995. A novel assay for apoptosis flow cytometric detection of phosphatidylserine expression on early apoptotic cells using fluorescein labelled Annexin V. Journal of Immunological Methods 184, 39–51.

Wolf, B.B and Green, D.R., 1999. Suicidal tendencies: apoptotic cell death by caspase family proteinases. Journal of Biological Chemistry, 274: 20049-20052.

Wong, R.S., 2011. Apoptosis in cancer: from pathogenesis to treatment. Journal of Experimental & Clinical Cancer Research, 30, 87.

Wang, X., Yu, H., Fang, H., Zhao, Y., Jin, Y., Shen, J., Zhou, Ch., Zhou, Y., Fu, Y., Wang, J., Zhang, J., 2019. Transcriptional profiling of zearalenone-induced inhibition of IPEC-J2 cell proliferation. Toxicon, 172, 8-14.

Wätjen, W., Debbab, A., Hohlfeld, A., Chovolou, Y., Proksch, P., 2014. The mycotoxin beauvericin induces apoptotic cell death in H4IIE hepatoma cells accompanied by an inhibition of NF-κB-activity and modulation of MAP-kinases, Toxicology Letters, 231(1), 9-16.

Zhang, R.Q., Sun, X.F., Wu, R.Y., Cheng, Sh.F., Zhang, G.L., Zhai, Q.Y., Liu, X.L., Zhao, Y., Shen, W., Li, L., 2018. Zearalenone exposure elevated the expression of tumorigenesis genes in mouse ovarian granulosa cells. Toxicology and Applied Pharmacology, 356, 191-203.

Zheng, W.L., Wang, B.J., Wang, L., Shan, Y.P., Zou, H., Song, R.L., Wang, T., Gu, J.H., Yuan, Y., Liu, X.Z., Zhu, G.Q., Bai, J.F., Liu, Z.P., Bian, J.C., 2018. ROS-Mediated Cell Cycle Arrest and Apoptosis Induced by Zearalenone in Mouse Sertoli Cells via ER Stress and the ATP/AMPK Pathway. Toxins, 10, 24.

Zhu, L., Yuan, H., Guo, C., Lu, Y., Deng, S., Yang, Y., Wei, Q., Wen, L., He Z., 2012. Zearalenone induces apoptosis and necrosis in porcine granulosa cells via a caspase-3- and caspase-9-dependent mitochondrial signaling pathway. Journal of Cellular Physiology. 227, 1814-1820.

Zingales, V., Fernández-Franzón, M., Ruiz, M.J., 2020. The role of mitochondria in sterigmatocystin-induced apoptosis on SH-SY5Y cells, Food and Chemical Toxicology, 142, 111493

4. GENERAL DISCUSSION

4. GENERAL DISCUSSION

To achieve the objectives of the present PhD thesis first it was carried out a prediction of ZEA, α-ZEL and β-ZEL toxicity, and defined the products of its metabolomics profile via an *in silico* study using three software of computational toxicology: MetaTox, SwissADME and PASS online. Furthermore, the cytotoxicological interactions between α-ZEL, β-ZEL, and BEA mycotoxins for 24, 48, and 72 h at different concentrations individually and in combination in human neuroblastoma SH-SY5Y cells, was performed via the MTT assay. Moreover, the effects of combinations of two and three mycotoxins were evaluated by isobologram analysis to determine whether their interaction was synergistic, additive, or antagonistic, as well as to understand how mycotoxins can act at the cellular level; and determining the amount of α-ZEL, β-ZEL, and BEA mycotoxins remaining in the medium by LC–ESI–qTOF-MS. In addition, it was evaluated the effects of these three mycotoxins on production of ROS; also determined the activity of non-enzymatic and enzymatic antioxidant of SH-SY5Y cells exposed to mentioned mycotoxins.

Afterward, the expression of genes that code for estrogen receptors (*ER2* (specifically *ERβ* and *GPER1*) were examined by all three mycotoxins. Moreover, to obtain more insight into the factors playing a role in the apoptotic process, the relative mRNA expression levels of *CASP3, BAX* and *BCL2* were evaluated in SH-SY5Y cell line, through RT-PCR. Ultimately, it was studied the neurotoxicity of α-ZEL, β-ZEL and BEA mycotoxins individually, in binary and in tertiary combinations on cell cycle regulation of SH-SY5Y cells exposed to

these three mycotoxins, and whether the cell death pathways is through apoptotic, apoptotic/necrotic or necrotic.

4.1. *In silico* study for metabolomic and toxicity prediction of zearalenone, α-zearalenone and β-zearalenone

MetaTox is used to obtain the metabolite products formed during Phase I and II reactions, contributing to describe the metabolomics profile (Rudik et al., 2017); SwissADME (Daina et al., 2017) has been used for assessing the ADMET processes suffered by three mycotoxins (ZEA, α-ZEL and β-ZEL) and its metabolites products (1z-5z for ZEA and 1 ab-7ab for α-ZEL and β-ZEL)(Figure 1, Study 1); and PASS online, predicted the toxic effect of activation and the biological activities with probability values (Pa, probability of activation).

Metabolites products predicted through MetaTox for the mycotoxins studied came from two Phase II reactions: O-glucuronidation and S-sulfation. Both are detoxication reactions of first line facilitating excretion. ZEA was predicted to generate two metabolites for each type of reaction (from 1z to 4z); while for α-ZEL and β-ZEL three metabolites (from 1 ab to 6 ab) (Figure 1 and Table 1, Study 1). For Phase I reaction, only hydrolysis reaction was predicted to take place from ZEA, α-ZEL and β-ZEL, generating only one metabolite product, 7z and 7 ab for ZEA and ZEA's metabolites, respectively. In summary a total of 12 compounds defined the metabolomic profile of ZEA, α-ZEL and β-ZEL (Figure 1 and Table 1, Study 1). Coinciding with other studies, these reactions take place and generate these compounds; however, their effects are unknown; in fact, the use of these metabolite products as biomarkers have been found in the literature in biomonitoring studies (Lorenz et al., 2019; Follmann

et al., 2016; Shephard et al., 2013; Wallin et al., 2015; Gerding et al., 2015) or directly detected in food and aromatic plants as masked mycotoxins (Berthiller et al., 2006, 2009; Mannani et al., 2019). However, an analysis of *in silico* prediction of toxic effects defined by the metabolomics profile is here the first time reported. EFSA has dealt in assessing the risk of ZEA, α-ZEL and β-ZEL and has indicated that metabolites products coming from them (also reported as modified forms) might have effects (oestrogenic effect, genotoxicity, endocrine receptor, …) (EFSA, 2011 and 2014) and contribute to the exposure evaluation but the uncertainty exists as there is a lack of data which entails difficulties in defining its toxic effects (EFSA et al., 2014, 2016, 2017). Not to mention the gap in effects of its mixtures or with other mycotoxins or contaminants.

In silico analysis show that ZEA, α-ZEL and β-ZEL are poorly achieving the BBB, have good distribution and are highly favored to be absorbed gastrointestinally (Table 2, Study 1). The interesting point noticed with the analysis of metabolites products of these mycotoxins, obtained from O-glucuronidation, S-sulfation and hydrolysis reactions, is that these properties change inversely, especially for achieving the BBB (see values from Table 2 and Table 3, Study 1) from low values to high values. There are studies coinciding and others opposite to the results predicted in here when compared with those reported by in vitro and in vivo studies. For all three mycotoxins it has been reported a good gastrointestinal absorption (rapid and extensive) as well as the formation of metabolites from hydrolysis, sulfation and glurcuronidation (Biehl et al., 1993; Frizzell et al., 2015; Pfeiffer et al., 2011; Plasencia et al., 1991); in fact, several strategies and recommendations have been also considered for the entire risk assessment (EFSA 2017; Lorenz et al., 2019). Optimal gastrointestinal

absorption predicted by Lipinsky RO5 is reported in Table 1 (Study 1), for the metabolomics profile. It also indicates that the probability of one compound to be absorbed orally is directly related to the ADMET and toxic effects. Only metabolites coming from O-glucuronidation were not following the Lipinsky's RO5 (HBA>10), because of not passing the gastrointestinal barrier; however, mycotoxins, and metabolites from S-sulfation and hydrolysis reactions did which indicates their good distribution.

According to the analysis of main effects predicted *in silico* for ZEA, α-ZEL, β-ZEL and its metabolite product defining the metabolomic profile, carcinogencity is the toxic effect predicted with high probability; however, IARC has classified ZEA (since 1993) as Group 3 (not classifiable as to their carcinogenicity to humans) based on inadequate evidence in humans and limited evidence in experimental animals (IARC 1993); to mention different behave in mice and mouse with limited evidence reported. This explains the prediction described in Figure 2 (Study 1), which although carcinogenicity indicates high probability (80–90%), the evidence is not coinciding with assays carried out for evaluating such effect. This is not happening with other effects reported in Figure 2 (Study 1) which coincide with studies carried out either *in vivo* or *in vitro* (especially for ZEA as it is the most studied): mutagenicity (Abbès et al., 2007; Ben Salah-Abbès et al., 2009); nephrotoxic in rats (Becci et al., 1982), genotoxic (Ouanes et al., 2003, 2005; El-Makawy et al., 2001). As mentioned before the prediction needs to be confirmed with further assays without forgetting that it is giving a valuable indication to start from.

Cytochrome P450 (CYP450) is an enzymatic complex important as mechanism of defense by the organism when in contact with contaminants. Its

main function is to metabolize the majority of toxic compounds through Phase I reactions. It is constituted by several isoforms to highlight the following as the most implicated in defense: CYP3A4, CYP2C9, CYP2C19, CYP1A1 and CYP1A2 (SwissADME). Expression of different isoforms occurs by exposure to contaminants as mycotoxins; which can act as inhibitors, inducers or substrates of this enzymatic complex. Results reveal that the highest predictions effects were for CYP3A4 (40–80%). When analyzing the action of mycotoxins, all three act as substrate, inducers and inhibitors ranging from 60% to 90%, from 21% to 38% and from 23% to 32%, respectively for isoforms CYP1A1 and CYP1A2 (Figure 3, Study 1); while as substrate (62%–71%) and inducers (89%) for CYP3A4. Finally, for isoform CYP2C9, ZEA act as substrate and inducer and, α-ZEL and β-ZEL as substrate and inhibitor. For metabolite products, probabilities of action were marked for isoform CYP3A4. This isoform jointly CYP1A2 have been reported to play an important role in metabolism of ZEA in humans (Pfeiffer et al., 2009); while jointly with CYP2C8 denotes a high activation hydroxylation of ZEA (Bravin et al., 2009). In summary, different isoforms of CYP seem to contribute in the metabolization of all 15 compounds according to *in silico* prediction which coincides with the studies performed in vitro (Pfeiffer et al., 2009; Bravin et al., 2009); and more specifically with the isoform CYP3A4 which has the highest values of probability.

Apoptotic cell death has been studied for ZEA *in vitro* revealing that activation of caspase 3 and 8 occurs (Banjerdpongchai et al., 2020; Gazzah et al., 2010; Othmen et al., 2008; Agahi et al., 2020 Zhu et al., 2012); as well as for α-ZEL and β-ZEL (Abid-Essefi et al., 2009). Nothing is known nor for its metabolite products defined in the metabolomics profile. Both caspases,

implicated in the cascade activation for apoptotic cell death, have been predicted *in silico* as reported in Figure 4 (Study 1). Results for ZEA coincide with those reported in the literature in vitro denoting a major activation for caspase 3 than caspase-8 (Barjerdpongchai et al., 2020). Among that, similar tendency was observed for all the other 14 compounds studied; and while O-glucuronidates present highest prediction of activation for both caspase-3 and 8 and all compounds, S-sulfation products from ZEA (3z and 4z) do not contribute to activation of cell death through caspase-8 (Figure 4B, Study 1). The prediction achieved in this thesis in cell death and the *in vitro* confirmation reported for ZEA, α- ZEL and β-ZEL reveal that the apoptosis pathway of cell death is contributed by its metabolite products, which are generated during its detoxification by Phase I and II reactions.

4.2. Cytotoxic effect of zearalenone's derivates and beauvericin mycotoxins on SH-SY5Y cells

4.2.1. Cytotoxicity effect of individual and combined mycotoxins

According to the IC_{50} values of single mycotoxins, β-ZEL was the most cytotoxic mycotoxin compared to the other mycotoxins assayed individually, which is in accordance with Marin et al. (2019) who studied the cytotoxicity of ZEA and its metabolites in HepG2 cells, individually and in double combinations. Regarding to double combinations, it was revealed that presence of two mycotoxins increased the cytotoxic potential in SH-SY5Y cells, as shown by the lower IC_{50} values. IC_{50} for α-ZEL and BEA was not reached in individual treatment however, binary combination α-ZEL + BEA (5:1) inhibited cell proliferation from up to 50 to 90% for all times studied. For the β-ZEL + BEA (5:1) binary combination, the IC_{50} values at 48 and 72 h were lower than that of

β-ZEL. This was also observed when β-ZEL was combined with α-ZEL, for which combination (α-ZEL + β-ZEL (1:1)), the IC_{50} value was the same as that found for β-ZEL alone. This result was not achieved by Tatay et al. (2014) in CHO-K1 cells, although the mycotoxin concentrations studied in binary assays in that work were two times higher than the concentrations assayed in our study. The proliferation of CHO-K1 cells treated with the α-ZEL + β-ZEL mixture at the highest concentration decreased only by 20% with respect to the values found when each mycotoxin was tested alone. For the triple combination (α-ZEL + β-ZEL + BEA, (5:5:1)), cell proliferation inhibition was lower than when β-ZEL was assayed individually, and the same result was found for β-ZEL + BEA after 48 and 72 h and for α-ZEL + β-ZEL after 48 h in SH-SY5Y cells. This is in contrast with the results obtained for the tertiary combination of α-ZEL + β-ZEL + ZEN in CHO-K1 cells, as this combination was more cytotoxic than each mycotoxin tested alone (Chou and Talalay, 1984).

In SH-SY5Y cells presented in this work, almost all the combinations tested reduced cell viability more than the individual mycotoxins, except the β-ZEL + BEA (5:1), α-ZEL + β-ZEL (1:1), and α-ZEL + β-ZEL + BEA (5:5:1) combinations, for which the reduction in cell viability was not significantly different from that obtained when β-ZEL was assayed individually. According to Dong et al. (2010), ZEA is degraded more efficiently to α-ZEL than to β-ZEL in almost all tissues, whereas it is converted more efficiently to β-ZEL than to α-ZEL in liver and lungs. Some studies demonstrated that β-ZEL is more cytotoxic than α-ZEL (Jia et al, 2019; Abid et al, 2009; Chou 2006), whereas other studies found that α-ZEL is more cytotoxic (Jia et al, 2019; Chou and Talalay, 1984).

4.2.2. α-ZEL, β-ZEL, and BEA present in cell medium after treatment with binary and tertiary combination

The IC_{50} values obtained by the MTT assay and the amount of mycotoxin detected in the media by LC–ESI–qTOF-MS were determined and translated into percentage values as an attempt to calculate the amount of each mycotoxin involved in the cytotoxic effect and in the type of interaction effect. Hence, the percentage of mycotoxin present in the media was considered in accordance with the IC_{50} value obtained from the MTT assay. The results showed that among the individual mycotoxins assayed, the amount of α-ZEL that remained in the culture medium was above 50% of the administered quantity at all times assayed. This can be related to the effect, which shows that the viability was above 100% for the doses reported. This can be justified by the chemical structure of this compound, which might impede its access in the cell. the results suggest that the availability and capacity of the tested mycotoxins to get into cells were greater than those of α-ZEL, and as a consequence, the amounts of these mycotoxins detected in the media were lower than that of α-ZEL. To notice that the higher the amount of mycotoxin in the medium (at 24 h), the higher the cell viability, which might be related to the lower amount of mycotoxin affecting the live cells. On the contrary, BEA seemed to have easier access the cells, as its percentage in the medium was generally below 50%, but cell viability was maintained above 50% for the doses assayed, indicating the lower potential toxicity of BEA in SH-SY5Y cells compared to ZEA metabolites. In fact, among all three mycotoxins tested, BEA reached the IC_{50} values after long exposures times (72 h), highlighting again the mild toxic effect of BEA in SHY-SY5Y cells compared to ZEA metabolites.

According to this and when analyzing combinations, the amounts of ZEA metabolites found in the medium were in most cases below BEA's amounts, indicating easier access of these compounds in SH-SY5Y compared to BEA. In detail, for the α-ZEL + BEA combination, it can be observed that the lower the amount of α-ZEL in the medium over time, the lower the viability of SH-SY5Y cells, in particular at 72 h. For triple mixtures, the cytotoxic effect was weaker at all times and for all mixtures compared with that of binary combinations; however, the amounts of each mycotoxin detected were all below 50%, and the cytotoxic effect seemed to be bearable for SH-SY5Y cells for doses administered in the first and second mixture but not for those of the third mixture (6.25 + 6.26 + 1.25) μM (α-ZEL + β-ZEL + BEA, 5:5:1), specifically at 48 h and 72 h. The results obtained in this assay suggest that cytotoxicity is due to the stimulation of different biochemical mechanisms that after a certain level of stimulation, cannot be controlled and cause cell death.

4.3. Determination of oxidative stress production and enzymatic defense system in SH-SY5Y cells exposed to zearalenone metabolites and beauvericin

There are limited studies to demonstrate the effects of ZEA´s metabolites and BEA on cells cytotoxicity according to their relationship on different factors such as oxidative stress and regulation of gene expression, individually and in combination (Marin et al., 2019; Fu et al., 2019; Tatay et al., 2016, 2017; Ferrer et al., 2009). In Study 2, the cytotoxicity of ZEA´s metabolites (α-ZEL and β-ZEL) and BEA were examined individually and in combination and it was observed that all treatments caused cytotoxic effect on SH-SY5Y cells.

Accordingly, it was aimed to determine the mechanism whereby these three mycotoxins induce oxidative stress in the same cell line and their possible effect on alteration of enzymatic and non-enzymatic defense system.

4.3.1. Intracellular ROS generation of individual and combined mycotoxins

Regarding to our results obtained from evaluating ROS generation, elevated ROS levels in combinations where α-ZEL was involved, were observed with increases of 2.8- to 8-fold compared to control, coinciding with that obtained by Tatay et al. (2017) on HepG2 cells that α-ZEL was the major contributor to ROS production. However, no significant difference in ROS levels were detected when each mycotoxins was tested alone.

On the other hand, opposite to results previously published for SH-SY5Y cells, HepG2 cells and CHO-K1 cells (Zingales et al., 2020; Tatay et al., 2016, 2017; Venkataramana et al., 2014) it was not observed any relationship between increasing time or concentration and the amount of ROS production in cells. The increased ROS generation in cells exposed to ZEA´s metabolites and BEA could be a consequent contribution to cell injury or oxidative stress.

4.3.2 Alteration of non-enzymatic defense system

With considering that the levels of GSH determine the balance in the antioxidant defense system, the impact on cellular GSH content present in two redox form (glutathione reduced (GSH) and glutathione disulfide (GSSG)), was evaluated after 24 h and 48 h in SH-SY5Y cells for α-ZEL, β-ZEL and BEA individually and combined, as all three have toxicological interest due to their potential to cause oxidative stress and damage.

The obtained results suggested that α-ZEL, β-ZEL and BEA, in individual and combination treatment after 24 h had induced GSH/GSSG in the SH-SY5Y cells, since the ratio was significantly elevated; whereas, after 48 h of exposure the same result was only observed for α-ZEL + BEA and α-ZEL + β-ZEL combination at the lowest concentration assayed.

4.3.3. Alteration of enzymatic defense system

The results obtained in this thesis, showed an increase of SOD activity in all treatments assayed, individually and in combination, from 2- to 5- folds after 48 h of exposure compared to unexposed cells, while after 24 h of exposure this activity remained unchanged. Afterwards, with accelerating the activity of SOD, H_2O_2 production increases, and consequently GPx antioxidant which detoxify H_2O_2 activity increases as well. According to our results, GPx activity increased significantly in all treatments individually and in combination after 24 h of exposure by 3.5- to 24- folds compared to untreated cells. According to the results achieved in Study 3, the effect of ROS activity on GSH levels demonstrated no change in the activity of this antioxidant; furthermore, regarding to the utilization of GPx from GSH as a substrate, no lack of GSH allowed GPx to enhance their activity when the levels of ROS started to increase. On the other hand, the activity of GPx decreased significantly in tertiary combination at 24 h and remained unchanged after 48 h of exposure in almost all treatments. In several studies, cells with increased levels of SOD showed to be hypersensitive to oxidative stress rather than protected from it (Weydert et al., 2006; Michiels et al., 1994). Hence, the dysfunctionality of H_2O_2 conversion by an adequate level of CAT and GPx, may be detrimental to the cell, which

consequently an accumulation of H_2O_2 might occur to end up cells dying. In the light of this, the high levels of SOD activity during 48 h of exposure can justify the inadequate levels of GPx at this time. Also, according to the study carried out on cytotoxicity of α-ZEL, β-ZEL and BEA, it was observed lower viability in SH-SY5Y cells after 48 h of exposure in all treatments and in tertiary mixture, which confirmed that the cytotoxicity was higher compare to other treatments; also, as confirmed in previously, the ROS levels increased when mycotoxins were assayed in combination at the same levels as reported in here for undifferentiated SH-SY5Y cells. This suggests that GPx activity in undifferentiated SH-SY5Y cell line is not the major implicated enzyme in detoxifying when cells viability decrease inversely with the increase of time of exposure, and when three mycotoxins engage. Moreover, Pigeolet et al., (1990) discovered that GPx itself is susceptible to oxidation by the oxidative reactive molecules and lipid peroxides and could be inactivated by its own substrates. Thus, the decrease of GPx activity in cells exposed to mycotoxins after 48 h and in tertiary combination, could be associated to the inactivation by higher ROS levels.

Similar results were obtained by Tatay et al., (2016 and 2017) where SOD and GPx activity increased in both HepG2 and CHO–K1 cells exposed to α-ZEL and β-ZEL individually for 24 h. Also, in another study by Krishnaswamy et al., (2010) which suggested SOD and GPx are enzymes primarily involved in combating cellular oxidative stress in HT-29 cells treated with deoxynivalenol (DON). Moreover, Mallebrera et al., (2014) observed an increase in GPx activity in CHO–K1 cells exposed to different concentrations of BEA for 24 h. Dinu et al., (2011) in Hek-293 cells exposed to DON mycotoxin between 6 to 24 h of exposure, reported a significant increase in SOD activity. However, opposite

results were obtained for sterigmatocystin (STE) mycotoxins in SH-SY5Y cells exposed during 24 h, where SOD and GPx enzymes decreased suggesting that these enzymes are unable to counteract the oxidative stress produced by STE exposure (Zingales et al., 2020).

According to the results obtained from CAT activity in cells treated with α-ZEL, β-ZEL and BEA, it was observed a significant decrease in all individual treatments at 24h) as well as in combinations except in the binary treatment β-ZEL + BEA. This decrease is probably because of the competition of GPx with CAT enzyme in detoxifying the effect of H_2O_2 activity in the stage of 24 h of exposure. In addition, this marked effect can be due to high concentrations of H_2O_2 produced under mycotoxin exposure, which depression or complete oxidation of CAT activity in situations of high peroxide concentrations may also occur, and it can be even inactivated (Williams., 1928). Contrary, in the stage of 48 h of exposure, the activity of CAT increased significantly in α-ZEL and β-ZEL mycotoxins individually and in combination up to 5-fold in comparison to control cells. Moreover, the excess of H_2O_2 can cross the mitochondrial membrane and can be degraded by CAT; thus, it could be speculated that it might be due to a compensatory manner for CAT to reduce H_2O_2 levels while GPx is inactivated in the same treatments during 48 h of exposure. Similar results were found by Tatay et al., (2016 and 2017) and Dinu et al., (2011) where CAT activity reduced in a dose-dependent manner, suggesting that the accumulation of superoxide anion produced by assayed mycotoxins may inhibit CAT activity (Kono and Fridovich., 1982).

At last, a down regulation of the antioxidant defense system by decreasing the activity of GST enzyme only in cells exposed to α-ZEL and β-ZEL individually was observed. Inversely, a significant increase was demonstrated in all combination treatments, particularly in the highest concentrations assayed (except in α-ZEL + β-ZEL). Increase in GST activity is considered a chemical stress signal; therefore, this effect can be due of increasing enzymatic activity in combination treatments by higher ROS produced, which was discussed in Study 3, where ROS activity increased significantly in all combination treatments from 2.8- to 8- fold compared to control. Conversely, the decrease or unchanged GST activity in individual treatments can be due of no changing in ROS activity.

4.4. Expression of apoptosis-related and estrogen receptors genes in SH-SY5Y cells exposed to zearalenone metabolites and beauvericin

According to the examination of *GPER1* and *Erβ*, as endocrine disruptor genes, it was observed that among all three mycotoxins assayed in individual and combination forms, only β-ZEL up-regulated the expression of *ERβ* mRNA significantly up to 2.7-fold at 12.5 μM compared to the reference gene (*18S*); while for *GPER1*, any significant regulation was observed.

Studies have shown that the *BCL2* and *BAX* pathways are involved in ZEA-induced apoptosis in primary rat cells (Li et al., 2011); also, the caspase family of proteins plays an important role in the initiation of apoptosis, of which caspase-3 is the primary initiator (Riedl and Salvesen, 2007). Nevertheless, there are no sufficient data about the two major metabolites of ZEA (α-ZEL and β-ZEL), since it is proved that it breaks down into their main metabolites during phase I metabolism (Metzler et al., 2010). The results of our study for individual treatments demonstrated that, while α-ZEL up-regulated the expression of cell

apoptosis genes, β-ZEL shows an adverse effect which was down-regulating of these genes. Additionally, BEA only up-regulated the expression of *BCL2* significantly. Moreover, β-ZEL + BEA was the only combination that elevated the expression of cell apoptosis genes. Then α-ZEL presented effect on gene expression, either cell apoptosis or estrogen receptors. However, in the combination, β-ZEL + BEA at [12.5 + 2.5] μM it was up-regulated the expression of all five studied gene expression involved in cell apoptosis (*CASP3, BAX, BCL2*) and estrogen receptors (*ERβ* and *GPER1*).

4.5. Cell cycle disruption and cell death pathway analysis of zearalenone's metabolites and beauvericin

4.5.1. Cell cycle alteration in neuroblastoma cells exposed to zearalenone metabolites and beauvericin

In accordance with the results, after 24 h of exposure, cell proliferation was arrested remarkably in G0/G1 phase by α-ZEL, β-ZEL and BEA mycotoxins individually and combined in comparison with non-treated SH-SY5Y cells. Such effect was mostly highlighted in treatments where β-ZEL was involved. Conversely, after 48 h of exposure, it was detected unchanged activity and/or decrease in number of cells in G0/G1 phase for all treatments except where β-ZEL engaged, which showed cells cycle arrest at their highest concentrations assayed. These findings were fortified by the results achieved in Study 2, where β-ZEL was the most cytotoxic mycotoxin when tested individually.

It is detected that growth arrest can be induced when DNA is damaged (Kastan et al. 1991; Linke et al, 1996); additionally, variations in neuronal cells death may arise from the alteration in the expression of several families of genes that regulate apoptosis which are identified in mammals as *Bcl-2*, *Casp-3* and *Bax*. The *Bcl*-2 is recognized as anti-apoptotic protein family (Merry et al, 1997); while *Bax*, member of the *Bcl-2* protein family, functions as an apoptotic activator or pro-apoptotic; likewise, Caspase-3 (*Casp-3*) as a member of caspase family, is believed to activate cell surface death receptors, which is a major commitment step for apoptosis (Wolf et al, 1999). Results of the expression of all three genes reported in Study 3 are in accordance with the results obtained here, as down regulation of genes *BCL-2* and *Casp3* in SH-SY5Y cells was observed when exposed to β-ZEL, and up regulation in all apoptotic genes when exposed to β-ZEL + BEA. It has been also evidenced that the G2/M checkpoint prevents cells from entering mitosis when DNA replication/repair is not complete (He et al, 2020); which coincide with Study 3 where α-ZEL + β-ZEL + BEA down-regulated *BCL-2* gene in SH-SY5Y cells; so it can be concluded that growth arrest in G2/M phase by more than 2 times, might be due to the DNA damage, and consequently this will result in increasing necrotic cells in subG0 phase by 4 times compared to control cells.

Along with the increment in G0/G1 phase, a significant decrease in S and G2/M phases for all treatments was observed, mainly at the highest concentration assayed for each treatment, remarkably in β-ZEL, β-ZEL + BEA and β-ZEL + α-ZEL for both phases. This could be due to DNA damage and mitosis impairment. Different studies on the cytotoxic and neurotoxic effects of several chemicals and toxins on the alteration of SH-SY5Y cell cycle have been carried out, but not for mycotoxins. For instance, in a study carried out by Sudo

et al., (2019) it was indicated that heavy metals (MeHg, $HgCl_2$, and $CdCl_2$) which are known to induce neurotoxicity, can alter SH-SY5Y cell cycle by arresting them in S and G2/M phases. When looking at studies of the assayed mycotoxins on other cell lines similar results have been revealed for ZEA in inducing G0/G1-phase arrest in hESCs cells and granulosa cells, (Cao et al., 2019; Zhang et al., 2018) but contradictory on prostate cancer (PCa) cells, intestinal epithelial cells (IECs) and sertoli cells, where cell cycle arrest occurred in the G2/M phase at highest doses assayed (Kowalska et al, 2020; Wang et al, 2019; Zheng et al, 2018). Also, in another study performed on RAW264.7 macrophages cells, accumulation of cells in the sub-G1 phase was significantly higher in the groups exposed to β-ZEL than α-ZEL after 24 h (Lu et al, 2013).

On the other hand, for BEA similar results was observed on CHO-K1 cells where cells were arrested in G0/G1 phase after 24 h and an opposite result after 48 h and 72 h where cell arrest happened through G2/M phase (Mallebrera et al, 2016); also on Caco-2 cells where cells were arrested mainly in G2/M phase (Prosperini et al, 2013). Although there are few studies about the effect of combined mycotoxins on cell cycle alteration, Juan-García et al., (2019) investigated the effect of BEA mycotoxin individually and combined with ochratoxin A (OTA) on HepG2 cells. Results of BEA showed a significant decrease in all phases of cell cycle but only in G0/G1 phase when combined with OTA. Gathering all, it can be concluded that alterations in SH-SY5Y cell cycle induced by ZEA's metabolites and BEA, differ with other studies; however, depending on the cell line and concentrations assayed, there is no doubt that these mycotoxins can interrupt cell cycle progression and initiate cell death.

4.5.2. Cell death pathway analysis in neuroblastoma cells exposed to zearalenone metabolites and beauvericin

According to the study of apoptosis-necrosis progression on SH-SY5Y cells, in individual treatments of mycotoxins, it was observed a significant tendency of growth in early apoptotic cells population for β-ZEL at its highest concentration assayed (12.5 μM); while for α-ZEL and BEA this tendency shifted considerably from apoptotic cells population to apoptotic/necrotic (late apoptotic) cells after 48 h of exposure. In spite of the fact that there are few studies carried out on ZEA's metabolites on cell death pathway, this could be fortified by results achieved by Lu et al., (2013) on RAW 264.7 macrophages which early apoptotic cells increased significantly when exposed to β-ZEL 50 μM, rather than α-ZEL. Also, in other studies, ZEA caused cell death in apoptotic pathway on pig granulosa cells, and in late apoptotic and necrotic pathways on RAW 264.7 macrophages cells, both studies after 24 h (Li et al, 2015; Zhu et al, 2012). Conversely, for BEA, it was observed an increase in early apoptotic cell death pathway in CHO-K1 cells (from 1and 5 μM), and in Caco-2 cells (from 1.5 μM and 3.0 μM) (Mallebrera et al, 2016; Prosperini et al, 2013); while an induction in necrotic cell death pathway in CHO-K1 cells (1 and 5 μM), and in C6 cells (1.5 μM) (Mallebrera et al, 2016; Wätjen et al, 2014). Despite the large number of studies about the effects of these mycotoxins on cell death pathway and the variety of results, all of them are focused only on studies performed in individual form.

Among binary and tertiary combinations, a remarkable increase in cell proportion was belonged to both early apoptotic and apoptotic/necrotic cell death pathways after 24 h of exposure, which was specifically detected at the

highest concentration assayed as described in sections 3.4; for tertiary mixture early apoptotic cells increased by 126%, and for binary combination β-ZEL + α-ZEL in apoptotic/necrotic (late apoptotic) cells by 128% both at the highest concentration. However, after 48 h of exposure a significant increase in apoptotic cell population was noticed for tertiary combination and β-ZEL + BEA at their highest concentration assayed by more than 60% compared to control cells.

4.6. References

Abbès S, Ouanes Z, Salah-Abbès J, Abdel-Wahhab MA, Oueslati R and Bacha H, 2007. Preventive role of aluminosilicate clay against induction of micronuclei and chromosome aberrations in bonemarrow cells of Balb/c mice treated with Zearalenone. Mutation Research Genetic Toxicology and Environmental Mutagenesis, 631, 85-92.

Abid, S., Bouaziz, C,El., Golli-Bennour, E., Ouanes Ben Othmen, Z., Bacha, H., 2009. Comparative study of toxic effects of zearalenone and its two major metabolites α-zearalenol and β-zearalenol on cultured human Caco-2 cells. Journal of Biochemical and Molecular Toxicology. 23, 233–243.

Bang O.Y., Hong H.S., Kim D.H., Kim H., Boo J.H., Huh K., Mook-Jung I., 2004. Neuroprotective effect of genistein against beta amyloid-induced neurotoxicity Neurobiology of Disease, 16 (1), 21-28.

Banjerdpongchai, R., Kongtawelert, P., Khantamat, O., Srisomsap, C., Chokchaichamnankit, D., Subhasitanont, P., Svasti, J. 2020. Mitochondrial and endoplasmic reticulum stress pathways cooperate in zearalenone-induced apoptosis of human leukemic cells. J. of Hematology & Oncology 3, 50.

Becci PJ, Voss KA, Hess FG, Gallo MA, Parent RA, Stevens KR and Taylor JM, 1982. Longterm carcinogenicity and toxicity study of zearalenone in the rat. Journal of Applied Toxicology, 2, 247-254.

Ben Salah-Abbès J, Abbès S, Abdel-Wahhab MA and Oueslati R, 2009. Raphanus sativus extract protects against Zearalenone-induced reproductive toxicity, oxidative stress and mutagenic alterations in male Balb/c mice. Toxicon, 53, 525-533.

Berthiller F, Hametner C, Krenn P, Schweiger W, Ludwig R, Adam G, Krska R and Schuhmacher R, 2009. Preparation and characterization of the conjugated Fusarium mycotoxins zearalenone-4O-beta-Dglucopyranoside, alpha-zearalenol-4O-beta-Dglucopyranoside and beta-zearalenol-4O-beta-D-glucopyranoside by MS/MS and two dimensional NMR. Food Additives & Contaminants. Part A: Chemistry, Analysis, Control, Exposure & Risk Assessment, 26, 207–213.

Berthiller F, Werner U, Sulyok M, Krska R, Hauser MT and Schuhmacher R, 2006. Liquid chromatography coupled to tandem mass spectrometry (LC-MS/MS) determination of phase II metabolites of the mycotoxin zearalenone in the model plant Arabidopsis thaliana. Food Additives and Contaminants, 23, 1194–1200.

Biehl ML, Prelusky DB, Koritz GD, Hartin KE, BuckWB, Trenholm HL., 1993. Biliary excretion and enterohepatic cycling of zearalenone in immature pigs. Toxicol Appl Pharmacol, 121:152–159.

Bravin F, Duca RC, Balaguer P and Delaforge M, 2009. In vitro cytochrome p450 formation of a monohydroxylated metabolite of zearalenone exhibiting estrogenic activities: possible occurrence of this metabolite in vivo. International Journal of Molecular Sciences, 10, 1824-1837.

Cao, H., Zhi, Y., Xu, H., Fang, H., Jia, X., 2019. Zearalenone causes embryotoxicity and induces oxidative stress and apoptosis in differentiated human embryonic stem cells. Toxicology in Vitro, 54, 243-250.

Chou, T.C., 2006. Theoretical basis, experimental design, and computerized simulation of synergism and antagonism in drug combination studies. Pharmacological Review. 58, 621–681.

Chou, T.C., Talalay, P., 1984. Quantitative analysis of dose-effect relationships: the combined effects of multiple drugs or enzyme inhibitors. Advances in Enzyme Regulation. 22:27-55.

Daina A., Michielin O., Zoete V., 2017. SwissADME: a free web tool to evaluate pharmacokinetics, drug-likeness and medicinal chemistry friendliness of small molecules. Scientific Reports, 7:42717.

Dinu, D., Bodea, G.O., Ceapa, C.D., Munteanu, M.C., Roming, F.I., Serban, A.I., 2011. Adapted response of the antioxidant defense system to

oxidative stress induced by deoxynivalenol in Hek-293 cells. Toxicon, 57, 1023-1032.

Dong, M., Tulayakul, P., Li, J-Y., Dong, K-S., Manabe, N., Kumagai, S., 2010. Metabolic Conversion of Zearalenone to α-Zearalenol by Goat Tissues. Journal of Veterinary Medical Science. 72, 307-312.

EFSA - European Food Safety Authority (2011) Scientific Opinion on the risks for public health related to the presence of zearalenone in food EFSA Journal, 9(6):2197.

EFSA - European Food Safety Authority (2014) Scientific opinion on the risks for human and animal health related to the presence of modified forms of certain mycotoxins in food and feed EFSA J 12:3916. 107pp.

EFSA - European Food Safety Authority (2016) Appropriateness to set a group health-based guidance value for ZEN and its modified forms. EFSA J 14:4425. 46pp.

EFSA, 2019. Guidance on harmonised methodologies for human health, animal health and ecological risk assessment of combined exposure to multiple chemicals. EFSA Journal. 17: 5634, 77. https://doi.org/10.2903/j.efsa.2019.5634

El-Makawy A, Hassanane MS and Abd Alla ES, 2001. Genotoxic evaluation for the estrogenic mycotoxin zearalenone. Reproduction, Nutrition, Development, 41, 79-89.

Ferrer, E., Juan-García, A., Font, G., Ruiz, M.J., 2009. Reactive oxygen species induced by beauvericin, patulin and zearalenone in CHO-K1 cells. Toxicology In Vitro. 23, 1504–1509.

Föllmann W, Ali N, Blaszkewicz M, Degen G., 2016. Biomonitoring of mycotoxins in urine: pilot study in mill workers. J Toxicol Environ Health A 79:1015–1025.

Frizzell C., Uhlig S., Miles C.O., Verhaegen S., Elliott C.T., Eriksen G.S., Sorlie M., Ropstad E., Connolly L., 2015. Biotransformation of zearalenone and zearalenols to their major glucuronide metabolites reduces estrogenic activity. Toxicol in Vitro 29:575–581.

Frizzell, C., Ndossi, D., Verhaegen, S., Dahl, E., Eriksen, G., Sørlie, M., Connolly, L., 2011. Endocrine disrupting effects of zearalenone, alpha- and beta-zearalenol at the level of nuclear receptor binding and steroidogenesis. Toxicology Letters, 206(2), 210–217.

Fu, Y., Jin, Y., Y.Z., Shan, A., Fang, H., Shen, J., Zhou, C., Yu, H., Zhou, Y.F., Wang, X., Wang, J., Li, R., Wang, R., Zhang, J., 2019. Zearalenone induces apoptosis in bovine mammary epithelial cells by activating endoplasmic reticulum stress. Journal of Dairy Science. 102, 10543-10553.

Gazzah AC, Bennour EE, Bouaziz C, Abid S, Ladjimi M and Bacha H, 2010. Sequential events of apoptosis induced by zearalenone in cultured hepatocarcinoma cells. Mycotoxin Research, 26, 187-197.

Gerding J, Ali N, Schwartzbord J, Cramer B, Brown DL, Degen GH, Humpf HU., 2015. A comparative study of the human urinary mycotoxin excretion patterns in Bangladesh, Germany, and Haiti using a rapid and sensitive LC-MS/MS approach. Mycotoxin Res, 31:127–136.

Grassi D., Bellini M.J., Acaz-Fonseca E., Panzica G., Garcia-Segura L.M., 2013. Estradiol and testosterone regulate arginine-vasopressin expression in SH-SY5Y human female neuroblastoma cells through estrogen receptors-α and-β Endocrinology, 154, 2092-2100.

He, P., Li, Z., Xu, F., Ru, G., Huang, Y., Lin, E., Peng, S., 2020. AMPK Activity Contributes to G2 Arrest and DNA Damage Decrease via p53/p21 Pathways in Oxidatively Damaged Mouse Zygotes. Frontiers in Cell and Developmental Biology. 8:539485.

IARC (International Agency for Research on Cancer), 1993. IARC Monographs on the Evaluation of the Carcinogenic Risk of Chemicals to Humans, Vol. 56, Some Naturally Occurring Substances: Heterocyclic Aromatic Amines and Mycotoxins, Lyon. 39-444.

Jia, J., Wang, Q., Wud, H., Xiaa, Sh., Guoa, H., Blaženovićc, I., Zhanga, Y., Suna, X., 2019. Insights into cellular metabolic pathways of the combined toxicity responses of Caco-2 cells exposed to deoxynivalenol, zearalenone and Aflatoxin B1. Food and Chemical Toxicology. 126, 106-112.

Juan-García, A., Juan, C., König, S., Ruiza, M.J., 2015. Cytotoxic effects and degradation products of three mycotoxins: Alternariol, 3-acetyl-deoxynivalenol and 15-acetyl-deoxynivalenol in liver hepatocelular carcinoma cells. Toxicology Letters. 235, 8–16.

Juan-García, A., Tolosa, J., Juan, C., Ruiz, M.J., 2019. Cytotoxicity, genotoxicity and disturbance of cell cycle in HepG2 cells exposed to OTA and BEA: single and combined actions. Toxins, 11, 341.

Kastan, M.B., Onyekwere, O., Sidransky, D., Vogelstein, B., Craig, R.W., 1991., Participation of p53 protein in the cellular response to DNA damage. Cancer Research, 51:6304–6311.

Kono, N.S., Fridovich, I., 1982. Superoxide radical inhibits catalase. Journal of Biological Chemistry, 257, 5751-5754.

Kowalska, K., Habrowska-Gorczynska, D.E., Dominska, K., Urbanek, K.A., Piastowska-Ciesielska, A.W., 2020. ER Beta and NF Kappa B-Modulators of Zearalenone-Induced Oxidative Stress in Human Prostate Cancer Cells. Toxins, 12(3), 199.

Krishnaswamy, R., Devaraj, S.N., Padma, V.V., 2010. Lutein protects HT-29 cells against Deoxynivalenol-induced oxidative stress and apoptosis: prevention of NF-kappaB nuclear localization and down regulation of NF-kappaB and Cyclo-Oxygenase-2 expression. Free Radical Biology and Medicine, 49, 50-60.

Le Guevel, R., Pakdel, F., 2001. Assessment of oestrogenic potency of chemicals used as growth promoter by in-vitro methods. Human Reproduction. 16, 1030–1036.

Li, G.Y., Xie, P., Li, H.Y., Hao, L., Xiong, Q., Qiu, T., 2011. Involment of p53, Bax, and Bcl-2 pathway in microcystins-induced apoptosis in rat testis. Environmental Toxicology. 26,111–117.

Li, Q., Zhang, Zh., Lin, P., Lei, L., 2015. Endoplasmic Reticulum Stress Cooperates in Zearalenone-Induced Cell Death of RAW 264.7 Macrophages. International journal of molecular sciences. 16(8), 19780–19795.

Linke, S.P., Clarkin, K.C., Di Leonardo, A., Tsou, A., Wahl, G.M., 1996. A reversible, p53-dependent G0/G1 cell cycle arrest induced by ribonucleotide depletion in the absence of detectable DNA damage. Genes & Development, 10:934–947.

Lu, J., Yu, J.Y., Lim, Sh.S., Son, Y.O., Kim, D.H., Lee, S.A., hi, X., Lee, J.Ch., 2013. Cellular mechanisms of the cytotoxic effects of the zearalenone metabolites α-zearalenol and β-zearalenol on RAW264.7 macrophages. Toxicology in Vitro, 27(3), 1007-1017.

Mallebrera, B., Font, G., Ruiz, M.J., 2014. Disturbance of antioxidant capacity produced by beauvericin in CHO-K1 cells. Toxicology Letters. 226, 337-342.

Mallebrera, B., Juan-Garcia, A., Font, G., Ruiz, M.J., 2016. Mechanisms of beauvericin toxicity and antioxidant cellular defense. Toxicology Letters, 246, 28-34.

Mannani, N., Tabarani, A., Abdennebi, E. H., and Zinedine, A. (2019). Assessment of aflatoxin levels in herbal green tea available on the Moroccan market. Food Control, 108:e106882.

Marin, D. E., Pistol, G. C., Bulgaru, C. V., Taranu, I., 2019. Cytotoxic and inflammatory effects of individual and combined exposure of HepG2 cells to zearalenone and its metabolites. Naunyn-Schmiedeberg's Archives of Pharmacology. 392, 937–947.

Merry, D.E and Korsmeyer, S.J., 1997. Bcl-2 gene family in the nervous system. Annual Review of Neuroscience, 20: 245-267.

Metzler, M., Pfeiffer, E., Hildebrand, A.A., 2010. Zearalenone and its metabolites as endocrine disrupting chemicals. World Mycotoxin Journal. 3, 385-401.

Michiels, C., Raes, M., Toussaint, O., Remacle, J., 1994. Importance of Se-glutathione peroxidase, catalase and Cu/Zn–SOD for cell survival against oxidative stress. Free Radical Biology and Medicine, 17, 235-248.

Organisation for Economic Co-operation and Development (OECD). 2011. In Environment, Health and Safety News: The OECD Environment, Health and Safety Programme: Achievements, no. 27 on December 2011, [online: http://www.oecd.org/env/chemicalsafetyandbiosafety/49171557.pdf]

Othmen ZO, Golli EE, Abid-Essefi S, Bacha H. 2008 Cytotoxicity effects induced by Zearalenone metabolites, alpha Zearalenol and beta Zearalenol, on cultured Vero cells. Toxicology, 252, 72-77.

Ouanes Z, Abid S, Ayed I, Anane R, Mobio T, Creppy EE and Bacha H, 2003. Induction of micronuclei by Zearalenone in Vero monkey kidney cells and in bone marrow cells of mice: protective effect of Vitamin E. Mutation Research, 538, 63-70.

Ouanes Z, Ayed-Boussema I, Baati T, Creppy EE and Bacha H, 2005. Zearalenone induces chromosome aberrations in mouse bone marrow: preventive effect of 17beta-estradiol, progesterone and Vitamin E. Mutation Research, 565, 139-149.

Pfeiffer E, Kommer A, Dempe JS, Hildebrand AA, Metzler M. 2011 Absorption and metabolism of the mycotoxin zearalenone and the growth promotor zeranol in Caco-2 cells in vitro. Mol Nutr Food Res 55:560–567

Pigeolet, E., Corbisier, P., Houbion, A., Lambert, D., Michiels, C., Raes, M., Zachary, M.D., Remacle, J., 1990. Glutathione peroxidase, superoxide dismutase, and catalase inactivation by peroxide and oxygen derived free radical. Mechanism of Ageing and Development, 51, 283-297.

Plasencia J, Mirocha CJ. 1991 Isolation and characterization of zearalenone sulfate produced by Fusarium spp. Appl Environ Microbiol 57, 146–150.

Prosperini, A., Juan-García, A., Font, G., Ruiz, M. J., 2013. Beauvericin-induced cytotoxicity via ROS production and mitochondrial damage in Caco-2 cells. Toxicology Letters. 222(2), 204–211.

Ranzenigo, G., Caloni, F., Cremonesi, F., Y.Aad, P., J.Spicer, L., 2008. Effects of Fusarium mycotoxins on steroid production by porcine granulosa cells. Animal Reproduction Science. 107, 115-130.

Riedl, S.J., and. Salvesen, G.S., 2007. The apoptosome: Signalling platform of cell death. Nature reviews molecular cell biology. 8, 405–413.

Rudik, A.V., Bezhentsev, V.M., Dmitriev, A. V., Druzhilovskiy, D.S., Lagunin, A.A, Filimonov, D.A., Poroikov V.V.2017. MetaTox: Web Application for Predicting Structure and Toxicity of Xenobiotics' Metabolites. J. Chem. Inf. Model. 57, 638−642.

Shephard GS, Burger HM, Gambacorta L, Gong YY, Krska R, Rheeder JP, Solfrizzo M, Srey C, Sulyok M, Visconti A, Warth B, van der Westhuizen L (2013) Multiple mycotoxin exposure determined by urinary biomarkers in rural subsistence farmers in the former Transkei, South Africa. Food Chem Toxicol 62:217–225.

Sudo, K., Dao, C.V., Atsushi, M., Mitsuya, Sh., 2019. Comparative analysis of in vitro neurotoxicity of methylmercury, mercury, cadmium, and hydrogen peroxide on SH-SY5Y cells. Journal of Veterinary Medical Science, 81(6) 828-837.

Tatay, E., Espin, S., Garcia-Fernandez, A.J., Ruiz, M.J., 2017. Oxidative damage and disturbance of antioxidant capacity by zearalenone and its metabolites in human cells. Toxicology In Vitro, 45, 334-339.

Tatay, E., Font, G and Ruiz, M.J., 2016. Cytotoxic effects of zearalenone and its metabolites and antioxidant cell defense in CHO-K1 cells. Food and Chemical Toxicology. 96, 43-49.

Tatay, E., Meca, G., Font, G., Ruiz, M.J., 2014. Interactive effects of zearalenone and its metabolites on cytotoxicity and metabolization in ovarian CHO-K1 cells. Toxicology in Vitro. 28, 95-103.

Venkataramana, M., Chandra Nayaka, S., Anand, T., Rajesh, R., Aiyaz, M., Divakara, S.T., Murali, H.S., Prakash, H.S., Lakshmana Rao, P.V., 2014. Zearalenone induced toxicity in SHSY-5Y cells: The role of oxidative stress evidenced by N-acetyl cysteine. Food and Chemical Toxicology. 65, 335-342.

Wallin S, Gambacorta L, Kotova N, Lemming EW, Nalsen C, Solfrizzo M, Olsen M (2015). Biomonitoring of concurrent mycotoxin exposure among adults in Sweden through urinary multi-biomarker analysis. Food Chem Toxicol 83, 133–139.

Wang, X., Yu, H., Fang, H., Zhao, Y., Jin, Y., Shen, J., Zhou, Ch., Zhou, Y., Fu, Y., Wang, J., Zhang, J., 2019. Transcriptional profiling of zearalenone-induced inhibition of IPEC-J2 cell proliferation. Toxicon, 172, 8-14.

Wätjen, W., Debbab, A., Hohlfeld, A., Chovolou, Y., Proksch, P., 2014. The mycotoxin beauvericin induces apoptotic cell death in H4IIE hepatoma cells accompanied by an inhibition of NF-κB-activity and modulation of MAP-kinases, Toxicology Letters, 231(1), 9-16.

Weydert, Ch.J., Waugh, T.A., Ritchie, J.M., Kanchan, S.I., Smith, J.L., Ling, L., Spitz, D.R., Oberley, L.W., 2006. Overexpression of manganese or copper-zinc superoxide dismutase inhibits breast cancer growth. Free Radical Biology and Medicine, 41, 226-237.

Wolf, B.B and Green, D.R., 1999. Suicidal tendencies: apoptotic cell death by caspase family proteinases. Journal of Biological Chemistry, 274: 20049-20052.

Xiao Z., Huang C., Wu J., Sun L., Hao W., Leung L.K., Huang J.., 2013. The neuroprotective effects of ipriflavone against H_2O_2 and amyloid beta induced toxicity in human neuroblastoma SH-SY5Y cells European journal of pharmacology, 721, 286-293.

Zhang, R.Q., Sun, X.F., Wu, R.Y., Cheng, Sh.F., Zhang, G.L., Zhai, Q.Y., Liu, X.L., Zhao, Y., Shen, W., Li, L., 2018. Zearalenone exposure elevated the expression of tumorigenesis genes in mouse ovarian granulosa cells. Toxicology and Applied Pharmacology, 356, 191-203.

Zheng, N., Gao, Y.N., Liu, J., Wang, H.W., Wang, J. Q., 2018. Individual and combined cytotoxicity assessment of zearalenone with ochratoxin A or α-zearalenol by full factorial design. Food Science Biotechnology. 27, 251–259.

Zheng, W.L., Wang, B.J., Wang, L., Shan, Y.P., Zou, H., Song, R.L., Wang, T., Gu, J.H., Yuan, Y., Liu, X.Z., Zhu, G.Q., Bai, J.F., Liu, Z.P., Bian, J.C., 2018. ROS-Mediated Cell Cycle Arrest and Apoptosis Induced by Zearalenone in Mouse Sertoli Cells via ER Stress and the ATP/AMPK Pathway. Toxins, 10, 24.

Zhu, L., Yuan, H., Guo, C., Lu, Y., Deng, S., Yang, Y., Wei, Q., Wen, L., He Z., 2012. Zearalenone induces apoptosis and necrosis in porcine granulosa

cells via a caspase-3- and caspase-9-dependent mitochondrial signaling pathway. Journal of Cellular Physiology. 227, 1814-1820.

Zingales, V., Fernández-Franzón, M., Ruiz, M.J., 2020. Sterigmatocystin-induced cytotoxicity via oxidative stress induction in human neuroblastoma cells. Food and Chemical Toxicology. 136, 110956.

Zouaoui, N., Mallebrera, B., Berrada, H., Abid-Essefi, S., Bacha, H., Ruiz, M.-J., 2016. Cytotoxic effects induced by patulin, sterigmatocystin and beauvericin on CHO–K1 cells. Food and Chemical Toxicology. 89, 92–103.

5. CONCLUSIONES

5. CONCLUSIONES

1. El estudio *in silico* de las micotoxinas ZEA, α-ZEL y β-ZEL reveló que el perfil metabolómico se describe con productos de reacciones de biotransformación de O-glucuronidación, S-sulfatación e hidrólisis; los cuales tienen mejores propiedades para alcanzar la BBB que las micotoxinas iniciales.

2. La predicción del efecto tóxico del perfil metabolómico descrito *in silico* para ZEA, α-ZEL y β-ZEL fue el de carcinogenicidad mientras que el efecto de inhibición e inducción enzimática varió en función del sustrato y para cada compuesto.

3. La metodología *in silico* ofrece una visión excelente previa al inicio de ensayos *in vitro* o *in vivo* contribuyendo al principio de las 3Rs además de ser una herramienta interesante que ayuda a predecir la alteración de sistemas/vías/mecanismos de moléculas pequeñas.

4. El estudio citotóxico de α-ZEL, β-ZEL y BEA individualmente y combinado en células indiferenciadas SH-SY5Y, mostró que β-ZEL individualmente y las combinaciones α-ZEL + β-ZEL + BEA y α-ZEL + BEA presentaban la mayor potencialidad tóxica. Los valores de IC_{50} oscilaron entre 95 y 0.2 μM para las micotoxinas estudiadas, el efecto potencial en la exposición combinada fue sinergismo para todos los escenarios estudiados y las combinaciones.
5. Las recuperaciones de α-ZEL, β-ZEL y BEA en los medios de cultivo celular de las células SH-SY5Y por LC-qTOF-MS y la contribución a los efectos observados en los ensayos de citotoxicidad, revelaron que los

porcentajes más altos en los tratamientos individuales fue para BEA (> 50%). En los tratamientos combinados, las recuperaciones en i) α-ZEL + BEA fueron mayores para α-ZEL que para BEA; ii) β-ZEL + BEA mayor para BEA que para β-ZEL; iii) α-ZEL + β-ZEL las recuperaciones fueron similares para ambas micotoxinas y en iv) la combinación terciaria, todas las recuperaciones permanecieron por debajo del 50%. Cabe destacar que la combinación β-ZEL + BEA fue para la que se obtuvieron mayores recuperaciones.

6. Los resultados del estrés oxidativo en las células SH-SY5Y expuestas a α-ZEL, β-ZEL y BEA revelaron niveles elevados de ROS en combinaciones en las que participaba α-ZEL (de 2.8 a 8 veces en comparación con el control); sin embargo, no se detectaron diferencias significativas en los niveles de ROS cuando se ensayó en tratamientos individuales de una sola micotoxina.

7. La evaluación del sistema de defensa enzimático y no enzimático en células SH-SY5Y para α-ZEL, β-ZEL y BEA, reveló aumentos significativos a las 24 h i) en la relación GSH/GSSG para todas las concentraciones ensayadas; ii) en GPx hasta 24 veces en tratamientos individuales y 15 veces en combinaciones binarias y iii) en GST hasta 10 veces en tratamientos combinados. Por otro lado, a 48 h, la SOD aumentó entre 3.5 y 5 veces en el tratamiento individual y combinado, respectivamente. Contrario a esto, la actividad CAT disminuyó significativamente en todos los tratamientos hasta un 92% después de 24 h excepto para β-ZEL + BEA que reveló un aumento.

8. Los resultados obtenidos por expresión génica implicada en apoptosis y receptores de estrógenos por RT-PCR en células SH-SY5Y expuestas a α-ZEL, β-ZEL y BEA de forma individual y combinada, revelaron que α-ZEL indujo la sobrerregulación de *CASP3* y *BAX*; mientras que se observó una regulación a la baja para los genes *CASP3* y *BCL2* por β-ZEL y de *BCL2* por BEA. Además, β-ZEL + BEA fue el único tratamiento de combinación que pudo regular a la baja los niveles de expresión génica de apoptosis celular (*CASP3, BAX* y *BCL2*).

9. El efecto en el ciclo celular de α-ZEL, β-ZEL y BEA en las células SH-SY5Y se alteró notablemente en todos los tratamientos en los que β-ZEL participó (β-ZEL, β-ZEL + BEA y β-ZEL + α-ZEL) por una interrupción en la fase G0/G1 (hasta un 43,6%) una disminución en la proliferación celular en las fases S y G2/M (hasta un 19,6%). De forma similar, para la muerte celular entre tratamientos individuales, β-ZEL mostró un crecimiento significativo en la población de células apoptóticas tempranas a la concentración más alta ensayada, así como para todos los tratamientos de combinación en los que participó β-ZEL, en las vías de muerte celular tanto apoptótica temprana como apoptótica/necrótica.

10. Confiando en nuestros resultados, α-ZEL, β-ZEL y BEA, inducen daño en las células SH-SY5Y elevando los niveles de estrés oxidativo, alterando el papel de la actividad antioxidante del sistema glutatión y finalmente, causando desorden en las expresiones y actividades de la célula apoptótica relacionada genes de muerte celular.

5. CONCLUSIONS

1. *In silico* study of ZEA, α-ZEL and β-ZEL revealed that the metabolomic profile was described with products from O-glucuronidation, S-sulfation and hydrolysis all from biotransformation reactions and with better properties to reach the BBB than initial mycotoxins.

2. Prediction of toxic effect from metabolomics profile described *in silico* for ZEA, α-ZEL and β-ZEL was carcinogenicity while enzymatic effect of inhibition, induction and substrate function varied for each compound systems.

3. *In silico* methodology gives an excellent sight before starting *in vitro* or *in vivo* assays contributing to 3Rs principle and it is an interesting tool that helps to predict alteration of systems/pathways/mechanisms of small molecules.

4. Cytotoxic study of α-ZEL, β-ZEL and BEA individually and combined in SH-SY5Y cells showed that β-ZEL individually and in combinations α-ZEL + β-ZEL + BEA and α-ZEL + BEA presented the highest cytotoxicological potency. IC_{50} values ranged from 95 to 0.2 μM, the potential effect in combination exposure was synergism for all scenarios assayed and combinations.

5. Recoveries of α-ZEL, β-ZEL and BEA in the cell culture media of SH-SY5Y cells by LC-qTOF-MS and contribution to the effects observed in cytotoxicity assays, revealed the highest percentages in individual treatments for BEA (>50%). In combined treatments the recoveries i) in α-ZEL + BEA were higher for α-ZEL than for BEA; ii) in β-ZEL +

BEA higher for BEA than for β-ZEL; iii) in α-ZEL + β-ZEL recoveries were similar for both mycotoxins and iv) in tertiary all remained below 50%. Nevertheless, β-ZEL + BEA was the combination with the highest recoveries.

6. Results of oxidative stress in SH-SY5Y cells exposed to α-ZEL, β-ZEL and BEA revealed elevated ROS levels in combinations where α-ZEL was involved (2.8- to 8-fold compared to control); however, no significant difference in ROS levels were detected when single mycotoxin was tested.

7. Evaluation of enzymatic and non-enzymatic defence system in SH-SY5Y cells for α-ZEL, β-ZEL and BEA revealed significant increases at 24h i) in GSH/GSSG ratio at all concentrations tested; ii) in GPx up to 24-fold in individual treatments and 15-fold in binary combination and iii) in GST up to 10-fold in combination treatments. On the other hand, after 48h SOD increased up to 3.5- and 5-fold in individual and combined treatment, respectively. In contrary, CAT activity decreased significantly in all treatments up to 92% after 24 h except for β-ZEL + BEA, which revealed an increase.

8. Results obtained by gene expression involved in apoptosis and receptors of estrogens by RT-PCR in SH-SY5Y cells exposed to α-ZEL, β-ZEL and BEA individually and combined revealed that α-ZEL induced the up-regulation of *CASP3* and *BAX*; while a down-regulation was observed for *CASP3* and *BCL2* genes by β-ZEL and of *BCL2* by BEA. Moreover, β-ZEL + BEA was the only combination treatment which

was able to down regulate the levels of cell apoptosis gene expression (*CASP3, BAX* and *BCL2*).

9. Effect in cell cycle by α-ZEL, β-ZEL and BEA in SH-SY5Y cells was markedly altered in all treatments where β-ZEL engaged (β-ZEL, β-ZEL + BEA and β-ZEL + α-ZEL) by arresting cells in G0/G1 phase (up to 43.6%) and decreasing cell proliferation in S and G2/M phases (up to 19.6%). Similarly, for cell death among individual treatments β-ZEL showed a significant growth in early apoptotic cells population at highest concentration assayed as well as for all combination treatments where β-ZEL was involved, in both early apoptotic and apoptotic/necrotic cell death pathways.

10. Relying to our findings, α-ZEL, β-ZEL and BEA, induce injury in SH-SY5Y cells elevating oxidative stress levels, disturbing the antioxidant activity role of glutathione system and finally, causing disorder in the expressions and activities of the related apoptotic cell death genes.

ANNEXO

Food and Chemical Toxicology 146 (2020) 111818

Contents lists available at ScienceDirect

Food and Chemical Toxicology

journal homepage: www.elsevier.com/locate/foodchemtox

In silico methods for metabolomic and toxicity prediction of zearalenone, α-zearalenone and β-zearalenone

Fojan Agahi, Cristina Juan *, Guillermina Font, Ana Juan-García

Laboratory of Food Chemistry and Toxicology, Faculty of Pharmacy, University of Valencia, Av. Vicent Andrés Estellés s/n, 46100, Burjassot, València, Spain

ARTICLE INFO

Keywords:
Zearalenone
Metabolomics
Prediction
SwissADME
PASS online
MetaTox
In silico

ABSTRACT

Zearalenone (ZEA), α-zearalenol (α-ZEL) and β-zearalenol (β-ZEL) (ZEA's metabolites) are co/present in cereals, fruits or their products. All three with other compounds, constitute a cocktail-mixture that consumers (and also animals) are exposed and never entirely evaluated, nor *in vitro* nor *in vivo*. Effect of ZEA has been correlated to endocrine disruptor alterations as well as its metabolites (α-ZEL and β-ZEL); however, toxic effects associated to metabolites generated once ingested are unknown and difficult to study. The present study defines the metabolomics profile of all three mycotoxins (ZEA, α-ZEL and β-ZEL) and explores the prediction of their toxic effects proposing an *in silico* workflow by using three programs of predictions: MetaTox, SwissADME and PASS online. Metabolomic profile was also defined and toxic effect evaluated for all metabolite products from Phase I and II reaction (a total of 15 compounds). Results revealed that products describing metabolomics profile were: from O-glucuronidation (1z and 2z for ZEA and 1 ab, 2 ab and 3 ab for ZEA's metabolites), S-sulfation (3z and 4z for ZEA and 4 ab, 5 ab and 6 ab for ZEA's metabolites) and hydrolysis (5z and 7 ab for ZEA's metabolites, respectively). Lipinsky's rule-of-five was followed by all compounds except those coming from O-glucuronidation (HBA>10). Metabolite products had better properties to reach blood brain barrier than initial mycotoxins. According to *Pa* values (probability of activation) order of toxic effects studied was carcinogenicity > nephrotoxic > hepatotoxic > endocrine disruptor > mutagenic (AMES TEST) > genotoxic. Prediction of inhibition, induction and substrate function on different isoforms of Cytochrome P450 (CYP1A1, CYP1A2, CYP2C9 and CYP3A4) varied for each compounds analyzed; similarly, for activation of caspases 3 and 8. Relying to our findings, the metabolomics profile of ZEA, α-ZEL and β-ZEL analyzed by *in silico* programs predicts alteration of systems/pathways/mechanisms that ends up causing several toxic effects, giving an excellent sight and direct studies before starting *in vitro* or *in vivo* assays contributing to 3Rs principle; however, confirmation can be only demonstrated by performing those assays.

1. Introduction

Mycotoxins are low-molecular-weight toxic compounds synthetized by different types of molds belonging mainly to the genera *Aspergillus, Penicillium, Fusarium* and *Alternaria* (Berthiller et al., 2013; Juan et al., 2020; Pascari et al., 2019). Effects associated are diverse according to the chemical structure which provides a great variety in ADME/T characteristics (absorption, distribution, metabolism, and excretion/toxicity) and still to elucidate for most of them.

Zearalenone (ZEA) is a *Fusarium* mycotoxin of primary concern. It is commonly found in cereals like barley, sorghum, oats, wheat, millet, and rice (Juan et al., 2017a, 2017b; Stanciu et al., 2017; Bakker et al., 2018; Oueslati et al., 2020). When ingested and metabolized, two major metabolites, α-zearalenol (α-ZEL) and β-zearalenol (β-ZEL), can be found in various tissues; nonetheless, their presence is starting to be commonly found in food and feed as natural contaminants (EFSA et al., 2011, 2017). Once ingested by the consumer, further metabolite products from all three mycotoxins (ZEA, α-ZEL and β-ZEL) can be generated by Phase I and II reactions, although their effect is unknown. Studies of these compounds contribute to metabolomics profile for following the compound transformation (metabolic changes) whose identification and quantification will help to elucidate the complete toxic effects. It can help to understand global metabolic disturbances.

Effects associated to ZEA, α-ZEL and β-ZEL have been studied *in vitro* and *in vivo* and estrogenic effect, oxidative stress, cytotoxicity, DNA damage, among others have been reported (Eze et al., 2019; Frizzell

* Corresponding author.
E-mail address: cristina.juan@uv.es (C. Juan).

https://doi.org/10.1016/j.fct.2020.111818
Received 16 September 2020; Received in revised form 8 October 2020; Accepted 13 October 2020
Available online 21 October 2020

et al., 2011; Agahi et al., 2020; Juan-García et al., 2020). On the other hand, the entire implication of these compounds in producing toxic effects are unknown, same as with its metabolite products originated in Phase I and II reactions. So that, there are many indirect or side effects associated yet not studied and their involvement in pathways, cascade or routes still need to be discovered. Nowadays, the development of computational and informatics programs facilitates to predict experimental approaches in toxicology which need to be confirmed with further assays. These systems use chemical structures, parameters and descriptors which by comparison with other studied compounds, can give as a result empirical knowledge of their effect to prevent against exposure or even to promote the development of therapeutics to avoid or decrease toxic effects, concerning drugs.

Combination of compounds is a routine practice in medicine for palliate diseases achieving successful results. Previous to this practice it is necessary to evaluate the potential effects that this might cause. For toxic compounds there have been developed several mathematical methods implemented in informatics programs for assessing the effect of compounds combination and effects contributing to computational toxicology: Chou and Talalay by using isobolograms, Simple Addition of Effect, Factorial Analysis of Variance by using simple 2-way ANOVA, Bliss Independence Criterion, Loewe's Additivity Law, Highest Single Agent (HSA) Model (Gaddums non-interaction), etc. (Kifer et al., 2020). For mycotoxins' mixture assessment, Choy and Talalay method has been widely used in predicting potential effects (synergism, addition and antagonism) (Juan-García et al, 2016, 2019a, 2019b; Agahi et al., 2020) even with strong differences in chemical structures as well as in the variety of fungi *spp*. producer.

The global research scenario for new therapies and development of new drugs for common diseases, or as it is happening nowadays in the global world pandemic SARS-COVID-19 for health side-effects, the use of virtual screening techniques for helping in the discovery of new strategies and without using or avoiding long-term biological assays, is a good alternative. All these strategies end-up in exploring profile of effects by application of computer programs. One of this alternative programs is PASS online (Prediction of Activity Spectra for Substances) an *in silico* approach that reveals biological activities of compounds, their mechanisms of action and connected side-effects (Lagunin et al., 2000). The available PASS online version predicts over 4000 kinds of biological activity, including pharmacological effects, mechanisms of action, toxic and adverse effects, interaction with metabolic enzymes and transporters, influence on gene expression, etc. as described on its web page (www.pharmaexpert.ru/passonline) (Lagunin et al., 2000). Prediction is based on the analysis of structure activity-relationships for more than 250,000 biologically active substances including drugs, drug-candidates, leads and toxic compounds (Lagunin et al., 2000).

The support of new compounds discoveries and knowledge of its toxicity is given by other on-line programs which work with different parameters, some of them are: SwissADME, Meta-Tox, GUSAR, ROSC-Pred, etc. Each program is focused in providing different predictions, and for example while MetaTox predicts the Phase I and II metabolite products that can be generated from one compound (Rudik et al., 2017), SwissADME is a computational program that allows to compute physicochemical descriptors as well as ADME parameters, pharmacokinetic properties, drug-like nature and medicinal chemistry friendliness of one or multiple small molecules (Daina et al., 2017).

To escape long-term biological assays and implementing the computational programs for testing compounds and their predicted metabolites, here it is presented an *in silico* working procedure and the prediction of the entire potential effects of three mycotoxins (zearalenone (ZEA), α-zearalenol (α-ZEL) and β-zearalenol (β-ZEL)) and its Phase I and II metabolite products, by using three *in silico* programs described for computational toxicology: MetaTox, SwissADME and PASS online; all available on-line.

2. Materials and methods

Mycotoxins herein studied for this predictive *in silico* study displayed endocrine disruptor effects associated and correspond to: zearalenone (ZEA) (MW: 318,37 g/mol), α-zearalenol (α-ZEL) and β-zearalenol (β-ZEL) (MW: 320,38 g/mol) (Fig. 1).

2.1. Procedure followed (workflow)

Firstly, prediction of Phase I and II metabolites products was obtained by MetaTox software (http://way2drug.com/mg2/) with a molecular sketcher based on Marvin JS chemical editor. This editor is used for input and visualization of molecular structure (in canonical SMILE) of each mycotoxin, obtaining a metabolomic profile. "No-limit" in metabolite likeness and "all" reactions in predicting metabolites for drawn structure were selected (Rudik et al., 2017). Secondly, all compounds predicted from reactions and mycotoxins were evaluated through i)SwissADME by obtaining physicochemical descriptors (http://www.swissadme.ch/index.php) (Daina et al., 2017; Cheng et al., 2012; Yang et al., 2018) and following the Lipinski's rule of five (RO5) (see section 2.2. below) and ii)SwissSimilarity which provides an identification number HMDB (Human Metabolome Database version 4.0, https://hmdb.ca/) with a score associated (Zoete et al., 2016). Afterwards, all compounds were predicted as active compounds or inactive compounds according to probability of activation values (Pa) and probability of inactivation values (Pi), respectively; as well as their biological activities through PASS online software (http://www.pharmaexpert.ru/passonline/info.php) (Workflow 1). Lastly, potential toxic effects were predicted for Pa > Pi with PASS online software.

2.2. In silico software: MetaTox, SwissADME and PASS online

Three *in silico* softwares available online for studying prediction of toxicity and biological activities were used: MetaTox, SwissADME and PASS online.

MetaTox is a software based in generating metabolites and calculating probability of their formation where metabolism pathway generation is integrated with the prediction of acute toxicity. Metabolomics' profile is predicted by the formation from nine classes of reactions (aliphatic and aromatic hydroxylation, N and O-glucuronidation, N-, S- and C-oxidation, and N- and O-dealkylation) that are catalyzed by five human isoforms of cytochromes P450s (1A2, 2C19, 2C9, 2D6, 3A4) and by human UDP glucuronosyltransferase without differentiation into isoforms. The calculation of probability for generated metabolites is based on analyses of "structure-biotransformation reactions" and "structure-modified atoms" relationships using a Bayesian approach (Rudik et al., 2017).

SwissADME is a web tool that enables to predict the computation of key physicochemical properties, pharmacokinetics, mycotoxin-likeness and medicinal chemistry friendliness (for one or multiple molecules), (Daina et al., 2017; Cheng et al., 2012; Yang et al., 2018). This predictive *in silico* model shows statistical significance, predictive power, intuitive interpretation, and straight forward translation to molecular design. This program uses Lipinski's rule-of-five (RO5) for the lead compounds. The compounds were then filtered through that rule (RO5) to predict their mycotoxins likeliness. Lipinski's descriptors evaluate the molecular properties for compound pharmacokinetics in the human body, especially for oral absorption. The rule states molecules to have: molecular weight (MW) $\leq$500, number of hydrogen bond donors (HBD) $\leq$5, number of hydrogen bond acceptors (HBA) $\leq$10, cLogP $\leq$5 and number of rotable bounds (n-ROTB) $\leq$10. Molar reactivity in the range of 40–130 and topological polar surface area (TPSA) were also considered. Targets of p-glycoprotein (P-gp) efflux and isoforms of cytochrome P450 that metabolize the majority of toxic compounds (CYP3A4, CYP2C9, CYP2C19, CYP1A1 and CYP1A2) were investigated.

The biological prediction of activity spectra for mycotoxins and

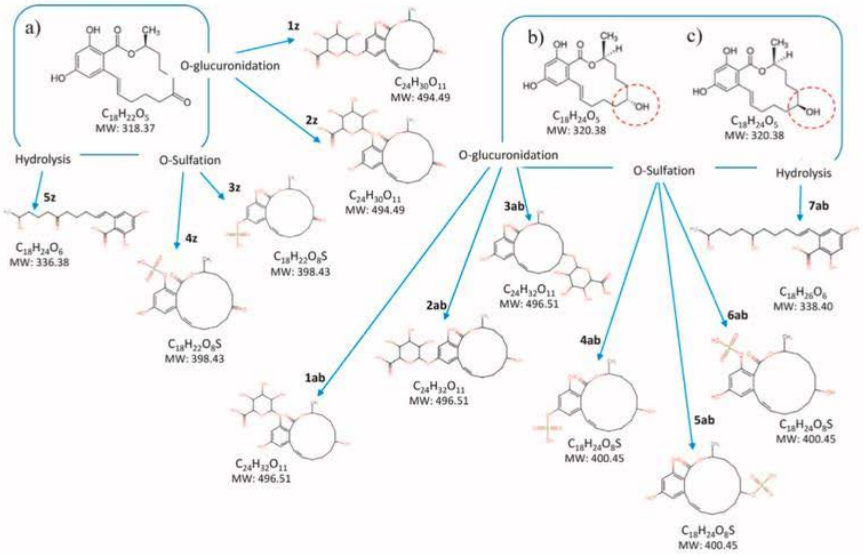

Fig. 1. Metabolomic profile and chemical structures of mycotoxins predicted by MetaTox: ZEA (a), α-ZEL (b) and β-ZEL (c).

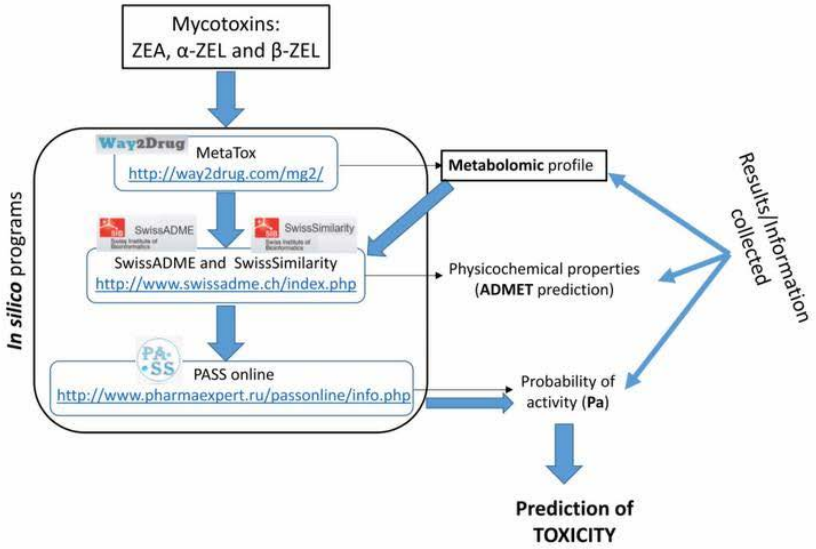

Workflow 1. Procedure followed to predict the toxic effect of mycotoxins and its metabolite products by using different in silico programs.

metabolite products were obtained by PASS online (available in www.pharmaexpert.ru/passonline) (Lagunin et al., 2000). This software was used to evaluate the general biological potential of all compounds and provided simultaneous prediction of several types of biological activity based on their chemical structure. It also estimated the predicted activity spectrum of mycotoxins as probable activity (Pa, probability to be active) and probable inactivity (Pi, probability to be inactive). Both probabilities, Pa and Pi values, vary from 0.000 to 1.000; nevertheless,

values are expressed as percentage of probability (%).

Among all toxic effects for all three mycotoxins and products of Phase I and II reactions provided from PASS, prediction was evaluated for: carcinogenesis, endocrine disruption, nephrotoxicity, mutagenicity (with and without AMES test), genotoxicity and hepatotoxicity. Biological activities prediction inhibiting, inducing or as substrate was evaluated for different isoforms of Cytochrome P450 and caspases 3 and 8. All predictions of probabilities were expressed as percentage of probability (%).

3. Results

3.1. Meta-Tox for predicting metabolite products: describing the metabolomics profile

Metabolite prediction included in MetaTox uses dictionaries of biotransformation based on preliminary prediction of possible classes of biotransformation describing also the metabolomics profile of the compounds. Mycotoxins' canonical SMILE structure were used to predict metabolite products in MetaTox. Fig. 1 collects chemical structure of mycotoxins and metabolite products predicted by MetaTox (five from ZEA (from 1z to 5z) and 7 for each ZEA's metabolite (from 1 ab to 7 ab)). Metabolite products predicted for ZEA were from: reaction of O-glucuronidation (metabolites 1z and 2z), reaction of S-sulfation (metabolites 3z and 4z) corresponding to Phase II products and one from reaction of hydrolysis (5z) corresponding to Phase I products. For α-ZEL and β-ZEL, products were equal for each one with a total of seven products for each isoform and corresponding to same reactions as ZEA: O-glucuronidation (metabolites: 1 ab, 2 ab and 3 ab), S-sulfation (metabolites: 4 ab, 5 ab and 6 ab) and hydrolysis (metabolite 7 ab) reactions. A total of 12 compounds were proposed as predicted metabolites products form Phase I and II reactions.

3.2. SwissADME for physicochemical descriptors of zearalenone, α-zearalenol, β-zearalenol and phase I and II metabolite products

Target of mycotoxins in organs and systems are wide and unknown for most of them; however, they are able to activate several routes or pathways. ZEA, α-ZEL and β-ZEL were analyzed through SwissADME online sever for molecular properties to validate them as potential inducers/activators of toxic mechanisms. All three mycotoxins were filtered through Lipinski's RO5 to predict their mycotoxin likeliness (Table 1). All three mycotoxins and metabolite products were studied and only metabolites coming from O-glucuronidation of ZEA (metabolites 1z and 2z) or α-ZEL and β-ZEL (metabolites 1 ab, 2 ab and 3 ab) violated Lipinski's rule because of HBA (hydrogen bond acceptor) (Table 1). It is also reported the human metabolome database identification number (HMDB ID) and the score of similarity predicted provided from SwissSimilarity. All compounds had one or more HMDB ID with score >50% (Table 1). To notice that values were the same for metabolite products coming from the same metabolization reaction.

Probability for ADMET and toxicity profile for all compounds was evaluated. Table 2 reports values for mycotoxins, while Table 3 for metabolite products of Phase I and II's reactions of all three mycotoxins. Results reveal that ZEA mycotoxin has very low prediction for BBB crossing (28.22%) and similar tendency was obtained for α-ZEL and

Table 2
Probability of ADMET and toxicity profile for ZEA, α-ZEL and β-ZEL.

	ZEA	α-ZEL and β-ZEL
	Probability (%)	Probability (%)
Absorption & Distribution		
BBB	28.22	31.47
HIA	97.61	97.50
P-gp substrate	85.50	84.12
Caco-2 permeability	48.84	59.94
LogPapp (cm/s)	−5.67	−5.39
Metabolism		
CYP450 2C9 substrate	57.95	60.44
CYP450 2D6 substrate	86.69	83.54
CYP450 3A4 substrate	55.40	57.08
CYP450 1A2 inhibitor	68.95	76.60
CYP450 2C9 inhibitor	84.90	89.37
CYP450 2D6 inhibitor	91.60	90.07
CYP450 2C19 inhibitor	75.95	72.46
CYP450 3A4 inhibitor	79.60	76.82
Toxicity		
AMES toxicity	90.0	85.00
Carcinogens	90.0	66.04
Rat acute toxicity (LD_{50}, mol/kg)	1.88	1.94

BBB: blood-brain barrier; HIA: human gastrointestinal absorption; P-gp: P-glycoprotein.

Table 1
Lipinski's molecular descriptors for ZEA, ZEA's metabolites (α-ZEL and β-ZEL) and its products of reaction (from O-glucuronidation, O-sulfation and hydrolysis) from SwissADME and SwissSimilarity.

	HMDB ID	MW(≤500)	HBD (≤5)	HBA(≤10)	cLog P (<5)	MR (≤10)	n-ROTB(≤10)	TPSA
ZEA	31,752 (99.6%)	318.37	2	5	3.58	88.40	0	83.83
O-Glucuronidation								
Metabolite 1z*	34,753 (74.1%)	494.49	5	11*	1.14	121.13	3	180.05
Metabolite 2z*	60,634 (84.3%)							
O-Sulfation								
Metabolite 3z	33,623 (99.6%)	398.43	2	8	3.06	98.60	2	135.58
Metabolite 4z	31,752 (87.6%)							
Hydrolysis								
Metabolite 5z	31,752 (52.4%)	336.38	4	6	3.10	92.16	10	115.06
α-ZEL and β-ZEL	41,838 (99.8%) 41,824 (99.7%)	320.38	3	5	3.37	89.36	0	86.99
O-Glucuronidation								
Metabolite 1 ab*	34,753 (86.8%)	496.51	6	11*	0.94	122.09	3	183.21
Metabolite 2 ab*	60,634 (75.6%)							
Metabolite 3 ab*	31,752 (53.9%)							
O-Sulfation								
Metabolite 4 ab	33,623 (91.5%)	400.45	3	8	2.85	99.56	2	138.74
Metabolite 5 ab	31,752 (90.4%)							
Metabolite 6 ab	41,838 (91.1%)							
Hydrolysis								
Metabolite 7 ab	41,824 (50.6%)	338.40	5	6	2.89	93.12	10	118.22

HMDB ID = Human Metabolome Database Identification; MW = Molecular weight; g/mol (acceptable range: <500); HBD = Hydrogen bond donor (acceptable range: ≤5); HBA = Hydrogen bond acceptor (acceptable range: ≤10); cLogP = High lipophilicity (expressed as LogP, acceptable range: <5); MR = Molar refractivity (acceptable range: 40–130); n-ROTB: number of rotatable bounds; TPSA = Topological polar surface area; Å2. *Denotes violation of Lipinski's RO5.

Table 3
Probability of ADMET and toxicity profile of products predicted by MetaTox from ZEA α-ZEL and β-ZEL.

	Metabolomic profile of ZEA					Metabolomic profile of α-ZEL and β-ZEL						
Reaction	O-Glucuronidation		S-Sulfation		Hydrolysis	O-Glucuronidation			S-Sulfation			Hydrolysis
Metabolites	1z	2z	3z	4z	5z	1 ab	2 ab	3 ab	4 ab	5 ab	6 ab	7 ab
Probability (Prob)	Prob (%)	Prob (%)	Prob (%)	Prob (%)	Prob (%)	Prob (%)	Prob (%)	Prob (%)	Prob (%)	Prob (%)	Prob (%)	Prob (%)
Absorption & Distribution												
BBB	37.65	37.65	97.05	97.05	79.17	31.47	50.00	37.65	97.00	97.04	97.00	79.17
HIA	72.33	70.65	95.94	96.20	96.75	97.50	68.84	71.40	95.72	96.97	95.90	97.43
P-gp substrate	89.04	78.58	82.69	75.15	75.38	84.12	78.48	80.17	81.59	80.54	73.72	73.06
Caco-2 permeability	81.87	87.20	76.48	80.89	62.41	59.94	86.25	86.09	66.51	55.72	70.99	61.16
LogPapp (cm/s)	−7.85	−8.24	−6.58	−6.97	−6.51	−7.96	−7.57	−7.42	−6.29	−6.14	−6.69	−6.16
Metabolism												
CYP450 2C9 substrate	100	100	79.13	59.58	59.92	60.44	79.88	80.22	58.95	61.28	61.74	61.90
CYP450 2D6 substrate	87.97	88.12	86.54	86.41	86.75	83.54	87.85	87.74	85.62	86.69	85.35	86.83
CYP450 3A4 substrate	63.85	64.20	60.69	61.92	50.71	57.08	64.36	63.41	62.04	60.19	63.23	51.50
CYP450 1A2 inhibitor	57.71		74.19		73.02	76.60	53.79	57.71	69.70	72.83	69.70	64.06
CYP450 2C9 inhibitor	92.01		82.74		84.24	89.37	92.95	92.01	82.61	81.81	82.61	79.70
CYP450 2D6 inhibitor	92.29		87.55		90.45	90.07	91.41	92.29	87.62	86.89	87.62	90.48
CYP450 2C19 inhibitor	74.09		77.83		82.96	72.46	79.05	74.09	75.21	76.29	75.21	74.04
CYP450 3A4 inhibitor	73.18		84.7		64.02	76.82	73.89	73.18	75.62	78.53	75.62	61.88
Toxicity												
AMES toxicity	68.00	66.00	73.00	66.00	79.00	85.00	67.00	70.00	68.79	76.79	60.79	74.00
Carcinogens	65.75	65.74	88.57	88.57	77.10	66.04	61.54	65.74	62.12	64.01	62.12	75.52
Rat acute toxicity (LD50, mol/kg)	2.65	2.22	2.50	2.03	2.36	1.94	2.36	2.45	2.77	2.37	2.3	2.27

BBB: blood-brain barrier; HIA: human gastrointestinal absorption; P-gp: P-glycoprotein.

β-ZEL (31.47%). However, high gastrointestinal absorption was reported for all three mycotoxins (HIA >97%, Caco-2 permeability >48% and P-glycoprotein substrate >84%) (Table 2). The results indicate moderate to high absorption by the gastrointestinal tract, but unlikely to penetrate into the brain on its current form unless metabolized (Table 3). Distribution (P-gp substrate) was favored with probability >84%. For metabolism prediction, several cytochrome P450 (CYP450) isoenzymes were evaluated showing similar pattern for all three mycotoxins. Probability of ZEA as substrate in CYP450 went from 55.40% (isoform 3A4) to 86.69% (isoform 2D6); while as inhibitor of CYP450 from 68.95% (isoform 1A2) to 91.60% (isoform 2D6). For α-ZEL and β-ZEL, as substrates of CYP450 probability went from 60.44% (isoform 2C9) to 83.54% (isoform 2D6); while as substrate from 72.46% (isoform 2C19) to 90.07% (isoform 2D6) (Table 2). For toxicity evaluation, ZEA reported higher values than α-ZEL and β-ZEL (Table 2).

For Phase I and II metabolite products of all three mycotoxins, ADMET probability values revealed that all 12 compounds (5 metabolite products from ZEA and 7 products from α-ZEL and β-ZEL) were able to pass the gastrointestinal tract (>70%), especially metabolite products originated in S-Sulfation and hydrolysis. Probability of BBB crossing was >95% for all same metabolites originated in same reaction mentioned above although quite low for O-glucuronidation metabolite products (<37%) (Table 3). Distribution (P-gp substrate) was favored for all compounds originated from all reactions (>73%). It is noticed that as long as the Phase I and II reactions take place, metabolite products become more suitable to reach BBB compartment (Table 3).

In metabolism, all ZEA's predicted products were substrate of CYP450 with probability from 100% (metabolites 1z and 2z) to 59.58% (metabolite 4z); while for α-ZEL and β-ZEL metabolites predicted products, it ranged from 51.5% (metabolite 7 ab) to 87.85% (metabolite 2 ab) (Table 3). Compounds were predicted as inhibitor for CYP450 with probabilities from 57.71% to 92.29% (metabolites 1z and 2z) for ZEA's predicted products; while from 53.79% (metabolite 2 ab) to 92.29% (metabolite 3 ab) for α-ZEL and β-ZEL's predicted products (Table 3). To notice that as inhibitors of CYP450 (for all five isoenzymes), ZEA's predicted products from O-glucuronidation (metabolites 1z and 2z) and S-sulfation (metabolites 3z and 4z) revealed the same probability; while this happened in α-ZEL and β-ZEL predicted products from S-sulfation (metabolites 4 ab and 6 ab) (Table 3).

Lastly in terms of toxicity evaluation, probability measured for AMES toxicity oscillated between 60.79% and 85% of no-AMES toxicity and carcinogenicity from 62.12 to 88.57%. Rat acute toxicity oscillated from 1.94 to 2.77 mol/kg.

3.3. Prediction of toxic effects by PASS online

Mycotoxins and products from metabolomics profile were studied by PASS online (Workflow 1). To validate them as suitable inducers/activator candidates, PASS online server was used which predicts possible effects of a compound based on its structural information. This tool compares more than 300 effects and biochemical mechanisms of compounds and gives the probability of activity (Pa) and inactivity (Pi) (Hasan et al., 2019).

Fig. 2 shows the probability for seven different toxic effects: carcinogenicity, endocrine disruptor, nephrotoxic, mutagenicity (and AMES test), genotoxicity and hepatotoxicity. It can be observed that ZEA had the highest probability in reporting carcinogenicity (78.2%); while α-ZEL and β-ZEL in genotoxicity (88.4%) (Fig. 2A). Among toxic effects studied, for all metabolite products (5 from ZEA and 7 from α-ZEL and β-ZEL), carcinogenicity reported the highest probability for all three mycotoxins followed by nephrotoxic > hepatotoxic > endocrine disruptor > mutagenic (AMES TEST) > genotoxic (Fig. 2B). Nonetheless, metabolite products from ZEA mycotoxin had the broadest range of probability in all toxic effects studied. Details of toxic effects per metabolite product from Phase I and II reactions are reported in Supplementary 1. Regarding the carcinogenicity effect predictions in rat and mouse (male and female), and the IARC classification is reported in Supplementary 2.

3.4. Prediction of biological activities by PASS online

Biological activities predicted by PASS online are reported in Figs. 3 and 4. It has been divided in one hand the most common isoforms of cytochrome P450 involved in metabolizing toxic compounds (Fig. 3); and in the other hand, cysteine proteases enzymes which are primary effectors in cell death: caspase 3 and caspase 8 (Fig. 4).

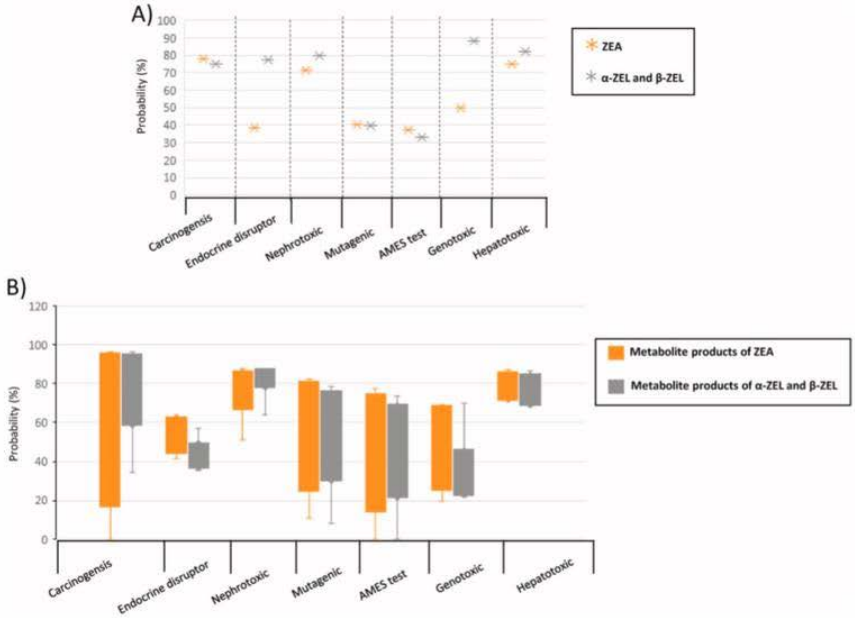

Fig. 2. Prediction of toxic effects (probability, %) for ZEA (orange star), α-ZEL and β-ZEL (grey star) (A) and all metabolite products (B, box diagram) of Phase I and II reactions obtained from those mycotoxins: ZEA (orange box) and ZEA's metabolites (grey box). Bars in (B) report the maximum and minimum value of prediction out of the box. (For interpretation of the references to colour in this figure legend, the reader is referred to the Web version of this article.)

3.4.1. Cytochrome P450

Prediction effects on isoforms of Cytochrome P450 (CYP1A1, CYP1A2, CYP2C9 and CYP3A4) are reported in Fig. 3 for all three mycotoxins and compounds defined in the metabolomics profile (from Phase I and II reactions). Effects are reported for each compounds acting as substrate, inducer or inhibitor. For all CYP450 isoforms all three mycotoxins reported effect as substrates, inducers and inhibitors; however, α-ZEL and β-ZEL reported higher probability prediction than ZEA in all of them independently of its mode of action (Fig. 3).

In detail, for isoform CYP1A1, all compounds had effects on it (Fig. 3A). Metabolite products coming from α-ZEL and β-ZEL had slightly higher probability prediction as substrate (>37%) than ZEA (>35%) for all O-glucuronidation, S-sulfation and hydrolysis products; as inducers, only metabolite products coming from O-glucuronidation reported this prediction effects. Finally, as inhibitor, only metabolite 5z from hydrolysis of ZEA and 6 ab from S-sulfation of α-ZEL and β-ZEL presented such prediction both in 30% (Fig. 3A).

For isoform CYP1A2, ZEA metabolite products had effects on it as substrate, except those coming from S-sulfation; and products of S-sulfation from α-ZEL and β-ZEL had no-effect (Fig. 3B). As inducers of this isoform (CYP1A2), only metabolite products of S-sulfation from ZEA (3z and 4z) were predicted in 16%. As inhibitor none of the compounds reported prediction in this direction (Fig. 3B).

For isoform CYP2C9, ZEA, α-ZEL and β-ZEL were predicted as substrate; while only ZEA as inducer and α-ZEL and β-ZEL as inhibitor (Fig. 3C). For metabolite products coming from O-glucuronidation of these mycotoxins all were predicted as i) substrate: 54% for those coming from ZEA and >60% for those coming from α-ZEL and β-ZEL; and as ii) inducers: >38% for all those coming from ZEA and from α-ZEL and β-ZEL. Metabolite product of hydrolysis coming from ZEA (5z) was predicted only as inducer (26%); while that coming from α-ZEL and β-ZEL (7 ab) was predicted as substrate (22%), inhibitor (23%) and inducer (26%). However, no-effect was predicted for S-sulfation compounds (neither as substrate, inhibitor or inducer).

Finally, ZEA, α-ZEL and β-ZEL were predicted as substrate and inducers with probabilities >60% for isoform CYP3A4 (Fig. 3D). All metabolite products from ZEA of O-glucuronidation and S-sulfation were predicted as substrate ranging from 32% (2z) to 61% (4z); and inducers ranging from 57% (4z) to 80% (1z). No effect was predicted for its hydrolysis product (5z). Similar prediction effect was observed for metabolite products from α-ZEL and β-ZEL as substrates ranging from 38% (1 ab) to 81% (5 ab) and as inducers ranging from 58% (6 ab) to 81% (3 ab). The hydrolysis product 7 ab, was only predicted as substrate (35%) (Fig. 3D).

3.4.2. Caspases 3 and 8

Caspases are involved in cascade activation of cell death, occurring either naturally or by exposure to toxic compounds. Prediction for caspases 3 and 8 activation (stimulation) is reported in Fig. 4A and B, respectively of all 15 compounds. Prediction of activation of both caspases, 3 and 8, was higher for α-ZEL and β-ZEL (86% and 49% for caspase 3 and 8, respectively) than for ZEA (73% and 43% for caspase 3 and 8, respectively).

Caspase 3 was activated for all compounds studied and for metabolite predicted from α-ZEL and β-ZEL probability was higher than those from ZEA (Fig. 4A). Metabolite products of i) O-glucuronidation from α-ZEL and β-ZEL reported caspase activation >80% while those from ZEA <77%; ii) S-sulfation from α-ZEL and β-ZEL reported caspase

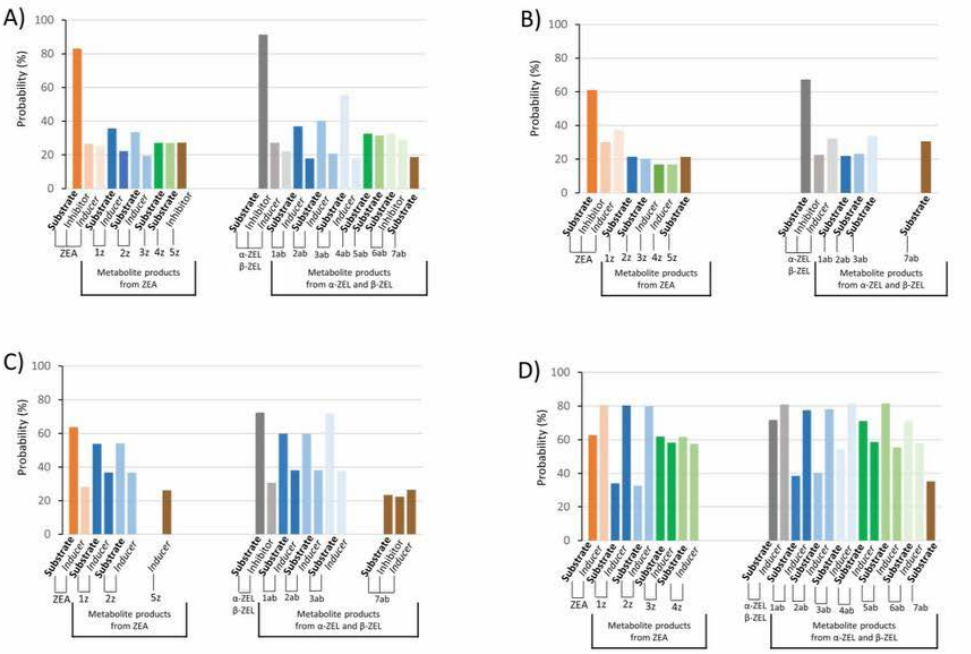

Fig. 3. Prediction of inhibition, induction and substrate function of different isoforms of Cytochrome P450 (probability, %) that metabolize the majority of xenobiotics: CYP1A1 (A); CYP1A2 (B); CYP2C9 (C) and CYP3A4 (D). Prediction is reported for each metabolite product from ZEA (from dark to light orange), α-ZEL and β-ZEL (from dark to light grey). O-glucuronidation products (from dark to light blue), S-sulfation products (from dark to light green) and hydrolysis products (in brown). (For interpretation of the references to colour in this figure legend, the reader is referred to the Web version of this article.)

activation >36% while those from ZEA <30% and iii) hydrolysis from α-ZEL and β-ZEL reported caspase activation 33% while those from ZEA 35% (Fig. 4A).

For caspase 8, ZEA metabolite products reported prediction of activation only from those coming from O-glucuronidation and hydrolysis, from 56% to 29%, respectively (Fig. 4B); while those metabolites products coming from α-ZEL and β-ZEL reported activation of caspases from 51% (1 ab) to 60% (3 ab) for O-glucuronidation products, from 25% (6 ab) to 27% (4 ab) for S-sulfation products and 34% (7 ab) for the hydrolysis product (Fig. 4B).

4. Discussion

The present study explores the prediction of toxicity of three mycotoxins (ZEA, α-ZEL and β-ZEL) and products defining its metabolomics profile by proposing an *in silico* workflow and by using three software of computational toxicology: MetaTox, SwissADME and PASS online. All three mycotoxins are well-known to be copresent in food and feed not following good manufacture/agricultural practices, generating a public health concern as well as agricultural economic losses. Its effect as endocrine disruptor has been widely reported although the implications of its metabolite products regarding that toxic effects (or others) are unknown.

The workflow proposed, uses MetaTox to obtain the metabolite products formed during Phase I and II reactions, contributing to describe the metabolomics profile (Rudik et al., 2017); SwissADME (Daina et al., 2017) here it has been used for assessing the ADMET processes suffered by three mycotoxins (ZEA, α-ZEL and β-ZEL) and its metabolites products (1z-5z for ZEA and 1 ab-7ab for α-ZEL and β-ZEL); and PASS online, predicted the toxic effect of activation and the biological activities with probability values (Pa, probability of activation). Different parameters are used for each software program which help in predictions, but as it occurs with *in vitro* or *in vivo* studies, they must be prudently assessed (Workflow 1).

Metabolites products predicted through MetaTox for the mycotoxins studied came from two Phase II reactions: O-glucuronidation and S-sulfation. Both are detoxication reactions of first line facilitating excretion. ZEA was predicted to generate two metabolites for each type of reaction (from 1z to 4z); while for α-ZEL and β-ZEL three metabolites (from 1 ab to 6 ab) (Fig. 1 and Table 1). For Phase I reaction, only hydrolysis reaction was predicted to take place from ZEA, α-ZEL and β-ZEL, generating only one metabolite product, 7z and 7 ab for ZEA and ZEA's metabolites, respectively. In summary a total of 12 compounds defined the metabolomic profile of ZEA, α-ZEL and β-ZEL (Fig. 1 and Table 1). Coinciding with other studies, these reactions take place and generate these compounds; however, their effects are unknown; in fact, the use of these metabolite products as biomarkers have been found in the literature in biomonitoring studies (Lorenz et al., 2019; Follmann et al., 2016; Shephard et al., 2013; Wallin et al., 2015; Gerding et al., 2015) or directly detected in food and aromatic plants as masked mycotoxins (Berthiller et al., 2006, 2009; Mannani et al., 2019). However, an analysis of *in silico* prediction of toxic effects defined by the metabolomics profile is here the first time reported. EFSA has dealt in assessing the risk of ZEA, α-ZEL and β-ZEL and has indicated that metabolites

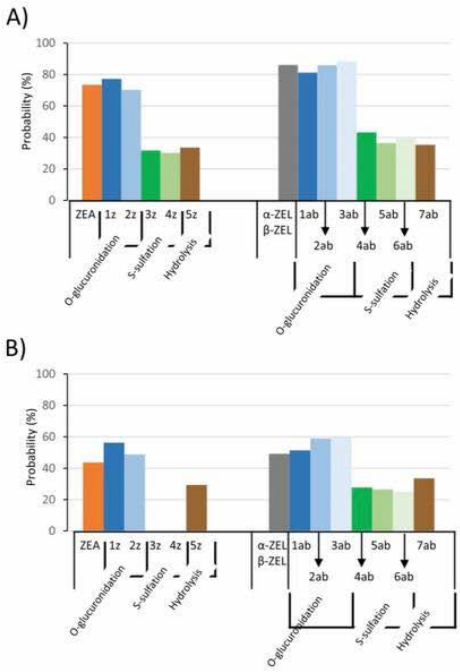

Fig. 4. Prediction of caspases activation (probability, %) implicated in cell death pathway: caspase 3 (A) and caspase 8 (B). Graphics are reported for ZEA, α-ZEL, β-ZEL and metabolites products of those generated during Phase I and II reactions: Oglucuronidation (in blue): 1z and 2z from ZEA, and 1 ab, 2 ab and 3 ab from ZEA's metabolites; S-sufation (in green): 3z and 4z from ZEA, and 4 ab, 5 ab and 6 ab from ZEA's metabolites; and hydrolysis (in brown): 5z from ZEA and 7 ab from ZEA's metabolites. (For interpretation of the references to colour in this figure legend, the reader is referred to the Web version of this article.)

products coming from them (also reported as modified forms) might have effects (oestrogenic effect, genotoxicity, endocrine receptor, …) (EFSA, 2011 and 2014) and contribute to the exposure evaluation but the uncertainty exists as there is a lack of data which entails difficulties in defining its toxic effects (EFSA et al., 2014, 2016, 2017). Not to mention the gap in effects of its mixtures or with other mycotoxins or contaminants.

In silico analysis show that ZEA, α-ZEL and β-ZEL are poorly achieving the BBB, have good distribution and are highly favored to be absorbed gastrointestinally (Table 2). The interesting point noticed with the analysis of metabolites products of these mycotoxins, obtained from O-glucuronidation, S-sulfation and hydrolysis reactions, is that these properties change inversely, especially for achieving the BBB (see values from Tables 2 and 3) from low values to high values. There are studies coinciding and others opposite to the results predicted in here when compared with those reported by *in vitro* and *in vivo* studies. For all three mycotoxins it has been reported a good gastrointestinal absorption (rapid and extensive) as well as the formation of metabolites from hydrolysis, sulfation and glurcuronidation (Biehl et al., 1993; Frizzell et al., 2015; Pfeiffer et al., 2011; Plasencia et al., 1991); in fact, several strategies and recommendations have been also considered for the entire risk assessment (EFSA 2017; Lorenz et al., 2019). Optimal gastrointestinal absorption predicted by Lipinsky RO5 is reported in Table 1 for the metabolomics profile. It also indicates that the probability of one compound to be absorbed orally is directly related to the ADMET and toxic effects. Only metabolites coming from O-glucuronidation were not following the Lipinsky's RO5 (HBA>10), because of not passing the gastrointestinal barrier; however, mycotoxins, and metabolites from S-sulfation and hydrolysis reactions did which indicates their good distribution.

Toxic effects associated to compounds from metabolomics profile and mycotoxins seem to contribute one to another. Related to this, EFSA has indicated to assume the toxic effects of one compound as the sum of all metabolites coming from that compound (EFSA, 2011; Lorenz et al., 2019). Nonetheless, it is possible to analyze individual predictions *in silico*. The most common effect associated to ZEA as well as ZEA's metabolites is as endocrine disruptors with a ranking of oestrogenic potential effect established by EFSA as follows: α- ZEL > ZEN > β-ZEL (EFSA 2011). Besides this common and demonstrated toxic effect through *in vitro* and *in vivo* assays (EFSA 2017; Eze et al., 2019), other effects according to several parameters can be predicted (Fig. 2A) as well as for its metabolite products (Fig. 2B). According to the analysis of main effects predicted *in silico* for ZEA, α- ZEL, β-ZEL and its metabolite product defining the metabolomic profile, carcinogencity is the toxic effect predicted with high probability; however, IARC has classified ZEA (since 1993) as Group 3 (not classifiable as to their carcinogenicity to humans) based on inadequate evidence in humans and limited evidence in experimental animals (IARC 1993); to mention different behave in mice and mouse with limited evidence reported. This explains the prediction described in Fig. 2, which although carcinogenicity indicates high probability (80–90%), the evidence is not coinciding with assays carried out for evaluating such effect. This is not happening with other effects reported in Fig. 2 which coincide with studies carried out either *in vivo* or *in vitro* (especially for ZEA as it is the most studied): mutagenicity (Abbès et al., 2007; Ben Salah-Abbès et al., 2009); nephrotoxic in rats (Becci et al., 1982), genotoxic (Ouanes et al., 2003, 2005; El-Makawy et al., 2001). As mentioned before the prediction needs to be confirmed with further assays without forgetting that it is giving a valuable indication to start from.

Cytochrome P450 (CYP450) is an enzymatic complex important as mechanism of defense by the organism when in contact with contaminants. Its main function is to metabolize the majority of toxic compounds through Phase I reactions. It is constituted by several isoforms to highlight the following as the most implicated in defense: CYP3A4, CYP2C9, CYP2C19, CYP1A1 and CYP1A2 (SwissADME). Expression of different isoforms occurs by exposure to contaminants as mycotoxins; which can act as inhibitors, inducers or substrates of this enzymatic complex. Results reported in Fig. 3 reveal that the highest predictions effects were for CYP3A4 (40–80%) (Fig. 3D). When analyzing the action of mycotoxins, all three act as substrate, inducers and inhibitors ranging from 60% to 90%, from 21% to 38% and from 23% to 32%, respectively for isoforms CYP1A1 and CYP1A2 (Fig. 3); while as substrate (62%–71%) and inducers (89%) for CYP3A4. Finally, for isoform CYP2C9, ZEA act as substrate and inducer and, α- ZEL and β-ZEL as substrate and inhibitor (Fig. 3). For metabolite products, probabilities of action were marked for isoform CYP3A4. This isoform jointly CYP1A2 have been reported to play an important role in metabolism of ZEA in humans (Pfeiffer et al., 2009); while jointly with CYP2C8 denotes a high activation hydroxylation of ZEA (Bravin et al., 2009). In summary, different isoforms of CYP seem to contribute in the metabolization of all 15 compounds according to *in silico* prediction which coincides with the studies performed *in vitro* (Pfeiffer et al., 2009; Bravin et al., 2009); and more specifically with the isoform CYP3A4 which has the highest values of probability (Fig. 3D).

Apoptotic cell death has been studied for ZEA *in vitro* revealing that activation of caspase 3 and 8 occurs (Banjerdpongchai et al., 2020; Gazzah et al., 2010; Othmen et al., 2008; Agahi et al., 2020 Zhu et al., 2012); as well as for α- ZEL and β-ZEL (Abid-Essefi et al., 2009). Nothing

is known nor for its metabolite products defined in the metabolomics profile. Both caspases, implicated in the cascade activation for apoptotic cell death, have been predicted *in silico* as reported in Fig. 4. Results for ZEA coincide with those reported in the literature *in vitro* denoting a major activation for caspase 3 than caspase-8 (Barjerdpongchai et al., 2010). Among that, similar tendency was observed for all the other 14 compounds studied; and while O-glucuronidates present highest prediction of activation for both caspase-3 and 8 and all compounds, S-sulfation products from ZEA (3z and 4z) do not contribute to activation of cell death through caspase-8 (Fig. 4B). The prediction presented in this work in cell death and the *in vitro* confirmation reported for ZEA, α- ZEL and β-ZEL reveal that the apoptosis pathway of cell death is contributed by its metabolite products, which are generated during its detoxification by Phase I and II reactions.

5. Conclusions

In conclusion, the results obtained in the present study indicate that toxicity of ZEA, α-ZEL and β-ZEL mycotoxins and their metabolomics' profile can be predicted *in silico*. MetaTox was able to predict a total of 12 metabolites defining the metabolomics profile of each mycotoxin studied (5 from ZEA and 7 from α-ZEL and β-ZEL). SwissADME permitted to analyze each compound by its physicochemical properties and predict the behave of each one according to its absorption, distribution, metabolism and toxicity. Among that it was possible to assign a HMDB ID according to a score of similarity. Lastly, PASS online provided an entire prediction of all compounds based on its structural information reported in Pa values. The results indicate moderate to high absorption by the gastrointestinal tract, but unlikely to penetrate into the brain on its current form unless metabolized. Slightly better properties to reach blood brain barrier than initial mycotoxins were observed. Toxic effects associated for all compounds revealed that carcinogenicity reported the highest probability for all three mycotoxins followed by nephrotoxic > hepatotoxic > endocrine disruptor > mutagenic (AMES TEST) > genotoxic. Prediction of inhibition, induction and substrate function on different isoforms of Cytochrome P450 varied for each compounds analyzed; similarly, for activation of caspases 3 and 8.

The metabolomics profile of ZEA, α-ZEL and β-ZEL analyzed by *in silico* programs (MetaTox, SwissADME and PASS online) predicts alteration of systems/pathways/mechanisms that ends up causing several toxic effects, giving an excellent sight and direct studies before starting *in vitro* or *in vivo* assays contributing to 3Rs principle by a reduction of animal testing. This innovative proposal in the field of computer toxicology helps (and opens a new window) to investigate the chemical risk assessment, a topic of great interest amongst researchers and safety authorities; nonetheless, it is necessary to continue developing and performing assays that confirm the predictions estimated to achieve solidest conclusions.

Source of funding

This research was supported by the Spanish Ministry of Science and Innovation PID2019-108070RB-100ALI and the Generalitat Valenciana GV2020/020, Generalitat Valenciana GVPROMETEO2018-126.

Compliance with ethical standards.

CRediT authorship contribution statement

Fojan Agahi: Data curation, Investigation, Methodology, Visualization, Writing - original draft. **Cristina Juan:** Conceptualization, Data curation, Formal analysis, Funding acquisition, Investigation, Methodology, Visualization, Writing - original draft, Writing - review & editing. **Guillermina Font:** Funding acquisition, Investigation, Writing - review & editing. **Ana Juan-García:** Conceptualization, Data curation, Formal analysis, Funding acquisition, Investigation, Methodology, Visualization, Writing - original draft, Writing - review & editing.

Declaration of competing interest

The authors declare that they have no known competing financial interests or personal relationships that could have appeared to influence the work reported in this paper.

Acknowledgements

Authors would like to thank Spanish Ministry of Science and Innovation PID2019-108070RB-I00ALI, Generalitat Valenciana GV2020/020 and Generalitat Valenciana GVPROMETEO2018-126.

Appendix ASupplementary data

Supplementary data to this article can be found online at https://doi.org/10.1016/j.fct.2020.111818.

References

Abbès, S., Ouanes, Z., Salah-Abbès, J., Abdel-Wahhab, M.A., Oueslati, R., Bacha, H., 2007. Preventive role of aluminosilicate clay against induction of micronuclei and chromosome aberrations in bonemarrow cells of Balb/c mice treated with Zearalenone. Mutat. Res. Genet. Toxicol. Environ. Mutagen 631, 85–92.

Abid-Essefi, S., Bouaziz, C., Golli-Bennour, E.E., Ouanes, Z., Bacha, H., 2009. Comparative study of toxic effects of zearalenone and its two major metabolites alpha-zearalenol and beta-zearalenol on cultured human Caco-2 cells. J. Biochem. Mol. Toxicol. 23, 233–243.

Agahi, F., Álvarez-Ortega, N., Font, G., Juan-García, A., Juan, C., 2020. Oxidative stress, glutathione, and gene expression as key indicators in SH-SY5Y cells exposed to zearalenone metabolites and beauvericin. Toxicology Letters 334, 44–52.

Agahi, F., Font, G., Juan, C., Juan-García, A., 2020. Individual and combined effect of zearalenone derivates and beauvericin mycotoxins on SH-SY5Y cells. Toxins 12, 212. https://doi.org/10.3390/toxins12040212.

Bakker, M.G., Brown, D.W., Kelly, A.C., Kim, H.S., Kurtzman, C.P., Mccormick, S.P., O'Donnell, K.L., Proctor, R.H., Vaughan, M.M., Ward, T.J., 2018. Fusarium mycotoxins: a trans-disciplinary overview. J. Indian Dent. Assoc. 40, 161–171.

Banjerdpongchai, R., Kongtawelert, P., Khantamat, O., Srisomsap, C., Chokchaichamnankit, D., Subhasitanont, P., Svasti, J., 2010. Mitochondrial and endoplasmic reticulum stress pathways cooperate in zearalenone-induced apoptosis of human leukemic cells. J. Hematol. Oncol. 3, 50. http://www.jhoonline.org/content/3/1/50.

Becci, P.J., Voss, K.A., Hess, F.G., Gallo, M.A., Parent, R.A., Stevens, K.R., Taylor, J.M., 1982. Long-term carcinogenicity and toxicity study of zearalenone in the rat. J. Appl. Toxicol. 2, 247–254.

Ben Salah-Abbès, J., Abbès, S., Abdel-Wahhab, M.A., Oueslati, R., 2009. Raphanus sativus extract protects against Zearalenone-induced reproductive toxicity, oxidative stress and mutagenic alterations in male Balb/c mice. Toxicon 53, 525–533.

Berthiller, F., Hametner, C., Krenn, P., Schweiger, W., Ludwig, R., Adam, G., Krska, R., Schuhmacher, R., 2009. Preparation and characterization of the conjugated Fusarium mycotoxins zearalenone-4O-beta-Dglucopyranoside, alpha-zearalenol-4O-beta-D-glucopyranoside and beta-zearalenol-4O-beta-D-glucopyranoside by MS/MS and two-dimensional NMR. Food Additives & Contaminants. Part. Accel.: Chemistry, Analysis, Control, Exposure & Risk Assessment 26, 207–213.

Berthiller, F., Werner, U., Sulyok, M., Krska, R., Hauser, M.T., Schuhmacher, R., 2006. Liquid chromatography coupled to tandem mass spectrometry (LC-MS/MS) determination of phase II metabolites of the mycotoxin zearalenone in the model plant Arabidopsis thaliana. Food Addit. Contam. 23, 1194–1200.

Berthiller, F., Crews, C., Dall'Asta, C., de Saeger, S., Haesaert, G., Karlovsky, P., Oswald, I.P., Seefelder, W., Speijers, G., Stroka, J., 2013. Masked mycotoxins: a review. Mol. Nutr. Food Res. 57, 165–186.

Biehl, M.L., Prelusky, D.B., Koritz, G.D., Hartin, K.E., Buck, W.B., Trenholm, H.L., 1993. Biliary excretion and enterohepatic cycling of zearalenone in immature pigs. Toxicol. Appl. Pharmacol. 121, 152–159.

Bravin, F., Duca, R.C., Balaguer, P., Delaforge, M., 2009. *In vitro* cytochrome p450 formation of a monohydroxylated metabolite of zearalenone exhibiting estrogenic activities: possible occurrence of this metabolite *in vivo*. Int. J. Mol. Sci. 10, 1824–1837.

Cheng, F., Li, W., Zhou, Y., Shen, J., Wu, Z., Liu, G., Lee, P.W., Tang, Y., 2012. AdmetSAR: a comprehensive source and free tool for evaluating chemical ADMET properties. J. Chem. Inf. Model. 52, 3099–3105.

Daina, A., Michielin, O., Zoete, V., 2017. SwissADME: a free web tool to evaluate pharmacokinetics, drug-likeness and medicinal chemistry friendliness of small molecules. Sci. Rep. 7, 42717. https://doi.org/10.1038/srep42717.

EFSA European Food Safety Authority, 2011. Scientific Opinion on the risks for public health related to the presence of zearalenone in food. EFSA Journal 9 (6), 2197.

EFSA European Food Safety Authority, 2014. Scientific opinion on the risks for human and animal health related to the presence of modified forms of certain mycotoxins in food and feed. EFSA J 12, 3916. https://doi.org/10.2903/j.efsa.2014.3916.

EFSA European Food Safety Authority, 2016. Appropriateness to set a group health-based guidance value for ZEN and its modified forms. EFSA J 14, 4425. https://doi.org/10.2903/j.efsa.2016.4425, 46pp.

EFSA European Food Safety Authority, 2017. Risks to human and animal health related to the presence of DON and its acetylated and modified forms in food and feed. EFSA J 15, 4718. https://doi.org/10.2903/j.efsa.2017.4718, 345pp.

El-Makawy, A., Hassanane, M.S., Abd Alla, E.S., 2001. Genotoxic evaluation for the estrogenic mycotoxin zearalenone. Reprod. Nutr. Dev. 41, 79–89.

Eze, U.A., Huntriss, J., Routledge, M.N., Gong, Y.Y., Connolly, L., 2019. The effect of individual and mixtures of mycotoxins and persistent organochloride pesticides on oestrogen receptor transcriptional activation using in vitro reporter gene assays. Food Chem. Toxicol. 130, 68–78.

Föllmann, W., Ali, N., Blaszkewicz, M., Degen, G., 2016. Biomonitoring of mycotoxins in urine: pilot study in mill workers. J. Toxicol. Environ. Health 79, 1015–1025.

Frizzell, C., Uhlig, S., Miles, C.O., Verhaegen, S., Elliott, C.T., Eriksen, G.S., Sørlie, M., Ropstad, E., Connolly, L., 2015. Biotransformation of zearalenone and zearalenols to their major glucuronide metabolites reduces estrogenic activity. Toxicol. Vitro 29, 575–581.

Frizzell, C., Ndossi, D., Verhaegen, S., Dahl, E., Eriksen, G., Sørlie, M., Connolly, L., 2011. Endocrine disrupting effects of zearalenone, alpha- and beta-zearalenol at the level of nuclear receptor binding and steroidogenesis. Toxicol. Lett. 206 (2), 210–217.

Gazzah, A.C., Bennour, E.E., Bouaziz, C., Abid, S., Ladjimi, M., Bacha, H., 2010. Sequential events of apoptosis induced by zearalenone in cultured hepatocarcinoma cells. Mycotoxin Res. 26, 187–197.

Gerding, J., Ali, N., Schwartzbord, J., Cramer, B., Brown, D.L., Degen, G.H., Humpf, H.U., 2015. A comparative study of the human urinary mycotoxin excretion patterns in Bangladesh, Germany, and Haiti using a rapid and sensitive LC-MS/MS approach. Mycotoxin Res. 31, 127–136.

Hasan, M.N., Bhuiya, N.M.M.A., Hossain, M.K., 2019. In silico molecular docking, PASS prediction, and ADME/T analysis for finding novel COX-2 inhibitor from Heliotropium indicum. J. Comp. Med. Res. 10, 142–154.

IARC (International Agency for Research on Cancer), 1993. IARC Monographs on the Evaluation of the Carcinogenic Risk of Chemicals to Humans, 56. Some Naturally Occurring Substances: Heterocyclic Aromatic Amines and Mycotoxins, Lyon, pp. 39–444.

Juan, C., Mañes, J., Font, G., Juan-García, A., 2017a. Determination of mycotoxins in fruit berry by-products using QuEChERS extraction method. LWT - Food Sci. Technol. (Lebensmittel-Wissenschaft -Technol.) 86, 344–351.

Juan, C., Berrada, H., Mañes, J., Oueslati, S., 2017b. Multi-mycotoxin determination in barley and derived products from Tunisia and estimation of their dietary intake. Food Chem. Toxicol. 103, 148–156.

Juan, C., Mannai, A., Ben Salem, H., Oueslati, S., Berrada, H., Juan-García, A., Mañes, J., 2020. Mycotoxin presence in pre- and post-fermented silage from Tunisia. Arabian Journal of Chemitry 13, 6753–6761.

Juan-García, A., Bind, M.A., Engert, F., 2020. Larval zebrafish as an in vitro model for evaluating toxicological effects of mycotoxins. Ecotoxicology and Environmental Safety 202, 110909.

Juan-García, A., Juan, C., Manyes, L., Ruiz, M.J., 2016. Binary and tertiary combination of alternariol, 3-acetyl-deoxynivalenol and 15-acetyl-deoxynivalenol on. In: HepG2 Cells: Toxic Effects and Evaluation of Degradation Products Toxicology in Vitro, vol. 34, pp. 264–273.

Juan-García, A., Tolosa, J., Juan, C., Ruiz, M.J., 2019a. Cytotoxicity, genotoxicity and disturbance of cell cycle in HepG2 cells exposed to OTA and BEA: single and combined actions. Toxins 11 (6), 341.

Juan-García, A., Tolosa, J., Juan, C., Ruiz, M.J., 2019b. Cytotoxicity, genotoxicity and disturbance of cell cycle in HepG2 cells exposed to OTA and BEA: single and combined actions. Toxins 11, 341. https://doi.org/10.3390/toxins11060341.

Kifer, D., Jaksi, D., Klari, M.S., 2020. Assessing the effect of mycotoxin combinations: which mathematical model is (the most) appropriate? Toxins 12, 153. https://doi.org/10.3390/toxins12030153.

Lagunin, A., Stepanchikova, A., Filimonov, D., Poroikov, V., 2000. PASS: prediction of activity spectra for biologically active substances. Bioinformatics 16 (8), 747–748.

Lorenz, N., Dänicke, s., Edler, L., Gottschalk, C., Lassek, E., Marko, D., Rychlik, M., Mally, A., 2019. A critical evaluation of health risk assessment of modified mycotoxins with a special focus on zearalenone. Mycotoxin Res. 35, 27–46. https://doi.org/10.1007/s12550-018-0328-z.

Mannani, N., Tabarani, A., Abdennebi, E.H., Zinedine, A., 2019. Assessment of aflatoxin levels in herbal green tea available on the Moroccan market. Food Contr. 108, e106882 https://doi.org/10.1016/j.foodcont.2019.106882.

Othmen, Z.O., Golli, E.E., Abid-Essefi, S., Bacha, H., 2008. Cytotoxicity effects induced by Zearalenone metabolites, alpha Zearalenol and beta Zearalenol, on cultured Vero cells. Toxicology 252, 72–77.

Ouanes, Z., Abid, S., Ayed, I., Anane, R., Mobio, T., Creppy, E.E., Bacha, H., 2003. Induction of micronuclei by Zearalenone in Vero monkey kidney cells and in bone marrow cells of mice: protective effect of Vitamin E. Mutat. Res. 538, 63–70.

Ouanes, Z., Ayed-Boussema, I., Baati, T., Creppy, E.E., Bacha, H., 2005. Zearalenone induces chromosome aberrations in mouse bone marrow: preventive effect of 17beta-estradiol, progesterone and Vitamin E. Mutat. Res. 565, 139–149.

Oueslati, S., Berrada, H., Juan-García, A., Mañes, J., Juan, C., 2020. Multiple mycotoxin determination on Tunisian cereals-based food and evaluation of the population exposure. Food Analytical Methods. https://doi.org/10.1007/s12161-020-01737-z.

Pfeiffer, E., Kommer, A., Dempe, J.S., Hildebrand, A.A., Metzler, M., 2011. Absorption and metabolism of the mycotoxin zearalenone and the growth promotor zeranol in Caco-2 cells *in vitro*. Mol. Nutr. Food Res. 55, 560–567.

Pascari, X., Rodriguez-Carrasco, Y., Juan, C., Mañes, J., Marín, S., Ramos, A.J., Sanchis, V., 2019. Transfer of Fusarium mycotoxins from malt to boiled wort. Food Chemistry 278, 700–710.

Pfeiffer, E., Herrmann, C., Altem_ller, M., Podlech, J., Metzler, M., 2009. Oxidative *in vitro* metabolism of the Alternaria toxins altenuene and isoaltenuene. Mol. Nutr. Food Res. 53, 452–459.

Plasencia, J., Mirocha, C.J., 1991. Isolation and characterization of zearalenone sulfate produced by *Fusarium spp*. Appl. Environ. Microbiol. 57, 146–150.

Rudik, A.V., Bezhentsev, V.M., Dmitriev, A.V., Druzhilovskiy, D.S., Lagunin, A.A., Filimonov, D.A., Poroikov, V.V., 2017. MetaTox: web application for predicting structure and toxicity of xenobiotics' metabolites. J. Chem. Inf. Model. 57, 638–642.

Shephard, G.S., Burger, H.M., Gambacorta, L., Gong, Y.Y., Krska, R., Rheeder, J.P., Solfrizzo, M., Srey, C., Sulyok, M., Visconti, A., Warth, B., van der Westhuizen, L., 2013. Multiple mycotoxin exposure determined by urinary biomarkers in rural subsistence farmers in the former Transkei, South Africa. Food Chem. Toxicol. 62, 217–225.

Stanciu, O., Juan, C., Miere, D., Loghin, F., Mañes, J., 2017. Occurrence and co-occurrence of Fusarium mycotoxins in wheat grains and wheat flour from Romania. Food Contr. 73, 147–155.

Wallin, S., Gambacorta, L., Kotova, N., Lemming, E.W., Nalsen, C., Solfrizzo, M., Olsen, M., 2015. Biomonitoring of concurrent mycotoxin exposure among adults in Sweden through urinary multi-biomarker analysis. Food Chem. Toxicol. 83, 133–139.

Yang, H., Lou, C., Sun, L., Li, J., Cai, Y., Wang, Z., Li, W., Liu, G., Tang, Y., 2018. AdmetSAR 2.0: web-service for prediction and optimization of chemical ADMET properties. Bioinformatics bty707.

Zhu, L., Yuan, H., Guo, C., Lu, Y., Deng, S., Yang, Y., Wei, Q., Wen, L., He, Z., 2012. Zearalenone induces apoptosis and necrosis in porcine granulosa cells via a caspase-3- and caspase-9-dependent mitochondrial signaling pathway. J. Cell. Physiol. 227, 1814–1820.

Zoete, V., Daina, A., Bovigny, C., Michielin, O., 2016. SwissSimilarity: a web tool for low to ultra high throughput ligand-based virtual screening. J. Chem. Inf. Model. 56 (8), 1399–1404.

toxins

MDPI

Article

Individual and Combined Effect of Zearalenone Derivates and Beauvericin Mycotoxins on SH-SY5Y Cells

Fojan Agahi, Guillermina Font, Cristina Juan * and Ana Juan-García

Laboratory of Food Chemistry and Toxicology, Faculty of Pharmacy, University of Valencia, Av. Vicent Andrés Estellés s/n, 46100 Burjassot, València, Spain; agahifozhan@gmail.com (F.A.); crisjua3@uv.es (G.F.); ana.juan@uv.es (A.J.-G.)

* Correspondence: cristina.juan@uv.es

Received: 9 February 2020; Accepted: 25 March 2020; Published: 27 March 2020

check for updates

Abstract: Beauvericin (BEA) and zearalenone derivatives, α-zearalenol (α-ZEL), and β-zearalenol (β-ZEL), are produced by several *Fusarium* species. Considering the impact of various mycotoxins on human's health, this study determined and evaluated the cytotoxic effect of individual, binary, and tertiary mycotoxin treatments consisting of α-ZEL, β-ZEL, and BEA at different concentrations over 24, 48, and 72 h on SH-SY5Y neuronal cells, by using the MTT assay (3-(4,5-dimethylthiazol-2-yl)-2,5diphenyltetrazoliumbromide). Subsequently, the isobologram method was applied to elucidate if the mixtures produced synergism, antagonism, or additive effects. Ultimately, we determined the amount of mycotoxin recovered from the media after treatment using liquid chromatography coupled with electrospray ionization–quadrupole time-of-flight mass spectrometry (LC–ESI–qTOF-MS). The IC_{50} values detected at all assayed times ranged from 95 to 0.2 μM for the individual treatments. The result indicated that β-ZEL was the most cytotoxic mycotoxin when tested individually. The major effect detected for all combinations assayed was synergism. Among the combinations assayed, α-ZEL + β-ZEL + BEA and α-ZEL + BEA presented the highest cytotoxic potential with respect to the IC value. In individual treatment, α-ZEL was the most recovered mycotoxin; while, this was observed for BEA in binary combination α-ZEL + BEA.

Keywords: SH-SY5Y cells; zearalenone derivates; beauvericin; MTT; qTOF–MS/MS

Key Contribution: Individual exposure of β-ZEL in SH-SY5Y cells presented the highest cytotoxicological potency compared to α-ZEL and BEA; while in combination, α-ZEL + β-ZEL + BEA and α-ZEL + BEA presented the highest cytotoxic potential with respect to the IC50 value obtained. Recoveries were the highest for α-ZEL in individual treatment in SH-SY5Y; while, this high recovery was observed for BEA in binary combination α-ZEL + BEA.

1. Introduction

Mycotoxins represent one of the most important categories of biologically produced natural toxins with potential effects on human and animal health. The worldwide contamination by these natural products of food, feed, and environment, represents a health risk for animals and humans [1].

Several *Fusarium* species produce toxic substances of considerable concern to livestock and poultry producers. The mycotoxins beauvericin (BEA) and zearalenone (ZEN) and their derivatives (α-zearalenol (α-ZEL), β-zearalenol (β-ZEL), zeranol, taleranol, and zearalanone) can be produced by several *Fusarium* species (mainly *Fusarium graminearum*, but also *Fusarium culmorum*, *Fusarium cerealis*, *Fusarium equiseti*, and *Fusarium semitectum*) that grow on crops in temperate and warm-climate zones [2].

These fungi are present in almost all continents, can grow under poor storage conditions, and mainly contaminate cereal grains, such as maize, wheat, oats, soybeans, and their derived food products [3,4].

It has been proved that ZEN and α-ZEL bind to human estrogen receptors and elicit permanent reproductive tract alterations, and consequently, chronical exposure to ZEN present contaminated food can be a cause of female reproductive changes as a result of its powerful estrogenic activity [5–8]. It has been also reported that ZEN induces genotoxic effects by induction of DNA adducts, DNA fragmentation, and apoptosis [9,10]. As reported by Dong et al. (2010) [5], metabolic conversion of ZEN mycotoxin to α-ZEL and β-ZEL was found in almost all tissues and occurred more efficiently to α-ZEL than to β-ZEL; these mycotoxins are endocrine disruptors which affect steroid hormones such as progesterone [7]. In 2016, EFSA (European food Safety Authorities) indicated that there is a high uncertainty associated with the exposure to ZEN and its modified forms and so that it would rather overestimate than underestimate any risk associated with exposure to modified ZEN [8]. Also, recent studies have indicated that ZEN is immunotoxic [4,11,12] and cytotoxic in various cell lines by inhibiting cell proliferation and increasing ROS (reactive oxygen species) generation [13–15].

On the other hand, BEA causes cytotoxic effects by reducing cell proliferation in a time- and concentration-dependent manner [16,17]. Moreover, it can increase ROS generation and lipid peroxidation and produces oxidative stress and depletion of antioxidant cellular mechanisms [14,18,19].

Neurotoxicological testing is mainly based on experimental animal models, but several cell lines and tissue culture models have been developed to study the mechanism of neurotoxicity. In general, cells of human origin are attractive alternatives to animal models for the exploration of toxicity to humans. Nonetheless, there are few studies about the effect of mycotoxins at the neuronal level [6,20–22].

Regarding the important role of the food industry in human health, studying the impact of mycotoxins and their combinations in feed and food commodities has gained attention over the last few years, due to the ability of most *Fusarium* spp. to simultaneously produce different mycotoxins [23–25]. Hence, EFSA has recently published a draft guidance document where a harmonized risk assessment methodology for combined exposure to multiple chemicals in all relevant areas is described [26].

Due to the importance of dietetic exposure to various mycotoxins and their impacts on human's health, there is an increasing concern about the hazard of co-occurrence of mycotoxins produced by *Fusarium* and of co-exposure to them through diet. Many studies have been conducted on the toxicity of individual mycotoxins; however, few studies have been dedicated to the toxicological interaction of mycotoxins when present in double and triple combinations on different cell lines [16–18,27–29].

The objective of the present study was to investigate the cytotoxicological interactions between α-ZEL, β-ZEL, and BEA mycotoxins in human neuroblastoma SH-SY5Y cells, via the MTT assay. The effects of combinations of two and three mycotoxins were evaluated by isobologram analysis [30] to determine whether their interaction was synergistic, additive, or antagonistic, as well as to understand how mycotoxins can act at the cellular level.

2. Results

2.1. Cytotoxicity Assay of Individual and Combined Mycotoxins

The cytotoxicity effects of α-ZEL, β-ZEL, and BEA mycotoxins on SH-SY5Y cells were evaluated by the MTT assays over 24, 48, and 72 h. Figure 1 shows the time- and concentration-dependent decrease in cell viability after exposure to each mycotoxin individually, while IC_{50} values are shown in Table 1. After 24 h, the IC_{50} value could be calculated only for β-ZEL and was 94.3 ± 2.0 μM; after 48 h of exposure, the IC_{50} values were 20.8 ± 0.5 μM for α-ZEL and 9.1 ± 1.8 μM for β-ZEL. After 72 h of exposure, the IC_{50} values were 14.0 ± 1.8 μM, 7.5 ± 1.2 μM. and 2.5 ± 0.2 μM for α-ZEL, β-ZEL, and BEA, respectively. According to the IC_{50} values obtained at 72 h, BEA showed the highest cytotoxic effect on SH-S5Y5 cells (Table 1).

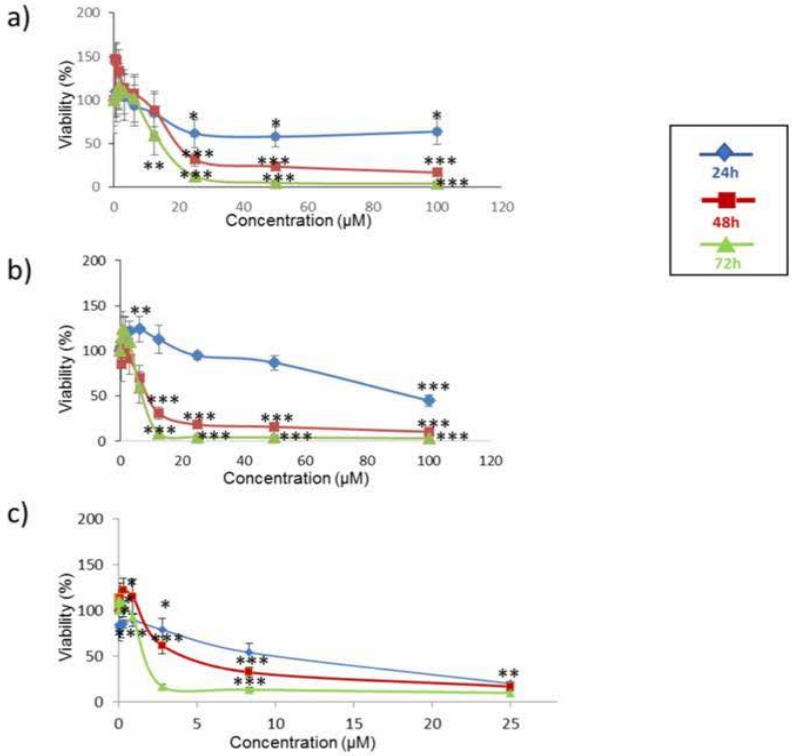

Figure 1. Cytotoxicity of the mycotoxins α-ZEL (**a**), β-ZEL (**b**), and BEA (**c**) individually at 24 h, 48 h, and 72 h. All values are the results of three independent experiments with eight replicates and are expressed as mean ± SD; $p \leq 0.05$ (*), $p \leq 0.01$ (**), $p \leq 0.001$ (***).

Table 1. Medium inhibitory concentration (IC_{50} ± SD) of α-zearalenol (α-ZEL), β-zearalenol (β-ZEL), and beauvericin (BEA) for SH-SY5Y cells after 24, 48, and 72 h of exposure, determined by the MTT assay. Three independent experiments were performed with eight replicates each.

Mycotoxin	IC_{50} (μM) ± SD		
	24 h	48 h	72 h
α-ZEL	n.a	20.8 ± 0.5	14.0 ± 1.8
β-ZEL	94.3 ± 2.0	9.1 ± 1.8	7.5 ± 1.2
BEA	n.a	n.a	2.5 ± 0.2

n.a: not available.

The cytotoxic effect of binary and tertiary combinations of α-ZEL, β-ZEL, and BEA on SH-SY5Y cells was evaluated by the MTT assays over 24, 48, and 72 h. The dose–response curves of the two- and three-mycotoxin combinations are shown in Figures 2 and 3, which demonstrate higher cytotoxicity of the combinations compared with individual mycotoxin. Figure 2 shows the concentration-dependent decrease in SH-SY5Y cell viability upon combined treatment with α-ZEL + BEA (5:1) (Figure 2a), β-ZEL + BEA (5:1) (Figure 2b), α-ZEL + β-ZEL (1:1) (Figure 2c); Figure 3 shows the results for α-ZEL + β-ZEL + BEA (5:5:1).

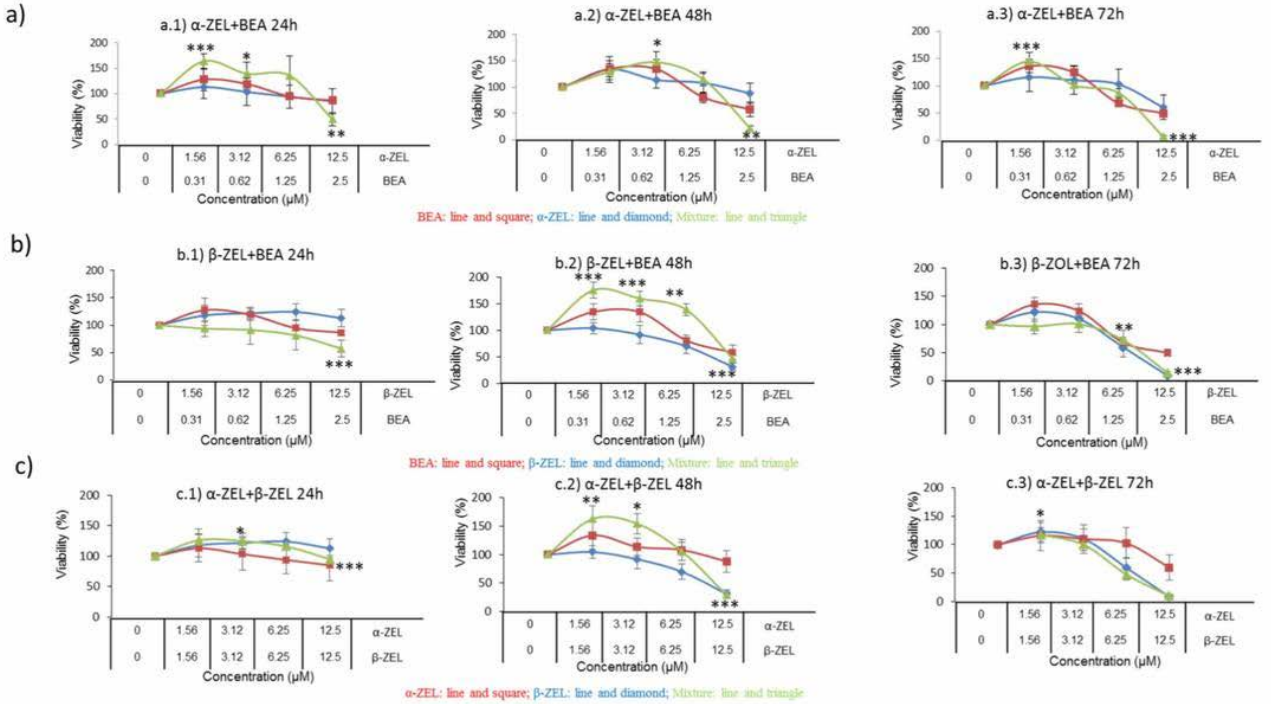

Figure 2. Cytotoxicity of the mycotoxin combinations of α-ZEL + BEA (5:1) (**a**), β-ZEL + BEA (5:1) (**b**), and α-ZEL + β-ZEL (1:1) (**c**) at 24 h (a.1, b.1, and c.1), 48 h (a.2, b.2, and c.2) and 72 h (a.3, b.3, and c.3). All values are the results of three independent experiments with eight replicates and are expressed as mean ± SD; $p \leq 0.05$ (*), $p \leq 0.01$ (**), $p \leq 0.001$ (***).

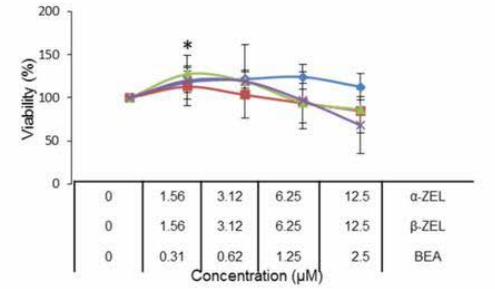

(a)

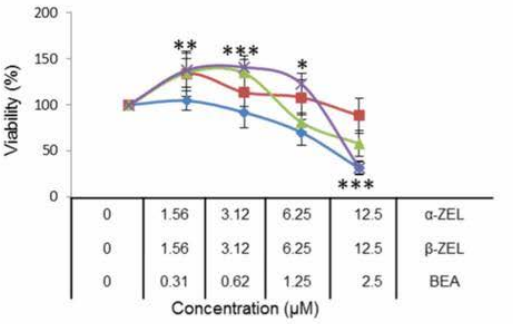

(b)

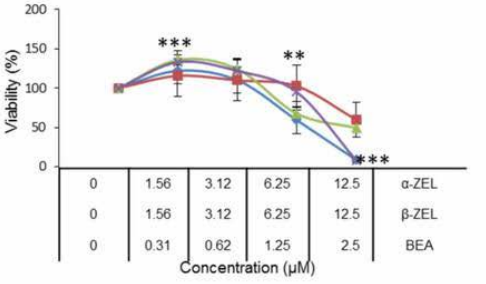

(c)

Figure 3. Cytotoxicity of the mycotoxin combination of α-ZEL + β-ZEL + BEA (5:5:1) at 24 h (**a**), 48 h, (**b**) and 72 h (**c**). All values are the results of three independent experiments with eight replicates and are expressed as mean ± SD; $p \leq 0.05$ (*), $p \leq 0.01$ (**), $p \leq 0.001$ (***). BEA: line and square; β-ZEL: line and diamond; α-ZEL: line and triangle; Mixture: line and ×.

The α-ZEL + BEA combination at the highest concentration induced a decrease in cell proliferation at 24 h of exposure (Figure 2a) of 35% with respect to the effect α-ZEL tested individually and of 37% with respect to the effect BEA. After 48 h of exposure, the decrease in cell proliferation was 67% with respect to that measured for α-ZEL and 36% with respect to that measured for BEA. After 72 h of exposure, the viability decreased 53% with respect to α-ZEL and 43% with respect to BEA. After 24 h of exposure, the β-ZEL + BEA combination (Figure 2b) decreased cell proliferation by about 55% and 29% at the highest concentration with respect to β-ZEL and BEA tested individually, respectively. After 48 h of exposure, the highest concentration of the combination reduced cell proliferation by 11% with respect to BEA tested individually. Also, at 72 h of exposure, the combination decreased cell proliferation by approximately 36% with respect to BEA individually tested. Such effect was not noticed after 48 and 72 h with respect to b-ZEL. In Figure 2c, the α-ZEL + β-ZEL combination after 24 h of exposure showed 17% of decrease in cell proliferation compared to β-ZEL individually assayed. After 48 and 72 h of exposure, the highest concentration of the combination reduced cell proliferation by 60% and 50%, respectively, compared to α-ZEL tested alone, whereas, this did not happen with respect to β-ZEL after 48 and 72 h of exposure. Figure 3 shows the dose–response curves for the tertiary combination of α-ZEL, β-ZEL, and BEA at 24, 48, and 72 h of exposure in SH-SY5Y cells. At 24 h of exposure, cell proliferation decreased by 16%, 44%, and 18% compared to cells exposed to α-ZEL, β-ZEL, and BEA alone. After 48 and 72 h of exposure, a significant reduction in cell proliferation, corresponding to 57% and 51%, was observed with respect to α-ZEL alone, and a reduction of 26% and 41% was observed with respect to BEA alone, while such effect was not observed with respect to β-ZEL alone.

The isobologram analysis was used to determine the type of interaction between α-ZEL, β-ZEL, and BEA. The values of the parameters *Dm*, *m*, and *r* of the double and triple combinations, as well as of the mean combination index (CI) are shown in Table 2. The IC_{50}, IC_{75}, and IC_{90} are the doses required to inhibit proliferation at 25%, 50%, 75%, and 90%, respectively. These CI values were calculated automatically by the computer software CalcuSyn. The CI fractional effect (*fa*) curves for α-ZEL, β-ZEL, and BEA combinations in SH-SY5Y cells are shown in Figure 4. Synergism for all concentration of the α-ZEL + BEA (5:1) mixture after 24 and 48 h of exposure was demonstrated; however, after 72 h of exposure, an additive effect for the α-ZEL + BEA combination was observed (Figure 4a, Table 2). The β-ZEL + BEA (5:1) mixture showed synergism after 24 h of exposure; however, after 48 and 72 h it showed antagonism at high concentrations and moderate synergism at low concentrations (Figure 4b, Table 2). The mixture of α-ZEL + β-ZEL showed antagonism after 24 h of exposure at all concentrations assayed but at 48 and 72 h, it showed antagonism at high concentration and a moderate synergism at low concentration (Figure 4c, Table 2). The tertiary mixture, after 24 h of exposure, showed antagonism at high concentration and synergism at low concentration, while after 48 h, it showed synergism and after 72 h, antagonism at all concentrations assayed (Figure 4d, Table 2).

Cytotoxicity after 24 h of incubation decreased in this order: α-ZEL + BEA > β-ZEL + BEA > α-ZEL + β-ZEL + BEA > α-ZEL + β-ZEL. After 48 and 72 h of incubation, the ranking was α-ZEL + BEA > β-ZEL + BEA >α-ZEL + β-ZEL > α-ZEL + β-ZEL + BEA.

2.2. *α-ZEL, β-ZEL, and BEA Present in Cell Medium after Treatment in Binary and Tertiary Combination*

The medium of SH-SY5Y cells containing α-ZEL, β-ZEL, and BEA after treatments (individual and combined after 24, 48, and 72h) was collected from each well. The amount of each mycotoxin remaining in the medium was calculated as a percentage with respect to the respective amount used in the exposure assays. In this sense, we determined whether the amounts were above or below 50% of those used for treatment (Figure 5). In individual exposures, the amounts of BEA and β-ZEL in the medium were below 50% at 48 and 72 h (Figure 5b,c), while, at 24 h, their concentrations tended to be higher and >50% for both mycotoxins. For α-ZEL, the concentration in the medium was maintained above 50% at all times studied (Figure 5a). This evidenced that a lower amount of α-ZEL exerted the

examined effect compared to the amount necessary for BEA and β-ZEL, as higher amounts of α-ZEL were detectable in the medium at all times and concentrations.

In the binary combination α-ZEL + BEA (5:1), the amounts of each mycotoxin after 24 and 48 h were below 50% (Figure 5d.1,d.2), although the amount of BEA was higher than that of α-ZEL once the concentration assayed overpassed 0.62 μM for BEA and 3.12 μM for α-ZEL, revealing that the effects exerted by this mixture in neuroblastoma cells depended on both mycotoxins and were due more to α-ZEL than to BEA. This tendency at 72 h was more accentuated, as the amount of BEA in the medium was above 50% for all concentrations, while that of α-ZEL was below 50% (Figure 5d.3).

Also, for the combination β-ZEL + BEA (5:1), the mycotoxin's percentage remaining in the media was the same as that found for α-ZEL + BEA; however, β-ZEL was detected in higher amount than BEA in all scenarios, revealing that the effect of this mixture and was due more to BEA than to β-ZEL (Supplementary Figure S1A). On the other hand, for the binary combination of ZEN metabolites, α-ZEL + β-ZEL (1:1), the amounts of mycotoxins recovered were below 50%, and slightly superior for α-ZEL than for β-ZEL. This revealed that both mycotoxins contributed to the effect of this mixture in SH-SY5Y cell line (Supplementary Figure S1B). For the tertiary combination (α-ZEL + β-ZEL + BEA, (5:5:1)), the mycotoxins' percentages detected were also below 50% of the administered concentration, and this percentage was higher for higher concentrations administered and lower time of exposure (Figure 5e). This revealed that high amounts of α-ZEL and β-ZEL accessed the neuroblastoma cells, and the effect was due more to β-ZEL at 48 and 72 h, according to the results in Figures 3 and 5.

Table 2. The parameters *Dm*, *m*, and *r* are the antilog of x-intercept, the slope, and the linear correlation of the median-effect plot, which means the shape of the dose–effect curve, the potency (IC_{50}), and the conformity of the data to the mass action law, respectively [30,31]. *Dm* and *m* values are used for calculating the combination index (CI) value (CI < 1, =1, and >1 indicate synergism (Syn), additive (Add) effect, and antagonism (Ant), respectively. IC_{50}, IC_{75}, and IC_{90} are the doses required to inhibit proliferation at 50%, 75%, and 90%, respectively. CalcuSyn software automatically provided theses values.

Mycotoxin	Time (h)	Dm (μM)	m	r	IC Values					
					IC_{50}		IC_{75}		CI_{90}	
α-ZEL	24	66.10	1.36	0.9679						
	48	31.59	1.82	0.9726						
	72	15.24	2.02	0.9873						
β-ZEL	24	171.33	1.28	0.9709						
	48	12.46	1.26	0.9715						
	72	11.65	2.28	0.9464						
BEA	24	21.65	0.98	0.9763						
	48	3.68	1.24	0.9945						
	72	2.59	1.40	0.9805						
α-ZEL+BEA	24	3.05	1.36	0.9736	0.37 ± 0.33	Syn	0.34 ± 0.35	Syn	0.31 ± 0.38	Syn
	48	1.16	1.56	0.9933	0.50 ± 0.24	Syn	0.47 ± 0.26	Syn	0.44 ± 0.29	Syn
	72	1.34	1.54	0.94708	0.96 ± 0.86	Add	1.00 ± 0.51	Add	1.20 ± 1.30	Ant
β-ZEL+BEA	24	3.78	1.20	0.9698	0.29 ± 0.19	Syn	0.26 ± 0.21	Syn	0.24 ± 0.24	Syn
	48	4.81	3.04	0.7744	3.24 ± 0.42	Ant	1.94 ± 0.32	Ant	1.00 ± 0.14	Add
	72	1.89	3.14	0.7585	1.35 ± 0.51	Ant	1.00 ± 0.12	Add	0.60 ± 0.52	Syn
α-ZEL+β-ZEL	24	133.46	1.73	0.7782	2.80 ± 1.01	Ant	2.32 ± 0.51	Ant	1.92 ± 0.62	Ant
	48	19.12	3.40	0.7782	2.14 ± 0.23	Ant	1.35 ± 0.18	Ant	0.30 ± 0.14	Syn
	72	7.89	5.01	0.9409	2.60 ± 0.90	Ant	1.42 ± 0.63	Ant	0.45 ± 0.42	Syn
α-ZEL+β-ZEL+BEA	24	3.74	3.14	0.9478	0.57 ± 0.30	Syn	0.32 ± 0.20	Syn	0.19 ± 0.14	Syn
	48	0.01	0.43	0.7465	0.23 ± 0.06	Syn	0.15 ± 0.07	Syn	0.18 ± 0.10	Syn
	72	7.47	2.30	0.8966	8.54 ± 0.77	Ant	7.60 ± 0.85	Ant	6.88 ± 0.95	Ant

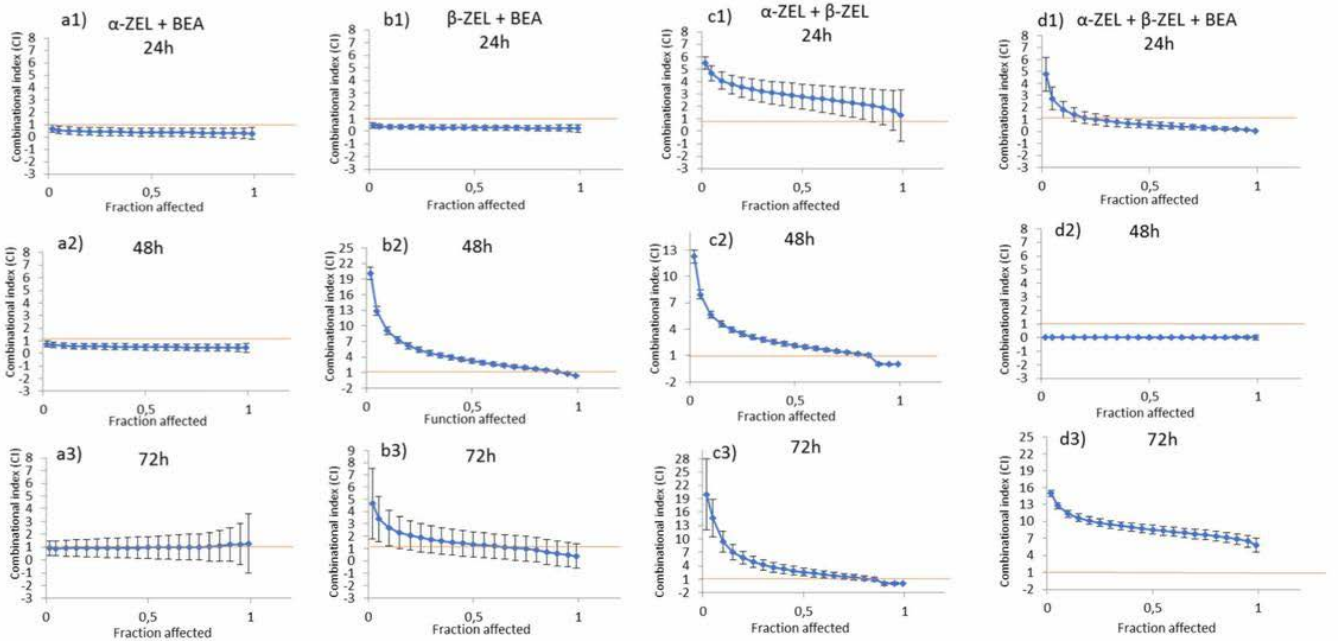

Figure 4. CI vs. fractional effect curve, as described by Chou and Talalay, for SH-SY5Y cells exposed to α-ZEL, β-ZEL, and BEA in binary and tertiary combinations. Each point represents the CI ± SD at a fractional effect as determined in our experiments. The line (CI = 1) indicates additivity, the area under this line indicates synergism, and the area above the line indicates antagonism. SH-SY5Y cells were exposed for 24, 48, and 72 h to α-ZEL + BEA and β-ZEL + BEA at a molar ratio of 5:1 (equimolar proportion), to α-ZEL + β-ZEL at a molar ratio of 1:1, and to α-ZEL + β-ZEL + BEA at a molar ratio of 5:5:1.

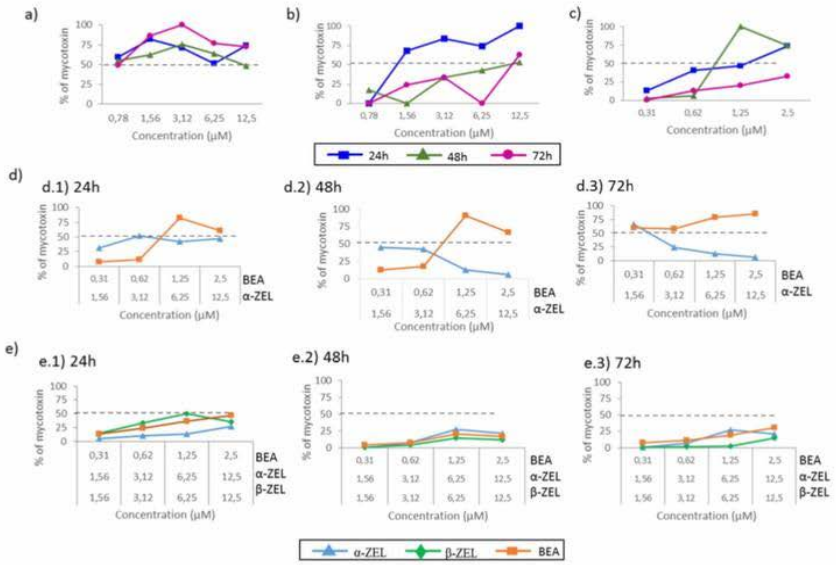

Figure 5. Percentage of α-ZEL, β-ZEL, and BEA remaining in the medium of SH-SY5Y cells after treatment for 24, 48, and 72 h at different concentrations individually or in combination by LC–ESI–qTOF-MS. (**a**) α-ZEL; (**b**) β-ZEL; (**c**) BEA; (**d**) α-ZEL + BEA and (**e**) α-ZEL + β-ZEL + BEA.

3. Discussion

Several studies have discussed the cytotoxic and an anti-proliferative effect of ZEN mycotoxin and its metabolites in various cell lines, such as Caco-2 [11], HepG2 cells [13], CHO-K1 cells [32], and SH-SY5Y [6], and hose of BEA mycotoxin in Caco [14], CHO-K1 [19], and Hep G2 cells [17]. However, there are no reports on the effect of ZEN metabolites and BEA in neuronal cells. In the present study, we proved the toxicity of ZEN metabolites (α-ZEL and β-ZEL) and BEA in human neuroblastoma SH-SY5Y cells in relation to exposure time, mycotoxin concentration, and mixture of mycotoxins.

According to the IC_{50} values of single mycotoxins, β-ZEL was the most cytotoxic mycotoxin compared to the other mycotoxins assayed individually, which is in accordance with Marin et al. (2019) [33] who studied the cytotoxicity of ZEN and its metabolites in HepG2 cells, individually and in double combinations. On the contrary, Tatay et al. (2014) [32] demonstrated that α-ZEL was the most cytotoxic among three mycotoxins tested (α-ZEL, β-ZEL, and ZEN) in CHO-K1 cells. Regarding to double combinations, it was revealed that presence of two mycotoxins increased the cytotoxic potential in SH-SY5Y cells, as shown by the lower IC_{50} values. According to Figure 2a, IC50 for α-ZEL and BEA was not reached in individual treatment however, binary combination α-ZEL + BEA (5:1) inhibited cell proliferation from up to 50 to 90% for all times studied. For the β-ZEL + BEA (5:1) binary combination, as it can be observed in Figure 2b, the IC_{50} values at 48 and 72 h were lower than that of β-ZEL. This was also observed when β-ZEL was combined with α-ZEL, for which combination (α-ZEL + β-ZEL (1:1)), the IC_{50} value was the same as that found for β-ZEL alone. This result was not achieved by Tatay et al. (2014) [31] in CHO-K1 cells, although the mycotoxin concentrations studied in binary assays in that work were two times higher than the concentrations assayed in our study. The proliferation of CHO-K1 cells treated with the α-ZEL + β-ZEL mixture at the highest concentration

decreased only by 20% with respect to the values found when each mycotoxin was tested alone. In addition, in that study, the IC_{50} value was never reached for binary mixtures, whereas in our study in SH-SY5Y cells, after 48 and 72 h, the α-ZEL + β-ZEL combination inhibited cell proliferation up to 70% and 90%, respectively (Figure 2c). For the triple combination (α-ZEL + β-ZEL + BEA, (5:5:1)), cell proliferation inhibition was lower than when β-ZEL was assayed individually, and the same result was found for β-ZEL + BEA after 48 and 72 h and for α-ZEL + β-ZEL after 48 h in SH-SY5Y cells. This is in contrast with the results obtained for the tertiary combination of α-ZEL + β-ZEL + ZEN in CHO-K1 cells, as this combination was more cytotoxic than each mycotoxin tested alone [30].

As the co-occurrence of mycotoxins in food and feed is very common, some studies evaluated the toxicity and cytotoxicity of several mycotoxins, both individually and in combination, in different cell lines, using the isobologram model. In these experiments, HepG2 cells were exposed to ochratoxin A (OTA) and BEA [16], to double and triple combinations of alternariol, 3-acetyl-deoxynivalenol, and 15-acetyl-deoxynivalenol [28], and to combinations of ZEN and OTA or α-ZEL (tested also individually) [33], CHO-K1 cells in vitro were used to examine the interactions between the mycotoxins beauvericin, deoxynivalenol (DON), and T-2 toxin [26] as well as the combination of BEA, patulin, and ZEN [17], whereas Caco-2 cells were exposed to DON, ZEN, and Aflatoxin B1 [34]. It is important to understand whether the interaction between mycotoxins shows synergism, additive effects, and/or antagonism concerning cell viability.

In SH-SY5Y cells, almost all the combinations tested reduced cell viability more than the individual mycotoxins, except the β-ZEL + BEA (5:1), α-ZEL + β-ZEL (1:1), and α-ZEL + β-ZEL + BEA (5:5:1) combinations, for which the reduction in cell viability was not significantly different from that obtained when β-ZEL was assayed individually. According to Dong et al. (2010) [5], ZEN is degraded more efficiently to α-ZEL than to β-ZEL in almost all tissues, whereas it is converted more efficiently to β-ZEL than to α-ZEL in liver and lungs. Some studies demonstrated that β-ZEL is more cytotoxic than α-ZEL [31,35,36], whereas other studies found that α-ZEL is more cytotoxic [30,35]. Hence, there is a necessity to clarify the cytotoxicity of these two mycotoxins with studies of the toxicity mechanisms involved.

The IC_{50} values obtained by the MTT assay and the amount of mycotoxin detected in the media by LC–ESI–qTOF-MS were determined and translated into percentage values as an attempt to calculate the amount of each mycotoxin involved in the cytotoxic effect and in the type of interaction effect. Hence, the percentage of mycotoxin present in the media was considered in accordance to the IC_{50} value obtained from the MTT assay (Table 1). The results showed that among the individual mycotoxins assayed, the amount of α-ZEL that remained in the culture medium was above 50% of the administered quantity at all times assayed (Figure 5a). This can be related to the effect in Figure 1a, which shows that the viability was above 100% for the doses reported in Figure 5. This can be justified by the chemical structure of this compound, which might impede its access in the cell. Our results suggest that the availability and capacity of the tested mycotoxins to get into cells were greater than those of α-ZEL, and as a consequence, the amounts of these mycotoxins detected in the media were lower than that of α-ZEL. To notice that the higher the amount of mycotoxin in the medium (at 24 h), the higher the cell viability, which might be related to the lower amount of mycotoxin affecting the live cells. On the contrary, BEA seemed to have easier access the cells, as its percentage in the medium was generally below 50%, but cell viability was maintained above 50% for the doses assayed, indicating the lower potential toxicity of BEA in SH-SY5Y cells compared to ZEN metabolites. In fact, among all three mycotoxins tested, BEA reached the IC_{50} values after long exposures times (72 h) (Table 1 and Figure 1c), highlighting again the mild toxic effect of BEA in SHY-SY5Y cells compared to ZEN metabolites.

According to this and when analyzing combinations, the amounts of ZEN metabolites found in the medium were in most cases below BEA's amounts, indicating easier access of these compounds in SH-SY5Y compared to BEA. In detail, for the α-ZEL + BEA combination (Figure 2a), it can be observed that the lower the amount of α-ZEL in the medium over time (Figure 5d), the lower the viability of SH-SY5Y cells, in particular at 72h. For triple mixtures, the cytotoxic effect was weaker

at all times and for all mixtures compared with that of binary combinations; however, the amounts of each mycotoxin detected were all below 50%, and the cytotoxic effect seemed to be bearable for SH-SY5Y cells for doses administered in the first and second mixture but not for those of the third mixture (6.25 + 6.26 + 1.25) μM (α-ZEL + β-ZEL + BEA, 5:5:1), specifically at 48 and 72 h. We suggest that cytotoxicity is due to the stimulation of different biochemical mechanisms that, after a certain level of stimulation, cannot be controlled and cause cell death. Therefore, it is necessary to study in detail the mechanisms of action implicated in the cytotoxic effects that occur when several mycotoxins are present in the same food or diet.

4. Conclusions

In conclusion, the treatment with β-ZEL alone presented the highest cytotoxicological potency compared to treatments with the other mycotoxins assayed (α-ZEL and BEA). The main type of interaction detected between mycotoxins for all combinations assayed was synergism. The potential interaction effects between combinations in this study are difficult to explain since α-ZEL + BEA for binary and α-ZEL + β-ZEL + BEA for tertiary combination were found more in favor of synergic effect respect to CI value, compared with other combinations, which could be related to the concentration range studied, ratio in each mixture, exposure time assayed and cell line studied. Moreover, among all mycotoxins assayed, α-ZEL appeared to remain in the culture medium and was less able to get into SH-SY5Y cells compared to BEA and β-ZEL. In combinations, such effect was observed for BEA reaching the highest in α-ZEL + BEA.

5. Materials and Methods

5.1. Reagents

The reagent-grade chemicals and cell culture components used, Dulbecco's Modified Eagle's Medium- F12 (DMEM/F-12), fetal bovine serum (FBS), and phosphate-buffered saline (PBS) were supplied by Thermofisher, Gibco ™ (Paisley, UK). Methanol (MeOH, HPLC LS/MS grade), was obtained from VWR International (Fontenay-sous-Bois, France). Dimethyl sulfoxide was obtained from Fisher Scientific Co, Fisher BioReagnts ™ (Geel, Belgium). The compound (3-(4,5-dimethylthiazol-2-yl)-2,5-diphenyltetrazolium bromide) (MTT) for the MTT assay, penicillin, streptomycin, and Trypsin–EDTA were purchased from SigmaAldrich (St. Louis, MO, USA). Deionized water (<18, MΩcm resistivity) was obtained in the laboratory using a Milli-QSP® Reagent Water System (Millipore, Beadford, MA, USA). Standard BEA (MW: 783.95 g/mol), α-ZEL, and β-ZEL (MW: 320.38 g/mol) were purchased from SigmaAldrich (St. Louis Mo. USA) (Figure 6). Stock solutions of mycotoxins were prepared in MeOH (α-ZEL and β-ZEL) and DMSO (BEA) and maintained at −20 °C in the dark. The final concentration of either methanol or DMSO in the medium was ≤1% (v/v) as previously established. All other reagents were of standard laboratory grade.

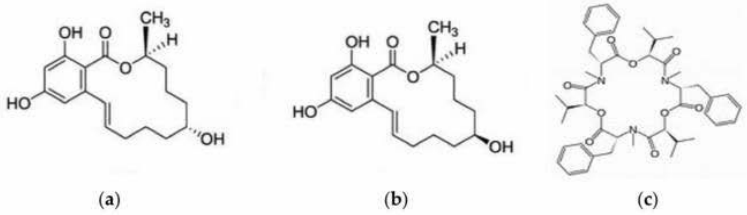

Figure 6. Chemical structures of the mycotoxins (**a**) α-ZEL, (**b**) β-ZEL, and (**c**) BEA.

5.2. Cell Culture

The human neuroblastoma cell line SH-SY5Y was obtained from the American Type Culture Collection (ATCC, Manassas, VA, USA) and cultured in Dulbecco's Modified Eagle's Medium/F12 (DMEM/F-12), supplemented with 10% FBS, 100 U/mL penicillin, and 100 mg/mL streptomycin. The cells were sub-cultivated after trypsinization once or twice a week and suspended in complete medium in a 1:3 split ratio. The cells were maintained as monolayers in 150 cm^2 cell culture flasks with filter screw caps (TPP, Trasadingen, Switzerland). Cell cultures were incubated at 37 °C, 5% CO_2 atmosphere.

5.3. Mycotoxin Exposure

Concentration of the mycotoxins and exposure time are two factors that were considered to in this study. The cells were exposed to α-ZEL, β-ZEL, and BEA mycotoxins individually for 24, 48, and 72 h at a concentration in the ranges of 0.39 to 100 μM for α-ZEL and β-ZEL and 0.009 to 25 μM for BEA, all with 1:2 dilution (Table 3). Also, the mycotoxins were assayed in combination in the following mixtures: α-ZEL + BEA, β-ZEL + BEA, α-ZEL + β-ZEL, and α-ZEL + β-ZEL + BEA at three exposure times 24, 48, and 72 h. The concentrations ranged from 1.87 to 25 μM for the binary combinations were studied and from 3.43 to 27.5 μM for the tertiary combination, including four dilutions of each mycotoxin: BEA (0.31, 0.62, 1.25, and 2.5 μM), α-ZEL and β-ZEL (1.56, 3.12, 6.25 and 12.5 μM) (Table 3). The dilution ratios of the concentrations for the binary combinations were 5:1 for α-ZEL + BEA and β-ZEL + BEA, 1:1 for α-ZEL + β-ZEL, and 5:5:1 for the tertiary combination (β-ZEL + α-ZEL + BEA) (Table 3).

Table 3. Concentration range (μM) of mycotoxins studied individually and in combinations. The dilution ratios were 5:1 for the combinations α-ZEL + BEA and β-ZEL + BEA, 1:1 for α-ZEL + β-ZEL, and 5:5:1 for α-ZEL + β-ZEL + BEA.

Combination Tested	Concentration Range (μM)
α-ZEL	(0.39–00)
β-ZEL	(0.39–100)
BEA	(0.009–25)
α-ZEL + BEA	(1.56–2.5) + (0.31–2.5)
β-ZEL + BEA	(1.56–2.5) + (0.31–2.5)
α-ZEL + β-ZEL	(1.56–12.5) + (1.56–12.5)
α-ZEL + β-ZEL + BEA	(1.56–12.5) + (1.56–12.5) + (0.31–2.5)

5.4. MTT Assay

Cytotoxicity was examined by the MTT assay, performed as described by Ruiz et al. (2006) [37], with few modifications. The assay consists in measuring the viability of cells by determining the reduction of the yellow soluble tetrazolium salt only in cells that are metabolically active via a mitochondrial reaction to an insoluble purple formazan crystal. Cells were seeded in 96-well culture plates at 2 × 96 cells/well and allowed to adhere for 18–24 h before mycotoxin additions. Serial dilutions of α-ZEL, β-ZEL, and BEA at 1:2 dilutions were prepared with supplemented medium and added to the respective plates (Table 3). Culture medium without mycotoxins and with 1% MeOH or DMSO was used as a control. After treatment, the medium was removed, and each well received 200 μL of fresh medium containing 50 μL of MTT solution (5 mg/mL; MTT powder dissolved in phosphate-buffered saline). After an incubation time of 4 h at 37 °C in the darkness, the MTT-containing medium was removed, and 200 μL of DMSO and 25 μL of Sorensen's solution were added to each well before reading the optical density at 620 nm with the ELISA plate reader Multiskan EX (Thermo Scientific, MA, USA). Each mycotoxin combination plus a control were tested in three independent experiments. Mean inhibition concentration (IC_{50}) values were calculated from full dose–response curves.

5.5. Experimental Design and Combination Index

The isobologram analysis (Chou–Talalay model) was used to determine the type of interaction (synergism, additive effect, and antagonism) that occurred when the mycotoxins studied were in combination. This model allows characterizing the interactions induced by combinations of mycotoxins in different cell lines and with different mycotoxins but it does not allow the elucidation of the mechanisms by which these types of interaction are produced. The median effect/combination index (CI) isobologram equation by Chou (2006) [31] and Chou and Talalay (1984) [30] permitted analyzing drug combination effects. The isobologram analysis involves plotting the dose–effect curves for each compound and its combinations in multiple diluted concentrations. Parameters such as *Dm* (median effect dose), *fa* (fraction affected by concentration), and *m* (coefficient signifying the shape of the dose–effect relationship) are relevant in the equation [30]. Therefore, the method considers both potency (*Dm*) and shape (*m*) parameters.

Chou and Talalay (1984) [30] introduced the term combination index (CI). CI values <1, =1, and >1 indicate synergism, additive effects, and antagonism of the combination, respectively. CalcuSyn software version 2.1. (Biosoft, Cambridge, UK, 1996–2007) was used to study the types of interactions assessed by the isobologram analysis. The IC_{25}, IC_{50}, IC_{75}, and IC_{90} are the doses required to produce toxicity at 25%, 50%, 75%, and 90%, respectively.

5.6. Extraction of α-ZEL, β-ZEL, and BEA from the Culture Media

To determine the intracellular accumulation of the mycotoxins studied, an extraction procedure of the culture media was carried out following the method described by Juan-García et al. (2015 and 2016) [27,28], with several modifications. Briefly, 0.8 mL of culture medium was collected and transferred into a polypropylene tube, 1.5 mL of ethyl acetate was added, and the mixture was shaken for 2 min with an Ultra-Turrax Ika T18 basic (Staufen, Germany). Afterwards, the mixture as sonicated in an ultrasound cleaning bath (VWR, USC1700TH) for 10 min. Finally, the mixture was centrifuged at ~5600× *g* for 5 min at 22 °C (Centrifuge 5810R, Eppendorf, Germany). The supernatant phase was collected. The liquid–liquid extraction process was repeated three times. Finally, the total volume obtained (approx. 4.5 mL) was evaporated to dryness at 45 °C in an N2 stream with a TurboVap-LV (Zymark, Allschwil, Switzerland) and then re-dissolved in 0.25 mL of a mixture of methanol and water (70:30, v/v) by vortexing vigorously (15 s), before being transferred into a vial for LC–ESI–qTOF-MS injection.

5.7. Determination of BEA, β-ZEL, and α-ZEL by LC–ESI–qTOF-MS

The analysis was performed using an LC–ESI–qTOF-MS system, consisting of an LC Agilent 1200-LC system (Agilent Technologies, Palo Alto, CA, USA) equipped with a vacuum degasser, an autosampler, and a binary pump. The columns were a Gemini NX-C18 column (150 × 2 mm, i.d. 3 µm, Phenomenex, Torrance, California) and a guard column C18 (4 × 2 mm, i.d. 3 µM).

Mobile phases consisted of milli-Q water with 0.1% of formic acid as solvent system A and acetonitrile and 0.1% of formic acid as solvent system B, with the following gradient elution: 3 min, 70% B; in 2 min 70–80% B; in 1 min get 90% of B, maintained 4 min; 90–100% B 4 min and maintained 2 min; in 2 min decrease to 50% B; in 2 min 90% B, maintained 2 min. The flow rate used was 0.250 mL min^{-1}, and the total run time was 22 min. The sample volume injected was 20 µL.

MS analysis was carried out using a 6540 Agilent Ultra- High-Definition Accurate-Mass q-TOF-MS, equipped with an Agilent Dual Jet Stream electrospray ionization (Dual AJS ESI) interface in negative and positive ionization modes. Operation conditions were as follows: sheath gas temperature 350 °C at a flow rate of 8 L/min, capillary voltage 3500 V, nebulizer pressure 45 psig, drying gas 10 L/min, gas temperature 300 °C, skimmer voltage 65 V, octopole RF peak 750 V, and fragmentor voltage 130 V. Analyses were performed using AutoMS/MS mode with fixed collision energy (10, 20 and 30) and in mass range of 50–1700 *m/z*. Acquisition rate was 3 spectra/second. Acquisition data were processed with Agilent MassHunter Workstation software.

5.8. Statistical Analysis

Statistical analysis of data was carried out using IBM SPSS Statistic version 23.0 (SPSS, Chicago, Il, USA) statistical software package. Data are expressed as mean ± SD of three independent experiments. The statistical analysis of the results was performed by student's T-test for paired samples. Difference between groups were analyzed statistically with ANOVA followed by the Tukey HDS post-hoc test for multiple comparisons. The level of $p \leq 0.05$ was considered statistically significant.

Supplementary Materials: The following are available online at http://www.mdpi.com/2072-6651/12/4/212/s1, Figure S1. Percentage of α-ZEL, β-ZEL, and BEA remaining in the medium of SH-SY5Y cells after treatment during 24, 48, and 72 h at different concentrations and combinations by LC–ESI–qTOF-MS. (**A**) β-ZEL+ BEA and (**B**) α-ZEL + β-ZEL.

Author Contributions: Data curation, F.A.; Formal analysis, C.J. and A.J.-G.; Funding acquisition, G.F., C.J., and A.J.-G.; Investigation, F.A., C.J., and A.J.-G.; Methodology, A.J.-G.; Supervision, C.J. and A.J.-G.; Writing—original draft, F.A, C.J. and A.J.-G.; Writing—review & editing, C.J. and A.J.-G. All authors have read and agreed to the published version of the manuscript.

Funding: This research was supported by the Spanish Ministry of Economy and Competitiveness AGL2016-77610-R and the Generalitat Valenciana GVPROMETEO2018-126.

Conflicts of Interest: The authors declare no conflict of interest.

References

1. Zain, M.E. Impact of mycotoxins on humans and animals. *J. Saudi Chem. Soc.* **2011**, *15*, 129–144. [CrossRef]
2. Mally, A.; Solfrizzo, M.; Degen, G.H. Volume Biomonitoring of the mycotoxin Zearalenone: Current state-of-the art and application to human exposure assessment. *Arch. Toxicol.* **2016**, *90*, 1281–1292. [CrossRef] [PubMed]
3. Richard, J.L. Some major mycotoxins and their mycotoxicoses—An overview. *Int. J. Food Microbiol.* **2007**, *119*, 3–10. [CrossRef] [PubMed]
4. Hueza, I.M.; Raspantini, P.C.; Raspantini, L.E.; Latorre, A.O.; Górniak, S.L. Zearalenone, an estrogenic mycotoxin, is an immunotoxic compound. *Toxins* **2014**, *6*, 1080–1095. [CrossRef]
5. Dong, M.; Tulayakul, P.; Li, J.-Y.; Dong, K.-S.; Manabe, N.; Kumagai, S. Metabolic Conversion of Zearalenone to α-Zearalenol by Goat Tissues. *J. Vet. Med. Sci.* **2010**, *72*, 307–312. [CrossRef]
6. Venkataramana, M.; Chandra Nayaka, S.; Anand, T.; Rajesh, R.; Aiyaz, M.; Divakara, S.T.; Murali, H.S.; Prakash, H.S.; Lakshmana Rao, P.V. Zearalenone induced toxicity in SHSY-5Y cells: The role of oxidative stress evidenced by N-acetyl cysteine. *Food Chem. Toxicol.* **2014**, *65*, 335–342. [CrossRef]
7. Gajecka, M.; Zielonka, L.; Gajecki, M. The effect of low monotonic doses of zearalenone on selected reproductive tissues in pre-pubertal female dogs-a review. *Molecules* **2015**, *20*, 20669–20687. [CrossRef]
8. EFSA CONTAM Panel (EFSA Panel on Contaminants in the Food Chain). Scientific opinion on the appropriateness to set a group health-based guidance value for zearalenone and its modified forms. *EFSA J.* **2016**, *14*, 4425.
9. Wang, J.J.; Wei, Z.K.; Han, Z.; Liu, Z.Y.; Zhu, X.Y.; Li, X.W.; Wang, K.; Yang, Z.T. Zearalenone Induces Estrogen-Receptor-Independent Neutrophil Extracellular Trap Release in Vitro. *J. Agric. Food Chem.* **2019**, *67*, 4588–4594. [CrossRef]
10. El-Makawy, A.; Hassanane, M.S.; Abd Alla, E.S.A.M. Genotoxic evaluation for the estrogenic mycotoxin zearalenone. *Reprod. Nutr. Dev* **2001**, *41*, 79–89. [CrossRef]
11. Abid-Essefi, S.; Baudrimont, I.; Hassen, W.; Ouanes, Z.; Mobio, T.A.; Anane, R.; Creppy, E.E.; Bacha, H. DNA fragmentation, apoptosis and cell cycle arrest induced by zearalenone in cultured DOK, Vero and Caco-2 cells: Prevention by Vitamin E. *Toxicology* **2003**, *192*, 237–248. [CrossRef]
12. Cai, G.; Pan, S.; Feng, N.; Zou, H.; Gu, J.; Yuan, Y.; Liu, X.; Liu, Z.; Bian, J. Zearalenone inhibits T cell chemotaxis by inhibiting cell adhesion and migration related proteins. *Ecotox. Environ. Safe* **2019**, *175*, 263–271. [CrossRef]
13. Hassen, W.; El Golli, E.; Baudrimont, I.; Mobio, A.T.; Ladjimi, M.M.; Creppy, E.E.; Bacha, H. Cytotoxicity and Hsp70 induction in HepG2 cells in response to zearalenone and cytoprotection by sub-lethal heat shock. *Toxicology* **2005**, *207*, 293–301. [CrossRef] [PubMed]

14. Prosperini, A.; Juan-García, A.; Font, G.; Ruiz, M.J. Beauvericin induced cytotoxicity via ROS production and mitochondrial damage in Caco-2 cells. *Toxicol. Lett.* **2013**, *222*, 204–211. [CrossRef] [PubMed]
15. Zhang, K.; Tan, X.; Li, Y.; Liang, G.; Ning, Z.; Ma, Y.; Li, Y. Transcriptional profiling analysis of Zearalenone-induced inhibition proliferation on mouse thymic epithelial cell line 1. *Ecotox. Environ. Safe* **2018**, *153*, 135–141. [CrossRef]
16. Zouaoui, N.; Mallebrera, B.; Berrada, H.; Abid-Essefi, S.; Bacha, H.; Ruiz, M.J. Cytotoxic effects induced by patulin, sterigmatocystin and beauvericin on CHO–K1 cells. *Food Chem. Toxicol.* **2016**, *89*, 92–103. [CrossRef]
17. Juan-García, A.; Tolosa, J.; Juan, C.; Ruiz, M.J. Cytotoxicity, Genotoxicity and Disturbance of Cell Cycle in HepG2 Cells Exposed to OTA and BEA: Single and Combined Actions. *Toxins* **2019**, *11*, 341. [CrossRef]
18. Ferrer, E.; Juan-García, A.; Font, G.; Ruiz, M.J. Reactive oxygen species induced by beauvericin, patulin and zearalenone in CHO-K1 cells. *Toxicol. In Vitro* **2009**, *23*, 1504–1509. [CrossRef]
19. Mallebrera, B.; Font, G.; Ruiz, M.J. Disturbance of antioxidant capacity produced by beauvericin in CHO-K1 cells. *Toxicol. Lett.* **2014**, *226*, 337–342. [CrossRef]
20. Stockmann-Juvala, H.; Mikkola, J.; Naarala, J.; Loikkanen, J.; Elovaara, E.; Savolainen, K. Oxidative stress induced by fumonisin B1 in continuous human and rodent neural cell cultures. *Free Radic. Res.* **2004**, *38*, 933–942. [CrossRef]
21. Zhang, X.; Boesch-Saadatmandi, C.; Lou, Y.; Wolffram, S.; Huebbe, P.; Rimbach, G. Ochratoxin A induces apoptosis in neuronal cells. *Genes Nutr.* **2009**, *4*, 41–48. [CrossRef]
22. Zingales, V.; Fernández-Franzón, M.; Ruiz, M.J. Sterigmatocystin-induced cytotoxicity via oxidative stress induction in human neuroblastoma cells. *Food Chem. Toxicol.* **2020**, *136*, 110956. [CrossRef]
23. Stanciu, O.; Juan, C.; Miere, D.; Loghin, F.; Mañes, J. Occurrence and co-occurrence of Fusarium mycotoxins in wheat grains and wheat flour from Romania. *Food Control.* **2017**, *73*, 147–155. [CrossRef]
24. Juan, C.; Berrada, H.; Mañes, J.; Oueslati, S. Multi-mycotoxin determination in barley and derived products from Tunisia and estimation of their dietary intake. *Food Chem. Toxicol.* **2017**, *103*, 148–156. [CrossRef] [PubMed]
25. Oueslati, S.; Berrada, H.; Mañes, J.; Juan, C. Presence of mycotoxins in Tunisian infant foods samples and subsequent risk assessment. *Food Control.* **2017**, *84*, 362–369. [CrossRef]
26. EFSA. Guidance on harmonised methodologies for human health, animal health and ecological risk assessment of combined exposure to multiple chemicals. *EFSA J.* **2019**, *17*, 5634. [CrossRef]
27. Ruiz, M.J.; Franzova, P.; Juan-García, A.; Font, G. Toxicological interactions between the mycotoxins beauvericin, deoxynivalenol and T-2 toxin in CHO-K1 cells in vitro. *Toxicon* **2011**, *58*, 315–326. [CrossRef] [PubMed]
28. Juan-García, A.; Juan, C.; König, S.; Ruiz, M.J. Cytotoxic effects and degradation products of three mycotoxins: Alternariol, 3-acetyl-deoxynivalenol and 15-acetyl-deoxynivalenol in liver hepatocelular carcinoma cells. *Toxicol. Lett.* **2015**, *235*, 8–16. [CrossRef]
29. Juan-García, A.; Juan, C.; Manyes, L.; Ruiz, M.J. Binary and tertiary combination of alternariol, 3-acetyl-deoxynivalenol and 15-acetyl-deoxynivalenol on HepG2 cells: Toxic effects and evaluation of degradation products. *Toxicol. In Vitro* **2016**, *34*, 264–273. [CrossRef]
30. Chou, T.C.; Talalay, P. Quantitative analysis of dose-effect relationships: The combined effects of multiple drugs or enzyme inhibitors. *Adv. Enzyme Regul.* **1984**, *22*, 27–55. [CrossRef]
31. Chou, T.C. Theoretical basis, experimental design, and computerized simulation of synergism and antagonism in drug combination studies. *Pharmacol. Rev.* **2006**, *58*, 621–681. [CrossRef] [PubMed]
32. Tatay, E.; Meca, G.; Font, G.; Ruiz, M.J. Interactive effects of zearalenone and its metabolites on cytotoxicity and metabolization in ovarian CHO-K1 cells. *Toxicol. In Vitro* **2014**, *28*, 95–103. [CrossRef] [PubMed]
33. Marin, D.E.; Pistol, G.C.; Bulgaru, C.V.; Taranu, I. Cytotoxic and inflammatory effects of individual and combined exposure of HepG2 cells to zearalenone and its metabolites. *N-S. Arch. Pharmacol.* **2019**, *392*, 937–947. [CrossRef] [PubMed]
34. Zheng, N.; Gao, Y.N.; Liu, J.; Wang, H.W.; Wang, J.Q. Individual and combined cytotoxicity assessment of zearalenone with ochratoxin A or α-zearalenol by full factorial design. *Food Sci. Biotechnol.* **2018**, *27*, 251–259. [CrossRef] [PubMed]
35. Jia, J.; Wang, Q.; Wud, H.; Xiaa, S.; Guoa, H.; Blaženovićc, I.; Zhanga, Y.; Suna, X. Insights into cellular metabolic pathways of the combined toxicity responses of Caco-2 cells exposed to deoxynivalenol, zearalenone and Aflatoxin B1. *Food Chem. Toxicol.* **2019**, *126*, 106–112. [CrossRef] [PubMed]

36. Abid, S.; Bouaziz, C.E.; Golli-Bennour, E.; Ouanes Ben Othmen, Z.; Bacha, H. Comparative study of toxic effects of zearalenone and its two major metabolites α-zearalenol and β-zearalenol on cultured human Caco-2 cells. *J. Biochem. Mol. Toxic.* **2009**, *23*, 233–243. [CrossRef] [PubMed]
37. Ruiz, M.J.; Festila, L.E.; Fernandez, M. Comparison of basal cytotoxicity of seven carbamates in CHO-K1 cells. *Environ. Toxicol. Chem.* **2006**, *88*, 345–354. [CrossRef]

Toxicology Letters 334 (2020) 44–52

Contents lists available at ScienceDirect

Toxicology Letters

journal homepage: www.elsevier.com/locate/toxlet

Oxidative stress, glutathione, and gene expression as key indicators in SH-SY5Y cells exposed to zearalenone metabolites and beauvericin

Fojan Agahi[a], Neda Álvarez-Ortega[b], Guillermina Font[a], Ana Juan-García[a,*], Cristina Juan[a]

[a] Laboratory of Food Chemistry and Toxicology, Faculty of Pharmacy, University of Valencia, Av. Vicent Andrés Estellés s/n, 46100 Burjassot, València, Spain
[b] Grupo de Química Ambiental y Computacional, Campus de Zaragocilla, Universidad de Cartagena, Cartagena, Colombia

ARTICLE INFO

Keywords:
α-ZEL
β-ZEL
BEA
ROS
GSH/GSSG
apoptosis
estrogen receptors

ABSTRACT

The co-presence of mycotoxins from fungi of the genus *Fusarium* is a common fact in raw food and food products, as trace levels of them or their metabolites can be detected, unless safety practices during manufacturing are carried out. Zearalenone (ZEA), its metabolites α-zearalenol (α-ZEL) and β-zearalenol (β-ZEL) and, beauvericin (BEA) are co/present in cereals, fruits or their products which is a mixture that consumer are exposed and never evaluated in neuronal cells. In this study the role of oxidative stress and intracellular defense systems was assessed by evaluating reactive oxygen species (ROS) generation and glutathione (GSH) ratio activity in a human neuroblastoma cell line, SH-SY5Y cells, treated individually and combined with α-ZEL, β-ZEL and BEA. It was further examined the expression of genes involved in cell apoptosis (*CASP3, BAX, BCL2*) and receptors of (endogenous or exogenous) estrogens (*ERβ* and *GPER1*), by RT-PCR in those same conditions. These results demonstrated elevated ROS levels in combinations where α-ZEL was involved (2.8- to 8-fold compared to control); however, no significant difference in ROS levels were detected when single mycotoxin was tested. Also, the results revealed a significant increase in GSH/GSSG ratio at all concentrations after 24 h. Expression levels of *CASP3* and *BAX* were up regulated by α-ZEL while *CASP3* and *BCL2* were down regulated by β-ZEL, revealing how ZEA´s metabolites can induce the expression of cell apoptosis genes. However, BEA down-regulated the expression of *BCL2*. Moreover, β-ZEL + BEA was the only combination treatment which was able to down regulate the levels of cell apoptosis gene expression. Relying to our findings, α-ZEL, β-ZEL and BEA, induce injury in SH-SY5Y cells elevating oxidative stress levels, disturbing the antioxidant activity role of glutathione system and finally, causing disorder in the expressions and activities of the related apoptotic cell death genes.

1. Introduction

Mycotoxins are low-molecular-weight toxic compounds synthetized by diff ;erent types of molds belonging mainly to the genera *Aspergillus*, *Penicillium*, *Fusarium* and *Alternaria* (Berthiller et al., 2013). The management of the *Fusarium* phytopathogens has been proven to be difficult due to their high genetic variability and broad host specificity (Ploetz et al., 2015). Mycotoxin-producing *Fusarium* species are major pathogens in cereals like wheat, oats, barley, and maize (Nganje et al., 2004; Stanciu et al., 2017a; Juan et al., 2017a, 2017b, 2017b; Oueslati et al., 2020).

Among the *Fusarium* mycotoxins, one of the primarily concerned is zearalenone (ZEA), commonly found in cereals like barley, sorghum, oats, wheat, millet, and rice. (Stanciu et al., 2017a; Bakker et al., 2018; Perincherry et al., 2019; Oueslati et al., 2020). The two major metabolites of ZEA are α-zearalenol (α-ZEL) and β-zearalenol (β-ZEL) which are metabolized in various tissues, particularly in the liver (Fig. 1) (EFSA, 2011 and 2017). There are various studies which have determined the effects of ZEA and its metabolites both *in vivo* and *in vitro* to characterize their estrogenic effect (Hueza et al., 2014; Tatay et al., 2017a; Zheng et al., 2019). It is also reported that they exert harmful health eff ;ect via decreasing fertility, increased fetal resorption, and changes in the weight of endocrine glands and serum hormone levels. However, exposure to these mycotoxins are not only limited to their estrogenic eff ;ect, but other mechanisms such as oxidative stress, cytotoxicity and DNA damages might be important mediators involved in their toxicity (Abid et al., 2009; Tatay et al., 2014, 2016, 2017b; Marin et al., 2019; Agahi et al., 2020).

On the other hand, beauvericin (BEA) also belongs to *Fusarium* species and can cause cytotoxic effects by reducing cell proliferation in time and in concentration dependent manner according to recent publications (Zouaoui et al., 2016; Juan-García et al., 2019a).

* Corresponding author.
E-mail address: ana.juan@uv.es (A. Juan-García).

https://doi.org/10.1016/j.toxlet.2020.09.011
Received 7 June 2020; Received in revised form 11 September 2020; Accepted 15 September 2020
Available online 18 September 2020
0378-4274/

Fig. 1. Chemical structures of the mycotoxins: α-ZEL and β-ZEL, BEA.

Moreover, it can increase ROS generation, lipid peroxidation and produce oxidative stress and depletion of antioxidant cellular mechanisms (Ferrer et al., 2009; Prosperini et al., 2013; Mallebrera et al., 2014; Manyes et al., 2018; Juan-García et al., 2019b; and 2020).

Since, in the real scenario, more than one mycotoxin can exist in food products, we dedicated our previous study to investigate the cytotoxic effect of co-presence of all three mentioned compounds on undifferentiated human neuroblastoma cell line (SH-SY5Y cells) and observed how they interfere with the normal functioning of cell proliferation (Agahi et al., 2020). According on our findings, the major effect detected in all combinations was synergism, and the highest cytotoxicity was observed when three mycotoxins were presented together. Therefore, there was a clear need for more comprehensive and reliable toxicology data to determine the reasons which lead to cytotoxicity and reduction of cell proliferation.

Undifferentiated SH-SY5Y cells endogenously express estrogen receptors (Grassi et al., 2013), which function as ligand-activated transcription factors to regulate gene transcription (Ding et al., 2019). The potential of ZEA´s metabolites in such direction plus mixtures with BEA add insights in elucidating that effect and not only through the most susceptible cells (Ventakarama et al., 2014). BEA reaches the blood brain barrier (BBB) if it passes to the systemic circulation and hence, it is capable of exerting central nervous system effects as demonstrated in a recent *in vitro* study of BBB transport (with homogenates of mouse brain) (Taevernier et al., 2016). Mycotoxins of the same family (enniatin B and B1) in a porcine BBB model using different cell lines demonstrated to reach the brain parenchyma, highlighting the neurotoxic effect of these mycotoxins (Krug et al., 2018). SH-SY5Y seems to be a good model for studying *in vitro* effects at neuronal level. A bottle-neck is the dose of exposure to study because of the low concentrations of α-ZEL and β-ZEL found in plasma and urine (Föllmann et al., 2016; Shephard et al., 2013; Wallin et al., 2015); so that, to get a good evaluation of toxic effect *in vitro*, the dose of exposure must be higher than those reported in circulation. In fact, some experiment performed to the BBB transport *in vivo* in mice used non-real exposure routes (intravenously and intracerebroventricularly) to ensure its experiments (Taevernier et al., 2016) as well as for bioavailability and toxicokinetic studies in pigs (Catteuw et al., 2019).

Cells have cellular protection mechanisms against biological reactive intermediates, xenobiotics (including mycotoxins) and metabolic products. When there is an imbalance between the production of oxidizing molecular species or ROS and the co-presence of cellular antioxidant agents in favor of the pro-oxidants, it can initiate events that contribute to production of oxidative stress and afterwards can damage mainly lipids, proteins and DNA (Hassen et al., 2007; Tatay et al., 2016; Juan-García et al., 2019b; and 2020). Moreover, the reduced glutathione (GSH)/glutathione disulfide (GSSG) redox couple is an important marker of oxidative stress due to its antioxidative role and high concentrations in cells.

In accordance with several studies, it has been shown that ZEA and its metabolites are generally hypothesized to mimic estrogen-like actions and compete with estrogens in binding to estrogen receptors (*ERs*) which is including the classical estrogen receptor alpha (*ERα*), estrogen receptor beta (*ERβ*) and G protein-coupled estrogen receptor (*GPER1*); these mycotoxins also decreased follicle stimulant hormone (FSH) synthesis and secretion through non-classical estrogen membrane receptor *GPR30* which it is also called *GPER1* (He et al., 2018; Kuiper-Goodman et al., 1987). Due to the structural similarity of these compounds to the endogenous estrogens (Parveen et al., 2009), their ability to activate the ERs leading to transcription of estrogen-responsive genes is a keypoint in this report.

Moreover, the *Bcl-2* family members are involved in the regulation of apoptosis by either inhibiting or promoting apoptosis (Martin et al., 1995). Other proteins, including the caspase family, play an additional role in the apoptotic process (Zamai et al., 1996). Several mycotoxins are able to activate caspases and *Bcl-2* family by triggering the apoptosis-inducing factor from the mitochondria. Accumulating evidence has indicated that ZEA induce apoptosis in bovine mammary epithelial cells via *CASP3, BAX, BCL2* genes (Fu et al., 2019); also in porcine granulosa cells via the caspase-3- and caspase-9-dependent mitochondrial signaling pathway (Liu et al., 2018; Zhu et al., 2012).

Hence, the objective of this study was to evaluate the effects of α-ZEL, β-ZEL and BEA, mycotoxins on production of reactive oxygen species (ROS) by using the H2-DCFDA probe on undifferentiated human neuroblastoma cell line (SH-SY5Y) during 120 min. It was also studied the GSH/GSSG ratio in these cells affected by all three mycotoxins individually and in combination. Because of the association of ZEA as endocrine disruptor, the expression of genes that code for estrogen receptors (*ER2* (specifically *ERβ*) and *GPER1*) by all three mycotoxins were examined. Furthermore, to obtain more insight into the factors playing a role in the apoptotic process, and since there are few studies about the ability of ZEA derivates and BEA on cell apoptosis, individually or in two or three combinations, the relative mRNA expression levels of *CASP3, BAX* and *BCL2* were evaluated in SH-SY5Y cell line, through RT-PCR.

2. Materials and Methods

2.1. Reagents

The reagent grade chemicals and cell culture components used, Dulbecco's Modified Eagle's Medium- F12 (DMEM/F-12), fetal bovine serum (FBS) and phosphate buffer saline (PBS) were supplied by Thermofisher, Gibco ™ (Paisley, UK). Methanol (MeOH, HPLC LS/MS grade), was obtained from VWR International (Fontenay-sous-Bois, France). Dimethyl sulfoxide was obtained from Fisher Scientific Co, Fisher BioReagnts ™ (Geel, Belgium). [3- (4,5-dimethylthiazol- 2-yl)-2,5-diphenyltetrazolium bromide] (MTT) for MTT assay, penicillin, streptomycin, and Trypsin–EDTA was purchased from SigmaAldrich (St. Louis, MO, USA). Deionized water (< 18, MΩcm resistivity) was obtained in the laboratory using a Milli-QSP® Reagent Water System (Millipore, Beadford, MA, USA). The standard of BEA (MW: 783.95 g/mol), α-ZEL and β-ZEL (MW: 320,38 g/mol) were purchased from SigmaAldrich (St. Louis Mo. USA). Stock solutions of mycotoxins were prepared in MeOH (α-ZEL and β-ZEL) and DMSO (BEA) and maintained at −20 °C in the dark. The final concentration of either MeOH or DMSO

in the medium was ≤1% (v/v) as per established. All other standards were of standard laboratory grade.

2.2. Cell culture

Human neuroblastoma cell line, SH-SY5Y, was obtained from American Type Culture Collection (ATCC, Manassas, VA, USA), and cultured in Dulbecco's Modified Eagle's Medium- F12 (DMEM/F-12), supplemented with 10% fetal bovine serum (FBS), 100 U/ml penicillin, and 100 mg/ml streptomycin. The cells were sub-cultivated after trypsinization once or twice a week and suspended in complete medium in a 1:3 split ratio. Cells were maintained as monolayer in 150 cm^2 cell culture flasks with filter screw caps (TPP, Trasadingen, Switzerland). Cell cultures were incubated at 37 °C, 5% CO_2 atmosphere.

2.3. Intracellular ROS generation

Early intracellular ROS production was monitored in SH-SY5Y cells by using the H2-DCFDA probe. DCFH-DA is taken up by the cells, and then deacetylated by intracellular esterase's and the resulting H_2-DCFDA is oxidized by ROS to the highly fluorescent DCF. Briefly, 2×10^4 cells/well were seeded in a 96-well black culture microplate. After reaching confluence, cells were loaded with 20 μM H_2-DCFDA in fresh medium for 20 min. Subsequently, H_2-DCFDA was removed and cells were washed with PBS and then exposed to α-ZEL and β-ZEL (25, 12.5, 6.25 and 3.12 μM), and BEA (2.5, 1.25, 0.78 and 0.39 μM) as an individual treatment. Afterwards, they were assayed in combination through the following mixtures: α-ZEL + BEA, β-ZEL + BEA, α-ZEL + β-ZEL and α-ZEL + β-ZEL + BEA with concentrations ranged from 25 to 1.87 μM for binary combinations, and from 27.5 to 3.43 μM for tertiary combination. The dilution ratio of concentration ranges in binary combinations was (1:1) for α-ZEL + β-ZEL, (5:1) for α-ZEL + BEA and β-ZEL + BEA, and (5:5:1) in tertiary combinations (α-ZEL + β-ZEL + BEA) (Table 1).

Data of single and combination treatments were obtained by considering the cytotoxicity assays for ZEA metabolites and BEA reported in our previous study (Agahi et al., 2020).

Increases in fluorescence were measured on a Perkin Elmer Wallac 1420 VICTOR2™ Multilabel Counter (Turku, Finland), at intervals up to 2 h at excitation/emission wavelengths of 485/535 nm, respectively. Results are expressed as increase in fluorescence in respect to control (untreated cells). Three independent experiments were performed with eight replicates each.

2.4. GSH determination

Determination of GSH and GSSG was assayed according to Maran et al (2009). Briefly, 7×10^5 cells/well were seeded in six-well plates. Once the cells reached 90% confluence, the culture medium was replaced with fresh medium containing different concentrations of: α-ZEL and β-ZEL (1.56, 3.12, 6.25 and 12.5 μM) BEA (0.31, 0.62, 1.25, and 2.5 μM), individually and in combination for 24 and 48 h of incubation. Afterwards, the medium was removed, and cells were washed with PBS and then homogenized in 0.25 ml of 20 mM Tris and 0.1% Triton.

For GSH determination, 10 μL of each homogenized cell sample was placed in 96 well black tissue culture plate, with 200 μL GSH buffer (pH 8.0) and 10 μL of OPT solution, mixed and incubated in darkness at room temperature for 15 min. For GSSG determination, 25 μL of each homogenized cell sample and 25 μL NEM (*N*-ethylmaleimide, 0.005 g/mL in deionized water) were placed in a 1.5 ml eppendorf, mixed and incubated at room temperature for 20 min. Afterwards, 50 μL of NaOH 0.1 N were added to achieve the correct pH to develop the GSSG assay. 10 μL of the mixture prepared was placed with 200 μL NaOH 1 N and 10 μL of the OPT (O-phthalaldehyde, 0.001 g/mL of in MeOH) solution in 96 well black tissue culture plate, mixed and incubated in darkness at room temperature for 15 min.

Concentrations of GSH and GSSG (prepared in plates described above) were determined using the microplate reader Wallace Victor2, model 1420 multilabel counter (Perkin Elmer, Turku, Finland) with excitation and emission wavelength of 345 and 424 nm, respectively. The GSH and GSSG levels were expressed in μg/mg proteins. Determinations were performed in two independent experiments with 4 replicates each.

Table 1
Sequence of the specific primers used in the analysis of the expression

Gene Symbol	Forward (5' - 3')	Reverse (5' - 3')
CASP3	GGAGGCCGACTTCTTGTATG	GCCATCCTTTGAATTTCGCC
BAX	ATGCGTTTTCCTTACGTGTCT	GAGGTCAGCAGGGTAGATGA
BCL2	CTTCTTTGAGTTCGGTGGGG	AAATCAAACAGAGGCCGCAT
ERβ	AATGCCGATGCCTATCCTCT	ATGGCAAATGAACAGGCAAAG
GPER1	CTCAGCGGACAAAGGATCAC	ACTTCAGCGAATCTCACTCC

2.5. Gene expression assay by RT-PCR

The real-time polymerase chain reaction (RT-PCR) was applied to do the gene expression assay on SH-SY5Y cells, which were counted and placed (7×10^5 cells/well) in 6-well tissue culture plates. After 24 h, the cells were exposed individually to α-ZEL (12.5 and 25 μM), β-ZEL (12.5 and 25 μM), and BEA (2.5 μM). In addition, the potential effects were evaluated using the following mixtures: α-ZEL + β-ZEL (12.5μM), α-ZEL + BEA (12.5 + 2.5μM), β-ZEL + BEA (12.5 + 2.5μM) and α-ZEL + β-ZEL + BEA (12.5 + 12.5 + 2.5μM), employing DMSO (1%) as vehicle control.

Total RNA was isolated from cell samples using the ReliaPrep™ RNA Cell Miniprep System kit (Promega, Madison, WI, USA) following the manufacturers' instructions. The RNA concentration was measured using a NanoDrop 2000 spectrophotometer (Thermo Scientific, Wilmington, USA), and its purity was evaluated by the absorbance ratios A260/A280 and A260/A230. Agarose gel electrophoresis (1.0%) was used to verify the RNA integrity (Alvarez-Álvarez-Ortega et al., 2017). Subsequently, the cDNA was synthesized from 500 ng of mRNA extracted using the TaqMan reverse transcription reagents kit (Applied Biosystems, Foster City, CA, USA) (Escrivá et al., 2019).

RT-PCR procedure was carried out as described previously by Álvarez-Ortega et al (2019) with some modifications. Briefly, RT-PCR amplification was performed and monitored using a StepOne Plus thermocycler (Applied Biosystems, Foster City, CA, USA). The reactions were performed in MicroAmp optical 96-well reaction plates (Applied Biosystems). Each 10 μL reaction mixture contained 5 μL of template cDNA, 5 μL of PowerUp SYBR Green Master Mix (Thermo Fisher Scientific Inc.), and 3 μL of forward and reverse primers (2.5 μM). In total, 5 genes were analyzed, the expression of three genes involved in cell apoptosis (*CASP3, BAX, BCL2*) and two genes that code for estrogen receptors (*ER2* (specifically *ERβ*) and *GPER1*) (Table 1). Changes in gene expression were determined using *18S* as the reference gene (housekeeping), and the comparative delta delta CT (ΔΔCT) method was utilized to estimate the relative mRNA amount of the target genes. Three experiments with two replicates were carried out. All experiments were run by duplicates and negative controls contained no cDNA.

2.6. Statistical analysis

Statistical analysis of data was carried out using IBM SPSS Statistic version 23.0 (SPSS, Chicago, Il, USA) statistical software package and GraphPad Prism 8.0 (GraphPad Prisma Software, Inc., San Diego, USA). Data were expressed as mean ± SD of three independent experiments. The statistical analysis of the results was performed by student's T-test for paired samples. Difference between groups were analyzed statistically with ANOVA followed by the Tukey HDS post hoc test for multiple comparisons. The level of $p \leq 0.05$ was considered statistically

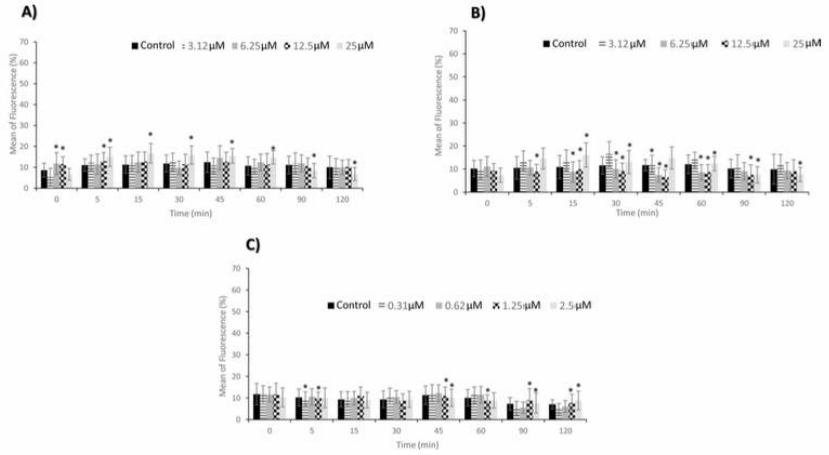

Fig. 2. Time dependence of ROS-induced fluorescence in SH-SY5Y cells exposed to α-ZEL (A), β-ZEL (B) and BEA (C), for 120 min at several concentrations (μM). Results are expressed as mean ± SEM (n = 3). (*) Represents significant diff ;erences ($p \leq 0.05$) versus control.

significant.

3. Results

3.1. Intracellular ROS generation of individual and combined mycotoxins

Changes in ROS generation inside SH-SY5Y cells in response to α-ZEL, β-ZEL and BEA (individually and in combinations) were determined. The production of ROS was determined by DCFH-DA assay. A treatment with all mycotoxins alone revealed a moderate change of ROS generation respect to the initial time (Fig. 2). According to α-ZEL tested alone, at 25 μM there is slight increase from 5 to 60 min and from 90 to 120 min decline moderately respect to their control ($p \leq 0.05$) (Fig. 2A). For individual test of β-ZEL, there is total decrease for 12.5 μM from 5 to 90 min and in addition, at 25 μM after 15 and 30 min and from 60 to 120 min it can be observed a moderate decrease compared to their control ($p \leq 0.05$) (Fig. 2B). Finally, for BEA, there is a slight decrease at 1.25 and 2.5 μM, from 45 to 120 min respect to control ($p \leq 0.05$) (Fig. 2C).

The mycotoxin mixture of α-ZEL + BEA increased ROS generation compared with control, after 45 and 120 min, at [1.56 + 0.31] μM ($p \leq 0.05$), while a gradual decrease at [6.25 + 1.25] μM and [12.5 + 2.5] μM at all times was obtained ($p \leq 0.05$) (Fig. 3A). For a combination of β-ZEL + BEA, a decrease of ROS generation with respect to control was observed (Fig. 3B) at [6.25 + 1.25] μM and [12.5 + 2.5] μM after 15 to 120 min ($p \leq 0.05$). For α-ZEL + β-ZEL, a statistically significant increase in ROS with respect to the control was obtained at the highest concentration assayed [12.5 + 12.5] μM from 15 to 120 min ($p \leq 0.05$), additionally, for [6.25 + 6.25] μM from 15 to 90 min (Fig. 3C). For the mixture containing all three compounds [α-ZEL + β-ZEL + BEA], as can be seen in Fig. 3, at [6.25 + 6.25 + 1.25] μM after 15 min and from 45 to 120 min ($p \leq 0.05$), decrease ROS generation slightly, also, at highest concentration [12.5 + 12.5 + 2.5] μM from 45 to 120 min ($p \leq 0.05$), there is a moderate decrease compared with control (Fig. 3D).

3.2. GSH determination

The alteration on GSH, GSSG and GSH/GSSG ratio was measured after 24 and 48 h of exposure to α-ZEL, β-ZEL (1.56, 3.12, 6.25 and 12.5 μM) and BEA (0.31, 0.62, 1.25, and 2.5 μM), individually and in combination in SH-SY5Y cells grown in fresh medium (Fig. 4 and 5).

In individual treatments, as shown in Fig. 4, GSH/GSSG ratio significantly increased after 24 h in cells exposed to mycotoxins in fresh medium at all concentrations from 111% to 148%, from 68% to 131% and from 103% to 142% for α-ZEL (Fig. 4A), β-ZEL (Fig. 4B) and BEA (Fig. 4C), respectively. However, after 48 h of exposure, GSH/GSSG ratio had a significant increase only after β-ZEL exposure of 12.5 μM by 37% and for the rest was not observed any considerable increase (Fig. 4B).

On the other hand, in combination treatments, GSH/GSSG ratio (Fig. 5) showed a significant increase in all cases for binary and tertiary mixtures respect to their controls; accordingly, from concentrations tested, percentages reached went from 102% to 157% for α-ZEL + BEA (Fig. 5A), from 102% to125% for α-ZEL + β-ZEL (Fig. 5C) and sequently, for β-ZEL + BEA binary combination it was observed a considerable increase in all concentrations assayed (from 81% to 127%) except for the lowest concentration assayed [1.56 + 0.31] μM) (Fig. 5B). Ultimately, in tertiary mixture GSH/GSSG ratio raised from 95% to 128% for the lowest and the highest concentration respect to control cells after 24 h of exposure (Fig. 5D).

After 48 h, in combination treatments GSH/GSSG ratio was not affected by any treatment except for binary mixtures α-ZEL + BEA (Fig. 5A) and α-ZEL + β-ZEL (Fig. 5C) in their respective lowest concentrations assayed ([1.56 + 031] μM and [1.56 + 1.56] μM) which increased significantly ($p \leq 0.05$) by 61% and 46%, respectively and respect to their control.

3.3. Gene expression assay in individual and combination

Findings in gene expression assay demonstrate that among all mycotoxins assayed individually. Compared to vehicle control, mRNA of *CASP3* and *BAX* mRNA were significantly overexpressed (up to 1.5-fold compared to the reference gene (*18S*)) for α-ZEL at concentrations of

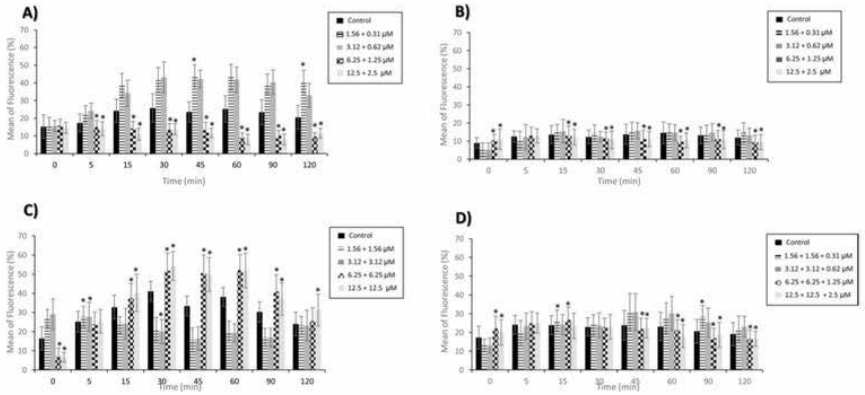

Fig. 3. Time dependence of ROS-induced fluorescence in SH-SY5Y cells exposed to mixtures of α-ZEL + BEA (A), β-ZEL + BEA (B) and α-ZEL + β-ZEL (C) and α-ZEL + β-ZEL + BEA (D) for 120 min at several concentrations (μM). Results are expressed as mean ± SEM (n = 3). (*) Represents significant diff ;erences ($p \leq 0.05$) versus control.

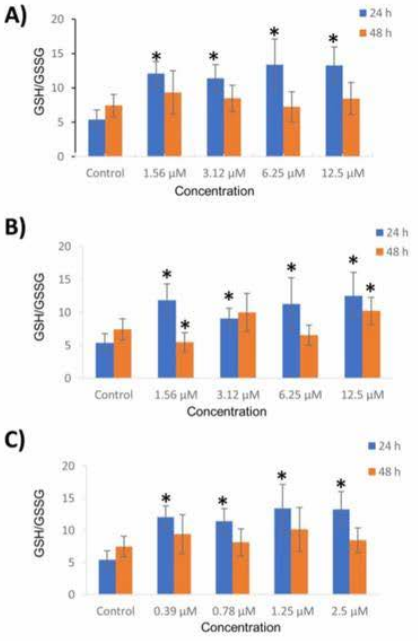

Fig. 4. Effect of zearalenone metabolites α-ZEL (A) and β-ZEL (B) (1.56, 3.12, 6.25 and 12.5 μM) and BEA (C) (0.39, 0.78, 1.25 and 2.5 μM) on the GSH/GSSG ratio after 24 h and 48 h of exposure. Data are expressed as mean values ± SEM of two independent experiments with 4 replicates each. *$p \leq 0.05$ indicates a significant difference from the respective control (fresh medium).

12.5 and 25 μM ($p \leq 0.05$) (Fig. 6A). On the other hand, β-ZEL up-regulated *ERβ* mRNA significantly up to 2.7-fold at 12.5 μM while down-regulated expression of *CASP3* and *BCL2* considerably (Fig. 6B). Additionally, BEA up-regulated only *BCL2* mRNA significantly while it was not able to induce the expression of other studied genes (Fig. 6C).

Among all combination treatments, β-ZEL + BEA was able to up-regulate the expression of all genes involved in cell apoptosis up to 1.5-fold (Fig. 7). Also, the expression of *BCL2* mRNA down-regulated significantly when cells were exposed to α-ZEL + β-ZEL combination (Fig. 7).

4. Discussion

Oxidative stress induced by mycotoxins has been explained by their ability to provoke generation of ROS in most of the cases. ZEA´s metabolites and BEA are known to be a common contaminant of important cereal and cereal-based products, such as corn, rice, wheat, barley and oats, throughout the world (Bertero et al., 2018); however, there are limited studies to demonstrate the effects of these mycotoxins on cells cytotoxicity according to their relationship on different factors such as oxidative stress and regulation of gene expression, individually and in combination (Ferrer et al., 2009; Tatay et al., 2016, 2017b; Marin et al., 2019; Fu et al., 2019).

In a previous study conducted in our laboratory, ZEA´s metabolites (α-ZEL and β-ZEL) and BEA were examined individually and in combination and it was observed that all caused cytotoxic effect on SH-SY5Y cells (Agahi et al., 2020). Accordingly, the present study aimed to determine the mechanism whereby α-ZEL, β-ZEL and BEA induce oxidative stress in the same cell line and its possible effect on alteration of GSH and GSSG levels. Also, to evaluate the effects of these three mycotoxins on expression of cell apoptosis and genes that code for estrogen receptors.

ZEA and its derivatives are known to be potent inducers of ROS in mammalian systems (Ben-Salem et al., 2015; Tatay et al., 2017b; Ben-Salem et al., 2017), also the studies of Ferrer et al. (2009), Prosperini et al. (2013) and Mallebrera et al. (2014) showed elevated level of ROS production by BEA when exposed to different cell lines (CHO-K1 and Caco-2 cells). Regarding to our results obtained from evaluating ROS generation, elevated ROS levels in combinations where α-ZEL was involved, were observed with increases of 2.8- to 8-fold compared to control (Fig. 3), coinciding with that obtained by Tatay et al. (2017b)

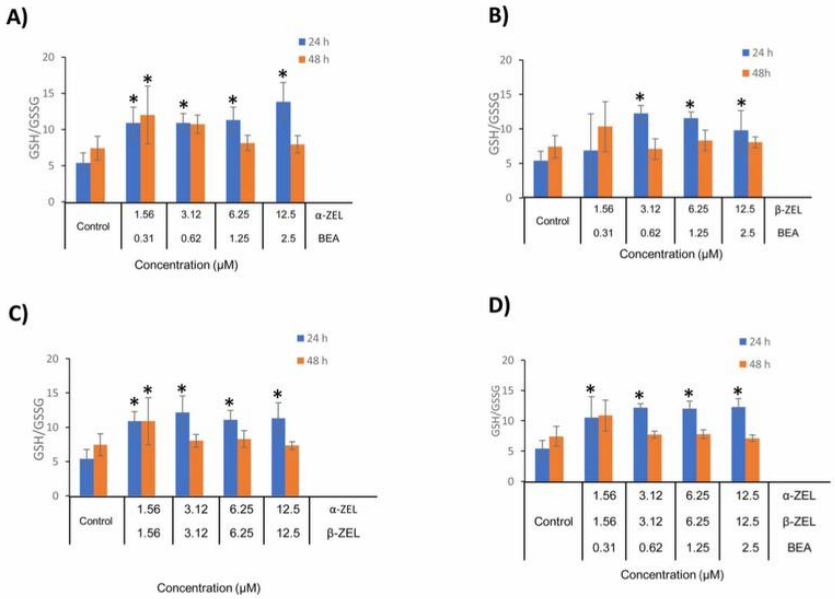

Fig. 5. Effect of mycotoxins mixtures α-ZEL + BEA (A), β-ZEL + BEA (B), α-ZEL + β-ZEL (C), and α-ZEL + β-ZEL + BEA (D) on the GSH/GSSG ratio after 24 h and 48 h of exposure. Data are expressed as mean values ± SEM of two independent experiments with 4 replicates each. $^{*}p \leq 0.05$ indicates a significant difference from the respective control (fresh medium).

on HepG2 cells that α-ZEL was the major contributor to ROS production. However, no significant difference in ROS levels were detected when each mycotoxins was tested alone (Fig. 2).

On the other hand, opposite to results previously published for SH-SY5Y cells, HepG2 cells and CHO-K1 cells (Venkataramana et al., 2014; Zingales et al., 2020; Tatay et al., 2016, 2017b) it was not observed any relationship between increasing time or concentration and the amount of ROS production in cells. The increased ROS generation in cells exposed to ZEA´s metabolites and BEA could be a consequent contribution to cell injury or oxidative stress. When the disruption occurred between the balance of antioxidant defense and ROS production, the cells try to survive so cellular antioxidant enzymes play their major role which is protecting cells from oxidative stress and damage. Regarding this fact, the first non-enzymatic antioxidant defense system in cells is GSH which plays a basic role in binding with ROS. Hence, with considering that the levels of GSH determine the balance in the antioxidant defense system, the impact on cellular GSH content present in two redox form (glutathione reduced (GSH) and glutathione disulfide (GSSG)), was evaluated after 24 h and 48 h in SH-SY5Y cells for α-ZEL, β-ZEL and BEA individually and combined, as all three have toxicological interest due to their potential to cause oxidative stress and damage (Fig. 2 and Fig. 3).

The obtained data suggested that α-ZEL, β-ZEL and BEA, in individual and combination treatment after 24 h had induced GSH/GSSG in the SH-SY5Y cells, since the ratio was significantly elevated (Fig. 4 and 5); whereas, after 48 h of exposure the same result was only observed for α-ZEL + BEA and α-ZEL + β-ZEL combination at the lowest concentration assayed (Fig. 5). The contrary effect was obtained by Zingales et al. (2020) when exposed to sterigmatocystin in the same cell line (SH-SY5Y cells), by depleting the GSH/GSSG ratio at the highest concentrations assayed.

Due to the increase in ROS levels and alteration in GSH/GSSG ratio, it was examined if such effects could be altering in SH-SY5Y cells the expression of genes involved in cell damage as apoptosis-related genes (*CASP3, BAX, BCL2*) and genes that code for estrogen receptors (*ERβ* and *GPER1*).

According to the OECD (Organization for Economic Cooperation and Development) EDTA (Endocrine Disrupter Testing and Assessment) meeting in April 2011, a possible endocrine disrupter is a chemical that is able to alter the functioning of the endocrine system but for which information about possible adverse consequences of that alteration in an intact organism is uncertain (Organisation for Economic Co-operation and Development (OECD, 2011). In the light of this fact, the research carried out by Ranzenigo et al. (2008) and Frizzell et al. (2011) had shown that ZEA and its metabolites, α-ZEL and β-ZEL, act as potential endocrine disruptors by interfering with nuclear receptor signaling and also by altering hormone production. Moreover, Le Guevel and Pakdel, 2001 have shown that ZEA and its derivates can exert their estrogenic effects through their ability to bind to the estrogen receptor (ER) since the expression of *ERβ* mRNA in SH-SY5Y cells has been shown in other studies (Bang et al., 2004; Grassi et al., 2013; Xiao et al., 2013). Hence, we examined *GPER1* and *ERβ*. In our study as it is indicated in Figs. 6 and 7, among all three mycotoxins assayed in individual and combination forms, only β-ZEL up-regulated the expression of *ERβ* mRNA significantly up to 2.7-fold at 12.5 μM compared to the reference gene (*18S*); while for *GPER1,* any significant regulation was observed (Fig. 6B).

Studies have shown that the *BCL2* and *BAX* pathways are involved in ZEA-induced apoptosis in primary rat cells (Li et al., 2011); also, the caspase family of proteins plays an important role in the initiation of

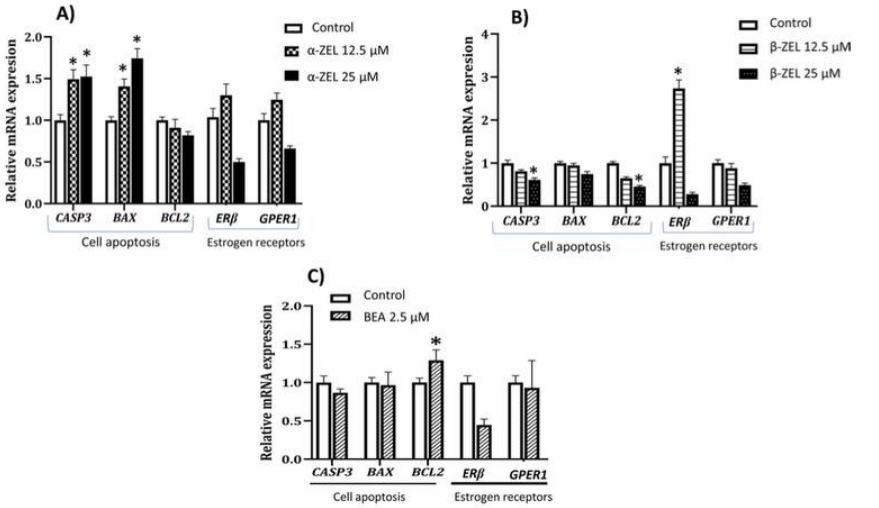

Fig. 6. Gene expression patterns of *CASP3, BAX, BCL, ERβ* and *GPER1* under different treatments in SH-SY5Y during 24 h by qRT-PCR. (A) for α-ZEL treatment, (B) for β-ZEL treatment and (C) for BEA treatment. *CASP3, BAX* and *BCL* are marker gene for cell apoptosis and *ERβ* and *GPER1* are markers of estrogen receptors. Three experiments with two replicates were carried out. Error bars represent standard deviations. Asterisks indicate significant ($p < 0.05$) differences in treated plants compared to mock-treated plants or to the time point before treatment.

apoptosis, of which caspase-3 is the primary initiator (Riedl and Salvesen, 2007). Nevertheless, there are no sufficient data about the two major metabolites of ZEA (α-ZEL and β-ZEL), since it is proved that it breaks down into their main metabolites during phase I metabolism (Metzler et al., 2010). The results of our study for individual treatments demonstrated that, while α-ZEL up-regulated the expression of cell apoptosis genes (Fig. 6A), β-ZEL shows an adverse effect which was down-regulating of these genes (Fig. 6B). Additionally, BEA only up-regulated the expression of *BCL2* significantly (Fig. 6C). Moreover, as it can be observed in Fig. 7, β-ZEL + BEA was the only combination that elevated the expression of cell apoptosis genes.

Then α-ZEL presented effect on gene expression, either cell apoptosis and estrogen receptors. However, in the combination, β-ZEL + BEA at [12.5 + 2.5] μM it was up-regulated the expression of all five studied gene expression involved in cell apoptosis (*CASP3, BAX, BCL2)* and estrogen receptors (*ERβ* and *GPER1)*.

5. Conclusion

In conclusion,the results obtained inthe present study indicate that α-ZEL, β-ZEL and BEA mycotoxins in SH-SY5Y cells, enhanced the oxidative damage by increasing ROS generation and GSH/GSSG ratio. In accordance to our findings, α-ZEL is more likely to induce oxidative stress in both individual and combination studies, also, this mycotoxin was found to be the most effective factor to enhance GSH/GSSG ratio in individual treatment and when it was involved in α-ZEL + BEA combination, which this can have consequences on initiation of oxidative damage. Regarding to expression genes effect, it is an unexplored area to investigate the endocrine-disruptive and cell apoptosis effects by up/down-regulation of implicated genes on SH-SY5Y cells exposed to mycotoxins and presented here for the first time. Our results show that β-ZEL might be considered a mycotoxin that induces apoptotic effect, individually and in combination while this happen for α-ZEL in individual exposure in SH-SY5Y cells. Nonetheless, there is no evidence how these genes can have further effects in more developed and complex cell systems closer to human or animal body exposed to α-ZEL, β-ZEL and BEA so that further studies are necessary.

Transparency document

The Transparency document associated with this article can be found in the online version.

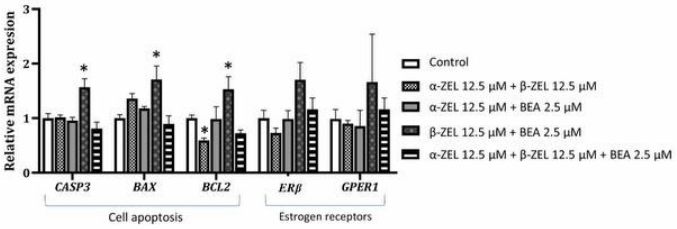

Fig. 7. Gene expression patterns of *CASP3, BAX, BCL, ERβ* and *GPER1* under different combination treatments in SH-SY5Y during 24 h by qRT-PCR. *CASP3, BAX* and *BCL* are marker gene for cell apoptosis and *ERβ* and *GPER1* are markers of estrogen receptors. Three experiments with two replicates were carried out. Error bars represent standard deviations. Asterisks indicate significant ($p < 0.05$) differences in treated plants compared to mock-treated plants or to the time point before treatment.

Declaration of Competing Interest

The authors declare that they have no known competing financial interests or personal relationships that could have appeared to influence the work reported in this paper.

Acknowledgements

This research has been supported by Spanish Ministry of Science and Innovation PID2019-108070RB-I00ALI, Generalitat Valenciana GVPROMETEO2018-126 and Generalitat Valenciana GV/2020/020. N.A.O. would like to thank Program for Doctoral Studies in Colombia (COLCIENCIAS 727.2015).

References

Abid, S., Bouaziz, C., El, Golli-Bennour, E, Ouanes Ben, Othmen, Z., Bacha, H., 2009. Comparative study of toxic effects of zearalenone and its two major metabolites α-zearalenol and β-zearalenol on cultured human Caco-2 cells. Journal of Biochemical and Molecular Toxicology. 23, 233–243.

Agahi, F., Font, G., Juan, C., Juan-García, A., 2020. Individual and combined effect of zearalenone derivates and beauvericin mycotoxins on SH-SY5Y cells. Toxins 12, 212. https://doi.org/10.3390/toxins12040212.

Álvarez-Ortega, N., Caballero-Gallardo, K., Olivero-Verbel, J., 2019. Toxicological effects in children exposed to lead: A cross-sectional study at the Colombian Caribbean coast. Environment international 130, 104809.

Álvarez-Ortega, N., Caballero-Gallardo, K., Olivero-Verbel, J., 2017. Low blood lead levels impair intellectual and hematological function in children from Cartagena, Caribbean coast of Colombia. Journal of Trace Elements in Medicine and Biology 44, 233–240.

Bakker, M.G., Brown, D.W., Kelly, A.C., Kim, H.S., Kurtzman, C.P., Mccormick, S.P., O'Donnell, K.L., Proctor, R.H., Vaughan, M.M., Ward, T.J., 2018. Fusarium mycotoxins: A trans-disciplinary overview. Canadian Journal of Plant Pathology. 40, 161–171.

Bang, O.Y., Hong, H.S., Kim, D.H., Kim, H., Boo, J.H., Huh, K., Mook-Jung, I., 2004. Neuroprotective effect of genistein against beta amyloid-induced neurotoxicity. Neurobiology of Disease 16 (1), 21–28.

Ben-Salem, I., Boussabbeh, M., Da-Silva, J.P., Guilbert, A., Bacha, H., Abid-Essefi, S., Lemaire, Ch., 2017. SIRT1 protects cardiac cells against apoptosis induced by zearalenone or its metabolites α- and β-zearalenol through an autophagy-dependent pathway. Toxicology and Applied Pharmacology. 314, 82–90.

Ben-Salem, I., Prola, A., Boussabbeh, M., Guilbert, A., Bacha, H., Lemaire, C., Abid-Essefi, S., 2015. Activation of ER stress and apoptosis by a- and b-zearalenol in HCT116 cells, protective role of Quercetin. NeuroToxicology. 53, 334–342.

Bertero, A., Spicer, L.J., Calonia, F., 2018. Fusarium mycotoxins and in vitro species-specific approach with porcine intestinal and brain in vitro barriers: A review. Food Chemical and Toxicology 121, 666–675.

Berthiller, F., Crews, C., Dall'Asta, C., de Saeger, S., Haesaert, G., Karlovsky, P., Oswald, I.P., Seefelder, W., Speijers, G., Stroka, J., 2013. Masked mycotoxins: A review. Molecular Nutrition and Food Research. 57, 165–186.

Catteuw, A., Broekaert, N., De Baere, S., Lauwers, M., Gasthuys, E., Huybrechts, B., Callebaut, A., Ivanova, L., Uhlig, S., De Boevre, M., De Saeger, S., Gehring, R., Devreese, M., Croubels, S., 2019. Insights into in vivo absolute oral bioavailability, biotransformation, and toxicokinetics of zearalenone, α- zearalenone, β- zearalenone, zearalenone-14-glucoside, and zearalenone-14-sulfate in pigs. J. Agric. Food Chem. 67, 3448–3458.

Ding, X.W., Gao, T., Gao, P., Meng, Y.Q., Zheng, Y., Dong, L., Luo, P., Zhang, G.H., Shi, X.Y., Rong, W.F., 2019. Activation of the G protein-coupled estrogen receptor elicits store calcium release and phosphorylation of the Mu-opioid receptors in the human neuroblastoma SH-SY5Y cells. Frontiers in Neurosci. 13, 1351.

EFSA, 2011. Scientific Opinion on the risks for public health related to the presence of zearalenone in food. EFSA Journal 9 (6), 2197.

EFSA, 2017. Scientific Opinion. Risks for animal health related to the presence of zearalenone and its modified forms in feed. https://doi.org/10.2903/j.efsa.2017.4851.

Escrivá, L., Alonso-Garrido, M., Font, G., Manyes, L., 2019. Transcriptional study after Beauvericin and Enniatin B combined exposure in Jurkat T cells. Food and Chemical Toxicology 130, 122–129.

Ferrer, E., Juan-García, A., Font, G., Ruíz, M.J., 2009. Reactive oxygen species induced by beauvericin, patulin and zearalenone in CHO-K1 cells. Toxicology In Vitro. 23, 1504–1509.

Föllmann, W., Ali, N., Blaszkewicz, M., Degen, G., 2016. Biomonitoring of mycotoxins in urine: pilot study in mill workers. J Toxicol Environ Health A 79, 1015–1025.

Frizzell, C., Ndossi, D., Verhaegen, S., Dahl, E., Eriksen, G., Sørlie, M., Connolly, L., 2011. Endocrine disrupting effects of zearalenone, alpha- and beta-zearalenol at the level of nuclear receptor binding and steroidogenesis. Toxicology Letters 206 (2), 210–217.

Fu, Y., Jin, Y., Y.Z, Shan, A., Fang, H., Shen, J., Zhou, C., Yu, H., Zhou, Y.F., Wang, X., Wang, J., Li, R., Wang, R., Zhang, J., 2019. Zearalenone induces apoptosis in bovine mammary epithelial cells by activating endoplasmic reticulum stress. Journal of Dairy Science. 102, 10543–10553.

Grassi, D., Bellini, M.J., Acaz-Fonseca, E., Panzica, G., Garcia-Segura, L.M., 2013. Estradiol and testosterone regulate arginine-vasopressin expression in SH-SY5Y human female neuroblastoma cells through estrogen receptors-α and-β. Endocrinology 154, 2092–2100.

Hassen, W., Ayed-Boussema, I., Oscoz, A.A., De Cerain Lopez, A., Bacha, H., 2007. The role of oxidative stress in zearalenone-mediated toxicity in Hep G2 cells: oxidative DNA damage. glutathione depletion and stress proteins induction Toxicology. 232, 294–302.

He, J., Wei, Ch., Li, Y., Liu, Y., Wang, Y., Pan, J., Liu, J., Wu, Y., Sheng Cui, Sh, 2018. Zearalenone and alpha-zearalenol inhibit the synthesis and secretion of pig follicle stimulating hormone via the non-classical estrogen membrane receptor GPR30. Molecular and Cellular Endocrinology. 461, 43–54.

Hueza, I.M., Raspantini, P.C., Raspantini, L.E., Latorre, A.O., Górniak, S.L., 2014. Zearalenone, an estrogenic mycotoxin, is an immunotoxic compound. Toxins. 6 (3), 1080–1095.

Juan, C., Mañes, J., Font, G., Juan-García, A., 2017a. Determination of mycotoxins in fruit berry by-products using QuEChERS extraction method. LWT - Food Science and Technology 86, 344–351.

Juan, C., Berrada, H., Mañes, J., Oueslati, S., 2017b. Multi-mycotoxin determination in barley and derived products from Tunisia and estimation of their dietary intake. Food Chem. Toxicol. 103, 148–156.

Juan-García, A., Juan, C., Tolosa, J., Ruíz, M.J., 2019a. Effects of deoxynivalenol, 3-acetyl-deoxynivalenol and 15-acetyl-deoxynivalenol on parameters associated with oxidative stress in HepG2 cells. Mycotoxin Res. https://doi.org/10.1007/s12550-019-00344-0.

Juan-García, A., Tolosa, J., Juan, C., Ruíz, M.J., 2019b. Cytotoxicity, genotoxicity and disturbance of cell cycle in HepG2 cells exposed to OTA and BEA: single and combined actions. Toxins 11, 341. https://doi.org/10.3390/toxins11060341.

Juan-García, A., Carbone, C., Ben-Mahmoud, M., Sagratini, G., Mañes, J., 2020. Beauvericin and ochratoxin A mycotoxins individually and combined in HepG2 cells alter lipid peroxidation, levels of reactive oxygen species and glutathione. Food Chem Toxicol 139, 111247.

Krug, I., Behrens, M., Esselen, M., Humpf, H.U., 2018. Transport of enniatin B and enniatin B1 across the blood-brain barrier and hints for neurotoxic effects in cerebral cells. PLOS ONE. https://doi.org/10.1371/journal.pone.0197406.

Kuiper-Goodman, T., Scott, P.M., Watanabe, H., 1987. Risk assessment of the mycotoxin zearalenone. Regulatory Toxicology and Pharmacology. 7 (3), 253–306.

Le Guevel, R., Pakdel, F., 2001. Assessment of oestrogenic potency of chemicals used as growth promoter by in-vitro methods. Human Reproduction. 16, 1030–1036.

Li, G.Y., Xie, P., Li, H.Y., Hao, L., Xiong, Q., Qiu, T., 2011. Involvement of p53, Bax, and Bcl-2 pathway in microcystins-induced apoptosis in rat testis. Environmental Toxicology. 26, 111–117.

Liu, X.L., Wu, R.Y., Sun, X.F., Cheng, S.F., Zhang, R.Q., Zhang, T.Y., Zhang, X.F., Zhao, Y., Shen, W., Li, L., 2018. Mycotoxin zearalenone exposure impairs genomic stability of swine follicular granulosa cells in vitro. Int. J. Biol. Sci. 14, 294–305.

Mallebrera, B., Font, G., Ruiz, M.J., 2014. Disturbance of antioxidant capacity produced by beauvericin in CHO-K1 cells. Toxicology Letters. 226, 337–342.

Manyes, L., Escrivá, L., Ruíz, M.J., Juan-García, A., 2018. Beauvericin and enniatin B effects on a human lymphoblastoid Jurkat T-cell model. Food Chem Toxicol 115, 127–135.

Maran, E., Fernandez, M., Barbieri, P., Font, G., Ruiz, M.J., 2009. Effects of four carbamate compounds on antioxidant parameters. Ecotoxicology and Environmental Safety 72, 922–930.

Marin, D.E., Pistol, G.C., Bulgaru, C.V., Taranu, I., 2019. Cytotoxic and inflammatory effects of individual and combined exposure of HepG2 cells to zearalenone and its metabolites. Naunyn-Schmiedeberg's Archives of Pharmacology. 392, 937–947.

Martin, S.J., Reutelingsperger, C.P., McGahon, A.J., Rader, J.A., van Schie, R.C., LaFace, D.M., Green, D.R., 1995. Early redistribution of plasma membrane phosphatidylserine is a general feature of apoptosis regardless of the initiating stimulus: inhibition by overexpression of Bcl-2 and Abl. Journal of Experimental Medicine 182, 1545–1556.

Metzler, M., Pfeiffer, E., Hildebrand, A.A., 2010. Zearalenone and its metabolites as endocrine disrupting chemicals. World Mycotoxin Journal. 3, 385–401.

Nganje, W.E., Bangsund, D.A., Leistritz, F.L., Wilson, W.W., Tiapo, N.M., 2004. Regional economic impacts of Fusarium head blight in wheat and barley. Review of Agricultural Economics. 26, 332–347.

Organisation for Economic Co-operation and Development (OECD), 2011. In Environment, Health and Safety News: The OECD Environment, Health and Safety Programme: Achievements. no. 27 on December 2011, [online:. http://www.oecd.org/env/chemicalsafetyandbiosafety/49171557.pdf].

Oueslati, S., Berrada, H., Juan-García, A., Mañes, J., Juan, C., 2020. Multiple mycotoxin determination on Tunisian cereals-based food and evaluation of the population exposure. Food Analytical Methods. https://doi.org/10.1007/s12161-020-01737-z.

Parveen, M., Zhu, Y., Kiyama, R., 2009. Expression profiling of the genes responding to zearalenone and its analogues using estrogen-responsive genes. FEBS Letters. 583, 2377–2384.

Perincherry, L., Lalak-Kanczugowska, J., Stępien, L., 2019. Fusarium-Produced Mycotoxins in Plant-Pathogen Interactions (review). Toxins. 11 (11), 664.

Ploetz, R.C., 2015. Fusarium wilt of banana. Phytopathology. 105, 1512–1521.

Prosperini, A., Juan-García, A., Font, G., Ruiz, M.J., 2013. Beauvericin-induced cytotoxicity via ROS production and mitochondrial damage in Caco-2 cells. Toxicology Letters. 222 (2), 204–211.

Ranzenigo, G., Caloni, F., Cremonesi, P., Y.Aad, P., J.Spicer, L., 2008. Effects of Fusarium mycotoxins on steroid production by porcine granulosa cells. Animal Reproduction Science. 107, 115–130.

Riedl, S.J., Salvesen, G.S., 2007. The apoptosome: Signalling platform of cell death. Nature reviews molecular cell biology. 8. pp. 405–413.

Shephard, G.S., Burger, H.M., Gambacorta, L., Gong, Y.Y., Krska, R., Rheeder, J.P., Solfrizzo, M., Srey, C., Sulyok, M., Visconti, A., Warth, B., van der Westhuizen, L., 2013. Multiple mycotoxin exposure determined by urinary biomarkers in rural subsistence farmers in the former Transkei, South Africa. Food Chem Toxicol 62, 217–225.
Stanciu, O., Juan, C., Miere, D., Dumitrescu, A., Bodoki, E., Loghin, F., Mañes, J., 2017b. Climatic conditions influence emerging mycotoxin presence in wheat grown in Romania – A 2-year survey. Crop Protection. 100, 124–133.
Stanciu, O., Juan, C., Miere, D., Loghin, F., Mañes, J., 2017a. Occurrence and co-occurrence of Fusarium mycotoxins in wheat grains and wheat flour from Romania. Food Control. 73, 147–155.
Tsevernier, L., Bracke, N., Veryser, L., Wynendaele, E., Gevaert, B., Peremans, K., De Spiegeleer, B., 2016. Blood-brain barrier transport kinetics of the cyclic depsipeptide mycotoxins beauvericin and enniatins. Toxicology Letters 258, 175–184.
Tatay, E., Espín, S., García-Fernández, A.J., Ruiz, M.J., 2017a. Estrogenic activity of zearalenone, α-zearalenol and β-zearalenol assessed using the E-Screen assay in MCF-7 cells. Toxicology Mechanisms and Methods. 1537–6524,
Tatay, E., Espín, S., García-Fernández, A.J., Ruiz, M.J., 2017b. Oxidative damage and disturbance of antioxidant capacity by zearalenone and its metabolites in human cells. Toxicology in Vitro. 45, 334–339.
Tatay, E., Font, G., Ruiz, M.J., 2016. Cytotoxic effects of zearalenone and its metabolites and antioxidant cell defense in CHO-K1 cells. Food and Chemical Toxicology. 96, 43–49.
Tatay, E., Meca, G., Font, G., Ruiz, M.J., 2014. Interactive effects of zearalenone and its metabolites on cytotoxicity and metabolization in ovarian CHO-K1 cells. Toxicology in Vitro. 28, 95–103.
Venkataramana, M., Chandra Nayaka, S., Anand, T., Rajesh, R., Aiyaz, M., Divakara, S.T., Murali, H.S., Prakash, H.S., Lakshmana Rao, P.V., 2014. Zearalenone induced toxicity in SH5Y-5Y cells: The role of oxidative stress evidenced by N-acetyl cysteine. Food and Chemical Toxicology. 65, 335–342.
Wallin, S., Gambacorta, L., Kolova, N., Lemming, E.W., Nalsen, C., Solfrizzo, M., Olsen, M., 2015. Biomonitoring of concurrent mycotoxin exposure among adults in Sweden through urinary multi-biomarker analysis. Food Chem Toxicol 83, 133–139.
Xiao, Z., Huang, C., Wu, J., Sun, L., Hao, W., Leung, L.K., Huang, J., 2013. The neuroprotective effects of ipriflavone against H2O2 and amyloid beta induced toxicity in human neuroblastoma SH-SY5Y cells. European journal of pharmacology 721, 286–293.
Zamai, L., Falcieri, E., Marhefka, G., Vitale, M., 1996. Supravital exposure to propidium iodide identifies apoptotic cells in the absence of nucleosomal DNA fragmentation. Cytometry 23, 303–311.
Zheng, W., Feng, N., Wang, Y., Noll, L., Xu, Sh., Liu, X., Lu, N., Zou, H., Gu, J., Yuan, Y., Liu, X., Zhu, G., Bian, J., Bai, J., Liu, Z., 2019. Eff ;ects of zearalenone and its derivatives on the synthesis and secretion of mammalian sex steroid hormones: A review. Food and Toxicology. 126, 262–276.
Zhu, L., Yuan, H., Guo, C., Lu, Y., Deng, S., Yang, Y., Wei, Q., Wen, L., He, Z., 2012. Zearalenone induces apoptosis and necrosis in porcine granulosa cells via a caspase-3- and caspase-9-dependent mitochondrial signaling pathway. Journal of Cellular Physiology. 227, 1814–1820.
Zingales, V., Fernández-Franzón, M., Ruiz, M.J., 2020. Sterigmatocystin-induced cytotoxicity via oxidative stress induction in human neuroblastoma cells. Food and Chemical Toxicology. 136, 110956.
Zouaoui, N., Mallebrera, B., Berrada, H., Abid-Essefi, S., Bacha, H., Ruiz, M.-J., 2016. Cytotoxic effects induced by patulin, sterigmatocystin and beauvericin on CHO–K1 cells. Food and Chemical Toxicology. 89, 92–103.

Food and Chemical Toxicology 152 (2021) 112227

Contents lists available at ScienceDirect

Food and Chemical Toxicology

journal homepage: www.elsevier.com/locate/foodchemtox

Study of enzymatic activity in human neuroblastoma cells SH-SY5Y exposed to zearalenone's derivates and beauvericin

Fojan Agahi, Ana Juan-García *, Guillermina Font, Cristina Juan

Laboratory of Food Chemistry and Toxicology, Faculty of Pharmacy, University of Valencia, Av. Vicent Andrés Estellés s/n, 46100, Burjassot, Valencia, Spain

ARTICLE INFO

Handling Editor: Dr. Jose Luis Domingo

Keywords:
Enzymatic antioxidant
Zearalenone's derivates
Beauvericin
Neuronal cells

ABSTRACT

Beauvericin (BEA), α-zearalenol (α-ZEL) and β-zearalenol (β-ZEL), are produced by several *Fusarium* species that contaminate cereal grains. These mycotoxins can cause cytotoxicity and neurotoxicity in various cell lines and they are also capable of produce oxidative stress at molecular level. However, mammalian cells are equipped with a protective endogenous antioxidant system formed by no-enzymatic antioxidant and enzymatic protective systems such as glutathione peroxidase (GPx), glutathione S-transferase (GST), catalase (CAT) and superoxide dismutase (SOD). The aim of this study was evaluating the effects of α-ZEL, β-ZEL and BEA, on enzymatic GPx, GST, CAT and SOD activity in human neuroblastoma cells using the SH-SY5Y cell line, over 24 h and 48 h with different treatments at the following concentration range: from 1.56 to 12.5 μM for α-ZEL and β-ZEL, from 0.39 to 2.5 μM for BEA, from 1.87 to 25 μM for binary combinations and from 3.43 to 27.5 μM for tertiary combination.

SH-SY5Y cells exposed to α-ZEL, β-ZEL and BEA revealed an overall increase in the activity of i) GPx, after 24 h of exposure up to 24-fold in individual treatments and 15-fold in binary combination; ii) GST after 24 h of exposure up to 10-fold (only in combination forms), and iii) SOD up to 3.5- and 5-fold in individual and combined treatment, respectively after 48 h of exposure. On the other hand, CAT activity decreased significantly in all treatments up to 92% after 24 h except for β-ZEL + BEA, which revealed the opposite.

1. Introduction

Many species of *Fusarium* produce a variety of mycotoxins which are widely distributed in nature and have serious health impacts in both humans and animals (Darwish et al., 2014; Dweba et al., 2017). The mycotoxins beauvericin (BEA) and zearalenone's (ZEA) derivatives (α-zearalenol (α-ZEL) and β-zearalenol (β-ZEL)), are produced mainly by *Fusarium* species in agricultural crops and can be co-present in the same foodstuffs, feed or in the diet (Oueslati et al., 2020). ZEA is one of the most common mycotoxins in Europe produced by fungi, which has a great agro-economic importance (Wei et al., 2020; Bocianowski et al., 2020). The major pathway for ZEA biotransformation by animals is based on hydroxylation resulting in the formation of α-ZEL and β-ZEL, presumably catalyzed by 3 α- and 3β-hydroxysteroid dehydrogenases (Olsen et al., 1981) which will follow a metabolization process with different effects as recently predicted *in silico* (Agahi et al., 2020c). This conversion has been shown to occur in the liver of various species (Malekinejad et al., 2006a) and in various cells, such as bovine and porcine granulosa cells (Malekinejad et al., 2006b), rat erythrocytes (Chang and Lin, 1984), the intestinal mucosa of swine (Biehl et al., 1993) and human intestinal Caco-2 cells (Pfeiffer et al., 2011; Videmann et al., 2008, 2009). Devreese et al. (2015) have also demonstrated that both α-ZEL and β-ZEL were absorbed equally after intravenous administration of ZEA in broiler chickens, laying hens, and turkey poults; whereas an increased biotransformation to β-ZEL was demonstrated after oral administration (Devreese et al., 2015). Beside this, it has been demonstrated that ZEA, α-ZEL and β-ZEL impaired cell proliferation, steroid production, and gene expression in bovine small-follicle granulosa cells *in vitro* (Pizzo et al., 2016); more importantly, it has been proved that α-ZEL and β-ZEL have a higher capacity to induce oxidative stress and damage in HepG2 cells than ZEA itself (Tatay et al., 2017). Brodehl et al. (2014) also showed that α-ZEL was 10-fold higher estrogenic than the parent ZEA, and in other study almost 500-fold stronger in comparison to ZEA, while β-ZEL was 16 times lower than ZEA (Drzymala et al., 2015; Molina-Molina et al., 2014). Moreover, in our previous study on SH-SY5Y cells reactive oxygen species (ROS) levels were higher in those combinations where α-ZEL was involved (2.8- to 8-fold compared to control) (Agahi et al., 2020b). Whereas when

* Corresponding author.
E-mail address: ana.juan@uv.es (A. Juan-García).

https://doi.org/10.1016/j.fct.2021.112227
Received 22 March 2021; Received in revised form 12 April 2021; Accepted 14 April 2021
Available online 18 April 2021
0278-6915/

cytotoxicity of ZEA's metabolites were studied individually on the same cells line, it was shown that β-ZEL was more cytotoxic compared to α-ZEL (Agahi et al., 2020b). However, there isn't information about combinations of these both metabolites jointly other mycotoxins that can be present in the same foodstuff.

Regarding beauvericin (BEA), it is characterized by allowing flux of cations on channel cells, (Kouri et al., 2003; Ojcius et al., 1991), thereby increasing the intracellular Ca^{2+} which can ultimately activate several biological pathways leading to cell death. Additionally, BEA was demonstrated to reduce calcium retention in isolated mitochondria (Tonshin et al., 2010). Ca^{2+} influx across the plasma membrane activate mitochondrial permeability transition pore opening and collapse the mitochondrial membrane potential. Moreover, BEA reduced cell viability and induced cytotoxic effects in different human cell lines which has been demonstrated through various *in vitro* studies (Prosperini et al., 2013; Mallebrera et al., 2014; Juan-García, 2019a, 2019b; Agahi et al., 2020b). Also, features characteristic of necrosis and apoptosis were observed in BEA-treated cells (Agahi et al., 2020a; Manyes et al., 2018; Prosperini et al., 2013; Klarić et al., 2008).

On the other hand, all organisms with a well-developed central nervous system have a blood–brain barrier (BBB) which is created by the endothelial cells that form the walls of the capillaries in the brain and spinal cord of humans (Abbott et al., 2005). It has been shown that BBB function as a protective barrier from neurotoxic substances circulating in the blood which maybe endogenous metabolites or proteins, or xenobiotics ingested in the diet or acquired from the environment. It has been proved by various studies that *Fusarium* mycotoxins are capable to cross the BBB and cause neuronal cell death (Taevernier et al., 2016; Behrens et al., 2015; Krug et al., 2018). However, there are limited studies about the effects of ZEA's derivates and BEA mycotoxins on BBB doses of which are studied here *in vitro* with an undifferentiated human neuroblastome cell line, SH-SY5Y. SH-SY5Y is a cell line commonly used as neuronal model (Xicoy et al., 2017). The implications or evidences of these mycotoxins in trigger brain disorders in humans still remains unclear; while for other mycotoxins as tremortoxins neurotoxic effects in animals have been reported (Reddy et al., 2019).

As it is known, oxidative stress is the answer of disbalance between the production of ROS and a biological system's ability to detoxify or repair the resulting damage, which potentially can cause lipid peroxidation, degradation of cytosolic proteins and damage to DNA, which ultimately may lead to cell death (Dinu et al., 2011; Tatay et al., 2017). Furthermore, excite-toxicity and oxidative stress may cause neuronal cell degeneration and death (Gandhi and Abramov, 2012). Oxidative stress generates negative effects in neurons and astrocytes, a phenomenon that has been associated with the progression of different conditions such as Parkinson's disease and Alzheimer's disease, and cancer (Albarracin et al., 2012). More recently, there are wide number of studies evidencing on the effects of oxidative stress damage caused by mycotoxins on different cell lines (Juan-García et al., 2020; Taroncher et al., 2020; Zingales et al., 2020; Tatay et al., 2016).

Considering this fact, enzymatic antioxidant function is to compensate the elevated ROS levels as well as non-enzymatic antioxidant system. However, depletion of these defense elements further promotes oxidative stress. In previous study we investigated the effects of α-ZEL, β-ZEL and BEA, mycotoxins on production of ROS on SH-SY5Y cell line (Agahi et al., 2020a). Hence, in the light of this, we further set out the present study to evaluate the enzymatic protective system in the same undifferentiated human neuroblastoma cell line, SH-SY5Y. As mentioned above it has been widely used as a cell model for the pathogenesis studies of neurotoxicity (Cai et al., 2020; Sirin et al., 2020; Lawana et al., 2020; Kim et al., 2020). Due to the lack of information in ZEA's metabolites jointly other mycotoxins that can be present in the same foodstuffs, SH-SY5Y have been exposed to α-ZEL, β-ZEL and BEA (both individually and combined exposures) establishing the first time to figure out the effect in antioxidant enzymes activities including glutathione peroxidase (GPX), glutathione transferase (GST), catalase (CAT), and superoxide dismutase (SOD) and its implications.

2. Material and methods

2.1. Reagents

The reagent grade chemicals and cell culture components used, Dulbecco's Modified Eagle's Medium- F12 (DMEM/F-12), fetal bovine serum (FBS) and phosphate buffer saline (PBS) were supplied by Thermofisher, Gibco ™ (Paisley, UK). Methanol (MeOH, HPLC LS/MS grade), was obtained from VWR International (Fontenay-sous-Bois, France). Dimethyl sulfoxide (DMSO) was obtained from Fisher Scientific Co, Fisher BioReagnts ™ (Geel, Belgium). Deionized water (<18, MΩcm resistivity) was obtained in the laboratory using a Milli-QSP® Reagent Water System (Millipore, Beadford, MA, USA). Penicillin, streptomycin, and Trypsin–EDTA, β –nicotinamide adenine dinucleotide phosphate (β-NADPH), sodium azide (NaN_3), glutathione reductase (GR), o-phtaldialdehyde (OPT), N-ethylmaleimide (NEM), t-octylphenoxypolyethoxyethanol (Triton-X 100), 1-chloro-2,4-dinitrobenzene (CDNB), ethylenediaminetetraacetic acid (EDTA), tris hydroxymethyl aminomethane (Tris), 4′,6-diamidine-2′-phenylindole dihydrochloride (DAPI), H_2O_2 and the standard of BEA (MW: 783.95 g/mol), α-ZEL and β-ZEL (MW: 320,38 g/mol) were purchased from SigmaAldrich (St. Louis Mo. USA). Stock solutions of mycotoxins were prepared in MeOH (α-ZEL and β-ZEL) and DMSO (BEA) and maintained at −20 °C in the dark. The final concentration of either MeOH or DMSO in the medium was ≤1% (v/v) as per established. All other standards were of standard laboratory grade.

2.2. Cell culture

Human neuroblastoma cell line, SH-SY5Y, was obtained from American Type Culture Collection (ATCC, Manassas, VA, USA), and cultured in Dulbecco's Modified Eagle's Medium- F12 (DMEM/F-12), supplemented with 10% fetal bovine serum (FBS), 100 U/ml penicillin, and 100 mg/ml streptomycin. The cells were sub-cultivated after trypsinization once or twice a week and suspended in complete medium in a 1:3 split ratio. Cells were maintained as monolayer in 150 cm^2 cell culture flasks with filter screw caps (TPP, Trasadingen, Switzerland). Cell cultures were incubated at 37 °C, 5% CO_2 atmosphere.

2.3. Determination of enzymatic activities

To determine the scavenging procedures in SH-SY5Y, cells got exposed to α-ZEL and β-ZEL (12.5, 6.25, 3.12 and 1.56 μM), and BEA (2.5, 1.25, 0.78 and 0.39 μM) for individual treatment. Afterward, they were assayed in combination through the following mixtures: α-ZEL + BEA, β-ZEL + BEA, α-ZEL + β-ZEL and α-ZEL + β-ZEL + BEA with concentrations ranging from 25 to 1.87 μM for binary combinations, and from 27.5 to 3.43 μM for tertiary combination. The dilution ratio of concentration ranges in binary combinations was (1:1) for α-ZEL + β-ZEL, (5:1) for α-ZEL + BEA and β-ZEL + BEA, and (5:5:1) in tertiary combinations (α-ZEL + β-ZEL + BEA).

For these assays, 7×10^5 cells/well were seeded in six-well plates. After cells achieved the 90% confluence, cells were treated with α-ZEL and β-ZEL and BEA at the concentrations above detailed for 24 h and 48 h. Then, the medium was removed, and cells were homogenized in 0.1 M phosphate buffer pH 7.5 containing 2 mM EDTA to a final volume of 0.5 mL. Aliquotes for each enzyme activity assay were prepared by disposing 125 μl in individual Eppendorfs.

2.3.1. Glutathione peroxidase activity

The glutathione peroxidase (GPx) activity was assayed spectrophotometrically using H_2O_2 as substrate for Se-dependent peroxidase activity of GPx by following oxidation of NADPH during the first 5 min in a coupled reaction with GR, as described by Maran et al. (2009). In 1 ml

final volume, the reaction mixture contained 500 μl of 0.1 M phosphate buffer, pH 7.5 with 4 mM NaN_3 and 2 mM EDTA, 100 μl of 20 mM GSH, 250 μl of ultrapure water, 2 U freshly prepared GR, 20 μl of 10 mM NADPH and 50 μl of 5 mM H_2O_2. 50 μL of homogenized cell sample was added to the reaction mixture. One unit of GPx will reduce 1 μmol of GSSG per min at pH 7.5. The GPx enzymatic activity was calculated by using a molar absorptivity of NADPH (6.22 mM^{-1} cm^{-1}) and expressed as μmol of NADPH oxidized/min/mg of protein. Assays were conducted at 25 °C in a thermocirculator of PerkinElmer UV/vis spectrometer Lambda 2 version 5.1. The absorbance was measured at 340 nm.

2.3.2. Glutathione S-transferase activity

The glutathione S-transferase (GST) activity was determined by following the conjugation of GSH with 1-chloro-2,4-dinitrobenzene (CDNB) during 5 min, according to the method of Maran et al. (2009). The reaction mixture contained in a final volume of 1 ml: 825 μl of 0.1 M Na/K phosphate buffer at pH 6.5, 100 μl of 20 mM GSH, 25 μl of 50 mM CDNB dissolved in ethanol and 50 μl of homogenized cell sample. The GST activity was expressed as mol of product formed/min/mg of protein using a molar absorptivity of CDNB (9.6 mM^{-1} cm^{-1}). Enzymatic activity was assayed in a thermocirculator of PerkinElmer UV/vis spectrometer Lambda 2 version 5.1. The absorbance was measured at 340 nm.

2.3.3. Catalase activity

The catalase (CAT) activity was measured according to Ueda et al. (1990). Briefly, 100 μl of homogenized cell sample was mixed with 500 μl of 0.5 M potassium phosphate buffer at pH 7.2 and 400 μl of 40 mM H_2O_2. The rate of enzymatic decomposition of H_2O_2 was determined as absorbance decrements at 240 nm for 3 min at 30 °C with a spectrophotometer (Super Aquarius CECIL 9500 CE). The CAT activity was calculated by using the molar absorptivity of H_2O_2 (43.6 mM^{-1} cm^{-1}) and expressed as μmol H_2O_2/min/mg of protein.

2.3.4. Superoxide dismutase activity

The superoxide dismutase (SOD) activity was determined using the Ransod kit (Randox Laboratories, United Kingdom) adapted for 1.5 ml cuvettes. The SOD destroys the free radical superoxide by converting it to peroxide. The SOD activity was monitored at 505 nm during 3 min at 37 °C with a spectrophotometer (PerkinElmer UV/Vis Lambda 2 version 5.1). The SOD results were expressed as units of SOD per mg protein. All the enzyme determinations were performed in duplicate.

2.4. Statistical analysis

Statistical analysis of data was carried out using IBM SPSS Statistic version 23.0 (SPSS, Chicago, Il, USA) statistical software package and GraphPad Prism 8.0 (GraphPad Software, Inc., San Diego, USA). Data were expressed as mean ± SD of three independent experiments. The statistical analysis of the results was performed by student's T-test for paired samples. Difference between groups were analyzed statistically with ANOVA followed by the Tukey HDS post hoc test for multiple comparisons. The level of $p \leq 0.05$ was considered statistically significant.

3. Results

The GPx, GST, CAT and SOD activities measured in undifferentiated SH-SY5Y cells after 24 h and 48 h of incubation with α-ZEL, β-ZEL and BEA in individual and in combination form, are presented in Figures from 1 to 5. Results of enzymes are expressed in folds and correspond to the number of times that increase or decrease respect to untreated cells (control).

3.1. Enzymatic activity of GPx

As shown in Fig. 1A and B the GPx activity in SH-SY5Y cells exposed to α-ZEL and β-ZEL, increased significantly at all concentrations assayed only after 24 h compared to control. Increases went by 13.5- to 23-fold for α-ZEL and 9- to 17-fold for β-ZEL. This increase was observed after both 24 h and 48 h of exposure at all concentrations in cells exposed to BEA from 9- to 17-fold and from 2- to 9-fold after 24 h and 48 h, respectively (Fig. 1C).

Similarly, for all binary treatments the level of GPx activity increased significantly after 24 h of exposure, for α-ZEL + BEA at all concentrations assayed from 7.6- to 14.5-fold (Fig. 1D)., for β-ZEL + BEA at all concentrations assayed from 4.7- to 10.3-fold (Fig. 1E); and for α-ZEL + β-ZEL at all concentrations except at the lowest one from 2.5- to 7.8-fold compared to unexposed cells (Fig. 1F). In contrary, the GPx activity in cells exposed to tertiary mixture of α-ZEL + β-ZEL + BEA an increase after 48 h of exposure at all concentrations assayed from 1- to 6-fold compared to control was observed (Fig. 5A). In summary, it was observed higher GPx activity in individual exposure than in combinations which could be due to the low concentration level of ROS activity when cells were treated with mycotoxins individually that was observed in the previous study (Agahi et al., 2020a).

3.2. Enzymatic activity of GST

Results for GST activity are described in percentage for individual treatments and compared to untreated cells (control). This enzyme activity increased significantly after 48 h of exposure in SH-SY5Y cells exposed to β-ZEL at 3.12 and 12.5 μM by 22% and 102%, respectively (Fig. 2B). Similarly, this happened after being exposed to BEA to doses above 0.78 μM for 48 h of exposure by 4%–32% (Fig. 2C).

In combination treatments, GST activity increased significantly after 24 h of exposure to α-ZEL + BEA at [1.56 + 0.39] μM, [6.25 + 1.25] μM and [12.5 + 2.5] μM from 5.6- to 8- fold compared to control (Fig. 2D), also after 48 h of exposure a notable increase at [6.25 + 1.25] was observed (Fig. 2D). For β-ZEL + BEA, a significant increase at [6.25 + 1.25] μM and [12.5 + 2.5] μM by 4- and 3- fold compared to untreated cells was observed after 24 h of exposure (Fig. 2E). As shown in Fig. 2F, GST activity in SH-SY5Y cells exposed to α-ZEL + β-ZEL, increased significantly at all concentrations assayed up to 8.8-fold after 24 h of exposure compared to control. For tertiary mixture, α-ZEL + β-ZEL + BEA, GST activity in SH-SY5Y cells increased significantly from 1- to 7.7-fold compared to control (Fig. 5B).

3.3. Enzymatic activity of CAT

The CAT activity increased significantly in SH-SY5Y cells exposed to α-ZEL and β-ZEL only after 48 h of exposure (from 0.4 to 1.4-fold for α-ZEL and 1–4.2-fold for β-ZEL) at all concentrations assayed (Fig. 3A and B); while this was not observed when cells were exposed to BEA mycotoxin (Fig. 3C).

For combination treatments, it was observed a significant increase mostly after 48 h of exposure except for β-ZEL + BEA. Accordingly, in cells exposed to α-ZEL + BEA, at [3.12 + 0.78] μM and [12.5 + 2.5] μM, by 2.1- and 1.5-fold respectively (Fig. 3D). for α-ZEL + β-ZEL at [1.56 + 0.39] μM, [6.25 + 1.25] μM and [12.5 + 2.5] μM from 0.8- to 3.5- fold (Fig. 3F), and for tertiary mixture at lowest concentration assayed ([1.56 + 1.5 + 0.39] μM by 0.6-fold (Fig. 5C), while for β-ZEL + BEA, this happened after 24 of exposure at all concentrations assayed from 0.6- to 3.2- folds, except when cells were exposed to the highest concentration ([12.5 + 2.5] μM) (Fig. 3E).

3.4. Enzymatic activity of SOD

As shown in Fig. 4, SOD activity increased significantly after being exposed to all treatments individually and in combination only after 48

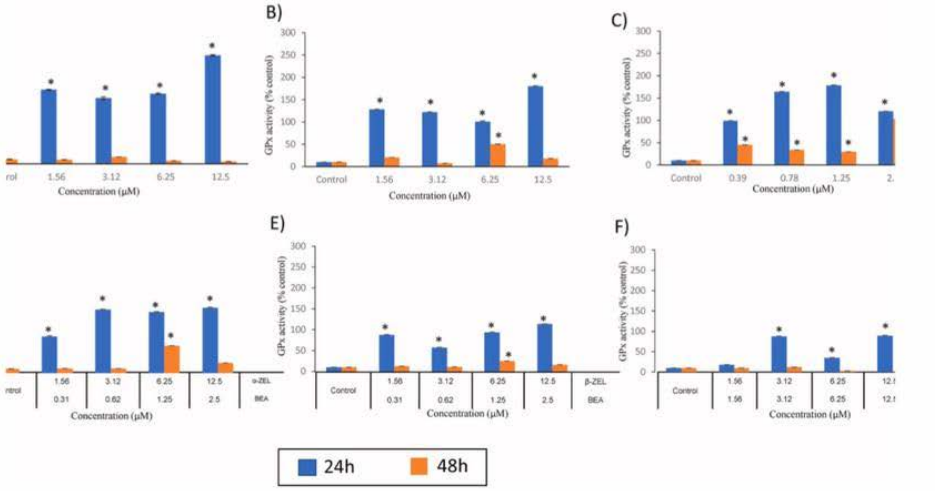

Fig. 1. Effect of α-ZEL (A), β-ZEL (B) and BEA (C), α-ZEL + BEA (D), β-ZEL + BEA (E), and α-ZEL + β-ZEL + BEA (F) on glutathione peroxidase (GPx) activity after 24 h and 48 h of exposure in SH-SY5Y cells. Data are expressed in % of the unexposed control. The GPx activity is expressed as μmol of NADPH oxidized/min/mg of protein; mean ± SEM (n = 3). *$p \leq 0.05$ indicates a significant difference from the respective solvent control.

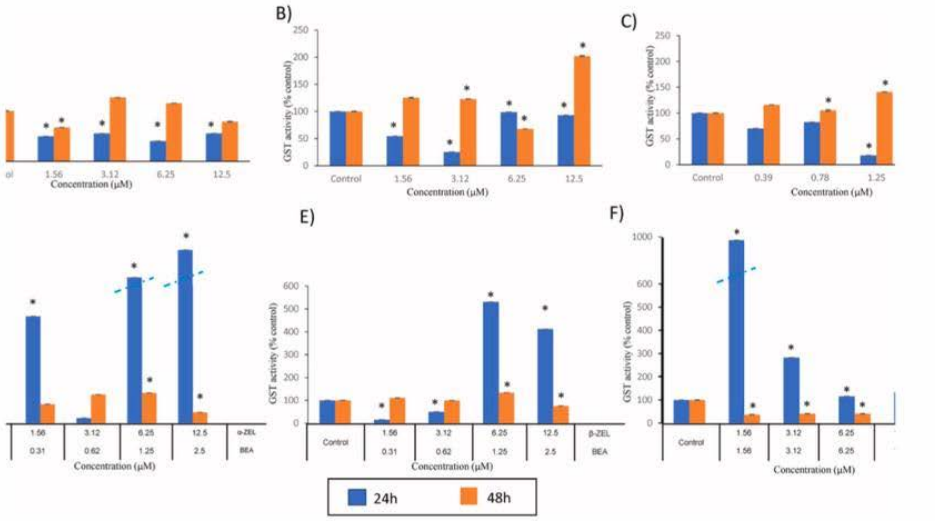

Fig. 2. Effect of α-ZEL (A), β-ZEL (B), BEA (C), α-ZEL + BEA (D), β-ZEL + BEA (E) and α-ZEL + β-ZEL (F) on glutathione S-transferase (GST) activity after 24 h and 48 h of exposure in SH-SY5Y cells. Data are expressed in % of the unexposed control. The GST activity is expressed as mol of product formed/min/mg of protein; mean ± SEM (n = 3). *$p \leq 0.05$ indicates a significant difference from the respective solvent control.

h of exposure at all concentrations assayed. Accordingly, for α-ZEL up to 1.4-fold (Fig. 4A), for β-ZEL up to 2.5-fold (Fig. 4B), for BEA up to 1-fold (Fig. 4C), and in binary and tertiary treatments, for α-ZEL + BEA from 2.7- to 3.3- fold (Fig. 4D), for β-ZEL + BEA from 2- to 4- fold (Fig. 4E), for α-ZEL + β-ZEL a minor increase up to 1-fold (Fig. 4F), and ultimately for α-ZEL + β-ZEL + BEA, from 1- to 2.5- fold in comparison to untreated

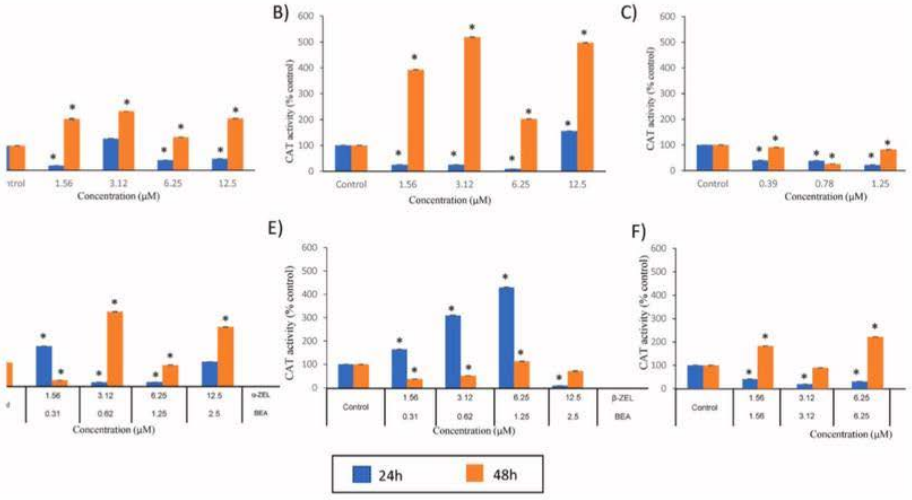

Fig. 3. Effect of α-ZEL (A), β-ZEL (B), BEA (C), α-ZEL + BEA (D), β-ZEL + BEA (E) and α-ZEL + β-ZEL (F) on catalase (CAT) activity after 24 h and 48 h of exposure in SH-SY5Y cells. Data are expressed in % of the unexposed control. The CAT activity is expressed as μmol H2O2/min/mg of protein; mean ± SEM (n = 3). *$p \leq 0.05$ indicates a significant difference from the respective solvent control.

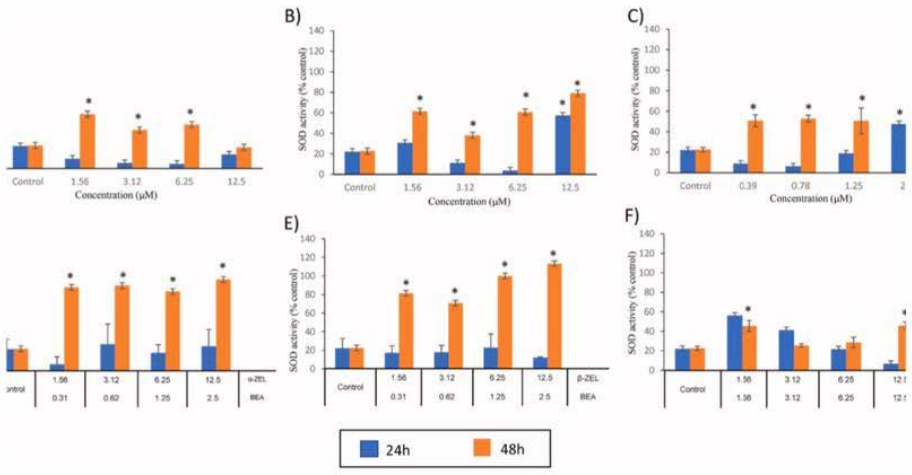

Fig. 4. Effect of α-ZEL (A), β-ZEL (B), BEA (C), α-ZEL + BEA (D), β-ZEL + BEA (E) and α-ZEL + β-ZEL (F) on superoxidase dismutase (SOD) activity after 24 h and 48 h of exposure in SH-SY5Y cells. Data are expressed in % of the unexposed control. The SOD activity is expressed as units of SOD/mg of protein; mean ± SEM (n = 3). *$p \leq 0.05$ indicates a significant difference from the respective solvent control.

cells (Fig. 5D). Therefore, as a result, binary combinations of α-ZEL + BEA and β-ZEL + BEA showed the major increase among other treatments.

4. Discussion

The study of α-ZEL, β-ZEL and BEA individually and combined for SH-SY5Y cells in enzyme activity for GPx, GST, CAT and SOD are here for the first time presented; however, in these same conditions oxidative stress and glutathione levels in our laboratory had been studied (Agahi

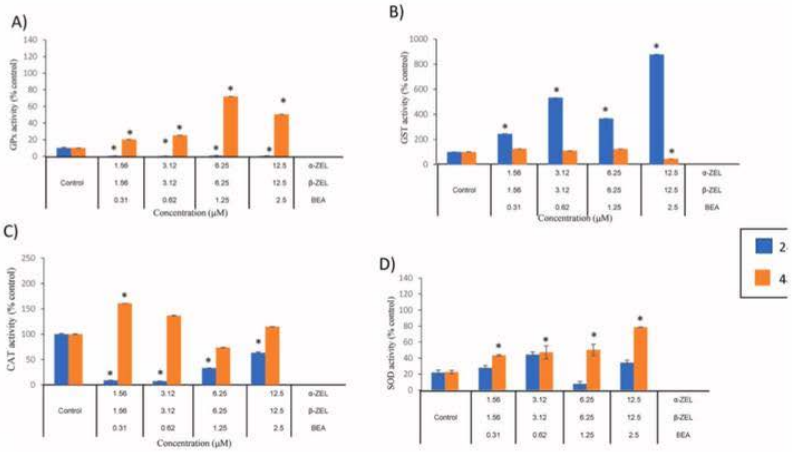

Fig. 5. Effect of α-ZEL + β-ZEL + BEA on glutathione peroxidase (GPx) (A), glutathione peroxidase (GPx) (B), catalase (CAT) (C) and superoxidase dismutase (SOD) (D) activity after 24 h and 48 h of exposure in SH-SY5Y cells. Data are expressed in % of the unexposed control. The GPx activity is expressed as μmol of NADPH oxidized/min/mg of protein; mean ± SEM (n = 3). *p ≤ 0.05 indicates a significant difference from the respective solvent control.

et al., 2020a). So that, although results in here are discussed and compared with other studies for any of the mycotoxins presented, results are mostly correlated with the effects obtained before in the same conditions in our laboratory. Same doses of exposure for individual and combined treatments (included the ratios for the mixtures) have been chosen according to previous results of cytotoxicity in undifferentiated SH-SY5Y cells (Agahi et al., 2020b) as well as not overpassing the levels found in food and the levels reaching the BBB.

Cellular systems are protected against oxidative damage by a multilayer network of mitochondrial anti-oxidant systems, which consist of SOD, CAT, GPx, GST and glutathione reductase (GR) enzymes. A number of low molecular weight antioxidants also intervene, such as α-tocopherol and ubiquinol and those coming from the food intake as zeaxanthin, lutein, polyphenols from goji berries and coffee, among others (Wei et al., 2001; Montesano et al., 2020; Juan-García et al., 2019a; Juan et al., 2020). These molecules are particularly effective in scavenging lipid peroxyl radicals and preventing free radical chain reactions of lipid peroxidation (Szeto et al., 2006).

Mitochondria converts 1–5% of the oxygen in cells to ROS which cannot be fully neutralized by defense systems completely (Wei et al., 2001). This can cause cumulative oxidative injuries to mitochondria, and progressively become less efficient in reducing ROS to end up undermining the mitochondria defense system and its consequences as induce mitochondrial DNA mutations, damage the mitochondrial respiratory chain, membrane permeability, Ca^{2+} homeostasis and mitochondrial defense systems (Brand et al., 2004). All these aspects are implicated in the development of neurodegenerative diseases as well and mediate or amplify the neuronal dysfunction during the course of neurodegeneration as previously reported in the literature (Szeto et al., 2006; Moreira et al., 2010; Michael et al., 2006).

The balanced enzymatic system in the mitochondrial matrix runs as follows: enzyme manganese superoxide dismutase (MnSOD or SOD2) or copper/zinc SOD (Cu/ZnSOD or SOD1) in the mitochondrial intermembrane space and cytosol convert $O_2^{\bullet}$ to hydrogen peroxide (H_2O_2) in the reaction $O_2^{\bullet} + O_2^{\bullet} + 2H+ \rightarrow H_2O_2 + O_2$ (Fridovich et al., 1995). H_2O_2 is more stable than $O_2^{\bullet}$ and can diffuse from mitochondria into the cytosol and nucleus. Afterward, H_2O_2 is detoxified by GPx in mitochondria and the cytosol by using glutathione (GSH) as a substrate, and by CAT in peroxisomes both by converting it to H_2O (Wei et al., 2001).

The results reported in here for BEA, α-ZEL and β-ZEL in undifferentiated SH-SY5Y cells, showed an increase of SOD activity in all treatments assayed, individually and combined, from 1- to 4- fold after 48 h of exposure compared to unexposed cells; while after 24 h of exposure, this activity remained unchanged (Figs. 4 and 5D). According to the connected enzymatic system described above, after accelerating the activity of SOD, the production of H_2O_2 increases, and consequently GPx antioxidant activity which is in charge of detoxifying H_2O_2 molecules, increases as well. Coinciding with this, GPx activity in SH-SY5Y exposed to mycotoxins increased significantly in all treatments individually and in binary combination after 24 h of exposure from 2.5- to 23- fold compared to untreated cells (Figs. 1 and 5A). GSH plays an important role in detoxifying H_2O_2 molecules but no changes in the activity of this antioxidant was observed when previously studied in our lab at the same conditions and for the same cell line (Agahi et al., 2020a). In fact, there is no GSH lack evidenced nor correlated with ROS levels and GPx activity. So that, results presented in here seem to have a close support to our previous findings (Agahi et al., 2020a).

In tertiary combination, the activity of GPx decreased significantly at 24 h and remained unchanged after 48 h of exposure for almost all treatments (Figs. 1 and 5A). In several studies, cells with increased levels of SOD showed to be hypersensitive to oxidative stress rather than protected from it (Michiels et al., 1994; Weydert et al., 2006). Hence, the dysfunctionality of H_2O_2 conversion by an adequate level of CAT and GPx, may be detrimental to the cell, by the consequence that H_2O_2 might accumulate to end up cells dying. In the light of this, the decreased activity level of GPx at 48 h can be justified by the increase of activity in SOD (Figs. 4 and 5D) coinciding with cytotoxicity and oxidative stress results reported by Agahi et al. (2020a and 2020b). This suggests that GPx activity in SH-SY5Y cell line is not the major implicated enzyme in detoxifying against cytotoxicity of BEA, α-ZEL and β-ZELIt is possible that GPx inactivates itself by its own substrates (Pigeolet et al., 1990) a fact that could be happening at 48 h in tertiary combination and associated to levels of ROS.

Similar results were obtained for sterigmatocystin (STE) mycotoxins in SH-SY5Y cells exposed during 24 h, where SOD and GPx enzymes decreased suggesting that these enzymes are unable to counteract the oxidative stress produced by STE exposure (Zingales et al., 2020). On the other hand, opposite results were obtained for HepG2 and CHO–K1 cells exposed to α-ZEL and β-ZEL individually for 24 h, where both SOD and GPx activity increased (Tatay et al., 2016, 2017); also for HT-29 cells exposed to deoxynivalenol (DON) during 24 h, where it was suggested that SOD and GPx were enzymes primarily involved in combating cellular oxidative (Krishnaswamy et al., 2010); and in CHO–K1 cells exposed to different concentrations of BEA for 24 h revealed an increase in GPx activity (Mallebrera et al., 2014). While in Hek-293 cells exposed to DON mycotoxin between 6 and 24 h of exposure, it was reported a significant increase in SOD activity (Dinu et al., 2011).

CAT enzyme is also involved in catalyze the decomposition of H_2O_2 along with GPx. CAT enzymes are abundant in the peroxisomes of liver cells while not as much in neuronal cells, and GPx is abundant in mitochondria and cytosol compartment. In this study, according to the results obtained from CAT activity in undifferentiated SH-SY5Y cells treated with α-ZEL, β-ZEL and BEA, it was observed a significant decrease in all individual treatments at 24 h (Fig. 2A, B and 2C) as well as in combinations except in the binary treatment β-ZEL + BEA (Fig. 2E). This decrease of CAT activity is probably associated to the competition of GPx with CAT enzyme in detoxifying H_2O_2 activity in the stage of 24 h of exposure mentioned above; although it is also possible that due to the high concentrations of peroxide, CAT inactivates or it is trying to equilibrate (Williams, 1928). Contrary, in the stage of 48 h of exposure, the activity of CAT in SH-SY5Y cells increased significantly for α-ZEL and β-ZEL mycotoxins in individual and combined treatments up to 4-fold in comparison to control cells (Figs. 2 and 5B). Moreover, the excess of H_2O_2 can cross the mitochondrial membrane and can be degraded by CAT; thus, it could be speculated that there is a compensation of CAT activity to reduce H_2O_2 levels, while GPx is inactivated for the same treatments during 48 h of exposure. Coinciding with this, similar results were found by Tatay et al. (2016, 2017) and Dinu et al. (2011) where CAT activity was reduced in a dose-dependent manner, suggesting that the accumulation of superoxide anion produced by assayed mycotoxins may inhibit CAT activity (Kono and Fridovich, 1982).

Finally, GST is a family of enzymes that catalyze the conjugation of GSH with a multitude of substrates to detoxify the exogenous and endogenous compounds. These enzymes are involved in the detoxification of xenobiotics and protective mechanism against cellular damage, such as oxidative stress. According to our results, a down regulation of the antioxidant defense system by decreasing the activity of GST enzyme only in cells exposed to α-ZEL and β-ZEL individually was observed (Fig. 3A and B). Inversely, a significant increase was demonstrated in all combination treatments, particularly in the highest concentrations assayed (except in α-ZEL + β-ZEL) (Fig. 3). In accordance with Grigutyte et al. (2009) increase in GST activity is considered a chemical stress signal, therefore, this effect can be in consequence of increasing enzymatic activity in combination treatments by augmenting the levels of ROS as previously reported, from 2.8- to 8- fold compared to control (Agahi et al., 2020a). Conversely, the decrease or unchanged GST activity in individual treatments can be as a result of no changing in ROS activity as it was proved previously (Agahi et al., 2020a).

5. Conclusions

In conclusion, the results achieved in the present study suggest that α-ZEL, β-ZEL and BEA mycotoxins in undifferentiated SH-SY5Y cells, individually and combined, increases the GPx activity after 24 h of exposure which can help to reduce the effects associated to these mycotoxins as the production of ROS originated at the same conditions (Agahi et al., 2020b). On the other hand, due to the balance of the enzymatic system the high activity detected for SOD enzyme after 48 h revealed decreases in the activity of GPx and CAT enzymes. CAT enzyme showed the highest activity for α-ZEL and β-ZEL in SH-SY5Y cells when exposed individually and in combined treatments. When mycotoxins merged together, GST enzyme activity increased which supports the fact that damage associated to oxidative stress by these mycotoxins is trying to be alleviated by GST activity. Ultimately, altogether and from achieved results it can be comprehended that antioxidant enzymatic system in SH-SY5Y cells, provide a strong protector role toward the damage caused by α-ZEL, β-ZEL and BEA mycotoxins in undifferentiated SH-SY5Y cells in individual and combined treatments.

CRediT authorship contribution statement

Fojan Agahi: Data curation, Investigation, Writing – original draft, Investigation, Methodology, Visualization, Writing – review & editing, Writing – original draft. **Ana Juan-García:** Data curation, Formal analysis. **Guillermina Font:** Funding acquisition. **Cristina Juan:** Data curation, Formal analysis, Funding acquisition, Investigation, Methodology, Visualization, Writing – original draft, Writing – review & editing.

Declaration of competing interest

The authors declare that they have no known competing financial interests or personal relationships that could have appeared to influence the work reported in this paper.

Acknowledgements

Authors would like to thank Spanish Ministry of Science and Innovation PID 2019-108070RB-I00ALI and Generalitat Valenciana GV 2020/020.

All persons who have made substantial contributions to the work reported in the manuscript (e.g., technical help, writing and editing assistance, general support), but who do not meet the criteria for authorship, are named in the Acknowledgements and have given us their written permission to be named. If we have not included an Acknowledgements, then that indicates that we have not received substantial contributions from non-authors.

References

Abbott, N.J., 2005. Dynamics of CNS barriers: evolution, differentiation, and modulation. Cell. Mol. Neurobiol. 25, 5–23.
Agahi, F., Alvarez-Ortega, A., Font, G., Juan-García, A., Juan, C., 2020a. Oxidative stress, glutathione, and gene expression as key indicators in SH-SY5Y cells exposed to zearalenone metabolites and beauvericin. Toxicol. Lett. 334, 44–52.
Agahi, F., Font, G., Juan, C., Juan-García, A., 2020b. Individual and combined effect of zearalenone derivates and beauvericin mycotoxins on SH-SY5Y cells. Toxins 12, 212.
Agahi, F., Juan, C., Font, G., Juan-García, A., 2020c. In silico methods for metabolomic and toxicity prediction of zearalenone, α-zearalenone and β-zearalenone. Food Chem. Toxicol. 146, 111818.
Albarracin, S.L., Stab, B., Casas, Z., Sutachan, J.J., Samudio, I., Gonzalez, J., Gonzalo, L., Capani, F., Morales, L., Barreto, G.E., 2012. Effects of natural antioxidants in neurodegenerative disease. Nutr. Neurosci. 15, 1–9.
Behrens, M., Hüwel, S., Galla, H.J., Humpf, H.U., 2015. Blood-brain barrier effects of the Fusarium mycotoxins deoxynivalenol, 3 acetyldeoxynivalenol, and moniliformin and their transfer to the brain. PloS One 10 (11), 0143640.
Biehl, M.L., Prelusky, D.B., Koritz, G.D., Hartin, K.E., Buck, W.B., Trenholm, H.L., 1993. Biliary-excretion and enterohepatic cycling of zearalenone in immature pigs. Toxicol. Appl. Pharmacol. 121 (1), 152–159.
Bocianowski, J., Szulc, P., Waskiewicz, A., Cyplik, A., 2020. The effect of agrotechnical factors on Fusarium mycotoxins level in maize. Agriculture 10 (11), 528.
Brand, M.D., Affourtit, C., Esteves, T.C., Green, K., 2004. Mitochondrial superoxide: production, biological effects, and activation of uncoupling proteins. Free Radic. Biol. Med. 37 (6), 755–767.
Brodehl, A., Möller, A., Kunte, H.J., Koch, M., Maul, R., 2014. Biotransformation of the mycotoxin zearalenone by fungi of the genera Rhizopus and Aspergillus. FEMS. Microbiology Letters 359, 124–130.
Cai, Y., Shen, H., Weng, H., Wang, Y., Cai, G., Chen, X., Ye, Q., 2020. Overexpression of PGC-1α influences the mitochondrial unfolded protein response (mtUPR) induced by MPP+ in human SH-SY5Y neuroblastoma cells. Sci. Rep. 10, 10444.
Chang, W., Lin, J., 1984. Transformation of zearalenone and zearalenol by rat erythrocytes. Food Chem. Toxicol. 22 (11), 887–891.
Darwish, W.S., Ikenaka, Y., Nakayama, ShM.M., Ishizuka, M., 2014. An overview on mycotoxin contamination of foods in africa. Toxicology 76, 789–797.

Devreese, M., Antonissen, G., Broekaert, N., De Baere, S., Vanhaecke, L., De Backer, P., Croubels, S., 2015. Comparative toxicokinetics, absolute oral bioavailability, and biotransformation of zearalenone in different poultry species. Agricultural and Food Chemistry 63 (20), 5092–5098.
Dinu, D., Bodea, G.O., Ceapa, C.D., Munteanu, M.C., Roming, F.I., Serban, A.I., 2011. Adapted response of the antioxidant defense system to oxidative stress induced by deoxynivalenol in Hek-293 cells. Toxicon 57, 1023–1032.
Drzymala, S.S., Binder, J., Brodehl, A., Penkert, M., Rosowski, M., Garbe, L.A., Koch, M., 2015. Estrogenicity of novel phase I and phase II metabolites of zearalenone and cis-zearalenone. Toxicon 105, 10–12.
Dweba, C.C., Figlan, S., Shimelis, H.A., Motaung, T.E., Sydenham, S., Mwadzingeni, L., Tsilo, T.J., 2017. Fusarium head blight of wheat: pathogenesis and control strategies. Crop Protect. 91, 114–122.
Fridovich, I., 1995. Superoxide radical and superoxide dismutases. Annu. Rev. Biochem. 64, 97–112.
Gandhi, S., Abramov, A.Y., 2012. Mechanism of Oxidative Stress in Neurodegeneration Oxidative Medicine and Cellular Longevity, pp. 1–11, 2012.
Juan García, A., Carbone, S., Ben Mahmoud, M., Sagratini, G., Mañes, J., 2020. Beauvericin and ochratoxin A mycotoxins individually and combined in HepG2 cells alter lipid peroxidation, levels of reactive oxygen species and glutathione. Food Chem. Toxicol. 139, 111247.
Juan, C., de Simone, G., Sagratini, G., Caprioli, G., Mañes, J., Juan-García, A., 2020. Reducing the effect of beauvericin on neuroblastoma SH-SY5Y cell line by natural products. Toxicon 188, 164–171.
Juan-García, A., Bind, M.A., Engert, F., 2020. Larval zebrafish as an in vitro model for evaluating toxicological effects of mycotoxins. Ecotoxicol. Environ. Saf. 202, 110909.
Juan-García, A., Montesano, D., Mañes, J., Juan, C., 2019a. Cytoprotective effects of carotenoids-rich extract from *Lycium barbarum L.* on the beauvericin-induced cytotoxicity on Caco-2 cells. Food Chem. Toxicol. 133, 110798.
Juan-García, A., Tolosa, J., Juan, C., Ruiz, M.J., 2019b. Cytotoxicity, genotoxicity and disturbance of cell cycle in HepG2 cells exposed to OTA and BEA: single and combined actions. Toxins 11, 341.
Kim, H.B., Yoo, J.Y., Yoo, S.Y., Lee, J.H., Chang, W., Kim, H.S., Baik, T.K., Woo, R.S., 2020. Neuregulin-1 inhibits CoCl2-induced upregulation of excitatory amino acid carrier 1 expression and oxidative stress in SH-SY5Y cells and the hippocampus of mice. Mol. Brain 13, 153.
Klarić, M.Š., Rumora, L., Ljubanović, D., Pepeljnjak, S., 2008. Cytotoxicity and apoptosis induced by fumonisin B1, beauvericin and ochratoxin A in porcine kidney PK15 cells: effects of individual and combined treatment. Arch. Toxicol. 82, 247–255.
Kono, N.S., Fridovich, I., 1982. Superoxide radical inhibits catalase. J. Biol. Chem. 257, 5751–5754.
Kouri, K., Lemmens, M., Lemmens-Gruber, R., 2003. Beauvericin-induced channels in ventricular myocytes and liposomes. Biochim. Biophys. Acta 1609, 203–210.
Krishnaswamy, R., Devaraj, S.N., Padma, V.V., 2010. Lutein protects HT-29 cells against Deoxynivalenol-induced oxidative stress and apoptosis: prevention of NF-kappaB nuclear localization and down regulation of NF-κB and Cyclo-Oxygenase - 2 expression, 49 (1), 50–60.
Krug, I., Behrens, M., Esselen, M., Humpf, H.U., 2018. Transport of enniatin B and enniatin B1 across the blood-brain barrier and hints for neurotoxic effects in cerebral cells. PloS One 13 (5), 0197406.
Lawana, V., Um, S.Y., Rochet, J.C., Turesky, R.J., Shannahan, J.H., Cannon, J.R., 2020. Neuromelanin modulates heterocyclic aromatic amine-induced dopaminergic neurotoxicity. Toxicol. Sci. 173, 171–188.
Malekinejad, H., Colenbrander, B., Fink-Gremmels, J., 2006a. Hydroxysteroid dehydrogenases in bovine and porcine granulosa cells convert zearalenone into its hydroxylated metabolites alpha-zearalenol and beta-zearalenol. Vet. Res. Commun. 30 (4), 445–453.
Malekinejad, H., Maas-Bakker, R., Fink-Gremmels, J., 2006b. Species differences in the hepatic biotransformation of zearalenone. Vet. J. 172 (1), 96–102.
Mallebrera, B., Font, G., Ruiz, M.J., 2014. Disturbance of antioxidant capacity produced by beauvericin in CHO-K1 cells. Toxicol. Lett. 226, 337–342.
Manyes, L., Escriva, L., Ruiz, M.J., Juan-García, A., 2018. Beauvericin and enniatin B effects on a human lymphoblastoid Jurkat T-cell model. Food Chem. Toxicol. 115, 127–135.
Maran, E., Fernandez, M., Barbieri, P., Font, G., Ruiz, M.J., 2009. Effects of four carbamate compounds on antioxidant parameters. Ecotoxicol. Environ. Saf. 72, 922–930.
Michiels, C., Raes, M., Toussaint, O., Remacle, J., 1994. Importance of Se-glutathione peroxidase, catalase and Cu/Zn–SOD for cell survival against oxidative stress. Free Radic. Biol. Med. 17, 235–248.
Molina-Molina, J.M., Real, M., Jimenez-Diaz, I., Belhassen, H., Hedhili, A., Torne, P., Fernandez, M.F., Olea, N., 2014. Assessment of estrogenic and anti-androgenic activities of the mycotoxin zearalenone and its metabolites using in vitro receptor-specific bioassays. Food Chem. Toxicol. 74, 233–239.
Montesano, D., Juan-García, A., Mañes, J., Juan, C., 2020. Chemoprotective effect of carotenoids from Lycium barbarum L. on SH-SY5Y neuroblastoma cells treated with beauvericin. Food Chem. Toxicol. 141, 111414.
Moreira, P.I., Zhu, X., Wang, X., Lee, H.G., Nunomura, A., Petersen, R.B., Perry, G., Smith, M.A., 2010. Mitochondria: a therapeutic target in neurodegeneration. Biochim. Biophys. Acta 1802 (1), 212–220.
Ojcius, D.M., Zychlinsky, A., Zheng, L.M., Young, J.D., 1991. Ionophore-induced apoptosis: role of DNA fragmentation and calcium fluxes. Exp. Cell Res. 197, 43–49.
Olsen, M., Pettersson, H., Kiessling, K.H., 1981. Reduction of zearalenone to zearalenol in female rat liver by 3 alpha-hydroxysteroid dehydrogenase. Toxicol. Appl. Pharmacol. 48, 157–161.
Ouesłati, S., Berrada, H., Juan-García, A., Mañes, J., Juan, C., 2020. Multiple mycotoxin determination on Tunisian cereals-based food and evaluation of the population exposure. Food Anal Meth. https://doi.org/10.1007/s12161-020-01737-z.
Pfeiffer, E., Kommer, A., Dempe, J.S., Hildebrand, A.A., Metzler, M., 2011. Absorption and metabolism of the mycotoxin zearalenone and the growth promotor zeranol in caco-2 cells in vitro. Mol. Nutr. Food Res. 55 (4), 560–567.
Pigeolet, E., Corbisier, P., Houbion, A., Lambert, D., Michiels, C., Raes, M., Zachary, M. D., Remacle, J., 1990. Glutathione peroxidase, superoxide dismutase, and catalase inactivation by peroxide and oxygen derived free radical. Mech. Ageing Dev. 51, 283–297.
Pizzo, F., Caloni, F., Schreiber, N.B., Cortinovis, C., Spicer, L.J., 2016. In vitro effects of deoxynivalenol and zearalenone major metabolites alone and combined, on cell proliferation, steroid production and gene expression in bovine small-follicle granulosa cells. Toxicon 109, 70–83.
Prosperini, A., Juan-García, A., Font, G., Ruiz, M.J., 2013. Beauvericin-induced cytotoxicity via ROS production and mitochondrial damage in Caco-2 cells. Toxicol. Lett. 222 (2), 204–211.
Reddy, P., Guthridge, K., Vassiliadis, S., Hemsworth, J., Hettiarachchige, I., Spangenberg, G., Rochfort, S., 2019. Tremorgenic mycotoxins: structure diversity and biological activity. Toxins 11, 302. https://doi.org/10.3390/toxins11050302.
Sirin, S., Aslim, B., 2020. Characterization of lactic acid bacteria derived exopolysaccharides for use as a defined neuroprotective agent against amyloid beta1–42-induced apoptosis in SH-SY5Y cells. Sci. Rep. 10, 8124.
Szeto, H.H., 2006. Mitochondria-targeted peptide antioxidants: novel neuroprotective agents. AAPS J. 8 (3), 521–531.
Taevernier, L., Bracke, N., Veryser, L., Wynendaele, E., Gevaert, B., Peremans, K., Spiegeleer, B.D., 2016. Blood-brain barrier transport kinetics of the cyclic depsipeptide mycotoxins beauvericin and enniatins. Toxicol. Lett. 258, 175–184.
Taroncher, M., Pigni, M.Ch, Diana, M.N., Juan-García, A., Ruiz, M.J., 2020. Does low concentration mycotoxin exposure induce toxicity in HepG2 cells through oxidative stress? Toxicol. Mech. Methods 30 (6), 417–426.
Tatay, E., Espin, S., Garcia-Fernandez, A.J., Ruiz, M.J., 2017. Oxidative damage and disturbance of antioxidant capacity by zearalenone and its metabolites in human cells. Toxicol. *Vitro* 45, 334–339.
Tatay, E., Font, G., Ruiz, M.J., 2016. Cytotoxic effects of zearalenone and its metabolites and antioxidant cell defense in CHO-K1 cells. Food Chem. Toxicol. 96, 43–49.
Tonshin, A.A., Teplova, V.V., Andersson, M.A., Salkinoja-Salonen, M.S., 2010. The Fusarium mycotoxins enniatins and beauvericin cause mitochondrial dysfunction by affecting the mitochondrial volume regulation, oxidative phosphorylation and ion homeostasis. Toxicology 276, 49–57.
Ueda, M., Mozaffar, S., Tanaka, A., 1990. Catalase from Candida boidinii 2201. Methods Enzymol. 188, 463–467.
Videmann, B., Mazallon, M., Prouillac, C., Delaforge, M., Lecoeur, S., 2009. ABCC1, ABCC2 and ABCC3 are implicated in the transepithelial transport of the myco-estrogen zearalenone and its major metabolites. Toxicol. Lett. (Shannon) 190 (2), 215–223.
Videmann, B., Mazallon, M., Tep, J., Lecoeur, S., 2008. Metabolism and transfer of the mycotoxin zearalenone in human intestinal caco-2 cells. Food Chem. Toxicol. 46 (10), 3279–3286.
Wei, J., Wu, B., 2020. Chemistry and bioactivities of secondary metabolites from the genus Fusarium. Fitoterapia 146, 104638.
Wei, Y.H., Lu, C.Y., Wei, C.Y., Ma, Y.S., Lee, H.C., 2001. Oxidative stress in human aging and mitochondrial disease? consequences of defective mitochondrial respiration and impaired antioxidant enzyme system. Chin. J. Physiol. 44 (1), 1–11.
Weydert, Ch.J., Waugh, T.A., Ritchie, J.M., Kanchan, S.I., Smith, J.L., Ling, L., Spitz, D.R., Oberley, L.W., 2006. Overexpression of manganese or copper-zinc superoxide dismutase inhibits breast cancer growth. Free Radical Biol. Med. 41, 226–237.
Williams, J., 1928. The decomposition of hydrogen peroxide by liver catalase. J. Gen. Physiol. 1, 309–337.
Xicoy, H., Wieringa, B., Martens, G.J., 2017. The SH-SY5Y cell line in Parkinson's disease research: a systematic review. Mol. Neurodegener. 12 (1), 10. https://doi.org/10.1186/s13024-017-0149-0. PMID: 28118852.

Toxicology 456 (2021) 152784

Contents lists available at ScienceDirect

Toxicology

journal homepage: www.elsevier.com/locate/toxicol

Neurotoxicity of zearalenone's metabolites and beauvericin mycotoxins via apoptosis and cell cycle disruption

Fojan Agahi, Cristina Juan *, Guillermina Font, Ana Juan-García

Laboratory of Food Chemistry and Toxicology, Faculty of Pharmacy, University of Valencia, Av. Vicent Andrés Estellés s/n, 46100, Burjassot, Valencia, Spain

ARTICLE INFO

Keywords:
Cell cycle
Cell death
Zearalenone's metabolites
Beauvericin
Neuronal cells

ABSTRACT

Cell cycle progression and programmed cell death are imposed by pathological stimuli of extrinsic or intrinsic including the exposure to neurotoxins, oxidative stress and DNA damage. All can cause abrupt or delayed cell death, inactivate normal cell survival or cell death networks. Nevertheless, the mechanisms of the neuronal cell death are unresolved. One of the cell deaths triggers which have been wildly studied, correspond to mycotoxins produced by *Fusarium* species, which have been demonstrated cytotoxicity and neurotoxicity through impairing cell proliferation, gene expression and induction of oxidative stress. The aim of present study was to analyze the cell cycle progression and cell death pathway by flow cytometry in undifferentiated SH-SY5Y neuronal cells exposed to α-zearalenol (α-ZEL), β-zearalenol (β-ZEL) and beauvericin (BEA) over 24 h and 48 h individually and combined at the following concentration ranges: from 1.56 to 12.5 μM for α-ZEL and β-ZEL, from 0.39 to 2.5 μM for BEA, from 1.87 to 25 μM for binary combinations and from 3.43 to 27.5 μM for tertiary combination. Alterations in cell cycle were observed remarkably for β-ZEL at the highest concentration in all treatments where engaged (β-ZEL, β-ZEL + BEA and β-ZEL + α-ZEL), for both 24 h and 48 h. by activating the cell proliferation in G0/G1 phase (up to 43.6 %) and causing delays or arrests in S and G2/M phases (up to 19.6 %). Tertiary mixtures revealed increases of cell proliferation in subG0 phase by 4-folds versus control. Similarly, for cell death among individual treatments β-ZEL showed a significant growth in early apoptotic cells population at the highest concentration assayed as well as for all combination treatments where β-ZEL was involved, in both early apoptotic and apoptotic/necrotic cell death pathways.

1. Introduction

Cell cycle and cell death are balanced routes that ensure the tissue structure and homeostasis which occurs through many pathways. There are two distinct routs of cell death, called apoptosis and necrosis, as per the structural and biochemical differences. Coupling the process of mitosis with apoptosis seem to be regulated through a specific set of precise factors (Pucci et al., 2000; King and Cidlowski, 1995). The occurrence of programmed cell death is a highly conserved mechanism in tissue remodeling, which enables an organism to eliminate redundant and malfunctioning cells through a process of cellular disintegration that has the advantage of not inducing an undesirable inflammatory response (Elmore, 2007; Thompson, 1995). However, unregulatable death events of cells can induce many disorders such as neurodegenerative disorders which can lead to various chronic disease states of amyotrophic lateral sclerosis (ALS) and Alzheimer's disease, and in neurological injury such as cerebral ischemia and trauma. It can also induce defense mechanisms of cancer cells against the apoptotic and necrotic signals where a loss of balance between cell division and cell death occurs (Wong, 2011; Okouchi et al., 2007).

The cell cycle is a set of events responsible for cell duplication, by which cells alternate DNA synthesis and mitosis and ensure that each of these processes finishes before the other begins. Such careful control is articulated at the level of checkpoints mechanisms that sense the progress of each cell cycle phase and only upon its completion allow progression into the next; hence, dysfunction of checkpoints can prove fatal for the affected cell (Pucci et al., 2000). Whether or not apoptosis and necrosis occur as a consequence of a defective cell cycle, it is clear that damage to the cell cycle or to genomic integrity is an extremely efficient trigger of cell death (Manickam et al., 2020; Zingales et al., 2020; Swomley et al., 2014). It has been proved that several cytotoxic agents induce cell death through oxidative stress in the form of increased reactive oxygen species (ROS), which not only triggers cell death but it is also implicated in several disorders (Manickam et al., 2020; Carri et al.,

* Corresponding author.
E-mail address: cristina.juan@uv.es (C. Juan).

https://doi.org/10.1016/j.tox.2021.152784
Received 27 January 2021; Received in revised form 18 March 2021; Accepted 12 April 2021
Available online 16 April 2021

2003; Jenner, 2003; Klein and Ackerman, 2003). ROS are considered to damage cells and ultimately apoptosis by destruction of cellular components including lipids, proteins, and nucleic acids (Kannan and Jain, 2000). In the sight of this fact, various *in vitro* and *in vivo* study suggested that ROS generation can be provoked by many toxins including one of the most recent studies as for mycotoxins (Agahi et al., 2020b; Tatay et al., 2017; Mallebrera et al., 2014; Prosperini et al., 2013). We previously demonstrated that α-ZEL, β-ZEL and BEA mycotoxins from fungi of the genus *Fusarium*, induce injury in human neuroblastoma SH-SY5Y cells by elevating oxidative stress levels which lead to the induction of cytotoxicity, ROS generation, disruption of enzymatic and non-enzymatic activity and more importantly causing disorders through alteration in the expression of genes *Casp-3, Bax* and *Bcl-2;* all three involved in cell apoptosis (Agahi et al., 2020a, 2020b). However, little is known about the effects of these mycotoxins or the implication of ROS levels on alterations of cell cycle progression nor in cell death route activation.

It is believed that the human-derived SH-SY5Y cells express a number of human-specific proteins and protein isoforms that would not be inherently present in rodent primary cultures. Both undifferentiated and differentiated SH-SY5Y cells have been utilized for *in vitro* experiments requiring neuronal-like cells. In the undifferentiated form, SH-SY5Y cells have catecholaminergic characteristic and recognized morphologically by neuroblast-like (Kovalevich and Langford, 2013). Hence, we set out the present study to investigate the cell cycle regulation in an undifferentiated SH-SY5Y neuronal cells line exposed by α-ZEL, β-ZEL and BEA mycotoxins individually, in binary and in tertiary combinations during 24 h and 48 h of exposure, and also determine the mechanism of cytotoxicity causing cell death whether is through apoptotic, apoptotic/necrotic or necrotic pathways.

2. Material and methods

2.1. Reagents

The reagent grade chemicals and cell culture components used, Dulbecco's Modified Eagle's Medium- F12 (DMEM/F-12), fetal bovine serum (FBS) and phosphate buffer saline (PBS) were supplied by Thermofisher, Gibco ™ (Paisley, UK). Methanol (MeOH, HPLC LS/MS grade) was obtained from VWR International (Fontenay-sous-Bois, France). Dimethyl sulfoxide was obtained from Fisher Scientific Co, Fisher BioReagnts ™ (Geel, Belgium). Deionized water (<18, MΩcm resistivity) was obtained in the laboratory using a Milli-QSP® Reagent Water System (Millipore, Beadford, MA, USA). HEPES, t-octylphenoxypolyethoxyethanol (Triton-X 100), tris-hydroxymethyl aminomethane (Tris), ribonuclease A from bovine pancreas (RNAase), Annexin V-FITC, propidium iodide (PI), the standard of BEA (MW: 783.95 g/mol), α-ZEL and β-ZEL (MW: 320.38 g/mol) were purchased from SigmaAldrich (St. Louis Mo. USA). Stock solutions of mycotoxins were prepared in MeOH (α-ZEL and β-ZEL) and DMSO (BEA) and maintained at −20 °C in the dark. The final concentration of either MeOH or DMSO in the medium was ≤1% (v/v) as per established. All other standards were of standard laboratory grade.

2.2. Cell culture

Human neuroblastoma cell line, SH-SY5Y, was obtained from American Type Culture Collection (ATCC, Manassas, VA, USA), and cultured in Dulbecco's Modified Eagle's Medium- F12 (DMEM/F-12), supplemented with 10 % fetal bovine serum (FBS), 100 U/mL penicillin, and 100 mg/mL streptomycin. The cells were sub-cultivated after trypsinization once or twice a week and suspended in complete medium in a 1:3 split ratio. Cells were maintained as monolayer in 150 cm^2 cell culture flasks with filter screw caps (TPP, Trasadingen, Switzerland). Cell cultures were incubated at 37 °C, 5% CO_2 atmosphere.

2.3. Cell cycle analysis

Cell cycle analysis was performed using Vindelov's PI staining solution as described previously by Juan-García et al. (2013). The PI solution is a fluorescent DNA intercalating agent able to bind and label double-stranded nucleic acids, making it possible to achieve rapid and precise evaluation of cellular DNA content by flow cytometric analysis. The cell cycle is monitored by different key checkpoints or decision points on whether the cell should divide, delay division, or enter a resting stage. 5-Fluorouracil (5-Fu) inhibits thymidylate synthase, which blocks synthesis of the nucleoside thymidine, and thus affects DNA synthesis in the S phase. The etoposide inhibits DNA topoisomerase II and exerts its effects at the G2-M checkpoint. Etoposide and 5-Fu were used as positive control. For this, 7×10^5 cells/well were seeded in six-well plates. After cells achieved the 90 % confluence, cells were treated with α-ZEL and β-ZEL (12.5, 6.25, 3.12 and 1.56 μM), and BEA (2.5, 1.25, 0.78 and 0.39 μM) as an individual treatment. In assays of combinations the following mixtures were tested: α-ZEL + BEA, β-ZEL + BEA, α-ZEL + β-ZEL and α-ZEL + β-ZEL + BEA with concentrations ranged from 25 to 1.87 μM for binary combinations, and from 27.5 to 3.43 μM for tertiary combination. The dilution ratio of concentration ranges in binary combinations was (1:1) for α-ZEL + β-ZEL, (5:1) for α-ZEL + BEA and β-ZEL + BEA, and (5:5:1) in tertiary combinations (α-ZEL + β-ZEL + BEA). Then, cells were trypsinized (0.14 mL) and removed after 3 min and placed on ice for 30 min with 0.36 mL of fresh medium containing 0.5 mL Vindelov's PI staining solution prepared as follows: 40 μg/mL RNAase, 0.1 % Triton X-100, 10 mM Tris, 10 mM NaCl and 50 μg/mL of PI in PBS. Fifty thousand cells for each sample were analyzed using BD LSRFortessa (BD Biosciences) flow cytometry. The experiments were carried out in duplicate, and the results were expressed as the mean ± SEM of different independent experiments.

2.4. Measurement of necrosis-apoptosis by Annexin V-FITC/PI

Cell death generally proceeds through two molecular mechanisms: necrosis and apoptosis. One of the characteristics of apoptosis is the externalization of phosphatidylserine (PS) to the outer leaflet of the plasma membrane. The differential of population of apoptotic cells (early or late), necrotic and dead cells was identified by Annexin V-FITC/PI double staining (Vermes et al., 1995). Cells considered as viable are both Annexin V-$FITC^-$/PI^- negative; cells in early apoptosis (pro-apoptotic/apoptotic cells) are Annexin V-$FITC^+$/PI^-. Cells stained negative for Annexin V-FITC and positive for PI represented necrotic cells. Cells stained positive for both Annexin V-FITC and PI corresponded to late apoptotic/necrotic cells. The assay was carried out as described by Juan-García et al. (2013). 10,000 cells were acquired and analyzed on a BD FACSCanto flow cytometer with FACSDiva software v 6.1.3 (BD Biosciences). Undifferentiated neuroblastoma SH-SY5Y cells were seeded and exposed to mycotoxins as detailed previously in section 2.3. Green (FL-1, 530 nm) and orange-red fluorescence (FL-2, 585 nm) were detected, emitted by FITC and PI, respectively. Quadrant statistics were performed to determine viable cells (live cells), early apoptotic, apoptotic/necrotic (late apoptotic) and necrotic (dead cells) from the total population of cells.

2.5. Statistical analysis

Statistical analysis of data was carried out using IBM SPSS Statistic version 23.0 (SPSS, Chicago, Il, USA) statistical software package and GraphPad Prism 8.0 (GraphPad Software, Inc., San Diego, USA). Data were expressed as mean ± SD of three independent experiments. The statistical analysis of the results was performed by student's T-test for paired samples. Difference between groups were analyzed statistically with ANOVA followed by the Tukey HDS post hoc test for multiple comparisons. The level of $p \leq 0.05$ was considered statistically significant.

3. Results

3.1. Cell cycle analysis in individual treatments

Flow cytometry was used to determine cell proliferation by cell cycle analysis with PI staining. As it is shown in Fig. 1a.1, in individual treatment of α-ZEL after 24 h of exposure, a significant concentration-dependent increase in G0/G1 phase was observed at 3.12 μM, 6.25 μM and 12.5 μM by 1.5 %, 4.5 % and 6% respectively, accompanied by a reduction in S phase at all concentrations up to 25.7 %, and in G2/M phase up to 32.4 % as compared to the control. Conversely, a concentration-dependent reduction in the number of cells in G0/G1 phase was detected after 48 h at 1.56 μM, 6.25 μM and 12.5 μM by 6.9 %, 7.6 % and 9%, respectively (Fig. 1a.2). For individual treatment of β-ZEL after 24 h of exposure, a significant dose-dependent increase in G0/G1 phase was observed at all concentrations assayed from 4.7%–34.6% versus the control (Fig. 1b.1); which was accompanied by a dose-dependent decline in S phase from 29 % to 87 %, and also in G2/M phase at the highest concentrations assayed of 6.25 μM and 12.5 μM by 46 % and 68 %, respectively (Fig. 1b.1).However, after 48 h of exposure in G0/G1 phase, this increase was only observed at the highest concentration assayed (12.5 μM) by 7.7 %, accompanied by unchanged activity in S phase and a significant decrease in G2/M phase at 3.12 μM and 6.25 μM by 30 % and 21 %, respectively (Fig. 1b.2). For BEA, after 24 h of exposure, a significant increase was observed in G0/G1 phase at the lowest concentrations assayed (0.39 μM and 0.78 μM,) by 10%–13.8%, followed by a notable reduction in S phase at the same concentrations from 19.8%–28.7% (Fig. 1c.1). The same increase happened for G2/M phase at 0.39 μM, 0.78 μM and 2.5 μM by 10.2 %, 13.2 % and 38.3 % respectively, in comparison to unexposed cells (Fig. 1c.1). Inversely, after 48 h exposure cell population remained unchanged in G0/G1 phase and G2/M phase, while in S phase a significant decrease was detected at 0.78 μM and 2.5 μM by 20 % and 42.3 %, respectively compared to control cells (Fig. 1c.2).

3.2. Cell cycle analysis in combination treatments

Fig. 2 reports the results of cell cycle progression for binary combinations. For α-ZEL + BEA (Fig. 2a), G0/G1 phase increased significantly at all concentrations assayed up to 15.4 % compared to untreated cells after 24 h of exposure (Fig. 2a.1). For S phase, a significant decrease was observed at the highest concentration assayed ([12.5 + 2.5] μM) by 31.6 % and 55.4 %, for 24 h and 48 h, respectively (Fig. 2a). For β-ZEL + BEA treatment (Fig. 2b), G0/G1 phase revealed a significant increase at [3.12 + 0.78] μM, [6.25 + 1.25] μM and [12.5 + 2.5] μM by 22.9 %, 34.3 % and 30 %, respectively at 24 h, followed by a dose-dependent decrease in S phase at the same concentrations from 37.5% to 66.5%, and in G2/M phase at all concentrations from 36 % to 6 compared to unexposed cells (Fig. 2b.1).On the other hand, after 48 h of exposure a marked alteration in all phases was observed at the highest concentrations assayed ([12.5 + 2.5] μM): cells in G0/G1 phase increased by 19.6 %, followed by a decrease in S and G2/M phases by 44 % and 78 %, respectively compared to unexposed cells (Fig. 2b.2). For α-ZEL + β-ZEL (Fig. 2c) cell distribution in G0/G1 phase was significantly high in a dose-dependent manner after 24 h of exposure at [1.56 + 0.39] μM, [6.25 + 1.25] μM and [12.5 + 2.5] μM by 17.9 %, 32.8 % and 43.6 %, respectively compared to control cells (Fig. 2c.1); this was accompanied by a significant reduction in cells population in S phase at the highest concentrations assayed [6.25 + 1.25] μM and [12.5 + 2.5] μM by 49 % and 84.6 %, respectively, and also in G2/M phase at all concentrations assayed in a concentration-dependent manner (from 35.7%–60%) (Fig. 2c.1). Remarkably, after 48 h of exposure a shift in percentage of cells distribution was observed at the highest concentrations assayed at all phases; increase in G0/G1 phase by 15 %, and decreased in S and G2/M phases by 38 % and 61 %, respectively (Fig. 2c.2).

Ultimately, tertiary combination of α-ZEL + β-ZEL + BEA is shown in Fig. 5. After 24 h of exposure a significant increase in cells number of G0/G1 phase was observed at all concentrations assayed, from 16.7%–34.6% in comparison to unexposed cells (Fig. 5a.1). This was followed by a considerable decline in S phase cells population at [3.12 + 3.12 + 0.78] μM, [6.25 + 6.25 + 1.25] μM and [12.5 + 12.5 + 2.5] μM by 37 %, 59.6 % and 55.3 %, respectively; and a dose-dependent decrease in G2/M phase at [1.56 + 1.56 + 0.39] μM, [3.12 + 3.12 + 0.78] μM and [6.25 + 6.25 + 1.25] μM by 29.2 %, 51.9 % and 61.2 %, respectively (Fig. 5a.1). After 48 h of exposure, the population of cells in G0/G1 and S phases decreased significantly at the highest concentration assayed ([12.5 + 12.5 + 2.5] μM) by 18.8 % and 41.4 %, respectively, while a significant increase in G2/M phase was observed at the highest concentration by 113 %, and lastly, a dramatic growth in cells number in subG0 phase was noticed at [3.12 + 3.12 + 0.78] and [6.25 + 6.25 + 1.25] μM by 2- and 3.2-folds respectively compare to control cells (Fig. 5a.2) which could be due to the increase in necrotic cells.

3.3. Necrosis-apoptosis analysis in individual treatments

To determine the death pathway underlying the observed decline on

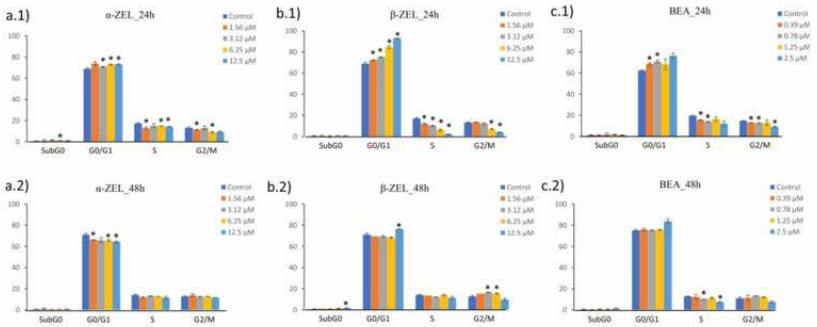

Fig. 1. Cell cycle progression of SH-SY5Y cells treated with α-ZEL (a), β-ZEL (b) and BEA (c) after 24 h (a.1, b.1, and c.1) and 48 h (a.2, b.2, and c.2) and analyzed by flow cytometry. The values were expressed as the mean ± SD for two replications. Data are expressed in % of the unexposed control. *$p \leq 0.05$ indicates a significant difference from the respective solvent control.

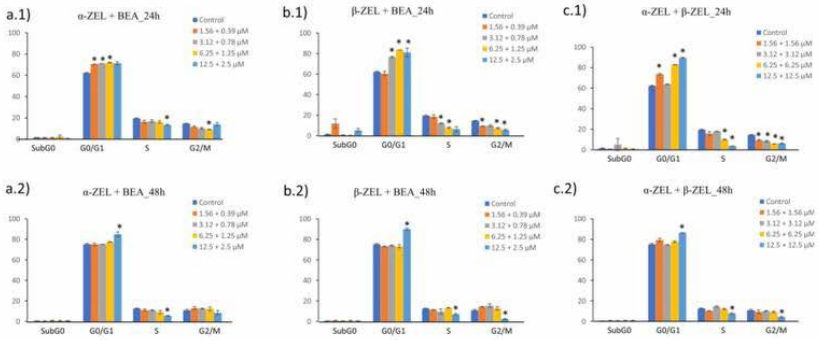

Fig. 2. Cell cycle progression of SH-SY5Y cells treated with binary combinations α-ZEL + BEA (a), β-ZEL + BEA (b) and α-ZEL + β-ZEL (c) after 24 h (a.1, b.1 and c.1) and 48 h (a.2, b.2 and c.2) and analyzed by flow cytometry. The values were expressed as the mean ± SD for two replications. Data are expressed in % of the unexposed control. $^{*}p \leq 0.05$ indicates a significant difference from the respective solvent control.

cell proliferation found by our previous study on cytotoxicity effect of α-ZEL, β-ZEL and BEA individually and in combinations, the mechanism of induction of cell death was decided to study in SH-SY5Y cells after 24 h and 48 h of exposure (Figs. 3, 4 and 5b). As it is shown in Fig. 3 a.1, after 24 h of exposure, α-ZEL treated cells increased significantly in apoptotic and apoptotic/necrotic cells by up to 83.3 % and 88.7 % compared to control, while conversely, after 48 h of exposure it was observed a notable decrease at all concentration assayed in apoptotic cells up to 52.9 % and an increase in apoptotic/necrotic cells at [6.25 + 1.25] and [12.5 + 2.5] μM by 23.7 % and 48.8 % versus control (Fig. 3a.2). Moreover, after 48 h of exposure it was observed a considerable increase in necrotic cells up to 95 % (Fig. 3a.2). For β-ZEL, a significant increase was observed in apoptotic cells exposed to the highest concentration assayed (12.5 μM) after both 24 h and 48 h of exposure by 43.9 % and 50 %, respectively (Fig. 3b.1). Also, apoptotic/necrotic cells increased significantly at 6.25 μM by 53 % after 24 h and at 1.56, 3.12 and 12.5 μM by 38.8 %, 24 % and 27.7 % respectively after 48 h of exposure compared to control cells (Fig. 3b). For BEA, after 48 h exposure a significant decrease was noticed at all concentrations from 8% to 44 %, versus control. in apoptotic/necrotic cells increased for both time of exposure, which was up to 89 % for 24 h and up to 38.8 % for 48 h (Fig. 3c). Also, after 48 h of exposure a notable increase was observed in necrotic cells at 0.39 and 0.78 μM by almost 2 times compare to control cells.

3.4. Necrosis-apoptosis analysis in combination treatments

The apoptosis-necrosis progression of binary combinations is shown in Fig. 4. For α-ZEL + BEA combination, it was observed a significant increase at 2.5 μM in both exposure time (by 57.6 % for 24 h and by 40.8 % for 48 h), similarly the same happened for apoptotic/necrotic cells at all concentrations assayed from 47.3%–83% for 24 h and from 37 % to 58.7 % for 48 h of exposure (Fig. 4a). After 24 h (Fig. 4b), apoptotic cells increased considerably at the highest concentration of [12.5 + 2.5] μM by 44 %, and at [6.25 + 1.25] and [12.5 + 2.5] μM by 28 % and 61.8 % for 48 h. Also, it was observed a significant increase in apoptotic/

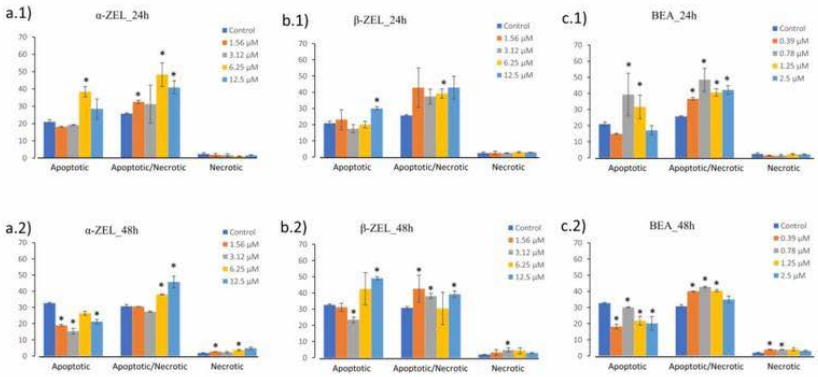

Fig. 3. Apoptosis-Necrosis progression of SH-SY5Y cells treated with α-ZEL (a), β-ZEL (b) and BEA (c) after 24 h (a.1, b.1, and c.1) and 48 h (a.2, b.2, and c.2), analysis by flow cytometry. The values were expressed as the mean ± SD for two replications. Data are expressed in % of the unexposed control. $^{*}p \leq 0.05$ indicates a significant difference from the respective solvent control.

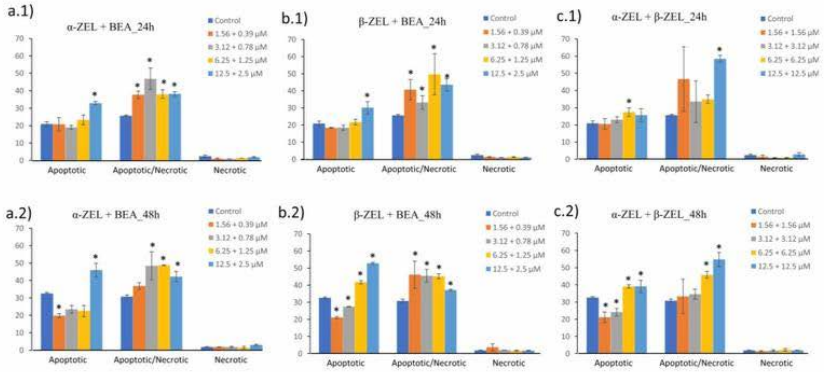

Fig. 4. Apoptosis-Necrosis progression of SH-SY5Y cells treated in binary combination of α-ZEL + BEA (a), β-ZEL + BEA (b), α-ZEL + β-ZEL (c) and α-ZEL + β-ZEL + BEA (c) after 24 h (a.1, b.1 and c.1) and 48 h (a.2, b.2 and c.2) and analyzed by flow cytometry. The values were expressed as the mean ± SD for two replications. Data are expressed in % of the unexposed control. $^*p \leq 0.05$ indicates a significant difference from the respective solvent control.

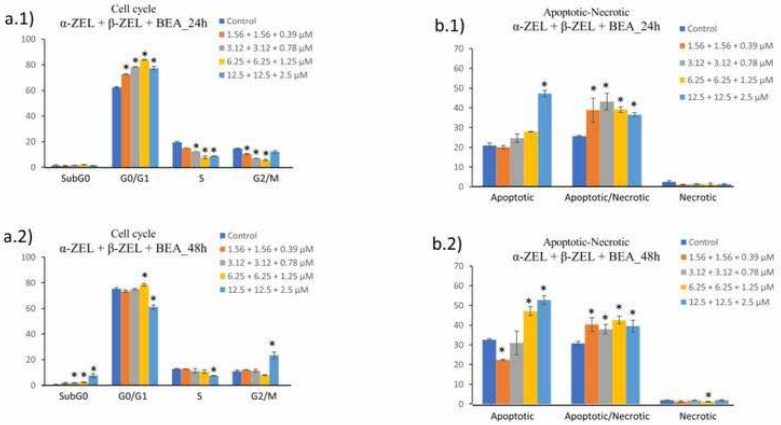

Fig. 5. Cell cycle progression (a) and apoptosis-necrosis progression (b) of SH-SY5Y cells treated in tertiary combination α-ZEL + β-ZEL + BEA after 24 h (a.1 and b.1) and 48 h (a.2 and b.2) and analyzed by flow cytometry. The values were expressed as the mean ± SD for two replications. Data are expressed in % of the unexposed control. $^*p \leq 0.05$ indicates a significant difference from the respective solvent control.

necrotic cells at all concentrations assayed for both times of exposure (from 29.7%–93.8% for 24 h, and from 20.8%–50% for 48 h), while necrotic cells population remained unchanged (Fig. 4b). For α-ZEL + β-ZEL treatments (Fig. 4c.1), after 24 h of exposure, a markable increase was observed at the highest concentration assayed ([12.5 + 2.5] μM) in apoptotic/necrotic cells by 128 %. On the other hand, after 48 h of exposure, a considerable increase was observed at [6.25 + 1.25] and [12.5 + 2.5] μM in both apoptotic (by 19.9 % and 19.8 %) and apoptotic/necrotic (by 49.3 % and 78.6 %) respect to unexposed cells (Fig. 4c.2).

Ultimately, for tertiary combination of α-ZEL + β-ZEL + BEA as it is show in Fig. 5b, a significant increment was noticed at the highest concentration assayed ([12.5 + 12.5 + 2.5] μM) for apoptotic cells for both exposure time (24 h and 48 h by 126 % and 61.6 %, respectively), and in the same way for apoptotic/necrotic cells at all concentrations assayed for both time of exposure (from 42.8%–68.6% for 24 h and from 23.6%–38.6% for 48 h) in comparison to unexposed cells (Fig. 5b).

4. Discussion

The cell cycle is typically divided into four phases: G1 (first gap), S (DNA synthesis), G2 (second gap), and M (mitosis) which are responsible for cell duplication (MacLachlan et al., 1995). Transmission of genetic information from one cell generation to the next requires genome replication during the S-phase, and its segregation to the two new daughter cells during mitosis or M-phase. These two phases are

crucial events in a cyclic process that allows the correct duplication of the cell without accumulating genetic abnormalities. In a normal cell cycle, M-phase does not occur until S-phase is complete. G1 separates M from S, and G2 is between S and M. The timing and order of cell cycle events are monitored during cell cycle checkpoints that occur at the G1/S boundary, in S-phase, and during the G2/M-phases (MacLachlan et al., 1995). These checkpoints can be activated or arrested by stimulation signals such as growth factors, DNA damage and by mis-aligned chromosomes at the mitotic spindle (Abid-Essefi et al., 2003; Prosperini et al., 2013). If the damage cannot be repaired, the cell ends up dying by apoptosis or necrosis.

In accordance with the results achieved from cell cycle analysis presented in here for SH-SY5Y cells, after 24 h of exposure, cell proliferation was arrested remarkably in G0/G1 phase by mycotoxins in comparison with non-treated cells. Such effect was mostly highlighted in treatments where β-ZEL was involved (Figs. 1b.1, 2b.1 and 2c.1). Conversely, after 48 h of exposure, it was detected unchanged activity and/or decrease in number of cells in G0/G1 phase for all treatments except where β-ZEL engaged, which showed cells cycle arrest at the highest concentrations assayed (Figs. 1b.2, Fig. 2b.2 and 2c.2). These findings were fortified by the results achieved in our previous study also in SH-SY5Y cells, where β-ZEL was the most cytotoxic mycotoxin when tested individually (Agahi et al., 2020a).

It is detected that growth arrest can be induced when DNA is damaged (Kastan et al., 1991; Linke et al., 1996); additionally, variations in neuronal cells death may arise from the alteration in the expression of several families of genes that regulate apoptosis which are identified in mammals as *Bcl-2, Casp-3* and *Bax*. The *Bcl-2* is recognized as anti-apoptotic protein family (Merry and Korsmeyer, 1997); while *Bax*, member of the *Bcl-2* protein family, functions as an apoptotic activator or pro-apoptotic; likewise, Caspase-3 (*Casp-3*) as a member of caspase family, is believed to activate cell surface death receptors, which is a major commitment step for apoptosis (Wolf and Green, 1999). Results of the expression of all three genes in SH-SY5Y cells with these mycotoxins treatments and combinations previously reported (Agahi et al., 2020b) are in accordance with the results obtained here (Figs. 1 and 2), as a down regulation of genes *Bcl-2* and *Casp3* in SH-SY5Y cells was observed when exposed to β-ZEL, and up regulation in all apoptotic genes when exposed to β-ZEL + BEA (Agahi et al., 2020b). It has been also evidenced that the G2/M checkpoint prevents cells from entering mitosis when DNA replication/repair is not complete (He et al., 2020); and coinciding with results from publication mentioned above it was proved that α-ZEL + β-ZEL + BEA down-regulate *Bcl-2* gene in SH-SY5Y cells (Agahi et al., 2020a,b), so it can be concluded that growth arrest in G2/M phase by more than 2 times, might be due to the DNA damage, and consequently this will result in increasing necrotic cells in subG0 phase by 4 times compared to control cells as shown in Fig. 5a.2.

Along with SH-SY5Y cells, increment in G0/G1 phase, and decrease in all treatments for S and G2/M phases was observed, mainly at the highest concentration assayed for each treatment, remarkably in β-ZEL, β-ZEL + BEA and β-ZEL + α-ZEL treatments for both phases (Figs. 1b, 2b and c). This could be due to DNA damage and mitosis impairment. Different studies on the cytotoxic and neurotoxic effects of several chemicals and toxins on the alteration of SH-SY5Y cell cycle have been carried out, but not for mycotoxins. For instance, in a study carried out by Sudo et al. (2019) it was indicated that heavy metals (MeHg, $HgCl_2$, and $CdCl_2$) which are known to induce neurotoxicity, can alter SH-SY5Y cell cycle by arresting them in S and G2/M phases. When looking at studies of the assayed mycotoxins on other cell lines similar results have been revealed for ZEA in inducing G0/G1-phase arrest in hESCs cells and granulosa cells, (Cao et al., 2019; Zhang et al., 2018) but contradictory on prostate cancer (PCa) cells, intestinal epithelial cells (IECs) and sertoli cells, where cell cycle arrest occurred in the G2/M phase at the highest doses assayed (Kowalska et al., 2020; Wang et al., 2019; Zheng et al., 2018). Also, in another study performed on RAW264.7 macrophages cells, accumulation of cells in the sub-G1 phase was significantly higher in the groups exposed to β-ZEL than α-ZEL after 24 h (Lu et al., 2013).

On the other hand, for BEA similar results was observed on CHO-K1 cells where cells were arrested in G0/G1 phase after 24 h and an opposite result after 48 h and 72 h where cell arrest happened through G2/M phase (Mallebrera et al., 2016); also on Caco-2 cells where cells were arrested mainly in G2/M phase (Prosperini et al., 2013). Although there are few studies about the effect of combined mycotoxins on cell cycle alteration, Juan-García et al. (2019) investigated the effect of BEA mycotoxin individually and combined with ochratoxin A (OTA) on HepG2 cells. Results of BEA showed a significant decrease in all phases of cell cycle but only in G0/G1 phase when combined with OTA. Gathering all, it can be concluded that alterations in SH-SY5Y cell cycle induced by ZEA's metabolites and BEA, differ with other studies; however, depending on the cell line and concentrations assayed, there is no doubt that these mycotoxins can interrupt cell cycle progression and initiate cell death.

The majority of cells that die by "apoptosis", have condensed nuclei and are eliminated by degradation of cell components for nearby cells (Thompson, 1995). In contrast, necrosis is a cell death initiated by rapid and severe failure to sustain homeostasis, which it involves damage to the structural and functional integrity of the cell and provokes an inflammatory response (Jacobson et al., 1997; Farber, 1994). Toxicological cell culture studies have verified that stimulus intensity influences the mode of cell death (Lennon et al., 1991; Fernandes and Cotter, 1994), although the modes of cell death are still viewed as mechanistically distinct as described above. It has been proposed that cell death occurs as an apoptosis-necrosis continuum, which occurs as hybrids ranging from apoptosis to necrosis (Martin, 2001). Several lines of evidence support a role for apoptosis in the toxicity of ZEA's metabolites and BEA mycotoxins in different cell models (Agahi et al., 2020b; Juan-García et al., 2019; Ben-Salem et al., 2017; Ayed-Boussema et al., 2008; Bouaziz et al., 2007).

According to our study of apoptosis-necrosis progression on SH-SY5Y cells, in individual treatments of mycotoxins, it was observed a significant tendency of growth in early apoptotic cells population for β-ZEL at the highest concentration assayed (12.5 μM) (Figs. 3b.1 and b.2); while for α-ZEL and BEA this tendency shifted considerably from apoptotic cells population to apoptotic/necrotic (late apoptotic) cells after 48 h of exposure (Figs. 3a.2 and c.2). In spite of the fact that there are few studies carried out on ZEA's metabolites on cell death pathway, this could be fortified by results achieved by Lu et al. (2013) on RAW 264.7 macrophages which early apoptotic cells increased significantly when exposed to β-ZEL 50 μM, rather than α-ZEL. Also, in other studies, ZEA caused cell death in apoptotic pathway on pig granulosa cells, and in late apoptotic and necrotic pathways on RAW 264.7 macrophages cells, both studies after 24 h (Li et al., 2015; Zhu et al., 2012). Conversely, for BEA, it was observed an increase in early apoptotic cell death pathway in CHO-K1 cells (from 1and 5 μM), and in Caco-2 cells (from 1.5 μM and 3.0 μM) (Mallebrera et al., 2016; Prosperini et al., 2013); while an induction in necrotic cell death pathway in CHO-K1 cells (1 and 5 μM), and in C6 cells (1.5 μM) (Mallebrera et al., 2016; Wätjen et al., 2014). Despite the large number of studies about the effects of these mycotoxins on cell death pathway and the variety of results, all of them are focused only on studies performed in individual form.

Among binary and tertiary combinations, a remarkable increase in cell proportion was belonged to both early apoptotic and apoptotic/necrotic cell death pathways after 24 h of exposure (Figs. 4, 5b.1 and 5b.2), which was specifically detected at the highest concentration assayed as described in sections 3.4; for tertiary mixture early apoptotic cells increased by 126 % (Fig. 5b.1) and for binary combination β-ZEL + α-ZEL in apoptotic/necrotic (late apoptotic) cells by 128 % both at the highest concentration (Fig. 4c.1). However, after 48 h of exposure a significant increase in apoptotic cell population was noticed for tertiary combination and β-ZEL + BEA at the highest concentration assayed by more than 60 % compared to control cells (Figs. 5b.2 and 4b.2).

The concept of an apoptosis-necrosis cell death progression could be important for understanding neuronal cell death, and thus may be important for the prevention of neuronal loss in human neurological disorder. Although, the death of neurons is not always strictly by apoptosis or necrosis pathways as described by Martin (2001), our results provide further novel information in the mechanisms of neuronal death and the route of dying neurons in an undifferentiated SH-SY5Y neuronal cells when exposed to α-ZEL, β-ZEL and BEA mycotoxins individually and combined. In summary, our results demonstrate that β-ZEL possessed the highest potential in disturbing cell cycle progression by activating and/or arresting cells in G0/G1 phase, and additionally causing cell death mainly in apoptotic pathway at the highest concentration in all treatments where engaged. Thus, these findings offer a better understanding of the cytotoxicity effect of α-ZEL, β-ZEL and BEA mycotoxins when coexist in food and feed, and their effect on the molecular mechanisms of neuronal cell death in nervous system which can lead to new approaches for the prevention of neurodegeneration and neurological disabilities. All this can expand the field of cell death biology, by regulating new norms in the levels of these mycotoxins in food and feed systems.

Declaration of Competing Interest

The authors report no declarations of interest.

Acknowledgements

Authors would like to thank Spanish Ministry of Science and Innovation PID2019-108070RB-I00ALI and Generalitat Valenciana GV 2020/020.

Appendix A. Supplementary data

Supplementary material related to this article can be found, in the online version, at doi:https://doi.org/10.1016/j.tox.2021.152784.

References

Abid-Essefi, S., Baudrimont, I., Hansen, W., Ouanes, Z., Mobio, T.A., Anane, R., Creppy, E.E., Bacha, H., 2003. DNA fragmentation, apoptosis and cell cycle arrest induced by zearalenone in cultured DOK, Vero and Caco-2 cells: prevention by Vitamin E. Toxicol. 192, 237–248.
Agahi, F., Font, G., Juan, C., Juan-García, A., 2020a. Individual and combined effect of zearalenone derivates and beauvericin mycotoxins on SH-SY5Y cells. Toxins 12, 212.
Agahi, F., Álvarez-Ortega, A., Font, G., Juan-García, A., Juan, C., 2020b. Oxidative stress, glutathione, and gene expression as key indicators in SH-SY5Y cells exposed to zearalenone metabolites and beauvericin. Toxicol. Lett. 334, 44–52.
Ayed-Be:surname>Ayed-Boussema, I., Bouaziz, C., Rjiba, K., Valenti, K., Laporte, F., Bacha, H., Hassen, W., 2008. The mycotoxin Zearalenone induces apoptosis in human hepatocytes (HepG2) via p53-dependent mitochondrial signaling pathway. Toxicol. Vitr. 22, 1671–1680.
Ben-Salem, I., Boussabbeh, M., Da-Silva, J.P., Guilbert, A., Bacha, H., Abid-Essefi, S., Lemaire, Ch., 2017. SIRT1 protects cardiac cells against apoptosis induced by zearalenone or its metabolites α- and β-zearalenol through an autophagy-dependent pathway. Toxicol. Appl. Pharmacol. 314, 82–90.
Bouaziz, C., Abid-Essefi, S., El Golli, E., Bacha, H., 2007. Cytotoxicity and apoptosis induction by the mycotoxin zearalenone and its metabolites alpha and beta zearalenol in the human Caco-2 cells. Toxicol. Lett. 172, 62–71.
Cao, H., Zhi, Y., Xu, H., Fang, H., Jia, X., 2019. Zearalenone causes embryotoxicity and induces oxidative stress and apoptosis in differentiated human embryonic stem cells. Toxicol. Vitr. 54, 243–250.
Carri, Mt., Ferri, A., Cozzolino, M., Calabrese, L., Rotilio, G., 2003. Neurodegeneration in amyotrophic lateral sclerosis: the role of oxidative stress and altered homeostasis of metals. Brain Res. Bull. 61, 365–374.
Elmore, S., 2007. Apoptosis: a review of programmed cell death. Toxicol. Pathol. 35, 495–516.
Farber, E., 1994. Programmed cell death: necrosis versus apoptosis. Mod. Pathol. 7, 605–609.
Fernandes, R.S., Cotter, T.G., 1994. Apoptosis or necrosis: intracellular levels of glutathione influence mode of cell death. Biochem. Pharmacol. 48, 675–681.
He, P., Li, Z., Xu, F., Ru, G., Huang, Y., Lin, E., Peng, S., 2020. AMPK activity contributes to G2 arrest and DNA damage decrease via p53/p21 pathways in oxidatively damaged mouse zygotes. Front. Cell Dev. Biol. 8, 539485.
Jacobson, M.D., Weil, M., Raff, M.C., 1997. Programmed cell death in animal development. Cell 88, 347–354.
Jenner, P., 2003. Oxidative stress in Parkinson's disease. Ann. Neurol. 53, 26–36.
Juan-García, A., Manyes, L., Ruiz, M.J., Font, G., 2013. Involvement of enniatins-induced cytotoxicity in human HepG2 cells. Toxicol. Lett. 218, 166–173.
Juan-García, A., Tolosa, J., Juan, C., Ruiz, M.J., 2019. Cytotoxicity, genotoxicity and disturbance of cell cycle in HepG2 cells exposed to OTA and BEA: single and combined actions. Toxins 11, 341.
Kannan, K., Jain, S.K., 2000. Oxidative stress and apoptosis. Pathophysiology 7, 153–163.
Kastan, M.B., Onyekwere, O., Sidransky, D., Vogelstein, B., Craig, R.W., 1991. Participation of p53 protein in the cellular response to DNA damage. Cancer Res. 51, 6304–6311.
King, K.L., Cidlowski, J.A., 1995. Cell cycle and apoptosis: common pathways to life and death. J. Cell. Biochem. 58, 175–180.
Klein, J.A., Ackerman, S.L., 2003. Oxidative stress, cell cycle, and neurodegeneration. J. Clin. Invest. 111, 785–793.
Kovalevich, J., Langford, D., 2013. Considerations for the use of SH-SY5Y neuroblastoma cells in neurobiology. In: Amini, S., White, M.K. (Eds.), Neuronal Cell Culture: Methods and Protocols. Humana Press, Totowa, NJ, pp. 9–21.
Kowalska, K., Habrowska-Gorczynska, D.E., Dominska, K., Urbanek, K.A., Piastowska-Ciesielska, A.W., 2020. ER Beta and NF kappa B-Modulators of zearalenone-induced oxidative stress in human prostate Cancer cells. Toxins 12 (3), 199.
Lennon, S.V., Martin, S.J., Cotter, T.G., 1991. Dose-dependent induction of apoptosis in human tumour cell lines by widely diverging stimuli. Cell Prolif. 24, 203–214, 1991.
Li, Q., Zhang, Zh., Lin, P., Lei, L., 2015. Endoplasmic reticulum stress cooperates in zearalenone-induced cell death of RAW 264.7 macrophages. Int. J. Mol. Sci. 16 (8), 19780–19795.
Linke, S.P., Clarkin, K.C., Di Leonardo, A., Tsou, A., Wahl, G.M., 1996. A reversible, p53-dependent G0/G1 cell cycle arrest induced by ribonucleotide depletion in the absence of detectable DNA damage. Genes Dev. 10, 934–947.
Lu, J., Yu, J.Y., Lim, Sh.S., Son, Y.O., Kim, D.H., Lee, S.A., hi, X., Lee, J.Ch., 2013. Cellular mechanisms of the cytotoxic effects of the zearalenone metabolites α-zearalenol and β-zearalenol on RAW264.7 macrophages. Toxicol. Vitr. 27 (3), 1007–1017.
MacLachlan, T.K., Sang, N., Giordano, A., 1995. Cyclins, cyclin-dependent kinases and cdk inhibitors: implications in cell cycle control and cancer. Crit. Rev. Eukaryot. Gene Expr. 5 (2), 127–156.
Mallebrera, B., Font, G., Ruiz, M.J., 2014. Disturbance of antioxidant capacity produced by beauvericin in CHO-K1 cells. Toxicol. Lett. 226, 337–342.
Mallebrera, B., Juan-García, A., Font, G., Ruiz, M.J., 2016. Mechanisms of beauvericin toxicity and antioxidant cellular defense. Toxicol. Lett. 246, 28–34.
Manickam, N., Radhakrishnan, R.K., Andrews, J.F.V., Selvaraj, D.B., Kandasamy, M., 2020. Cell cycle re-entry of neurons and reactive neuroblastosis in Huntington's disease: possibilities for neural-glial transition in the brain. Life Sci. 263, 118569.
Martin, L., 2001. Neuronal cell death in nervous system development, disease, and injury (Review). Int. J. Mol. Med. 7, 455–478.
Merry, D.E., Korsmeyer, S.J., 1997. Bcl-2 gene family in the nervous system. Annu. Rev. Neurosci. 20, 245–267.
Okouchi, M., Ekshyyan, O., Maracine, M., Aw, T.Y., 2007. Neuronal apoptosis in neurodegeneration. Antioxid. Redox Signal. 9, 1059–1096.
Prosperini, A., Juan-García, A., Font, G., Ruiz, M.J., 2013. Beauvericin-induced cytotoxicity via ROS production and mitochondrial damage in Caco-2 cells. Toxicol. Lett. 222 (2), 204–211.
Pucci, B., Kasten, M., Giordano, A., 2000. Cell cycle and apoptosis. Neoplasia 2, 291–299.
Sudo, K., Dao, C.V., Atsushi, M., Mitsuya, Sh., 2019. Comparative analysis of in vitro neurotoxicity of methylmercury, mercury, cadmium, and hydrogen peroxide on SH-SY5Y cells. J. Vet. Med. Sci. 81 (6), 828–837.
Swomley, A.M., Förster, S., Keeney, J.T., Triplett, J., Zhang, Z., Sultana, R., Butterfield, D.A., 2014. Abeta, oxidative stress in Alzheimer disease: evidence based on proteomics studies. Biochim. Biophys. Acta 1842 (8), 1248–1257.
Tatay, E., Espin, S., Garcia-Fernandez, A.J., Ruiz, M.J., 2017. Oxidative damage and disturbance of antioxidant capacity by zearalenone and its metabolites in human cells. Toxicol. Vitr. 45, 334–339.
Thompson, C.B., 1995. Apoptosis in the pathogenesis and treatment of disease. Science 267, 1456–1462.
Vermes, I., Haanen, C., Steffens-Nakken, H., Reutellingsperger, C., 1995. A novel assay for apoptosis flow cytometric detection of phosphatidylserine expression on early apoptotic cells using fluorescein labelled Annexin V. J. Immunol. Methods 184, 39–51.
Wang, X., Yu, H., Fang, H., Zhao, Y., Jin, Y., Shen, J., Zhou, Ch., Zhou, Y., Fu, Y., Wang, J., Zhang, J., 2019. Transcriptional profiling of zearalenone-induced inhibition of IPEC-J2 cell proliferation. Toxicon 172, 8–14.
Wätjen, W., Debbab, A., Hohlfeld, A., Chovolou, Y., Proksch, P., 2014. The mycotoxin beauvericin induces apoptotic cell death in H4IIE hepatoma cells accompanied by an inhibition of NF-κB-activity and modulation of MAP-kinases. Toxicol. Lett. 231 (1), 9–16.
Wolf, B.B., Green, D.R., 1999. Suicidal tendencies: apoptotic cell death by caspase family proteinases. J. Biol. Chem. 274, 20049–20052.
Wong, R.S., 2011. Apoptosis in cancer: from pathogenesis to treatment. J. Exp. Clin. Cancer Res. 30, 87.
Zhang, R.Q., Sun, X.F., Wu, R.Y., Cheng, Sh.F., Zhang, G.L., Zhai, Q.Y., Liu, X.L., Zhao, Y., Shen, W., Li, L., 2018. Zearalenone exposure elevated the expression of tumorigenesis genes in mouse ovarian granulosa cells. Toxicol. Appl. Pharmacol. 356, 191–203.

Zheng, W.L., Wang, B.J., Wang, L., Shan, Y.P., Zou, H., Song, R.L., Wang, T., Gu, J.H., Yuan, Y., Liu, X.Z., Zhu, G.Q., Bai, J.F., Liu, Z.P., Bian, J.C., 2018. ROS-mediated cell cycle arrest and apoptosis induced by Zearalenone in mouse sertoli cells via ER stress and the ATP/AMPK pathway. Toxins 10, 24.

Zhu, L., Yuan, H., Guo, C., Lu, Y., Deng, S., Yang, Y., Wei, Q., Wen, L., He, Z., 2012. Zearalenone induces apoptosis and necrosis in porcine granulosa cells via a caspase-3- and caspase-9-dependent mitochondrial signaling pathway. J. Cell. Physiol. 227, 1814–1820.

Zingales, V., Fernández-Franzón, M., Ruiz, M.J., 2020. The role of mitochondria in sterigmatocystin-induced apoptosis on SH-SY5Y cells. Food Chem. Toxicol. 142, 111493.